frontiers | Research Topics

Ovarian aging: Pathophysiology and recent development of maintaining ovarian reserve, volume III

Edited by
Antonio Simone Laganà, Akira Iwase and Osamu Hiraike

Published in
Frontiers in Endocrinology

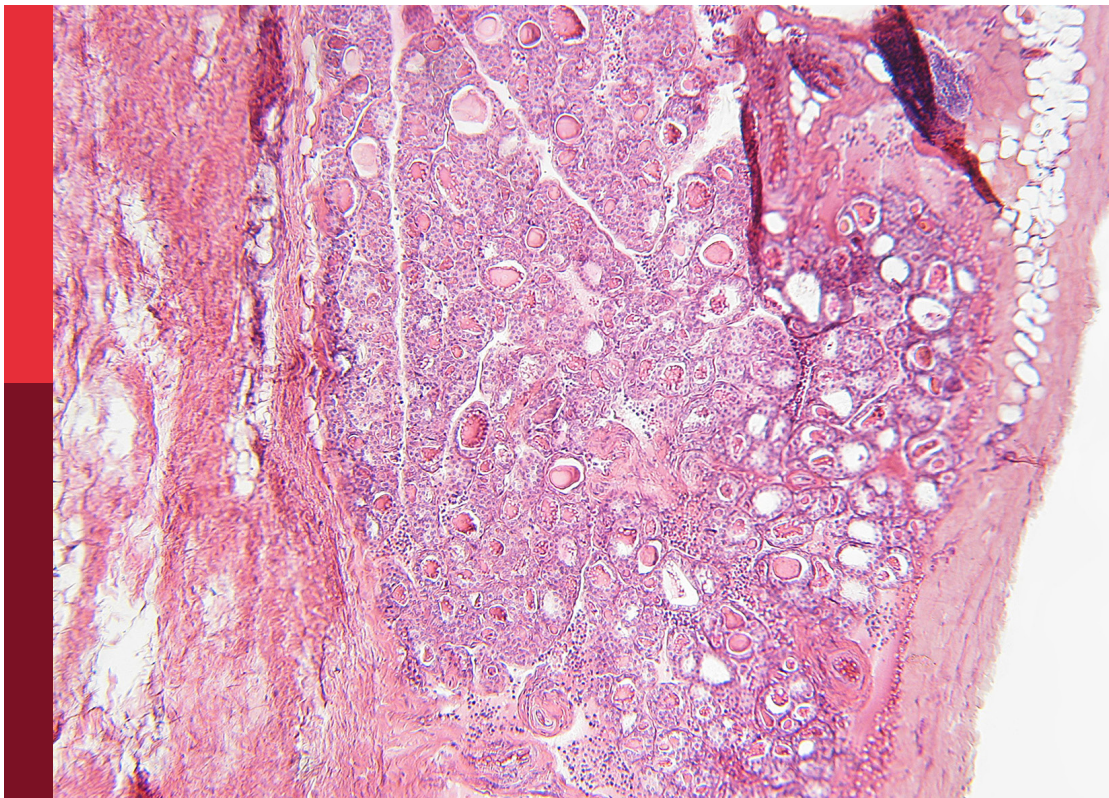

ISSN 1664-8714
ISBN 978-2-8325-5325-1
DOI 10.3389/978-2-8325-5325-1

About Frontiers

Frontiers is more than just an open access publisher of scholarly articles: it is a pioneering approach to the world of academia, radically improving the way scholarly research is managed. The grand vision of Frontiers is a world where all people have an equal opportunity to seek, share and generate knowledge. Frontiers provides immediate and permanent online open access to all its publications, but this alone is not enough to realize our grand goals.

Frontiers journal series

The Frontiers journal series is a multi-tier and interdisciplinary set of open-access, online journals, promising a paradigm shift from the current review, selection and dissemination processes in academic publishing. All Frontiers journals are driven by researchers for researchers; therefore, they constitute a service to the scholarly community. At the same time, the *Frontiers journal series* operates on a revolutionary invention, the tiered publishing system, initially addressing specific communities of scholars, and gradually climbing up to broader public understanding, thus serving the interests of the lay society, too.

Dedication to quality

Each Frontiers article is a landmark of the highest quality, thanks to genuinely collaborative interactions between authors and review editors, who include some of the world's best academicians. Research must be certified by peers before entering a stream of knowledge that may eventually reach the public - and shape society; therefore, Frontiers only applies the most rigorous and unbiased reviews. Frontiers revolutionizes research publishing by freely delivering the most outstanding research, evaluated with no bias from both the academic and social point of view. By applying the most advanced information technologies, Frontiers is catapulting scholarly publishing into a new generation.

What are Frontiers Research Topics?

Frontiers Research Topics are very popular trademarks of the *Frontiers journals series*: they are collections of at least ten articles, all centered on a particular subject. With their unique mix of varied contributions from Original Research to Review Articles, Frontiers Research Topics unify the most influential researchers, the latest key findings and historical advances in a hot research area.

Find out more on how to host your own Frontiers Research Topic or contribute to one as an author by contacting the Frontiers editorial office: frontiersin.org/about/contact

Ovarian aging: Pathophysiology and recent development of maintaining ovarian reserve, volume III

Topic editors

Antonio Simone Laganà — University of Palermo, Italy

Akira Iwase — Gunma University, Japan

Osamu Hiraike — The University of Tokyo, Japan

Citation

Laganà, A. S., Iwase, A., Hiraike, O., eds. (2024). *Ovarian aging: Pathophysiology and recent development of maintaining ovarian reserve, volume III*. Lausanne: Frontiers Media SA. doi: 10.3389/978-2-8325-5325-1

Table of contents

frontiers | Frontiers in Endocrinology

TYPE Editorial
PUBLISHED 05 August 2024
DOI 10.3389/fendo.2024.1460934

OPEN ACCESS

EDITED AND REVIEWED BY
Antonello Lorenzini,
University of Bologna, Italy

*CORRESPONDENCE
Osamu Hiraike
osamuwh-tky@umin.ac.jp

RECEIVED 07 July 2024
ACCEPTED 15 July 2024
PUBLISHED 05 August 2024

CITATION
Hiraike O, Iwase A and Laganà AS (2024) Editorial: Ovarian aging: pathophysiology and recent development of maintaining ovarian reserve, volume III.
Front. Endocrinol. 15:1460934.
doi: 10.3389/fendo.2024.1460934

Editorial: Ovarian aging: pathophysiology and recent development of maintaining ovarian reserve, volume III

Osamu Hiraike[1]*, Akira Iwase[2] and Antonio Simone Laganà[3]

[1]Department of Obstetrics and Gynecology, Faculty of Medicine, The University of Tokyo, Tokyo, Japan, [2]Department of Obstetrics and Gynecology, Gunma University Graduate School of Medicine, Maebashi, Japan, [3]Unit of Obstetrics and Gynecology, "Paolo Giaccone" Hospital, Department of Health Promotion, Mother and Child Care, Internal Medicine and Medical Specialties (PROMISE), University of Palermo, Palermo, Italy

KEYWORDS

ovary, ageing, artificial reproductive technologies, ovarian follicle, estrogen

Editorial on the Research Topic
Ovarian aging: pathophysiology and recent development of maintaining ovarian reserve, volume III

The function of the ovary must be considered both quantitatively and qualitatively. It is important to know the number of remaining of oocytes in the ovary, and it is also important to know whether the oocyte can become a good embryo after fertilization for the establishment of conception. The oocyte, granulosa cells, and theca cells form a follicle, and these components are indispensable for the development of mature oocytes. For the oocyte to function properly, it must undergo an elaborate process of ovarian development and oocyte formation, utilizing the central and local control mechanisms of ovulation and follicular development, luteinization, and follicle atresia, which is important in human reproduction. The development of experimental methods to predict ovarian dysfunction is an important issue in the management of reproductive-aged women and women after menopause. Establishment of appropriate diagnostic and therapeutic methods remains a major challenge.

Against this background, "Ovarian Aging: Pathophysiology and Recent Development of Maintaining Ovarian Reserve" was first proposed in 2019. Since then, the III volume was introduced. A further volume reflects the interests of researchers in this area, proving it remains a fascinating issue. In assisted reproductive technologies (ART), a number of new technologies have been introduced including cryopreservation of eggs and ovarian tissue. A recent trend of using next-generation sequencing technologies in the clinical field has provided us important insights and analysis of preimplantation embryos and bacterial flora has become a daily setting. The study of follicle development was previously impossible, but recent progress in molecular biology significantly improved our understanding of the differentiation of oocytes and the microenvironment of ovarian follicles.

We aimed to overview the recent studies related to ovarian function, including follicular pathophysiology, development of ovarian markers, drugs that maintain or improve ovarian reserve, and technologies of cryopreservation of oocyte and ovarian tissues. With the aim of this Research Topic, nine groups responded to our recruitment and

contributed and gave us useful insights into the underlying mechanisms of ovarian aging. The results shown here are interesting and we are confident that these studies offer a comprehensive collection on ovarian aging and its related issues. Fortunately, this third volume of Ovarian Ageing resulted in 25,207 total views, 8,148 article views, 3,024 downloads, and 17,059 topic views (accessed on 29 Jun, 2024).

In this series, three researchers provided clinical suggestions on ART. The clinical study [He et al.] showed that the ratio of basal FSH/LH could predict ovarian response and they developed an ovarian sensitivity index that can be used as an indicator of ovarian response in ART treatment. Sun et al. showed the progesterone to number of mature oocytes index levels can be useful for predicting pregnancy outcome in fresh IVF/ICSI cycles. A clinical randomized trial [Chu et al.] has proven beneficial for women with decreased ovarian reserve because it showed that intake of flaxseed oil contributed to the formation of MII oocytes. The manuscript using a machine learning model [Ding et al.] clearly demonstrated that the representative ovarian reserve marker, anti-Müllerian hormone (AMH), and antral follicle count (AFC) were applicable to a group of women aged 20 to 35 years.

Since the discovery of estrogen receptor α (ERα), its function in the ovary was investigated because estrogens play crucial roles in the development of ovarian follicles. It was known that ovaries of mice deficient in ERα exhibit multiple hemorrhagic cysts in the ovaries, but the physiological role of the cyst formation was not known. Schröder et al. showed iron deposits in the ovaries and significant increases in ovarian mast cells involved in iron-mediated foam cell formation, resembling signs of aging [Luo et al.].

Vasomotor symptoms such as hot flashes and sweating are representative climacteric symptoms and can be reversed by the supplementation of estrogens, known as hormonal therapy (HT). However, we sometimes encounter postmenopausal patients with vasomotor symptoms that are resistant to the conventional HT. A clinical trial [Li et al.] showed the beneficial effects of stellate ganglion block on perimenopausal hot flashes, and we can apply the result of this study in daily clinical settings.

The review manuscripts shed light on the role of mitochondria in ovarian aging [Ju et al.] and the usefulness of acupuncture, which is known as a less invasive technique and can be applied to various diseases [Cao et al.].

Concluding remarks

Altogether, the clinical studies, research studies, and reviews contained in this topic are insightful and beneficial both for clinicians and researchers. The wide range of data provides a good overview of the topic, and we are sure that these novel studies might enhance future studies with the aim to improve and maximize infertility treatment and the medical care of postmenopausal women.

Author contributions

OH: Conceptualization, Data curation, Formal analysis, Funding acquisition, Investigation, Methodology, Project administration, Resources, Software, Supervision, Validation, Visualization, Writing – original draft, Writing – review & editing. AI: Writing – review & editing. AL: Writing – review & editing.

Conflict of interest

The authors declare that the research was conducted in the absence of any commercial or financial relationships that could be construed as a potential conflict of interest.

Publisher's note

frontiers | Frontiers in Endocrinology

TYPE Original Research
PUBLISHED 23 February 2023
DOI 10.3389/fendo.2023.1086998

OPEN ACCESS

EDITED BY
Osamu Hiraike,
The University of Tokyo, Japan

REVIEWED BY
Jinhui Liu,
Nanjing Medical University, China
Feng Jiang,
Fudan University, China

*CORRESPONDENCE
Chenyu Sun
drsunchenyu@yeah.net
Ling Liu
eye99@163.com

†These authors have contributed equally to this work

SPECIALTY SECTION
This article was submitted to Endocrinology of Aging, a section of the journal Frontiers in Endocrinology

RECEIVED 01 November 2022
ACCEPTED 30 January 2023
PUBLISHED 23 February 2023

CITATION
Sun X, Yao F, Yin C, Meng M, Lan Y, Yang M, Sun C and Liu L (2023) Independent value of PMOI on hCG day in predicting pregnancy outcomes in IVF/ICSI cycles.
Front. Endocrinol. 14:1086998.
doi: 10.3389/fendo.2023.1086998

Independent value of PMOI on hCG day in predicting pregnancy outcomes in IVF/ICSI cycles

Xingyu Sun[1,2†], Fei Yao[1†], Chengliang Yin[3], Muzi Meng[4,5], Yunzhu Lan[6], Ming Yang[7], Chenyu Sun[8*†] and Ling Liu[2*†]

[1]Department of Gynecology, The Affiliated Traditional Chinese Medicine Hospital of Southwest Medical University, Luzhou, Sichuan, China, [2]Reproductive Medicine Center, the Affiliated Hospital of Southwest Medical University, Luzhou, China, [3]Faculty of Medicine, Macau University of Science and Technology, Macau, Macau SAR, China, [4]United Kingdom (UK) Program Site, American University of the Caribbean School of Medicine, Preston, United Kingdom, [5]Bronxcare Health System, New York City, NY, United States, [6]Obstetrics Department, The Fourth Affiliated Hospital, College of Medicine, Zhejiang University, Hefei, China, [7]Obstetrics Department, The First Dongguan Affiliated Hospital Of Guangdong Medical University, Dongguan, China, [8]Department of Thyroid and Breast Surgery, The Second Hospital of Anhui Medical University, Hefei, China

Objectives: The aim of this study was to determine whether, on the day of human chorionic gonadotropin (hCG) injection, the progesterone to number of mature oocytes index (PMOI) can be used alone or together with other parameters in a fresh embryo transfer *in vitro* fertilization (IVF)/intracytoplasmic sperm injection (ICSI) cycle to predict pregnancy outcome.

Methods: This was a retrospective cohort study of all couples who underwent a clinical pregnancy and received a fresh IVE/ICSI cycle at a single large reproductive medical center between June 2019 and March 2022. The study involved a total of 1239 cycles. To analyze risk factors associated with pregnancy outcomes on the day of HCG injection, univariate and multivariate logistic regression analyses were used. The area under the curve (AUC) was determined, and PMOI and other factors were compared using receiver operating characteristic (ROC) curves.

Results: The clinical pregnancy rate was significantly higher in group A (60.76%) than in the other groups (Group B: 52.92% and Group C:47.88%, respectively, p =0.0306). Univariate and multivariate logistic regression revealed that PMOI levels were significantly correlated with the probability of pregnancy outcome, independent of other risk factors. More importantly, PMOI levels independently predict the occurrence of pregnancy outcome, comparable to the model combining age. The optimal serum PMOI cutoff value for pregnancy outcome was 0.063 ug/L.

Conclusion: Our results suggest that PMOI levels have an independent predictive value for pregnancy outcome in fresh IVF/ICSI cycles.

KEYWORDS

progesterone to number of mature oocytes index, HCG day, pregnancy outcomes, IVF/ICSI cycle, prediction

Introduction

The term "infertility" refers to the inability to achieve a successful pregnancy after 12 months or more of appropriate, time-limited unprotected intercourse or therapeutic donor insemination. Nevertheless, early evaluation and treatment after six months may be reasonable for women over 35 years of age (1). A distressing fact about infertility is that the number of infertility patients is increasing every year, and infertility has become a major health problem, affecting 8%–15% of couples of reproductive age worldwide (2). Reassuringly, in recent years, assisted reproductive technology (ART), consisting of *in vitro* fertilization (IVF) and intracytoplasmic sperm injection (ICSI), has become an important treatment for many infertile women (3). However, despite recent advances in assisted reproductive technologies, success rates remain low, causing public socioeconomic distress regarding the health of individuals and women. Thus, achieving high pregnancy rates is our main challenge today with regard to assisted reproductive technologies (ART). Therefore, predicting pregnancy outcomes after assisted reproductive technologies has been a research hotspot, and more evidence is needed to help inform couples undergoing assisted reproduction, clinicians and policy makers. Currently, the factors that predict pregnancy outcomes on the day of HCG injection are not fully understood.

Progesterone (P) is essential before and during pregnancy as it plays a key role in supporting the endometrium and thus fetal survival (4). In the natural cycle, preovulatory P secretion facilitates the action of estrogen on the pituitary gland; the latter is a key factor in producing a mid-cycle luteinizing hormone (LH) peak. In addition, progesterone also stimulates a mid-cycle follicle-stimulating hormone (FSH) surge, which is important to support the expression of LH receptors in the granulosa layer (5, 6). Notably, the majority of circulating P (~95%) is produced in the follicle by granulosa cells (GCs) through the action of 3β-HSD catalyzing the conversion of pregnenolone (delta-4 pathway) under the influence of LH (7, 8). After ovulation, the corpus luteum is formed, and both the corpus luteum and GCs produce P in response to endogenous LH activity (9). In early pregnancy, human chorionic gonadotropin (hCG), secreted by syncytial trophoblasts, rescues the corpus luteum and maintains luteal function until the establishment of placental steroidogenesis (10). Therefore, elevated progesterone (PE) and its sustained levels are considered essential to be key in eliciting the endocrine signals responsible for initiating the endometrial receptive phase to embryo implantation (11, 12).

Nevertheless, it has been debated in the literature for over two decades that elevated serum progesterone (SP) is possible deleterious effects on the day of human chorionic gonadotropin (hCG) administration in relation to the outcome of assisted reproductive technology (ART) cycles (13, 14). Previous studies have reported that the decrease in clinical pregnancy rates (CPRs) was statistically significant ($P<0.05$), whereas no association was found in others (15, 16). Simultaneously, it is not widely accepted that serum progesterone (SP) has an adverse effect on cycle outcomes at a specific threshold level. Hence, serum progesterone (SP) cannot serve as a sole predictor of clinical pregnancy (CP). To our knowledge, SP level may correlate with the number of hormonally active follicles. In addition, the number of mature oocytes was a more objective parameter. As such it may be possible to use a new parameter of measurement: the progesterone to number of mature oocytes index (PMOI) to predict successful clinical pregnancy (CP) compared to SP levels alone.

Wu et al. showed that elevated progesterone on the day of hCG triggering was associated with a detrimental effect on live birth rate in low and intermediate ovarian responders, but not in high responders (17). It was a retrospective study with 2,351 patients receiving fresh assisted reproduction technology (ART) transfer cycles with GnRH agonist using a long or short protocol. Currently, the underlying mechanism of PE on IVF pregnancy outcome remains unclear, endometrial receptivity and embryo quality are two key factors to the success of implantation (18). Lu et al. has demonstrated PE influences endometrial receptivity during fresh ET cycles (19). It is possible that PE will promote the endometrium without affecting the embryo, which can lead to a dyssynchrony between the embryo and endometrium, which could lead to a decrease in the implantation rate, thereby reducing pregnancy rates. Furthermore, Sahar et al. also displayed that pregnancy rates were significantly lower on the day of hCG administration with progesterone thresholds above 1.5ng/mL compared to progesterone levels lower than 1.5ng/mL (20). Since progesterone (P) alone will not predict pregnancy outcome, various markers have been proposed to predict the outcome of assisted reproductive cycles more accurately.

As for strengths of PMOI, on the one hand, a correlation has been found between serum progesterone levels and the number of follicles with hormonal activity (21). It is possible for the number of follicles seen on ultrasound examination to vary between observers. On the other hand, it was suggested that the number of oocytes retrieved could be used as an objective parameter to calculate the progesterone to number of mature oocytes index (PMOI) (22, 23).

This aim of this study was to investigate the risk factors for pregnancy outcome in patients treated with fresh cycles of *in vitro* fertilization (IVF) or intracytoplasmic sperm injection (ICSI) and to elucidate the predictive power of PMOI level on the day of human chorionic gonadotropin (hCG) injection on pregnancy outcome based on retrospective data analysis. These results can help medical professionals take steps to minimize pregnancy failure and aid in decision-making for fresh embryo transfer cycle.

Materials and methods

Study population

In the cross-sectional retrospective study, enrolled patients underwent IVF/ICSI cycles at the reproductive center of the Affiliated hospital of Southwest Medical University, located in Luzhou, China. Medical records of all patients treated by IVF/ICSI from June 2019 and March 2022 were screened. The criteria for inclusion and exclusion of patients from this study are listed below. The flow chart for patient selection is shown in Figure 1.

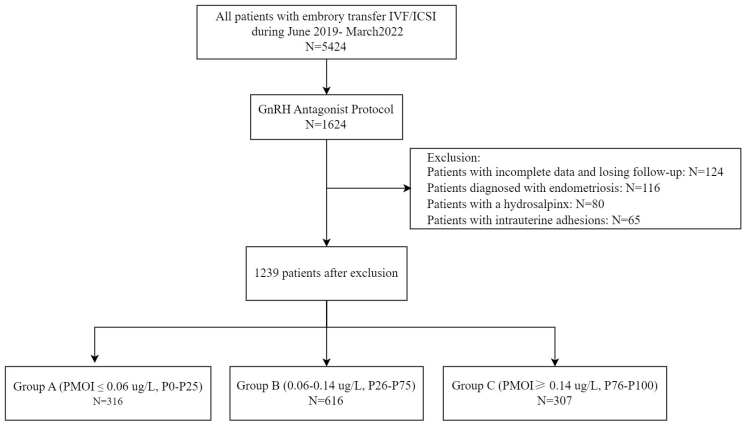

FIGURE 1
Flow chart of the research.

Inclusion criteria

(1) Women undergoing their first IVF/ICSI cycle for unexplained infertility, tubal infertility, stage I/II endometriosis, or a partner diagnosed with male-factor infertility were included in the study.

(2) Patients were treated with a gonadotropin-releasing hormone (GnRH) long-acting agonist regimen and received IVF/ICSI-ET.

Exclusion criteria

(1) Patients with incomplete data and loss to follow-up were excluded.

(2) Patients diagnosed with endometriosis prior to embryo transfer were excluded from the study.

(3) Patients with hydrosalpinx by hysterosalpingography (HSG) prior to embryo transfer were excluded.

(4) Patients with intrauterine adhesions diagnosed by hysterosalpingography (HSG) were excluded.

(5) Patients with no available embryos for transfer or canceled cycles for other reasons were excluded.

GnRH antagonist protocol

All women underwent controlled ovarian stimulation (COS) with a GnRH antagonist fixed regimen. Bilateral antral follicles (10mm) were counted by transvaginal ultrasonography on the second day of the menstrual cycle, and women started COS treatment with gonadotrophins (Gonal-F, Merck Serono Europe Ltd or Puregon, N. V. Organon). The levels of serum progesterone (SP) were measured using an automated electrochemiluminescence immunoassay (Roche Diagnostics Elecsys Cortisol II assays and COBAS E801), and values were expressed in ng/ml. At our center, the starting dose of gonadotrophins was 150 IU/day for women aged ≤ 34 years, with BMI <24 kg/m^2, 6≤AFC<15, and the dosage would be increased if the woman was older (age ≥ 35 years), heavier (BMI ≥ 24 kg/m2), or had poorer ovarian reserve AFC<6 or basal FSH>10 IU/L or AMH <1 ng/ml. Conversely, if the woman is lean (BMI < 19 kg/m2) or has a good ovarian reserve (AFC≥ 15 or AMH≥ 4 ng/ml), the dosage will be reduced. Dose adjustments were determined by the physician based on individual clinical experiences. GnRH antagonists (Cetrorelix, BaxterorGanirelix, N.V.Organon) were given daily starting on day 5 or 6 of stimulation. Human chorionic gonadotrophin (Chorionic Gonadotrophin for Injection, Livzon) was injected once there were at least three follicles >17 mm in diameter or at least two follicles >18 mm in diameter. Oocyte retrieval was performed under ultrasound guidance 34-36 hours after triggering.

Grouping

Patients were divided into three concentration groups according to the percentage of PMOI levels on the day of hCG injection: Group A (PMOI ≤ 0.06 ug/L, P0-P25), Group B (0.06-0.14 ug/L, P26-P75), and Group C (PMOI≥ 0.14 ug/L, P76-P100). Clinical data, including age, infertility duration, BMI, and other relevant clinical data, were compared between the groups.

Statistical analysis

Data analysis was performed using SPSS 23.0. Continuous variables were expressed as mean ± standard deviation (SD), and categorical variables were expressed as N (%). Univariate and multivariate logistic regression analyses were performed to assess risk factors associated with pregnancy outcomes. Receiver operating characteristic (ROC) curves were plotted, the area under the curve (AUC) was calculated, and the relationship between PMOI and other factors was compared. Optimal cutoff values were estimated by using the Youden index.

Results

Comparison of clinical data in each group

Patients were divided into three concentration groups according to the percentage of PMOI levels on the day of hCG injection: Group A (PMOI ≤ 0.06 ug/L, P0-P25), Group B (0.06-0.14 ug/L, P26-P75), and Group C (PMOI≥ 0.14 ug/L, P76-P100). There were significant differences in the general characteristics of the three groups, including AFC, FSH, FSH/LH, AMH, T, P, E2 on hCG day, number of eggs obtained, number of M_{II} oocytes, number of available embryos and clinical pregnancy rate. Group A had the highest AFC, FSH, FSH/LH, AMH, P, E2 on HCG day, number of eggs obtained, number of M_{II} oocytes, number of available embryos, and clinical pregnancy rate. Table 1 summarizes these data and provides additional information.

Univariate and multivariate analyses of clinical factors

A univariate logistic regression analysis was performed, considering all factors that may have an impact on clinical pregnancy rates. The results showed that age (OR=0.772, P=0.027), available embryos (OR=1.287, P=0.034), and PMOI (OR=0.002, P=0.010) were all associated with clinical pregnancy rate (P<0.05). The results are shown in the logistic regression table. Later, independent factors such as age, available embryos, and PMOI were included together in a multivariate logistic regression model. These results showed that age and PMOI were independent risk factors for clinical pregnancy rate. Detailed results are shown in Table 2.

Predictive value of PMOI for pregnancy outcomes

We performed a ROC curve analysis to explore the predictive value of PMOI levels and other risk factors for pregnancy outcome (Figure 2). The AUC for PMOI levels was 0.621ug/L (Figure 2A). The optimal PMOI threshold for predicting pregnancy outcome was 0.063, with a specificity of 79.2% and a sensitivity of 42.7%, according to the Youden index algorithm in the ROC curve. Meanwhile, the age-level AUC was 0.546 (Figure 2B). In the ROC curve, the optimal age threshold for predicting pregnancy outcome based on the Youden index algorithm was 34.5, with a specificity of 27.4% and a sensitivity of 83.5%. In addition, a prediction model combining PMOI and age was developed. The AUC of this model was 0.592 (95%CI:0.561–0.624). As for age, the AUC of the model increased from 0.546 to 0.592 (95% CI 0.561-0.624; P < 0.05) after including PMOI in age (Figures 2C, Table 3). Therefore, we can

TABLE 1 Comparison of clinical data in each group.

Parameters	Group A	Group B	Group C	*P value*
No. of cases	316	616	307	–
Age(year)	30.14 ± 4.36	31.06 ± 4.47	32.06 ± 5.14	0.765
Infertility duration	4.59 ± 3.48	4.56 ± 3.47	4.58 ± 3.53	0.991
BMI	23.34 ± 3.43	22.41 ± 3.24	22.32 ± 3.18	0.664
AFC	10.91 ± 4.41	10.12 ± 4.53	8.79 ± 4.18	<0.05
FSH	7.49 ± 2.16	8.15 ± 2.21	8.22 ± 1.99	<0.05
FSH/LH	2.79 ± 2.74	3.28 ± 3.54	3.29 ± 3.14	0.042
E2	53.63 ± 48.33	63.88 ± 79.04	66.32 ± 80.06	0.0589
AMH	5.24 ± 4.24	4.09 ± 3.50	2.89 ± 2.79	<0.05
PRL	12.75 ± 7.68	14.60 ± 15.86	14.65 ± 8.64	0.0766
T	45.90 ± 19.35	42.96 ± 19.90	46.56 ± 18.79	0.843
P	0.60 ± 0.42	0.65 ± 0.43	0.72 ± 0.38	0.0462
Endometrial thickness on transfer day	6.50 ± 2.42	6.63 ± 2.45	6.96 ± 2.54	0.0539
Total dosage of Gn used	2279.45 ± 743.23	2429.19 ± 712.90	2522.23 ± 805.24	0.324
Gn used duration	9.80 ± 2.34	9.84 ± 2.15	9.72 ± 2.64	0.849
E2 on HCG day	2810.39 ± 1278.89	2755.21 ± 1494.15	2027.26 ± 1002.33	< 0.05
No. of eggs obtained	11.29 ± 4.46	9.88 ± 4.23	6.67 ± 3.96	< 0.05
No.of MII oocytes	10.32 ± 4.27	8.98 ± 4.04	6.06 ± 3.78	< 0.05
No.of available embryos	4.12 ± 1.23	3.56 ± 1.25	2.54 ± 1.01	<0.001
No.of transferred embryos	1.69 ± 0.58	1.71 ± 0.48	1.53 ± 0.52	0.465
Clinical pregnancy rate	60.76(192/316)	52.92(326/616)	47.88(147/307)	0.0306

TABLE 2 Univariate and multivariate analyses of clinical factors.

Variables	Univariate analysis		Multivariate analysis	
	P	*OR (95%CI)*	*P*	OR (95%CI)
Age	0.027	0.772(0.644-0.942)	0.032	0.742(0.578-0.863)
E2 on the day of hCG injection	0.524	1.000(1.000-1.0000)	–	–
P on the day of hCG injection	0.267	0. 817(0.571-1.168)	–	–
No.of M_{II} oocytes	0.315	0.941(0.836-1.059)	–	–
No.of available embryos	0.034	1.287(1.057-1.363)	0.126	1.194(0.857-01.384)
No.of 2PN	0.604	1.070(0.828-1.383)	–	–
No.of transferred embryos	0.130	1.353(0.879-2.556)	–	–
PMOI on hCG injection day	0.010	0.002(0.000-0.227)	0.043	0.005(0.000-0.780)

naturally conclude that PMOI levels can be used as an independent predictor of clinical pregnancy rate. Detailed results are shown in Table 3 and Figure 2.

Discussion

In this study, we demonstrated that in fresh IVF/ICSI cycles, PMOI levels were significantly associated with the risk of pregnancy outcome on the day of hCG injection, independent of other risk factors, including age, E2 on the day of hCG injection, P on the day of hCG injection, number of M_{II} oocytes, number of available embryos, 2PN count, and number of transferred embryos. In addition, PMOI showed a more significant AUC than age in predicting pregnancy outcome on the day of hCG injection. More importantly, our findings suggest that PMOI has a more significant predictive value than the model including PMOI and age.

Progesterone (P) is known to perform an important physiological function during the menstrual cycle and pregnancy (24). The use of late follicular P levels to predict pregnancy outcome in assisted reproductive therapy (ART) remains controversial. A recent study showed that elevated P levels on the day of human chorionic gonadotropin (HCG) administration had a negative impact on live birth rate and were associated with high miscarriage rates. However, the adverse effects of high P levels during pregnancy were not associated with endometrial receptivity (25). A different study reported that low P levels (≤ 0.5 ng/ml) on the day of hCG administration were associated with a low live birth rate (LBR) (26). Several studies have reported that prematurely elevated P levels on the day of hCG administration were negatively associated with IVF outcomes in cycles with gonadotropin-releasing hormone (GnRH). Sangisapu et al. showed no predictive association with either IVF outcomes or progesterone levels in their study, a single-center retrospective cohort study conducted on 306 fresh IVF cycles of normozoospermic semen samples and COS by long protocol with GnRH agonists followed by hCG trigger from 2016 to 2018 (27). In addition, different P thresholds were used in different studies. Deng et al. demonstrated a negative correlation and saturation effect between serum progesterone and first pregnancy outcome. When progesterone was <90.62 nmol/L, a 1 nmol/L increase in serum progesterone was associated with 3% reduction in the risk of miscarriage (OR: 0.97, 95% CI: 0.95-0.98) (28). To address these deficiencies, we conducted a retrospective cohort study of PMOI levels to predict pregnancy outcomes in patients.

In this study, the lowest clinical pregnancy rate (60.76%) was found in group C among groups A, B, and C. This may be partly due to the identified increase in serum progesterone levels. Our findings are supported by a number of studies that report a significant decrease in pregnancy rates due to increased progesterone levels (29–31). Sahar et al. demonstrated that progesterone levels > 1 ng/mL on the day of hCG administration decreased HOXA10 expression so that endometrial reception during the implantation period was already impaired (20). Various factors of clinical pregnancy on the day of hCG were examined by both univariate and multivariate analyses.

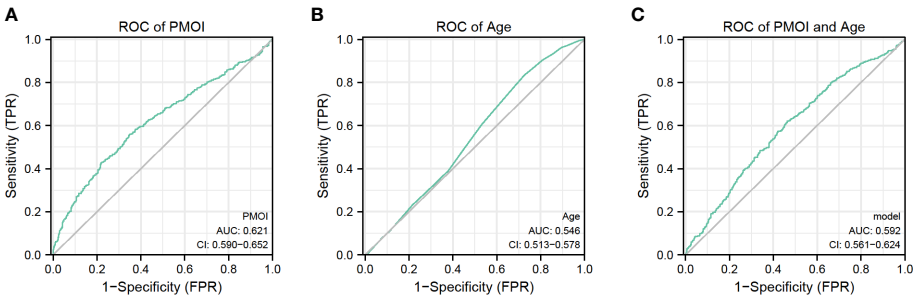

FIGURE 2
Predictive value of PMOI and age for pregnancy outcomes.

TABLE 3 Accuracy of different variables and model in IVF/ICSI to predict clinical pregnancy rate.

Parameters	AUC	95% CI	P valve	Best threshold	Specificity(%)	Sensitivity(%)
PMOI	62.1	0.590-0.652	<0.05	0.063	78.2	42.7
Age	0.546	0.513-0.578	<0.05	34.5	27.4	83.5
Model	0.592	0.561-0.624	<0.05	0.160	53.7	62.1

AUC, area under the curve; CI, confidence interval; NPV, negative predictive valve; PPV, positive predictive valve.
Model included PMOI and Age.

The results showed that PMOI (OR: 0.005, 95%CI: 0.000-0.780, P=0.043) was an independent risk factor for pregnancy outcome. In our study, the risk of obtaining the number of eggs, the number of M_{II} oocytes, and the number of available embryos decreased as PMOI increased. Our study suggests that PMOI may have a negative impact on pregnancy outcome. However, this study was a single-centre study with a small overall sample size, so whether PMOI on hCG day is associated with poor pregnancy outcomes remains to be further confirmed in a large-scale clinical studies. Grin et al. noted that higher serum progesterone levels are associated with follicular counts and that higher P affects endometrial receptivity, as well as oocyte and embryo quality (32). Their study showed POI (ration of number of oocytes aspirated) was inversely related to CP (clinical pregnancy) with an adjusted OR of 0.063 (95% CI: 0.016-0.249, p <.001). POI is a simple predictor of IVF-ET cycle outcome, and it can advocate a limit beyond which embryo transfer should be reconsidered. Simon et al. showed that PMOI recorded in the same patient in a single attempt was similar and partially correlated with basal FSH, anti-Müllerian hormone, antral follicle count, and OSI (33). In the current study, univariate and multivariate regression analyses showed that age and PMOI on the day of hCG injection were independent prognostic factors affecting the outcome of IVF/ICSI-ET pregnancies. Also, in the current study, the results of the ROC curve showed that the threshold value of PMOI on the day of hCG injection to predict pregnancy outcome was 0.063. The sensitivity was 42.7%, and the specificity was 78.2%. The AUC obtained was 62.1 (P<0.05), which shows that PMOI on the day of hCG has some value in predicting pregnancy outcome.

The PMOI seems to be elevated mainly in patients with low ovarian reserves and low ovarian response as evaluated by ovarian sensitivity index (OSI). Indeed, PMOI seemed to be reproducible from one attempt to another in the same patient and is related to low AMH and AFC levels. As a matter of fact, in poor responders, the higher administrated FSH doses result in a higher FSH dose to recruited follicle ratio, probably leading to a higher follicular fluid progesterone concentration. Therefore, the freeze-all strategy and reducing the FSH doses are probably the right way to avoid or limit oocyte damage. Due to the respective parts of the effect on the endometrium and on embryo developmental ability are difficult to discriminate, the use of PMOI could help to identify an oocyte effect rather than an endometrial one. In brief, the PMOI seemed to be more predictive of IVF outcomes than blood progesterone levels.

The underlying mechanism of the premature rise of progesterone (P) on hCG day is not fully understood and may be related to the following factors. First, granulosa cells have abundant receptors on their surface, such as follicle-stimulating hormone (FSH), luteinizing hormone (LH), and estrogen receptors (34). High-dose FSH increase the sensitivity of FSH-incuded LH receptors in granulosa cells, leading to increased LH levels (26). Secondly, ovarian stimulation leads to maturation of multiple follicles and therefore supraphysiological concentrations of progesterone in the early luteal phase (35). Third, premature rise in progesterone (P) is associated with a low ovarian reserve and poor ovarian response (36). Fourth, patients with poor ovarian response are more likely to have an elevated estradiol/testosterone ratio (32). Patients who obtain fewer than five eggs may see more elevated POI (36). This was confirmed by the present study. We found that the highest FSH levels were in group A (PMOI ≤ 0.06 ug/L). While the results for groups A to C were 7.49 ± 2.16, 8.15 ± 2.21, and 8.22 ± 1.99, respectively. In addition, the lowest AMH and AFC were found in group A (PMOI ≤ 0.06 ug/L). These differences showed statistical significance. This present study suggests that patients with low ovarian response are more likely to have elevated PMOI on the day of hCG injection.

The strength of the present study is based on a specific population living in Southwest China, suitable for economically undeveloped areas, but with an increasing trend of infertility patients. In addition, these measurements were performed in the same laboratory using the same equipment. This greatly reduces the variability caused by laboratory testing. Our study, however, has some limitations. On the one hand, this was a retrospective study. On the other hand, the current PMOI predictive values in this study showed an average performance in predicting pregnancy outcomes, with a specification of 78.2% and a sensitivity of 42.7%. Therefore, there is a need to improve the ability to predict pregnancy outcomes in fresh IVF/ICSI cycles beyond the current capabilities.

In conclusion, the present study shows that PMOI is an independent and meaningful predictor of pregnancy outcome on the day of hCG injection in fresh IVF/ICSI cycles and that combining age and PMOI levels does not improve the prediction effect.

Data availability statement

The original contributions presented in the study are included in the article/supplementary material. Further inquiries can be directed to the corresponding authors.

Ethics statement

Ethics approval for this study was obtained from The Affiliated Hospital Of Southwest Medical University Ethics Committee (No.KY2022312). Informed consent from study participants was not required.

Author contributions

LL and CS: Conceptualization. XS and FY: Data curation, Writing-Original draft preparation. MM, CY, MY, and YL: revising the manuscript critically for important intellectual content. All authors contributed to the article and approved the submitted version.

Acknowledgments

We thank the survey participants and all members involved in this study for their painstaking efforts in conducting the data collection.

Conflict of interest

The authors declare that the research was conducted in the absence of any commercial or financial relationships that could be construed as a potential conflict of interest.

Publisher's note

All claims expressed in this article are solely those of the authors and do not necessarily represent those of their affiliated organizations, or those of the publisher, the editors and the reviewers. Any product that may be evaluated in this article, or claim that may be made by its manufacturer, is not guaranteed or endorsed by the publisher.

References

1. Zaake D, Kayiira A, Namagembe I. Perceptions, expectations and challenges among men during *in vitro* fertilization treatment in a low resource setting: a qualitative study. *Fertil Res Pract* (2019) 5:6. doi: 10.1186/s40738-019-0058-8

2. Zhang Z, Zhang Y, Liu C, Zhao M, Yang Y, Wu H, et al. Serum metabolomic profiling identifies characterization of non-obstructive azoospermic men. *Int J Mol Sci* (2017) 18(2):238. doi: 10.3390/ijms18020238

3. Zhang M, Liu C, Chen B, Lv M, Zou H, Liu Y, et al. Identification of novel biallelic TLE6 variants in female infertility with preimplantation embryonic lethality. *Front Genet* (2021) 12:666136. doi: 10.3389/fgene.2021.666136

4. Spencer TE, Johnson GA, Burghardt RC, Bazer FW. Progesterone and placental hormone actions on the uterus: insights from domestic animals. *Biol Reprod* (2004) 71 (1):2–10. doi: 10.1095/biolreprod.103.024133

5. Gougeon A. Dynamics of human follicular growth: morphologic, dynamic, and functional aspects. *Ovary* (2004) 2:25–43. doi: 10.1016/B978-012444562-8/50003-3

6. Hoff JD, Quigley ME, Yen SS. Hormonal dynamics at midcycle: a reevaluation. *J Clin Endocrinol Metab* (1983) 57(4):792–6. doi: 10.1210/jcem-57-4-792

7. Payne AH, Hales DB. Overview of steroidogenic enzymes in the pathway from cholesterol to active steroid hormones. *Endocr Rev* (2004) 25(6):947–70. doi: 10.1210/er.2003-0030

8. Seger R, Hanoch T, Rosenberg R, Dantes A, Merz WE, Strauss JF3rd, et al. The ERK signaling cascade inhibits gonadotropin-stimulated steroidogenesis. *J Biol Chem* (2001) 276(17):13957–64. doi: 10.1074/jbc.M006852200

9. Leão Rde B, Esteves SC. Gonadotropin therapy in assisted reproduction: an evolutionary perspective from biologics to biotech. *Clinics (Sao Paulo)* (2014) 69(4):279–93. doi: 10.6061/clinics/2014(04)10

10. Czyzyk A, Podfigurna A, Genazzani AR, Meczekalski B. The role of progesterone therapy in early pregnancy: from physiological role to therapeutic utility. *Gynecol Endocrinol* (2017) 33(6):421–4. doi: 10.1080/09513590.2017.1291615

11. Lessey BA. Two pathways of progesterone action in the human endometrium: implications for implantation and contraception. *Steroids* (2003) 68(10-13):809–15. doi: 10.1016/j.steroids.2003.09.004

12. Blakemore JK, Kofinas JD, McCulloh DH, Grifo J. Serum progesterone trend after day of transfer predicts live birth in fresh IVF cycles. *J Assist Reprod Genet* (2017) 34 (3):339–43. doi: 10.1007/s10815-016-0859-1

13. Nayak S, Ochalski ME, Fu B, Wakim KM, Chu TJ, Dong X, et al. Progesterone level at oocyte retrieval predicts *in vitro* fertilization success in a short-antagonist protocol: a prospective cohort study. *Fertil Steril* (2014) 101(3):676–82. doi: 10.1016/j.fertnstert.2013.11.022

14. Venetis CA, Kolibianakis EM, Bosdou JK, Tarlatzis BC. Progesterone elevation and probability of pregnancy after IVF: a systematic review and meta-analysis of over 60 000 cycles. *Hum Reprod Update* (2013) 19(5):433–57. doi: 10.1093/humupd/dmt014

15. Venetis CA, Kolibianakis EM, Papanikolaou E, Bontis J, Devroey P, Tarlatzis BC. Is progesterone elevation on the day of human chorionic gonadotrophin administration associated with the probability of pregnancy in *in vitro* fertilization? a systematic review and meta-analysis. *Hum Reprod Update* (2007) 13(4):343–55. doi: 10.1093/humupd/dmm007

16. Martinez F, Rodriguez I, Devesa M, Buxaderas R, Gómez MJ, Coroleu B. Should progesterone on the human chorionic gonadotropin day still be measured? *Fertil Steril* (2016) 105(1):86–92. doi: 10.1016/j.fertnstert.2015.09.008

17. Wu Z, Dong Y, Ma Y, Li Y, Li L, Lin N, et al. Progesterone elevation on the day of hCG trigger has detrimental effect on live birth rate in low and intermediate ovarian responders, but not in high responders. *Sci Rep* (2019) 9(1):5127. doi: 10.1038/s41598-019-41499-1

18. Roque M, Lattes K, Serra S, Solà I, Geber S, Carreras R, et al. Fresh embryo transfer versus frozen embryo transfer in *in vitro* fertilization cycles: A systematic review and meta-analysis. *Fertil Steril.* (2013) 99(1):156–62. doi: 10.1016/j.fertnstert.2012.09.003

19. Lu X, Chen Q, Fu Y, Ai A, Lyu Q, Kuang YP. Elevated progesterone on the trigger day does not impair the outcome of human menotrophins gonadotrophin and medroxyprogesterone acetate treatment cycles. *Sci Rep* (2016) 6:31112. doi: 10.1038/srep31112

20. Sahar N, Mujihartini N, Pudjianto DA, Pradhita AD, Thuffi R, Kusmardi K. Increased progesterone on the day of administration of hCG in controlled ovarian hyperstimulation affects the expression of HOXA10 in primates' endometrial receptivity. *Biomedicines* (2019) 7(4):83. doi: 10.3390/biomedicines7040083

21. Shufaro Y, Sapir O, Oron G, Ben Haroush A, Garor R, Pinkas H, et al. Progesterone-to-follicle index is better correlated with *in vitro* fertilization cycle outcome than blood progesterone level. *Fertil Steril* (2015) 103(3):669–74.e3. doi: 10.1016/j.fertnstert.2014.11.026

22. Roque M, Valle M, Sampaio M, Geber S, Checa MA. Ratio of progesterone-to-number of follicles as a prognostic tool for *in vitro* fertilization cycles. *J Assist Reprod Genet* (2015) 32(6):951–7. doi: 10.1007/s10815-015-0487-1

23. Singh N, Malik N, Malhotra N, Vanamail P, Gupta M. Impact of progesterone (on hCG day)/oocyte ratio on pregnancy outcome in long agonist non donor fresh IVF/ICSI cycles. *Taiwan J Obstet Gynecol.* (2016) 55(4):503–6. doi: 10.1016/j.tjog.2015.09.005

24. Dozortsev D, Pellicer A, Diamond MP. Progesterone is a physiological trigger of ovulatory gonadotropins. *Fertil Steril* (2020) 113(5):923–4. doi: 10.1016/j.fertnstert.2019.12.024

25. Lepage J, Keromnes G, Epelboin S, Luton D, Yazbeck C. Premature progesterone rise on day of hCG negatively correlated with live birth rate in IVF cycles: An analysis of 1022 cycles. *J Gynecol Obstet Hum Reprod* (2019) 48(1):51–4. doi: 10.1016/j.jogoh.2018.05.005

26. Santos-Ribeiro S, Polyzos NP, Haentjens P, Smitz J, Camus M, Tournaye H, et al. Live birth rates after IVF are reduced by both low and high progesterone levels on the day of human chorionic gonadotrophin administration. *Hum Reprod* (2014) 29(8):1698–705. doi: 10.1093/humrep/deu151

27. Sangisapu S, Karunakaran S. Comparative study of serum progesterone levels at the time of human chorionic gonadotropin trigger and ovum PickUp in predicting outcome in fresh *in vitro* fertilization cycles. *J Hum Reprod Sci* (2019) 12(3):234–9. doi: 10.4103/jhrs.JHRS_156_18

28. Deng Y, Chen C, Chen S, Mai G, Liao X, Tian H, et al. Baseline levels of serum progesterone and the first trimester pregnancy outcome in women with threatened abortion: A retrospective cohort study. *BioMed Res Int* (2020) 2020:8780253. doi: 10.1155/2020/8780253

29. Elnashar AM. Progesterone rise on the day of HCG administration (premature luteinization) in IVF: an overdue update. *J Assist Reprod Genet* (2010) 27(4):149–55. doi: 10.1007/s10815-010-9393-8

30. Kyrou D, Al-Azemi M, Papanikolaou EG, Donoso P, Tziomalos K, Devroey P, et al. The relationship of premature progesterone rise with serum estradiol levels and number of follicles in GnRH antagonist/recombinant FSH-stimulated cycles. *Eur J Obstet Gynecol Reprod Biol* (2012) 162(2):165–8. doi: 10.1016/j.ejogrb.2012.02.025

31. Papanikolaou EG, Pados G, Grimbizis G, Bili E, Kyriazi L, Polyzos NP, et al. GnRH-agonist versus GnRH-antagonist IVF cycles: is the reproductive outcome affected by the incidence of progesterone elevation on the day of HCG triggering? a randomized prospective study. *Hum Reprod* (2012) 27(6):1822–8. doi: 10.1093/humrep/des066

32. Grin L, Mizrachi Y, Cohen O, Lazer T, Liberty G, Meltcer S, et al. Does progesterone to oocyte index have a predictive value for IVF outcome? a retrospective cohort and review of the literature. *Gynecol Endocrinol* (2018) 34(8):638–43. doi: 10.1080/09513590.2018.1431772

33. Simon C, Branet L, Moreau J, Gatimel N, Cohade C, Lesourd F, et al. Association between progesterone to number of mature oocytes index and live birth in GnRH antagonist protocols. *Reprod BioMed Online*. (2019) 38(6):901–7. doi: 10.1016/j.rbmo.2019.01.009

34. Xie S, Zhang Q, Zhao J, Hao J, Fu J, Li Y. MiR-423-5p may regulate ovarian response to ovulation induction *via* CSF1. *Reprod Biol Endocrinol* (2020) 18(1):26. doi: 10.1186/s12958-020-00585-0

35. Xu B, Li Z, Zhang H, Jin L, Li Y, Ai J, et al. Serum progesterone level effects on the outcome of *in vitro* fertilization in patients with different ovarian response: an analysis of more than 10,000 cycles. *Fertil Steril.* (2012) 97(6):1321–7.e1-4. doi: 10.1016/j.fertnstert.2012.03.014

36. Younis JS, Matilsky M, Radin O, Ben-Ami M. Increased progesterone/estradiol ratio in the late follicular phase could be related to low ovarian reserve in *in vitro* fertilization-embryo transfer cycles with a long gonadotropin-releasing hormone agonist. *Fertil Steril.* (2001) 76(2):294–9. doi: 10.1016/s0015-0282(01)01918-5

frontiers | Frontiers in Endocrinology

TYPE Original Research
PUBLISHED 15 March 2023
DOI 10.3389/fendo.2023.1087429

OPEN ACCESS

EDITED BY
Antonio Simone Laganà,
University of Palermo, Italy

REVIEWED BY
Adriana Vita Streva,
University of Palermo, Italy
Jiaqiang Xiong,
Zhongnan Hospital, Wuhan University, China

*CORRESPONDENCE
Yan Li
liyan@tjh.tjmu.edu.cn
Shixuan Wang
shixuanwang@tjh.tjmu.edu.cn

†These authors have contributed equally to this work and share first authorship

SPECIALTY SECTION
This article was submitted to Endocrinology of Aging, a section of the journal Frontiers in Endocrinology

RECEIVED 02 November 2022
ACCEPTED 24 February 2023
PUBLISHED 15 March 2023

CITATION
Ding T, Ren W, Wang T, Han Y, Ma W, Wang M, Fu F, Li Y and Wang S (2023) Assessment and quantification of ovarian reserve on the basis of machine learning models.
Front. Endocrinol. 14:1087429.
doi: 10.3389/fendo.2023.1087429

Assessment and quantification of ovarian reserve on the basis of machine learning models

Ting Ding†, Wu Ren†, Tian Wang†, Yun Han, Wenqing Ma, Man Wang, Fangfang Fu, Yan Li* and Shixuan Wang*

Department of Obstetrics and Gynecology, Tongji Hospital, Tongji Medical College, Huazhong University of Science and Technology, Wuhan, Hubei, China

Background: Early detection of ovarian aging is of huge importance, although no ideal marker or acknowledged evaluation system exists. The purpose of this study was to develop a better prediction model to assess and quantify ovarian reserve using machine learning methods.

Methods: This is a multicenter, nationwide population-based study including a total of 1,020 healthy women. For these healthy women, their ovarian reserve was quantified in the form of ovarian age, which was assumed equal to their chronological age, and least absolute shrinkage and selection operator (LASSO) regression was used to select features to construct models. Seven machine learning methods, namely artificial neural network (ANN), support vector machine (SVM), generalized linear model (GLM), K-nearest neighbors regression (KNN), gradient boosting decision tree (GBDT), extreme gradient boosting (XGBoost), and light gradient boosting machine (LightGBM) were applied to construct prediction models separately. Pearson's correlation coefficient (PCC), mean absolute error (MAE), and mean squared error (MSE) were used to compare the efficiency and stability of these models.

Results: Anti-Müllerian hormone (AMH) and antral follicle count (AFC) were detected to have the highest absolute PCC values of 0.45 and 0.43 with age and held similar age distribution curves. The LightGBM model was thought to be the most suitable model for ovarian age after ranking analysis, combining PCC, MAE, and MSE values. The LightGBM model obtained PCC values of 0.82, 0.56, and 0.70 for the training set, the test set, and the entire dataset, respectively. The LightGBM method still held the lowest MAE and cross-validated MSE values. Further, in two different age groups (20–35 and >35 years), the LightGBM model also obtained the lowest MAE value of 2.88 for women between the ages of 20 and 35 years and the second lowest MAE value of 5.12 for women over the age of 35 years.

Conclusion: Machine learning methods combining multi-features were reliable in assessing and quantifying ovarian reserve, and the LightGBM method turned

out to be the approach with the best result, especially in the child-bearing age group of 20 to 35 years.

KEYWORDS

ovarian aging, ovarian reserve, machine learning, quantification, light gradient boosting machine

Introduction

Ovarian reserve represents the number of oocytes remaining in the ovary; both the number and quality of oocytes impact reproductive potential and aging (1, 2). Ovarian aging is due to a variety of causative factors, such as chromosomal, genetic, mitochondrial, and cytoplasmic changes in oocyte quantity and quality (3–8). Evaluation of present ovarian reserve and ovarian aging degree could offer helpful advice for women regarding evaluating their reproductive potential and preventing early menopause or related disorders because few treatments are effective in preventing ovarian aging.

So far, the most classical and commonly used evaluation system for ovarian aging is the Stages of Reproductive Aging Workshop criteria (STRAW+10), which is widely considered the gold standard for characterizing reproductive aging through menopause. STRAW classified the stages of a woman's adult life into three general categories: reproductive, menopausal transition, and postmenopause. However, the STRAW staging approach lacks specific diagnostic criteria for evaluating ovarian reserve, and the assessment system is too generalized to reliably assess each individual's ovarian aging degree. In addition, the current evaluation of ovarian reserve can draw on clinical indicators, such as biochemical tests and ultrasound imaging of the ovaries (2). Biochemical tests include follicle-stimulating hormone (FSH), estradiol (E2), or inhibin B in early-follicular-phase, cycle-day-independent anti-Müllerian hormone (AMH), and provocative tests, while ultrasonographic measures include antral follicle count (AFC) and ovarian volume. Among these indicators, AMH is regarded as the most sensitive and reliable marker of ovarian reserve because it is independent of the menstrual cycle and tends to decline before FSH rises (9). However, several studies have reported the limited use of these markers. In reproductive-aged women without a history of infertility, markers of lower ovarian reserve were found to be unrelated to reduced fertility, and in women with a history of one to two previous miscarriages, AMH levels were found to be unrelated to clinical pregnancy loss (10, 11). These findings highlight the limitations of these single markers.

Machine learning holds considerable advantages for analyzing and integrating large amounts of medical data (12, 13). Machine learning can fully account for the interactions between characteristics and incorporate new data to update models, in contrast to traditional statistical analysis approaches, which rely on a preset equation (14). In the realm of assisted reproduction, machine learning methods have previously been applied to evaluate and predict pregnancy rates (15–17). Researchers also have attempted to construct regression models to assess ovarian reserve by integrating single biochemical and ultrasound markers (18–21). However, more machine learning methods should be utilized to determine a suitable evaluation model. The main aim of this study is to develop a more accurate machine learning model to estimate and quantify ovarian reserve in terms of predicting reproductive possibility and time to menopause.

Method

Population selection

This is a multicenter, nationwide population-based study. The participants were recruited from seven centers in six different cities of China, including the city of Shenyang (northern China), Foshan (southern China), Chengdu (western China), Zhengzhou, Yichang, and Wuhan (central China). From October 2011 to December 2014, a total of 2,055 women, aged 20 to 55, were recruited through advertisements. Of the initial recruits, 1,020 women met the following strict inclusion criteria for the healthy population used for modeling: 1) regular menstrual cycles between 21 and 35 days for women <40 years old having regular menstrual cycles and for women >40 not required to have regular menstrual cycles, considering that they may be in normal perimenopause or menopause; 2) no hormone use in the past 6 months; 3) no history of radiotherapy or chemotherapy; 4) no history of hysterectomy, oophorectomy, or any other type of ovarian surgery; 5) no ovarian cysts or ovarian tumors, as confirmed by ultrasound; and 6) no known chronic, systemic, metabolic, or endocrine diseases such as hyperandrogenism or hyperprolactinemia.

All volunteers were interviewed one-on-one using prepared questionnaires that included questions about their demographic, geographic, and reproductive characteristics. The participants were physically examined and received free hormone and ultrasound testing. The study was approved by the Tongji Ethics Committee, and written informed consent was obtained from each woman for the anonymous use of clinical data for statistical evaluation and research purposes.

Blood sample collection

All blood samples were taken from the participants' antecubital vein between 7:00 AM and 11:00 AM, after a 12 h overnight fast, on days 2 to 5 of a spontaneous menstrual cycle or any day if

amenorrhea had lasted more than 3 months in those aged over 40 years. The samples were then centrifuged using standard conditions within 2 h of venipuncture. After centrifugation, serums were obtained, aliquoted, transported to the central laboratory, and stored at −80°C for no more than 2 weeks until the assays were performed. To avoid the potential bias produced by differences between laboratory test results, we chose the gynecologic endocrine laboratory of Tongji Hospital as the central laboratory; all serums were transported to the central laboratory using dry ice within 48 h of collection, and all serum hormones were tested in the central laboratory.

Hormone detection

Serum concentrations of AMH at the time of recruitment were measured using the AMH Gen II ELISA kit (Beckman Coulter, Inc., Brea, CA, USA) and Ultra-Sensitive AMH ELISA assays (AL-105, Ansh Labs, Webster, TX, USA). Two commercial assays and the mean value were decided as the final AMH level, and all serum AMH measurements were performed in the same laboratory using the above kits. The controls were used at two concentrations to monitor the accuracy of the assay. The intra- and interassay coefficients of variation (CVs) were 3.6% and 4.5%, respectively. The lowest amount of AMH that could be detected with a 95% probability in a sample was 0.08 ng/ml for Gen II ELISA and 0.04 ng/ml for Ansh Labs; therefore, we replaced all values recorded as <min (undetectable) with a value of 0.08 or 0.04 ng/ml for the purpose of this analysis. Serum FSH, luteinizing hormone (LH), E2, testosterone (T), prolactin (PRL), and progesterone (PRG) levels were measured using a chemiluminescence-based immunometric assay on an ADVIA Centaur immunoassay system (Siemens Healthcare Diagnostics Inc., Tarrytown, NY, USA). All the serum hormone levels were measured in the same laboratory using the same kit. The intra- and interassay coefficients of variation were all <15%. Due to missing values, the three hormones—T, PRL, and PRG—were not included in the analysis.

Ultrasound examination

A transvaginal ultrasound scan of the ovaries was performed to determine the AFC. This ultrasound examination was performed at the seven centers. All participating research institutes were modernized large comprehensive hospitals and received our regular supervision and verification. The unified standard for this examination was formulated in the beginning, and all ultrasound doctors were strictly trained to test AFCs according to the same standard. In this study, the AFC was defined as the total number of visible round or oval structures with diameters of 2 to 10 mm in both ovaries. All ultrasound examinations were performed on days 2 to 5 of a spontaneous menstrual cycle or in the follicular phase for non-menstruating women. None of the eligible participants had follicles larger than 10 mm. No significant differences were found between each center. The intra-analysis coefficient of variation for the follicle diameter measurements was <5%, and the lower limit of detection was 0.1 mm.

Establishment and assessment of models

In this study, ovarian reserve was quantified in the form of ovarian age for healthy women, and ovarian age was regarded as equal to their chronological age. The least absolute shrinkage and selection operator (LASSO) regression was used for data regularization and feature selection (22). With the use of seven features (AMH, body mass index (BMI), Inhibin B, FSH, E2, LH, and AFC), quantifying work was performed. As for the construction of prediction models, seven different machine learning algorithms were used, namely artificial neural network (ANN), support vector machine (SVM), generalized linear model (GLM), K-nearest neighbors regression (KNN), gradient boosting decision tree (GBDT), extreme gradient boosting (XGBoost), and light gradient boosting machine (LightGBM), in which their chronological age was regarded as ovarian age in healthy women who were supposed to have a normal ovarian function (23–29). All the above-mentioned models were trained and tested on a partitioned 50/50 percentage split of the dataset by stratified random sampling. Parameter tuning was based on the grid search method and 10-fold cross-validation in training the dataset (30). The parameters of the machine learning models are listed in Table S1. For model assessment, Pearson's correlation coefficient (PCC) and mean absolute error (MAE) values were applied to indicate how well a model explains the variation in the dependent variables. The mean squared error (MSE) value was calculated to measure the stability of the model. All machine learning techniques were programmed in R language (version 3.6.3) using packages including neuralnet, e1071, kknn, gbm, xgboost, and lightgbm.

Results

From October 2011 to December 2014, a total of 2,055 women, aged from 18 to 55, were recruited through advertisements. According to exclusion and inclusion criteria, a total of 1,020 women from seven centers were enrolled and analyzed (Figure 1). Table 1 summarizes the statistics of included women for age, AMH value, Inhibin B, BMI value, FSH, LH, E2, and AFC value. Figure 2A shows PCC between age and AMH (−0.45), Inhibin B (−0.08), BMI (0.28), FSH (0.24), LH (−0.07), E2 (0.04), and AFC (−0.43), from which AMH and AFC had the highest absolute value. In Figures 2B, C, the distribution curves are depicted for AMH and AFC within specific ages, which are similar to each other.

Holding the assumption that ovarian age was equal to chronological age in healthy women, we performed LASSO regression analysis on the total data to select those features suitable for constructing the models (Figure S1). Finally, these seven features were all left with the lowest CP value for the follow-up study (Table S2). We randomly chose half of the datasets as training data to make the prediction and half as test data, and we then checked the results on different datasets.

10.3389/fendo.2023.1087429

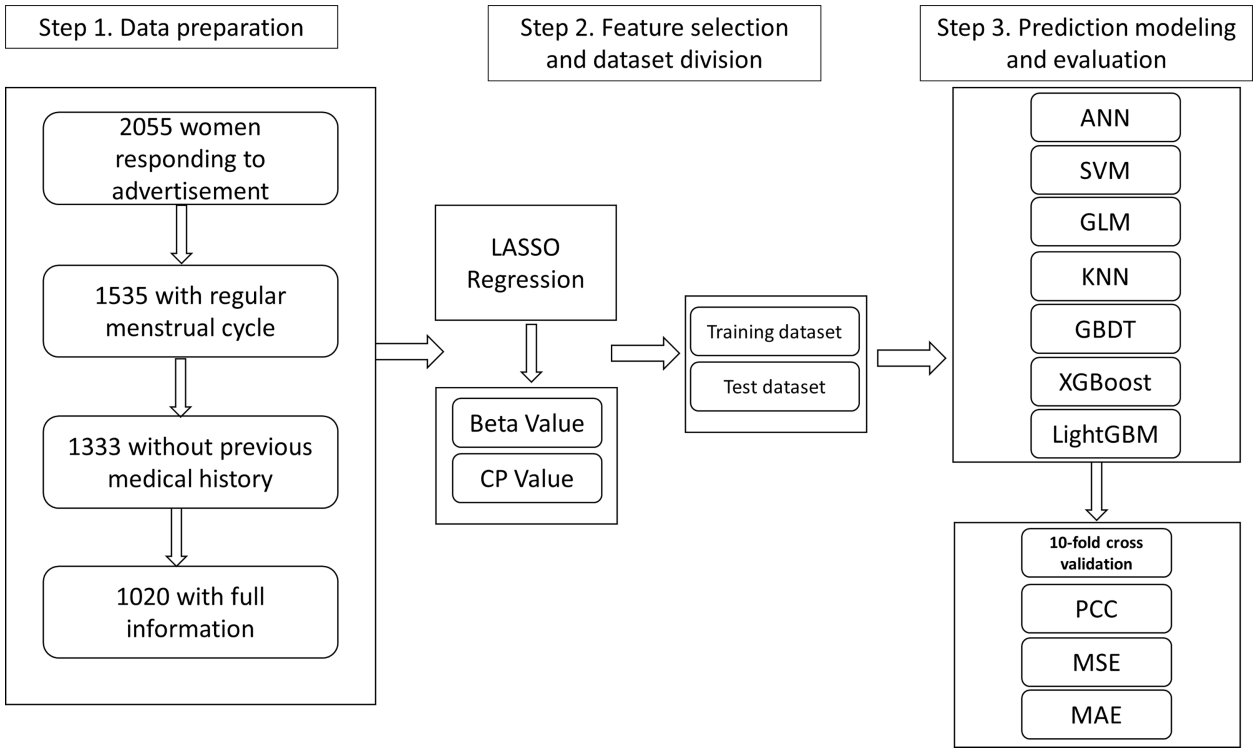

FIGURE 1
The flowchart of the study design.

The results of the prediction analyses were compared in terms of PCC and MAE values for the seven machine learning models (ANN, SVM, GLM, KNN, GBDT, XGBoost, and LightGBM) (Table 2). The table shows the PCC values for the training dataset, the test dataset, and the entire dataset, as well as the MAE values for the entire dataset. Focusing on the PCC values, it can be observed that the XGBoost, LightGBM, and ANN method had better performance. While PCC just describes the correlation trend, the MAE value represents the detailed difference, which reflects the prediction bias. The LightGBM model had the lowest MAE value for all the data of 3.41 years. As there were five datasets with more than 90 women, the seven models were also tested in the datasets of Chengdu, Foshan, Tongji, Shenyang, and Zhengzhou. The XGBoost and LightGBM models also obtained the highest PCC value in all center-based datasets. While the XGBoost model had the highest PCC value on the Shenyang dataset, at 0.90, the GLM model

TABLE 1 Description of the features and centers from which the data were obtained.

Center	Number	Age (year)	AMH (ng/ml)	Inhibin B (pg/ml)	BMI	FSH (mIU/ml)	E2 (pmol/L)	LH (mIU/ml)	AFC
Chengdu	191	31.69 ± 5.20	3.79 ± 2.64	93.02 ± 31.95	21.52 ± 2.89	7.00 ± 1.87	53.07 ± 33.37	3.77 ± 1.92	10.68 ± 4.64
Foshan	246	31.40 ± 4.68	5.32 ± 3.34	95.56 ± 39.68	20.65 ± 2.72	8.00 ± 2.02	40.81 ± 20.19	4.81 ± 2.27	12.60 ± 2.62
SFY	13	33.19 ± 6.94	3.76 ± 4.00	83.16 ± 38.77	21.16 ± 4.06	8.42 ± 3.34	40.54 ± 20.91	4.33 ± 1.07	9.77 ± 5.33
Tongji	302	30.45 ± 5.54	4.89 ± 3.11	80.25 ± 29.55	21.30 ± 2.83	6.94 ± 2.81	41.85 ± 18.94	4.55 ± 2.71	13.32 ± 5.19
Shenyang	95	28.29 ± 7.74	5.72 ± 3.79	80.79 ± 38.13	20.58 ± 2.05	5.99 ± 3.23	45.06 ± 25.80	4.43 ± 2.04	11.68 ± 5.52
Yichang	15	33.17 ± 5.95	4.68 ± 3.35	76.39 ± 20.59	22.08 ± 3.11	7.40 ± 1.13	63.98 ± 25.18	4.40 ± 3.36	15.87 ± 6.45
Zhengzhou	158	33.32 ± 6.92	3.34 ± 2.73	78.62 ± 35.33	22.90 ± 3.26	7.67 ± 4.73	51.62 ± 46.89	5.35 ± 4.30	9.34 ± 4.96

AMH, anti-Müllerian hormone; BMI, body mass index; FSH, follicle-stimulating hormone; E2, estradiol; LH, luteinizing hormone; AFC, antral follicle count.

10.3389/fendo.2023.1087429

had the lowest value on the Foshan and Tongji datasets, at just 0.43 (Figure 3A). As for the MAE value, the GBDT model had the highest MAE value on the Shenyang dataset, at 5.52 years, and the LightGBM model had the lowest value on the Foshan dataset, at just 3.05 years (Figure 3B).

Further, we cross-validated the models using the 10-fold method in which we randomly chose 90% of the entire dataset as the training dataset and 10% of the data as the test dataset. We iterated the method 100 times and obtained a mean MSE value. Figure 4 shows the MSE value broken down for the seven different methods. The lowest mean MSE was gained for the LightGBM technique, which showed the stability of this method.

In order to evaluate the performance of the models and select the most suitable one, we combined the three indexes of PCC value, MAE value, and MSE value. The models that ranked in the top three under each index were left. As shown in Table 3, the LightGBM model was the only one that ranked in the top three in all the lists. Though the PCC value of XGBoost was a little higher than that in the LightGBM model, the MSE and MAE values were much better in the LightGBM model.

As 35 years is the boundary age of childbearing, here, we divided the datasets into two different age groups (20–35 and >35 years) and analyzed the mean prediction errors by age groups. Figures 5A, B show absolute prediction errors in different age groups under the seven models. The LightGBM model obtained the lowest MAE value of 2.88 in the 20–35 age group than other methods. As there were 778 women under 35 years old (778/1,020, 76.30%), the LightGBM model could distinguish 774 (99.49%) women from them, and only 4 (0.51%) women were left. In addition, while the XGBoost model obtained the lowest MAE value of 4.20 years in the >35 years age group, the LightGBM model obtained the second lowest MAE value of 5.12.

TABLE 2 Summary of prediction analyses for the training dataset (correlation value), the test dataset (correlation value), and the entire dataset (correlation value and mean absolute prediction errors value).

	Train	Test	Total	MAE*
ANN	0.68	0.56	0.62	3.68
SVM	0.57	0.55	0.56	3.91
GLM	0.61	0.51	0.56	3.93
KNN	0.58	0.62	0.60	3.87
GBDT	0.58	0.63	0.61	3.90
XGBoost	0.80	0.62	0.71	3.64
LightGBM	0.82	0.56	0.70	3.41

ANN, artificial neural network; SVM, support vector machine; GLM, generalized linear model; KNN, K-nearest neighbors regression; GBDT, gradient boosting decision tree; XGBoost, extreme gradient boosting; LightGBM, light gradient boosting machine.
*Mean absolute prediction errors for the entire dataset.

Discussion

In this study, we collected data on clinical, biochemical, and basic ultrasonographic features in a population of healthy women with the aim of constructing a quantitative system for ovarian reserve. We compared different machine learning models with respect to their prediction accuracy and stability in order to find a better one to reflect the ovarian reserve status.

In recent years, mathematical methods have been used by researchers to evaluate ovarian reserves. Younis et al. developed a multivariable scoring system, combining biochemical tests, imaging measures, and BMI to assess ovarian reserve and pregnancy rate (21). Xu and colleagues developed two models to evaluate ovarian reserve, clinical pregnancy rate, and live-birth rate (18, 19). Although these models are simple and easy to use, they are only used for infertile patients who require fertility treatments and *in vitro* fertilization (IVF) cycles, which means that they do not adequately reflect the majority of women of childbearing age. Additionally, the output result from these models is categorized, which makes it impossible to quantify ovarian function. Even though they could evaluate the reproductive prognosis, it would be challenging for these models to forecast the timing of menopause. As a result, Roberta's study attempted to measure and describe ovarian function using the quantitative variable

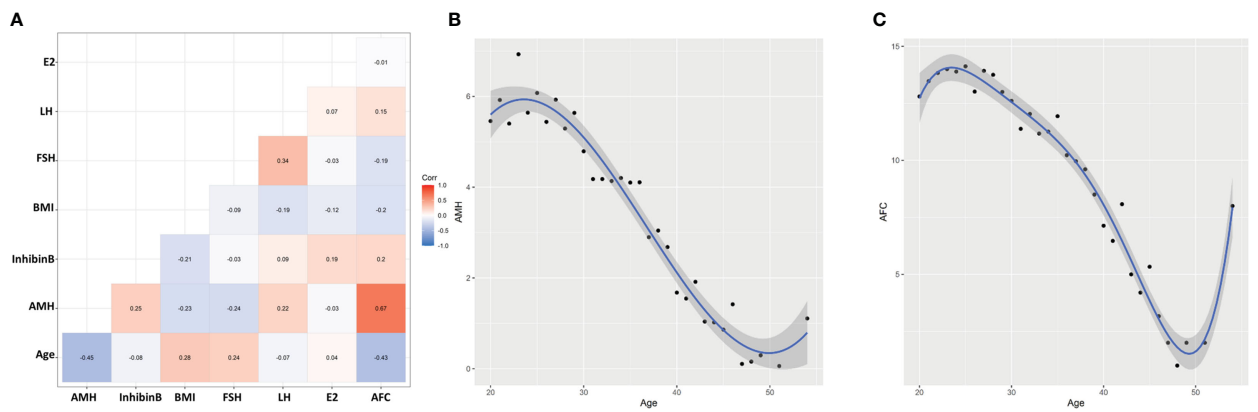

FIGURE 2
Correlation and distribution between features and age. **(A)** Pearson's correlation coefficients between age and different features. **(B)** Age-specific anti-Müllerian hormone (AMH) value distribution and fitting curve. **(C)** Age-specific antral follicle count (AFC) value distribution and fitting curve.

OvAge, a numeric variable that accurately reflects ovarian reserve in terms of both reproductive potential and time to menopause (20). They employed a single generalized linear model method since their study was the first to utilize a multi-factor model to assess and quantify ovarian age, and other characteristics like BMI that affect ovarian reserve should also be included in the model (31). Meanwhile, there were many ultrasonic measurement indicators in the model, for which special hardware was needed, and the subjective judgment of different ultrasound staff might result in an artificial mistake. In contrast to their study, we developed assessment models using a variety of machine learning methods and straightforward, objective indicators. Furthermore, seven machine learning models were constructed and analyzed to choose the most effective model for ovarian reserve quantification.

In our study, we first calculated the PCC value between different indicators and age. AFC value and AMH obtained the highest absolute PCC value, which is in accordance with the studies that said that AFC and AMH were the two most important single tests in evaluating ovarian reserve. The PCC value between AMH and AFC was as high as 0.67, indicating the effect of AMH on the stage of pre-antral and small antral follicles (32). We also revealed the AFC and AMH distributions, referring to age, and obtained fitting curves. With the prevailing age-specific reference values obtained for AMH levels based on samples from an American population in 2011, age-specific AMH reference values for Chinese women are needed (33). Our age-specific AMH distribution curve here is also similar to that of a Japanese study revealing an age-specific AMH reference for Japanese women to evaluate reproductive potential (34).

We used the assumption that ovarian age corresponds to chronological age in healthy women to investigate this novel variable of ovarian reserve. The key findings of this research are that clinical variables, blood biomarkers, and ultrasonographic characteristics may all be used to estimate ovarian reserve. After ranking analysis, including PCC, MAE, and MSE values, we determined the LightGBM model to be the best appropriate

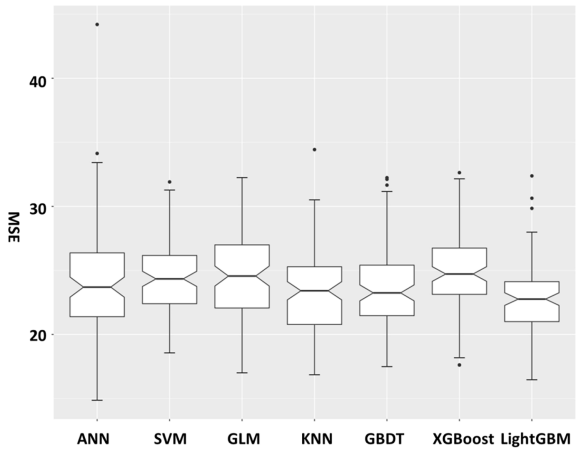

FIGURE 4
Mean squared error (MSE) after 10-fold cross-validation for the seven methods.

model of the seven prediction models we constructed. The LightGBM approach, which was developed to be dispersed and effective with the benefits of faster training speeds, more efficiency, and better accuracy, utilized histogram-based algorithms. In our study, the performance of the LightGBM model, which had the second-best PCC value of all the models, obtained PCC values of 0.82, 0.56, and 0.70 for the training set, the test set, and the entire dataset, respectively. MAE measures the exact differences between ovarian age and predicted ovarian age, and the LightGBM model obtained the lowest MAE value, indicating better accuracy. Moreover, the MSE value of the LightGBM model was the lowest, which showed better stability in this method. Other models, such as XGBoost and ANN, also exhibited good performance on prediction accuracy but did not perform as well in terms of stability. As a previous study used the GLM method to construct a predictive system for ovarian reserve evaluation, the results here showed that

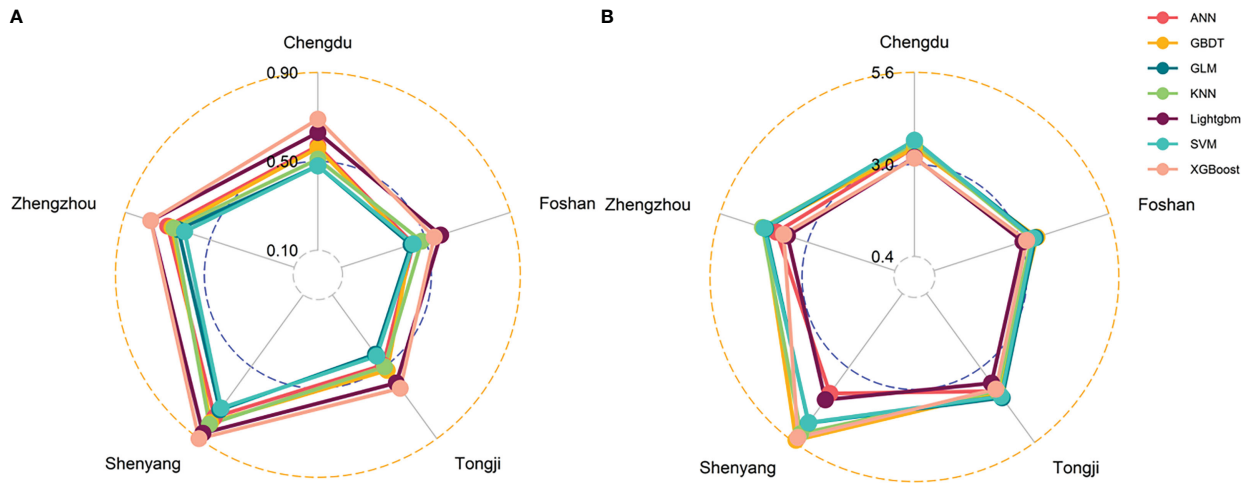

FIGURE 3
Radar plot showing correlation values **(A)** and mean absolute prediction errors (MAE) values **(B)** for the five datasets using the seven different prediction models.

TABLE 3 Models ranked top three under different evaluation indexes.

PCC	MAE	MSE
XGBoost	LightGBM	LightGBM
LightGBM	XGBoost	GBDT
ANN	ANN	KNN

PCC, Pearson's correlation coefficient; MAE, mean absolute error; MSE, mean squared error; XGBoost, extreme gradient boosting; LightGBM, light gradient boosting machine; GBDT, gradient boosting decision tree; ANN, artificial neural network.

the predictive power of this method was lower than that of other methods (20). Considering that a model combining markers would not be superior to a model with a single marker, we found that the PCC values of the seven models were all higher than those of single markers, such as AMH (−0.45) and AFC (−0.43), which indicated that machine learning methods may lessen the influence of correlated markers in combined ovarian reserve marker models (35, 36).

Further, we performed an age-stratified analysis, and we found that the LightGBM model was the most suitable model for women under the age of 35, with the lowest MAE value of 2.88 years. This model could distinguish the ovarian age for women under 35 years old with an accuracy of 99.49%. As we know, 35 years is the boundary for childbearing age, and the model has the potential to be used for evaluating reproductive function and guiding childbearing (37).

Our study has several strengths. First, we assessed and quantified ovarian reserve in terms of ovarian age in a way that could be easily implemented in the clinic. For example, as the recognized natural menopause age is around 51, it is easy to evaluate the distance to an individual's menopause (38). Further, as 35 years is the boundary for childbearing age, it is easy to predict ovarian age and compare it to this boundary, then design individual reproductive plans (37). Second, the data included in this study came from multi-centers, which covered several geographical regions of China; this made the study population more representative and improved the credibility of the results. Third, we compared the performances of seven models and selected the most effective one. Our result may be more reasonable than the former study, which used only one method.

This study has several limitations. First, our model regards ovarian age as chronological age in healthy women, which would need more strict inclusion criteria for the population. Second, due to incomplete information, limited features were used in this study. As ovarian aging is associated with additional features including lifestyle and genetic factors, these features should also be incorporated into future studies (3, 4, 39). Third, this is a cross-sectional study involving healthy population data; an external validation test should be conducted in polycystic ovarian syndrome and diminished ovarian reserve patients. A longitudinal follow-up study should be performed to assess the predicting ability. Additionally, though this is a nationwide study, the sample size from some centers was too small, which could potentially cause bias. More samples are needed to further test the model and explore more clinical applications.

Conclusion

Taken together, machine learning methods combining multi-features, including simple and easily obtained clinical, biochemical, and ultrasonographic parameters were reliable in quantifying ovarian reserve and were better than a single indicator, providing another possible measurement to reflect ovarian reserve accurately and predict the aging degree of female ovaries individually. After comparison, the LightGBM method revealed itself to be the approach with the best quantitative effect and stability, especially in the specific age group of 20 to 35 years. In the future, this model should be tested and improved on a larger cohort.

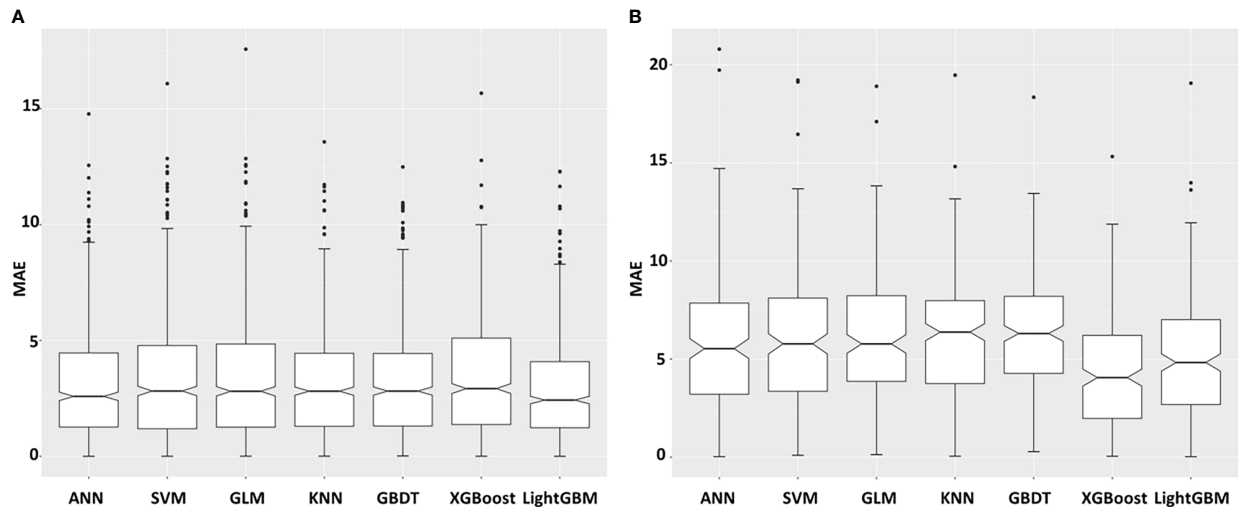

FIGURE 5
Mean absolute prediction errors (MAE) broken down for the seven different prediction models and different age groups: **(A)** 20–35 **(B)** >35 years.

Data availability statement

The raw data supporting the conclusions of this article will be made available by the authors, without undue reservation.

Ethics statement

The studies involving human participants were reviewed and approved by Tongji Hospital, Tongji Medical College, Huazhong University of Science and Technology. The patients/participants provided their written informed consent to participate in this study.

Author contributions

SW and YL conceived and designed the study. TD and TW collected the data and developed the analytic pipeline. WR, YH, and WM led the analysis, generated the tables and figures, and wrote the manuscript. MW and FF verified and processed the underlying data. All authors contributed to the article and approved the submitted version.

Funding

This work was supported by the National Natural Science Foundation of China (grant numbers 81873824 and 81902669).

Conflict of interest

The authors declare that the research was conducted in the absence of any commercial or financial relationships that could be construed as a potential conflict of interest.

Publisher's note

Supplementary material

The Supplementary Material for this article can be found online at: https://www.frontiersin.org/articles/10.3389/fendo.2023.1087429/full#supplementary-material

SUPPLEMENTARY FIGURE 1
Coefficient values for features in different steps of LASSO regression.

References

1. Park SU, Walsh L, Berkowitz KM. Mechanisms of ovarian aging. *Reprod Camb Engl* (2021) 162:R19–33. doi: 10.1530/REP-21-0022

2. Practice Committee of the American Society for Reproductive Medicine. Testing and interpreting measures of ovarian reserve: a committee opinion. *Fertil Steril* (2020) 114:1151–7. doi: 10.1016/j.fertnstert.2020.09.134

3. Hipp HS, Charen KH, Spencer JB, Allen EG, Sherman SL. Reproductive and gynecologic care of women with fragile X primary ovarian insufficiency (FXPOI). *Menopause NYN* (2016) 23:993–9. doi: 10.1097/GME.0000000000000658

4. He C, Murabito JM. Genome-wide association studies of age at menarche and age at natural menopause. *Mol Cell Endocrinol* (2014) 382:767–79. doi: 10.1016/j.mce.2012.05.003

5. Rizzo A, Roscino MT, Binetti F, Sciorsci RL. Roles of reactive oxygen species in female reproduction. *Reprod Domest Anim Zuchthyg* (2012) 47:344–52. doi: 10.1111/j.1439-0531.2011.01891.x

6. Duncan FE, Gerton JL. Mammalian oogenesis and female reproductive aging. *Aging* (2018) 10:162–3. doi: 10.18632/aging.101381

7. Briley SM, Jasti S, McCracken JM, Hornick JE, Fegley B, Pritchard MT, et al. Reproductive age-associated fibrosis in the stroma of the mammalian ovary. *Reprod Camb Engl* (2016) 152:245–60. doi: 10.1530/REP-16-0129

8. Foley KG, Pritchard MT, Duncan FE. Macrophage-derived multinucleated giant cells: hallmarks of the aging ovary. *Reprod Camb Engl* (2021) 161:V5–9. doi: 10.1530/REP-20-0489

9. de Vet A, Laven JSE, de Jong FH, Themmen APN, Fauser BCJM. Antimüllerian hormone serum levels: A putative marker for ovarian aging. *Fertil Steril* (2002) 77:357–62. doi: 10.1016/s0015-0282(01)02993-4

10. Steiner AZ, Pritchard D, Stanczyk FZ, Kesner JS, Meadows JW, Herring AH, et al. Association between biomarkers of ovarian reserve and infertility among older women of reproductive age. *JAMA* (2017) 318:1367–76. doi: 10.1001/jama.2017.14588

11. Zarek SM, Mitchell EM, Sjaarda LA, Mumford SL, Silver RM, Stanford JB, et al. Antimüllerian hormone and pregnancy loss from the effects of aspirin in gestation and reproduction trial. *Fertil Steril* (2016) 105:946–952.e2. doi: 10.1016/j.fertnstert.2015.12.003

12. Van Calster B, Wynants L. Machine learning in medicine. *N Engl J Med* (2019) 380:2588. doi: 10.1056/NEJMc1906060

13. Ngiam KY, Khor IW. Big data and machine learning algorithms for health-care delivery. *Lancet Oncol* (2019) 20:e262–73. doi: 10.1016/S1470-2045(19)30149-4

14. Waljee AK, Higgins PDR. Machine learning in medicine: A primer for physicians. *Am J Gastroenterol* (2010) 105:1224–6. doi: 10.1038/ajg.2010.173

15. Blank C, Wildeboer RR, DeCroo I, Tilleman K, Weyers B, de Sutter P, et al. Prediction of implantation after blastocyst transfer in in vitro fertilization: A machine-learning perspective. *Fertil Steril* (2019) 111:318–26. doi: 10.1016/j.fertnstert.2018.10.030

16. Liao S, Pan W, Dai W-Q, Jin L, Huang G, Wang R, et al. Development of a dynamic diagnosis grading system for infertility using machine learning. *JAMA Netw Open* (2020) 3:e2023654. doi: 10.1001/jamanetworkopen.2020.23654

17. Qiu J, Li P, Dong M, Xin X, Tan J. Personalized prediction of live birth prior to the first *in vitro* fertilization treatment: A machine learning method. *J Transl Med* (2019) 17:317. doi: 10.1186/s12967-019-2062-5

18. Xu H, Feng G, Wang H, Han Y, Yang R, Song Y, et al. A novel mathematical model of true ovarian reserve assessment based on predicted probability of poor ovarian response: A retrospective cohort study. *J Assist Reprod Genet* (2020) 37:963–72. doi: 10.1007/s10815-020-01700-1

19. Xu H, Shi L, Feng G, Xiao Z, Chen L, Li R, et al. An ovarian reserve assessment model based on anti-müllerian hormone levels, follicle-stimulating hormone levels, and age: Retrospective cohort study. *J Med Internet Res* (2020) 22:e19096. doi: 10.2196/19096

20. Venturella R, Lico D, Sarica A, Falbo MP, Gulletta E, Morelli M, et al. OvAge: A new methodology to quantify ovarian reserve combining clinical, biochemical and 3D-ultrasonographic parameters. *J Ovarian Res* (2015) 8:21. doi: 10.1186/s13048-015-0149-z

21. Younis JS, Jadaon J, Izhaki I, Haddad S, Radin O, Bar-Ami S, et al. A simple multivariate score could predict ovarian reserve, as well as pregnancy rate, in infertile women. *Fertil Steril* (2010) 94:655–61. doi: 10.1016/j.fertnstert.2009.03.036

22. Zhang H, Wang J, Sun Z, Zurada JM, Pal NR. Feature selection for neural networks using group lasso regularization. *IEEE Trans Knowl Data Eng* (2020) 32:659–73. doi: 10.1109/TKDE.2019.2893266

23. Mishra M, Srivastava M. *A view of artificial neural network*. (IEEE.) (2014). pp. 1–3. doi: 10.1109/ICAETR.2014.7012785.

24. Basak D, Srimanta P, Patranbis DC. Support vector regression. *Neural Inf Process Lett Rev* (2007) 11. doi: 10.1007/978-1-4302-5990-9_4

25. Friedman J. Greedy function approximation: A gradient boosting machine. *Ann Stat* (2001) 29:1189–232. doi: 10.2307/2699986

26. Zhang Z. Introduction to machine learning: K-nearest neighbors. *Ann Transl Med* (2016) 4:218–8. doi: 10.21037/atm.2016.03.37

27. Nwanganga F, Chapple M. *K-nearest neighbors*. (Wiley) (2020). pp. 221–49. doi: 10.1002/9781119591542.ch6.

28. Chen T, Guestrin C. XGBoost: A scalable tree boosting system. In: *Proceedings of the 22nd ACM SIGKDD international conference on knowledge discovery and data mining*. San Francisco California USA: ACM (2016). p. 785–94. doi: 10.1145/2939672.2939785

29. Meng Q. LightGBM: A highly efficient gradient boosting decision tree. Neural Information Processing Systems Curran Associates Inc. (2017) 3149–3157.

30. Xiao J, Ding R, Xu X, Guan H, Feng X, Sun T, et al. Comparison and development of machine learning tools in the prediction of chronic kidney disease progression. *J Transl Med* (2019) 17:119. doi: 10.1186/s12967-019-1860-0

31. >Sermondade N, Huberlant S, Bourhis-Lefebvre V, Arbo E, Gallot V, Colombani M, et al. Female obesity is negatively associated with live birth rate following IVF: A systematic review and meta-analysis. *Hum Reprod Update* (2019) 25:439–51. doi: 10.1093/humupd/dmz011

32. Traversari J, Aepli H, Knutti B, Lüttgenau J, Bruckmaier RM, Bollwein H. Relationships between antral follicle count, blood serum concentration of anti-müllerian hormone and fertility in mares. *Schweiz Arch Tierheilkd* (2019) 161:627–38. doi: 10.17236/sat00225

33. Seifer DB, Baker VL, Leader B. Age-specific serum anti-müllerian hormone values for 17,120 women presenting to fertility centers within the united states. *Fertil Steril* (2011) 95:747–50. doi: 10.1016/j.fertnstert.2010.10.011

34. Segawa T, Omi K, Watanabe Y, Sone Y, Handa M, Kuroda M, et al. Age-specific values of access anti-müllerian hormone immunoassay carried out on Japanese patients with infertility: A retrospective large-scale study. *BMC Womens Health* (2019) 19:57. doi: 10.1186/s12905-019-0752-z

35. Lorusso F, Vicino M, Lamanna G, Trerotoli P, Serio G, Depalo R. Performance of different ovarian reserve markers for predicting the numbers of oocytes retrieved and mature oocytes. *Maturitas* (2007) 56:429–35. doi: 10.1016/j.maturitas.2006.11.007

36. Broer SL, van Disseldorp J, Broeze KA, Dolleman M, Opmeer BC, Bossuyt P, et al. Added value of ovarian reserve testing on patient characteristics in the prediction of ovarian response and ongoing pregnancy: an individual patient data approach. *Hum Reprod Update* (2013) 19:26–36. doi: 10.1093/humupd/dms041

37. West C. Age and infertility. *Br Med J Clin Res Ed* (1987) 294:853–4. doi: 10.1136/bmj.294.6576.853

38. Zhu D, Chung H-F, Dobson AJ, Pandeya N, Giles GG, Bruinsma F, et al. Age at natural menopause and risk of incident cardiovascular disease: A pooled analysis of individual patient data. *Lancet Public Health* (2019) 4:e553–64. doi: 10.1016/S2468-2667(19)30155-0

39. Laisk T, Tšuiko O, Jatsenko T, Hõrak P, Otala M, Lahdenperä M, et al. Demographic and evolutionary trends in ovarian function and aging. *Hum Reprod Update* (2019) 25:34–50. doi: 10.1093/humupd/dmy031

frontiers | Frontiers in Endocrinology

TYPE Original Research
PUBLISHED 03 May 2023
DOI 10.3389/fendo.2023.1086924

OPEN ACCESS

EDITED BY
Osamu Hiraike,
The University of Tokyo, Japan

REVIEWED BY
Amelia Caruana,
Azienda Ospedaliera Ospedali Riuniti Villa Sofia Cervello, Italy
Zhongbao Zhou,
Capital Medical University, China
Yujia Zhang,
Centers for Disease Control and Prevention (CDC), United States

*CORRESPONDENCE
Chengliang Yin
chengliangyin@163.com
Xingyu Sun
sxy6636@yeah.net

†These authors have contributed equally to this work

SPECIALTY SECTION
This article was submitted to Endocrinology of Aging, a section of the journal Frontiers in Endocrinology

RECEIVED 01 November 2022
ACCEPTED 10 April 2023
PUBLISHED 03 May 2023

CITATION
He Y, Liu L, Yao F, Sun C, Meng M, Lan Y, Yin C and Sun X (2023) Assisted reproductive technology and interactions between serum basal FSH/LH and ovarian sensitivity index.
Front. Endocrinol. 14:1086924.
doi: 10.3389/fendo.2023.1086924

Assisted reproductive technology and interactions between serum basal FSH/LH and ovarian sensitivity index

Yumei He[1], Ling Liu[2], Fei Yao[1], Chenyu Sun[3], Muzi Meng[4,5], Yunzhu Lan[6], Chengliang Yin[7*†] and Xingyu Sun[1*†]

[1]Department of Gynecology, The Affiliated Traditional Chinese Medicine Hospital of Southwest Medical University, Luzhou, Sichuan, China, [2]Department of Reproductive Medicine Center, The Affiliated Hospital of Southwest Medical University, Luzhou, China, [3]Department of Thyroid and Breast Surgery, The Second Affiliated Hospital of Anhui Medical University, Hefei, China, [4]UK Program Site, American University of the Caribbean School of Medicine, Preston, United Kingdom, [5]Bronxcare Health System, New York City, NY, United States, [6]The Fourth Affiliated Hospital, Zhejiang University School of Medicine, Hangzhou, China, [7]Faculty of Medicine, Macau University of Science and Technology, Macau, Macao SAR, China

Objectives: This study aimed to investigate whether the FSH (follicle-stimulating hormone)/LH (Luteinizing hormone) ratio correlates with ovarian response in a cross-sectional retrospective study of a population with normal levels of anti-Müllerian hormone (AMH).

Methods: This was a retrospective cross-sectional study with data obtained from medical records from March 2019 to December 2019 at the reproductive center in the Affiliated Hospital of Southwest Medical University. The Spearmans correlation test evaluated correlations between Ovarian sensitivity index (OSI) and other parameters. The relationship between basal FSH/LH and ovarian response was analyzed using smoothed curve fitting to find the threshold or saturation point for the population with mean AMH level (1.1<AMH<6μg/L). The enrolled cases were divided into two groups according to AMH threshold. Cycle characteristics, cycle information and cycle outcomes were compared. The Mann-Whitney U test was used to compare different parameters between two groups separated by basal FSH/LH in the AMH normal group. Univariate logistic regression analysis and multivariate logistic regression analysis were performed to find the risk factor for OSI.

Results: A total of 428 patients were included in the study. A significant negative correlation was observed between OSI and age, FSH, basal FSH/LH, Gn total dose, and Gn total days, while a positive correlation was found with AMH, AFC, retrieved oocytes, and MII egg. In patients with AMH <1.1 ug/L, OSI values decreased as basal FSH/LH levels increased, while in patients with 1.1<AMH<6 ug/L, OSI values remained stable with increasing basal FSH/LH levels. Logistic regression analysis identified age, AMH, AFC, and basal FSH/LH as significant independent risk factors for OSI.

Conclusions: We conclude that increased basal FSH/LH in the AMH normal group reduces the ovarian response to exogenous Gn. Meanwhile, basal FSH/LH of 3.5 was found to be a useful diagnostic threshold for assessing ovarian response in people with normal AMH levels. OSI can be used as an indicator of ovarian response in ART treatment.

KEYWORDS

FSH/LH, ovarian sensitivity index (OSI), anti-Mullerian hormone, pregnancy, assisted reproductive technology

Introduction

In recent years, infertility, which affects human development and health, has become a global medical and sociological problem (1). Assisted reproductive technologies (ART) have been developed for more than 40 years. In recent decades, assisted reproduction techniques have evolved. However, even when good quality embryos are selected for transfer to the uterus, the implantation rate remains low. Sunderam et al. showed that despite a gradual increase in clinical pregnancy rates among infertile women treated with ART over the past decades, the live birth rate per *in vitro* fertilization-embryo transfer (IVF-ET) was only 38.1% (2). Fertility practitioners should be fully aware of the failure of IVF cycles to improve the success rate of ART. Controlled ovarian hyperstimulation (COH) is critical to the success of IVF-ET (3). However, COH can lead to two adverse outcomes (high ovarian response or low ovarian response) due to the different ovarian responses to COH (4). Accurate prediction of ovarian response is critical to improve *in vitro* fertilization (IVF) or intracytoplasmic sperm injection (ICSI) (5). Currently, there are no relevant informative markers that directly predict ovarian response. The ovarian response is predicted based on the assessment of ovarian reserve indicators (6).

Anti-Müllerian hormone (AMH) levels are positively correlated with follicle number and decrease with increasing age and decreasing follicle number. AMH levels are constant throughout the menstrual cycle and its serum levels are not affected by FSH, LH, and E2 levels. These unique characteristics make AMH a good predictor of ovarian reserve (7). In addition, many studies have shown that age, AMH levels and antral follicle count (AFC) may be predictors of ovarian response (8). However, in clinical practice, the above parameters may not always be evaluated satisfactorily and accurately, and there is a need for more reliable factors to evaluate ovarian reserve. Several potential indicators of ovarian function are influenced by both cyclic variability and aging, and both factors must be taken into account in assessing ovarian function, which makes interpretation a challenge. Du et al. have demonstrated no factors can unconditionally assess ovarian reserve (9). Although AMH and AFC are widely considered as ovarian markers, they do not correctly detect hyporesponsive patients with normal ovarian reserve markers (10–12). A study related to the basal FSH/LH ratio predicting *in vitro* fertilization outcome showed that the basal FSH/LH was associated with poor outcome of *in vitro* fertilization treatment and may be a predictor of decreased ovarian reserve (13).

It has been observed that both the absolute number of oocytes retrieved and total gonadotrophin dose are essential measures of ovarian responsiveness, and the ratio of the two is a better representation of ovarian responsiveness than either parameter alone.

Ovarian sensitivity index (OSI), was first proposed by Biasoni et al. (14). OSI has been found correlated to AMH and AFC, which have been suggested as predictors of ovarian responsiveness (15, 16). Using OSI as a measure of ovarian responsiveness would be better than the number of retrieved oocytes for different gonadotrophin dosages applied to different subjects daily. Pan et al. showed that when OSI values were low, ovarian sensitivity was lower and pregnancy rates were lower; when OSI values were high, the incidence of OHSS was higher and pregnancy rates were lower (17). Huber et al. showed that an OSI below 1.7 was considered a low ovarian response (18). We defined OSI as the number of retrieved oocytes/the total dose of administered gonadotrophins. The use of gonadotropins for ovulation induction is related to a variety of factors, including the patient's age, body mass index (BMI), ovarian function, hormone levels, personal and family history, and the patient's personal preferences and treatment goals. The use of gonadotropins may also be influenced by the patient's lifestyle and environmental factors. Therefore, when using gonadotropins for ovulation induction, these factors should be considered to ensure the treatment's effectiveness and safety. Therefore, searching for new accurate, safe and effective markers is very important.

In the present study, we focused our research mainly on normal AMH population. The study aims were: (1) to detect the association between ovarian sensitivity index (OSI) and varieties of ovarian reserve, (2) to examine whether serum basal FSH/LH is corelated to OSI, (3) to assess whether OSI affects ovarian response, and (4) to find the threshold/saturation point in the study population.

Methods

Patients enrollment

In the cross-sectional retrospective study, infertile women underwent IVF/ICSI treatment at the reproductive center in the Affiliated Hospital of Southwest Medical University between March 2019 and December 2019.

Inclusion criteria

(1) Aged<40 years;
(2) FSH < 25 U/L;
(3) Patients received IVF/ICSI treatment;
(4) Complete case information.

Exclusion criteria

(1) Patients with polycystic ovarian syndrome (PCOS), endometriosis, premature ovarian insufficiency (POI);
(2) Patients with a high incidence of ovarian stimulation hyperresponsiveness;
(3) Patients with a history of ovarian tumors and other malignancies;
(4) Patients with a history of endocrine abnormalities such as diabetes, hyperthyroidism, and hypothyroidism.

Data collection

Collected data included age, duration of infertility, BMI, AFC, AMH, basal FSH, basal LH, basal estradiol (E2) and basal P (progesterone), total Gn dose, total Gn days, oocytes recovered, number of embryos transferred, number of MII eggs, HCG day E2 level, HCG day LH level and HCG day P level.

Ovarian sensitivity index calculation

Ovarian sensitivity index (OSI) was calculated by the following formula: OSI= Retrieved oocytes×1000/total Gn doses

Hormone detection and analyses

Venous blood was collected into plain serum tubes and all samples were centrifuged (2–8°C, 2,000 g, 10 min) within 1 h of blood collection to separate the serum. In order to separate serum from venous blood, all samples were centrifuged (2–8°C, 2,000 g, 10 minutes) within 1 h of blood collection. Each aliquot from each patient was evaluated in random order in the same run, and all hormones were analyzed simultaneously. Each hormone was measured with an Elecsys® assay in conjunction with a cobas e 601 module of a cobas® 6000 analyzer (Roche Diagnostics, Mannheim, Germany) according to the producer's instructions.

Ovulation induction

All patients received the same ovulation promotion protocols, using the same hormones and the same dose adjustment criteria. Ovulation was induced using antagonists or long-term protocols. Recombinant follicle-stimulating hormone (rFSH, Gonal-F, Merck-Serono, Brazil) was given daily on day 2 of the menstrual cycle as the start of the antagonist protocol. The dose of rFSH was adjusted according to the ovarian response measured by estradiol serum concentrations, and follicular growth was monitored by vaginal ultrasound. When follicles reached 14 mm, patients started receiving gonadotropin-releasing hormone (GnRH) antagonists (Cetrotide, MerckSerono, Brazil) associated with rFSH. For the long-term regimen, treatment began with subcutaneous administration of 3.75 mg of GnRH agonist (Gonapeptyl, Ferring, Brazil) on day 21 of their menstrual cycle to suppress pituitary function. To confirm the downregulation of estradiol, serum estradiol concentrations and vaginal ultrasonography were performed approximately 10 days later. If the estradiol concentration was <30 pg/ml and ultrasound showed an endometrial thickness of <3 mm, patients were considered ready to start ovulation induction. After confirmation of suppression, patients received daily doses of rFSH for ovulation induction. In both regimens, oocyte maturation was induced with recombinant human chorionic gonadotrophin (hCG, Ovidrel, Merck-Serono, Brazil) when at least two follicles reached a mean size of 17 mm with concordant estradiol levels (approximately 200 pg/ml).

Embryo transfer technique

All embryo transfers were performed under ultrasound control. Therefore, patients were asked to fill their bladders to provide an acoustic window for uterine visualization. The catheter tip (Wallace, Smits-Medical, Dublin, Ireland) was placed 1.0–2.0 cm below the apex of the uterine cavity. Avoiding uterine contractions, a pipette was inserted slowly from the cervical os into the uterine cavity until it reached the fundus uteri.

Outcome measure

The pregnancy diagnosis was made by a positive hCG test on Day 14 after embryo transfer. The patient underwent transrectal ultrasonography to monitor the gestational sac and the clinical pregnancy diagnosis was confirmed on day 28 post-transfer. Luteal phase support was continued until 12 weeks of gestation. The ratio of basal FSH/LH was computed to detect the turning point of OSI.

Statistical analysis

SPSS-22.0 software (SPSS Inc. Chicago, IL, USA) was used for statistical analysis. Continuous variables were expressed as median scores and compared using the Mann-Whitney U test. Categorical variables were applied as percentages and compared using Fisher's exact test. Median [P25%, P75%] and Mann-Whitney U tests were

used to represent and compare continuous variables. The t-test (2-tailed) was used for comparison between groups of measures, and the Kruskal-Wallis test was used when normality was not satisfied for comparison between groups. Enumeration data were expressed as percentages using the χ^2 test. The Spearman correlation coefficient was applied to explore the correlation between variables. Differences were considered statistically significant at a P-value < 0.05. An additional logistic regression analysis was performed, and the outcome was a binary OSI variable obtained using the detected turning point as cutoff, which differs from the continuous OSI mentioned elsewhere.

Results

General characteristics of this study

Four hundred twenty-eight patients who met the selection criteria were included in this study. Figure 1 shows the study procedure flowchart. Patient information included in this study is shown in Table 1. The median age of the patients was 31 years and the median duration of infertility was 3 years. The median AMH and AFC are 4.06 ug/L and 8, respectively. The clinical pregnancy rate in this study was 28%. Additional patient information is shown in Table 1.

The correlation between OSI and other parameters

The results of the correlation analysis between OSI and other parameters in this study are shown in Table 2. There was a significant negative correlation as follows, for OSI with Age (r_s=-0.115, p=0.017) (Figure 2A), FSH (r_s=-0.267, P<0.001) (Figure 2D), basal FSH/LH (r_s=-0.203, P<0.001) (Figure 2E), Gn total dose (r_s=-0.551, P<0.001) (Figure 2F), and Gn total days (r_s=-0.319, P=0.004) (Figure 2G). There is also a significant positive correlation as follows, for OSI with AMH (r_s= 0.340, P<0.001) (Figure 2B), AFC (r_s=0.223, P<0.001) (Figure 2C), Retrieved oocytes (r_s=0.789, P<0.001) (Figure 2H) and MII egg (r_s=0.099, P=0.040) (Figure 2I). More detailed results were shown in Table 2.

The relationship between basal FSH/LH and ovarian response in AMH <1.1 ug/L and 1.1<AMH<6 ug/L groups

A total of 50 patients with AMH < 1.1ug/L and 243 patients with 1.1<AMH<6ug/L were analyzed to examine the relationship between basal FSH/LH and OSI while excluding ovarian response-related factors such as age, BMI, AMH, E2, and AFC. In the AMH<1.1ug/L group, OSI values decreased as basal FSH/LH levels increased (Figure 3). In contrast, for the 1.1<AMH<6ug/L group, OSI values remained stable and the curve was smooth with increasing basal FSH/LH levels (Figure 4). Table 3 (revised) presents the threshold effect analysis for the association between FSH/LH and OSI in two groups with different AMH levels: AMH <1.1 ug/L and 1.1<AMH<6 ug/L. The table is divided into two sections, with one section for each group. Each section contains two models (Models I and II) and their respective adjusted beta coefficients (95% CI) and P-values. In Model I (linear analysis) for the group with AMH <1.1 ug/L, the one-line slope has an adjusted beta coefficient of -0.3 with a 95% CI of (-0.9, 0.3) and a P-value of 0.413. For the group with 1.1<AMH<6 ug/L, the one-line slope has an adjusted beta coefficient of -0.1 with a 95% CI of (-0.2, 0.1) and a P-value of 0.358. In Model II (non-linear analysis), a turning point is identified for each group. For the group with AMH <1.1 ug/L, the turning point is 2.3, with a slope1 of 2.1 (95% CI: -4.4, 8.7) and P-value of 0.513 for values below 2.3, and a slope2 of -0.1 (95% CI: -0.3, 0.3) and P-value of 0.316 for values above 2.3. For the group with 1.1<AMH<6 ug/L, the turning point is 3.5, with a slope1 of -0.2 (95% CI: -0.6, -0.1) and P-value of 0.049 for values below 3.5, and a slope2 of 0.1 (95% CI: -0.1, 0.3) and P-value of 0.052 for values above 3.5. The LRT test results indicate that there is a significant difference between Models I and II for both groups, with P-values of 0.03 for the AMH <1.1 ug/L group and 0.042 for the 1.1<AMH<6 ug/L group, suggesting a non-linear relationship between FSH/LH and OSI in both groups.

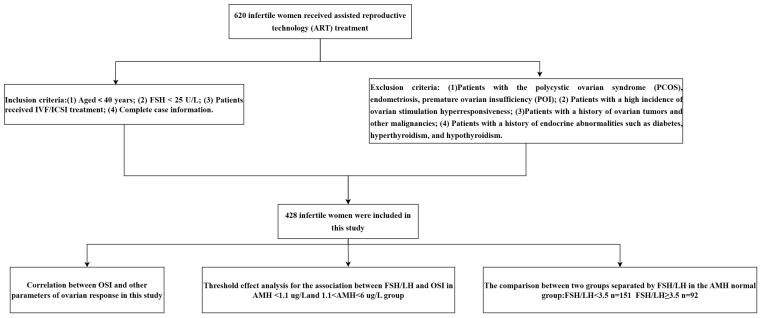

FIGURE 1
The flow chart of this research.

TABLE 1 Baseline characteristics of the patients enrolled.

Parameters		Value
Age(years)		31(28-34)
Infertility duration (years)		3(2-5)
Body mass index (BMI, kg/m^2)		22.03(19.81-24.65)
AFC(pieces)		8(6-9)
Anti-Müllerian hormone (AMH, ug/L)		4.06(2.25-7.55)
Basal Follicle-stimulating hormone(FSH, U/L)		8.57(7.26-10.39)
Basal Luteinizing hormone(LH, mU/L)		3.15(2.21-4.65)
basal E2(ng/L)		41.88(32.50-59.50)
basal P(ug/L)		0.61(0.39-0.97)
Gn total dose(U)		2400(1800-3000)
Gn total days (days)		11(9-13)
Retrieved oocytes(pieces)		9(6-13)
No. of transferred embryos(pieces)		2(1-2)
No. of MII eggs (pieces)		8(5-11)
E_2 level on HCG day(ng/L)		2706.46(1671.46-3370.23)
LH level on HCG day(mU/L)		0.81(0.46-1.36)
P level on HCG day(ug/L)		0.79(0.55-1.08)
Outcomes	No pregnancies	308(71.9%)
	Pregnancies	120(28%)

BMI, body mass index; AFC, antral follicle count; AMH, anti-Müllerian hormone; FSH, Follicle-stimulating hormone; LH, Luteinizing hormone; E_2, estrogen; Gn, gonadotropin; Values are expressed as Medians [P25%, P75%].

The comparison between two groups separated by basal FSH/LH in the AMH normal group

The results comparing age, infertility duration, BMI, AFC, AMH, and FSH (basal FSH/LH<3.5 and basal FSH/LH≥3.5) in the two groups are shown in Table 4. The following variables were statistically significant: Age, BMI, AFC, AMH, FSH, LH, E2, total Gn dose, and retrieved oocytes. Age, BMI, FSH, and total Gn dose were significantly higher in the basal FSH/LH≥3.5 group than in the basal FSH/LH<3.5 group (P<0.05). AFC, AMH, LH, and E2 were significantly lower in the basal FSH/LH≥3.5 group than in the basal FSH/LH<3.5 group (P<0.05). Although the pregnancy rate was also significantly higher than in the basal FSH/LH<3.5 group, the difference in pregnancy rate was not statistically significant (P=0.66). The retrieved oocytes, MII eggs, E_2, and P on HCG day were lower than those in the basal FSH/LH<3.5 group (P<0.05).

Logistics regression analysis of OSI risk factors

In the univariate and multivariate logistic regression analyses, there were finally four parameters significantly correlated with OSI

TABLE 2 Correlation between OSI and other parameters of ovarian response in this study.

Parameter	Ovarian sensitivity index	
	Correlation coefficient	*p*-value
Ages(years)	-0.115	0.017
Infertility duration(years)	-0.044	0.362
Body mass index (BMI, kg/m^2)	-0,043	0.374
basal E2(ng/L)	0.078	0.107
basal P(ug/L)	0.004	0.927
Anti-Müllerian hormone (AMH, ug/L)	0.340	P<0.001
Antral follicle count (AFC)	0.223	P<0.001
Basal Follicle-stimulating hormone(FSH, U/L)	-0.267	P<0.001
Basal Luteinizing hormone(LH, mU/L)	0.057	0.238
FSH/LH	-0.203	P<0.001
Gn total dose(IU)	-0.551	P<0.001
Gn total days (d)	-0.139	0.004
Retrieved oocytes(pieces)	0.789	P<0.001
No. of transferred embryos(pieces)	-0.037	0.448
No. of MII eggs (pieces)	0.099	0.040
E_2 level on HCG day(ng/L)	0.032	0.512
LH level on HCG day(mU/L)	-0.041	0.397
P level on HCG day(ug/L)	-0.134	0.006

BMI, body mass index; AFC, antral follicle count; AMH, anti-Müllerian hormone; FSH, Follicle-stimulating hormone; LH, Luteinizing hormone; E_2, estrogen, E_2;Gn, gonadotropin; Statistically significant(P<0.05,P<0.001).
Models I, linear analysis; Models II, non-linear analysis. LRT test, Logarithmic likelihood ratio test (p value<0.05 means Models II is significantly different from Models I, which indicates a non-linear relationship). Adjusted: adjusted for age, BMI, AMH, E2, and AFC; BMI, body mass index: AMH, anti-Müllerian hormone; E_2, estrogen, E_2, AFC, antral follicle count; OSI, Ovarian sensitivity index.

(Table 5), namely age (odds ratio (OR) 0.72, 95% CI 0.66–0.94, P = 0.026), AMH (odds ratio (OR): 1.32, 95% CI 1.26–1.74, P<0.001), AFC (odds ratio (OR): 1.55, 95% CI 1.46–1.88, P<0.001), and basal FSH/LH (odds ratio (OR): 0.84, 95% CI 0.72–0.94, P=0.042). The logistics regression model showed Age, AMH, AFC, FSH, and basal FSH/LH were independent risk factors of OSI (P<0.05 for all, shown in Table 5; Figures 5A, B).

Discussion

In vitro fertilization (IVF) and intracytoplasmic sperm injection (ICSI) in Assisted reproductive technology (ART) are effective methods for the treatment of infertile women (19). However, the response to exogenous gonadotropins (Gn) may vary between women undergoing controlled ovarian hyperstimulation (COH), which is associated with patient prognosis, including cycle cancellation rate, exogenous gonadotropin dose, and pregnancy

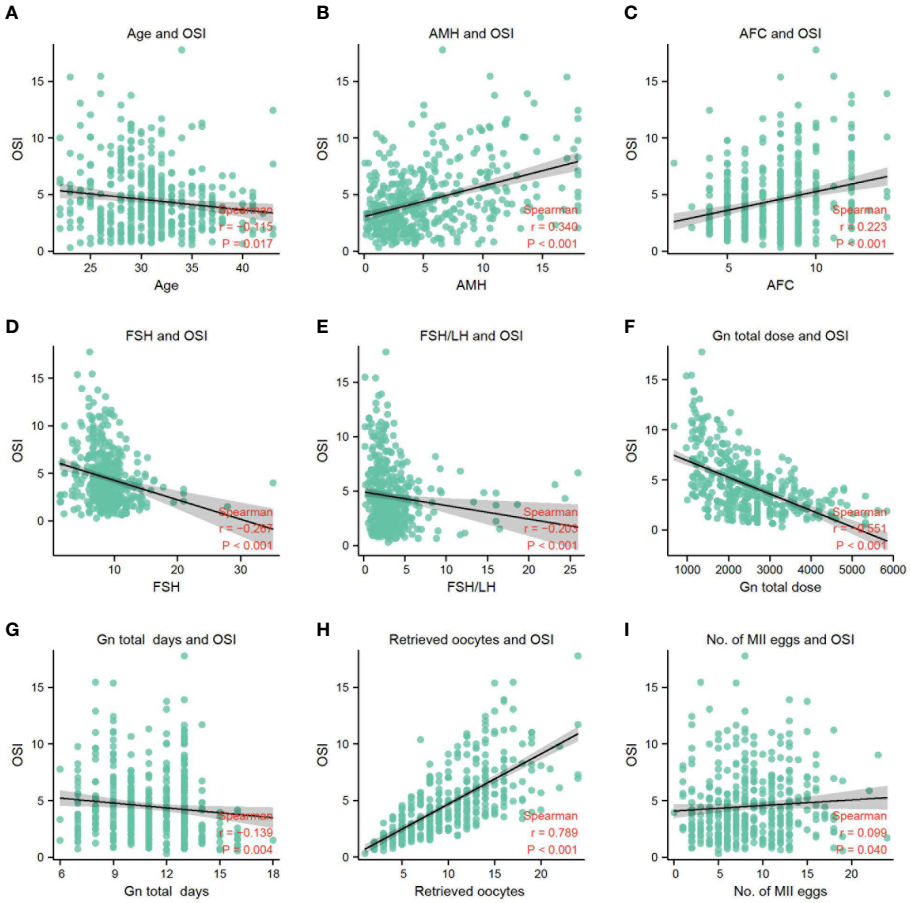

FIGURE 2
(A) The correlation between OSI and age. **(B)** The correlation between OSI and AMH. **(C)** The correlation between OSI and AFC. **(D)** The correlation between OSI and FSH. **(E)** The correlation between OSI and FSH/LH. **(F)** The correlation between OSI and Gn total dose. **(G)** The correlation between OSI and Gn total days. **(H)** The correlation between OSI and retrieved oocytes. **(I)** The correlation between OSI and No. of MII eggs.

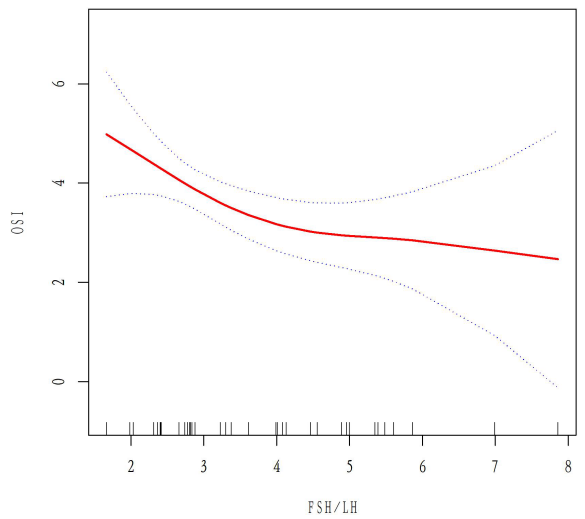

FIGURE 3
Relationship between basal FSH/LH levels and OSI values in the AMH<1.1ug/L group.

outcome (20). Poor ovarian response (POR) is an important issue in clinic infertility treatment. Even when appropriate ovarian stimulation is given, the prognosis for poor ovarian response (POR) remains unfavorable pregnancy outcome (21). Fertility declines gradually with age in women, starting to decline significantly around the age of 32 years and accelerating significantly after the age of 37 years (22). Screening for individuals and groups at risk of declining fertility is critical. In clinical practice, it is crucial to identify patients at risk of low ovarian response, and individualized ovulatory treatment for different ovarian responses may improve clinical pregnancy rates in infertile patients.

Reduced ovarian reserve is the dominant factor for poor ovarian response, and clinical indicators reflecting ovarian reserve include age, AMH AFC basic FSH level, and other relevant indicators (23). However, the evaluation of ovarian response is unsatisfactory and even the results can be inaccurate (24). Some new indicators such as AFC/TOC and FSH/LH may be a recent approaches in treating ovarian stimulation on COH therapy (10, 25). In early clinical practice, basic FSH was often used as an index to assess ovarian reserve, but ovarian response has been found to be lower in patients with normal FSH (26). The AFC is susceptible to human factors,

10.3389/fendo.2023.1086924

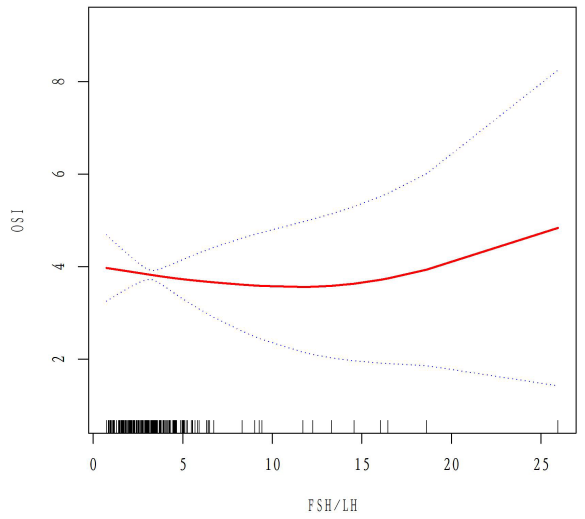

FIGURE 4
Relationship between basal FSH/LH levels and OSI values in the1.1<AMH<6ug/L group.

resulting in a lack of accuracy and objectivity. In recent years, the combined use of AMH and AFC has allowed the assessment ovarian reserve. Patients with the low response, normal or high to exogenous Gn, can be identified by AFC and AMH (27). Mutlu et al. has shown that AMH is less sensitive in predicting low ovarian response (28). Overall, there are no specific markers to evaluate ovarian reserve and response independently, and a combined application for evaluation is still needed. Basal FSH/LH reflects ovarian response to exogenous Gn and is also associated with the length of the menstrual cycle prior to IVF/ICSI-ET (29). Kofinas et al. showed that elevated basal FSH/LH ratio >3 was more likely to result in individual menstrual cycle cancellation (15 vs 5.24%; p = 0.0001) in a total of 676 patients in the USA involved (30). Seckin et al. demonstrated that older women with a high basal FSH/LH (n = 23) had a significantly lower number of good grade embryos transferred (p = 0.04) and a significantly lower pregnancy rate (p = 0.03) compared to older women with a low basal FSH/LH ratio. However, in younger women, treatment outcomes were similar in both subgroups (31). Thus, they concluded that basal FSH/LH ratio is useful in predicting IVF outcomes in older women but does not appear to be an accurate predictor in younger women.

Patients with normal serum AMH levels but low ovarian response still exist and are easily overlooked by clinicians in clinical practice. In this study, we found that AMH and AFC decreased with increasing basal FSH/LH with increasing age by analyzing the normal AMH group. Therefore, we believe that the basal FSH/LH levels can reflect the reserve function of ovaries to some extent. Also, patients with elevated basal FSH/LH levels had higher total Gn doses but significantly fewer MII eggs than those with low basal FSH/LH levels in this study. Thus, patients with elevated basal FSH/LH levels had reduced sensitivity to exogenous Gn and reduced ovarian response. Previous studies found that the number of mature oocytes was reduced in those with elevated basal FSH/LH (23) levels and suggested that elevated basal FSH/LH levels were associated with a decreased final pregnancy rate (13). However, Arat et al. confirmed basal FSH/LH levels were not associated with the final cycle outcome (23) and that age and number of embryos transferred were independent factors affecting the final live birth rate (30). In the present study, we found no significant reduction in the number of mature eggs, number of embryos transferred, and final pregnancy rate in the population with basal FSH/LH ≥3.5. Therefore, we concluded that the number of mature eggs and the number of embryos transferred were not related to the level of basal FSH/LH. There was no significant difference in the number of mature eggs and final cycle outcomes. However, due to the small sample size, further follow-up is needed to calculate the cumulative pregnancy rate to determine whether the pregnancy outcome is affected by basal FSH/LH. In the present study, we found a decreasing trend in LH levels from the basal FSH/LH<3.5 group to the basal FSH/LH>3.5 group. We can further speculate that the decrease in ovarian response to exogenous Gn

TABLE 3 Threshold effect analysis for the association between FSH/LH and OSI in AMH <1.1 ug/L and 1.1<AMH<6 ug/L group.

Models	OSI (group: AMH<1.1 ug/L)		Models	OSI (group:1.1<AMH<6ug/L)	
	Adjustedβ (95%CI)	*P*-valve		Adjustedβ(95%CI)	*P*-valve
Models I			**Models I**		
One line slope	-0.3(-0.9,0.3)	0.413	One line slope	-0.1(-0.2,0.1)	0.358
Models II			**Models II**		
Turning point	2.3		Turning point	3.5	
< 2.3 slope1	2.1(-4.4,8.7)	0.513	<3.5 slope1	-0.2(-0.6,-0.1)	0.049
>2.3 slope2	-0.1(-0.3,0.3)	0.316	>3.5 slope2	0.1(-0.1,0.3)	0.052
LRT test		0.03	**LRT test**		0.042

Models I, linear analysis; Models II, non-linear analysis. LRT test, Logarithmic likelihood ratio test (p value<0.05 means Models II is significantly different from Models I, which indicates a non-linear relationship). Adjusted: adjusted for age, BMI, AMH, E2, and AFC; BMI: body mass index: AMH, anti-Müllerian hormone; E2, estrogen, E2; AFC, antral follicle count; OSI, Ovarian sensitivity index.

TABLE 4 The comparison between two groups separated by FSH/LH in the AMH normal group.

Parameter	FSH/LH<3.5 n=151	FSH/LH≥3.5 n=92	*P-value*
Age(years)	31(28-34)	32(29-35)	0.042
Infertility duration (years)	3(2-5)	3(2-5)	0.265
Body mass index (BMI, kg/m^2)	21.33(19.53-24.22)	21.77(19.82-24.65)	0.024
Antral follicle count (AFC)	8(6-9)	7(6-8)	0.049
Anti-Müllerian hormone (AMH, ug/L)	3.36(2.26-4.80)	3.05(2.39-4.02)	0.039
Follicle-stimulating hormone(FSH, U/L)	8.28(7.37-10.06)	9.78(7.88-11.24)	0.001
Luteinizing hormone(LH, mU/L)	3.68(2.67-4.97)	2.13(1.28-2.56)	P<0.001
basal E2(ng/L)	47.03(34.40-64.94)	41.24(31.13-62.37)	0.031
basal P(ng/L)	0.67(0.38-1.08)	0.61(0.43-1.01)	0.417
Gn total dose	2475 (2025.00-2475)	2700 (2050-3375)	0.024
Gn total days	11(9-13)	11(9-13)	0.877
Retrieved oocytes	9(5-13)	8(6-12)	0.038
mature eggs	1(0.83-1.00)	1(0.88-1.00)	0.900
No. of transferred embryos(pieces)	2(1-2)	2(1-2)	0.805
No. of MII eggs (pieces)	8(6-11)	7(5-10)	0.043
E_2 level on HCG day(ng/L)	2758.42(1863.22-3326.22)	2386.82(1473.28-3370.23)	0.045
LH level on HCG day(mU/L)	0.80(0.46-1.34)	0.94(0.56-1.18)	0.054
P level on HCG day(ug/L)	0.83(0.55-1.19)	0.81(0.58-1.23)	0.047
outcomes (Pregnancies %)	41(27.15%)	28(30.43%)	0.66

BMI, body mass index; AFC, antral follicle count; AMH, anti-Müllerian hormone; FSH, Follicle-stimulating hormone; LH, Luteinizing hormone; E_2, estrogen, E_2;Gn, gonadotropin; Statistically significant(P<0.05,P<0.001).

may be related to the increase in FSH and the decrease in LH level. A study found that a decrease in the basal LH level on the third day of the menstrual cycle reduced the number of retrieved oocytes and decreased the risk of hyperstimulation syndrome (OHSS) (32). Also, a decrease in LH may lead to a decrease in the number of antral follicles (33), as studied at the genetic level in rats. Noel et al. also demonstrated a reduced requirement for exogenous Gn during COH (34) in individuals with elevated endogenous LH levels to a

TABLE 5 Risk factors for OSI* identified by univariate logistic regression analysis and multivariate logistic regression analysis.

Characteristics	Univariate logistic regression analysis			Multivariate logistic regression analysis		
	OR	95%CI	P	OR	95%CI	P
Age	0.78	0.68-0.92	0.003	0.72	0.66-0.94	0.026
AMH	1.54	1.15-1.91	<0.001	1.32	1.26-1.74	<0.001
AFC	1.63	1.27-1.81	<0.001	1.55	1.46-1.88	<0.001
FSH	0.69	0.56-0.94	0.011	–	–	–
FSH/LH	0.86	0.73-0.96	0.023	0.84	0.72-0.94	0.042
Gn total dose	0.67	0.55-0.92	0.039	–	–	–
Gn total days	0.56	0.55-0.89	0.041	–	–	–
Retrieved oocytes	0.89	0.79-0.99	0.032	–	–	–
No. of MII eggs	0.78	0.69-0.79	0.044	–	–	–
P level on HCG day	0.84	0.81-0.92	0.049	–	–	–

AFC, antral follicle count; AMH, anti-Müllerian hormone; FSH, Follicle-stimulating hormone; LH, Luteinizing hormone. OSI*, a binary variable obtained using the detected turning point as cutoff.

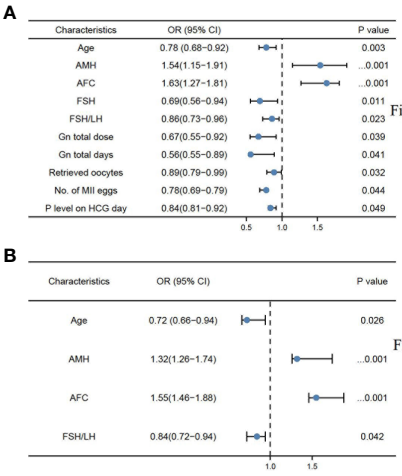

Figure 5A Univariate logistic regression analysis

Figure 5B Multivariate logistic regression analysis

FIGURE 5
(A) Univariate logistic regression analysis. **(B)** Multivariate logistic regression analysis.

certain extent. A complex interaction of molecular pathways occurs between female and male gametes during clinical pregnancies and live births. Olszewska et al. have demonstrated the relationship between methylation (5mC) and hydroxymethylation (5hmC) in sperm DNA concerning sperm chromatin protamination in three subpopulations of fertile normozoospermic controls and infertile patients with oligo-/oligoasthenozoospermia (35). Furthermore, Giebler et al. showed that PIWI-LIKE 1 and 2 transcript levels in the spermatozoa of the swim-up fraction were positively correlated with each other by analyzing how PIWI-LIKE 1-4 mRNA expression in ejaculated spermatozoa predicts outcomes of assisted reproductive techniques (ART), evaluating swim-up spermatozoa used for fertilization from 160 *in vitro* fertilization (IVF) or intracytoplasmic sperm injection (ICSI) cycles (36). In conclusion, our study sheds light on the potential impact of basal FSH/LH levels on ovarian response and ART outcomes, but it is essential to recognize the multifactorial nature of infertility and the diverse molecular pathways that come into play during the process of fertilization and embryo development. By expanding our knowledge in this area and exploring additional factors such as sperm DNA methylation and PIWI-LIKE transcript levels, we may be able to develop a more comprehensive understanding of infertility and improve the prognosis and treatment options for infertile couples seeking assistance through ART.

This study has the advantage of focusing on a specific population in Southwest China, an area that may not be economically developed but has an increasing trend of infertility patients. Additionally, these measurements were made in the same laboratory using the same equipment. As a result, laboratory testing is much less likely to be variable. There are three limitations to our study. First, we generated our findings from a relatively small number of individuals, which should be validated in larger cohorts of Chinese Han patients. Second, this study is limited by its retrospective nature and its confinement to a single center. In the future, the sample size will be expanded, or multicenter studies will be performed for further validation. Third, in this study, only associations between ART pregnancy outcomes and basal FSH/LH and OSI were investigated without addressing other confounders' impacts.

Conclusions

Firstly, in individuals with normal AMH levels, we observed that an increase in basal FSH/LH leads to a reduced ovarian response to exogenous Gn. Secondly, the OSI exhibited a strong correlation with female parameters associated with ovarian reserve. Thirdly, we identified threshold effects for basal FSH/LH and OSI in both normal and low anti-Müllerian hormone populations, with turning points at 3.5 and 2.3, respectively. Additionally, the ovarian sensitivity index (OSI) independently impacted the ovarian response. These findings could assist clinicians in evaluating ovarian response in patients with normal AMH levels undergoing assisted reproductive technology (ART) treatments for infertility. By employing factor analysis, we may be able to better understand the underlying relationships among variables like AMH, AFC, FSH/LH, and others, and potentially reveal novel patterns or factors that contribute to ovarian reserve and response. Consequently, further research is required to elucidate the relevant underlying mechanisms.

Data availability statement

The original contributions presented in the study are included in the article/supplementary material. Further inquiries can be directed to the corresponding authors.

Ethics statement

The study was approved by the Ethics Committee of the Affiliated Hospital of Southwest Medical University (ethics code number: KY2022300). Informed consent from study participants was not required.

Author contributions

XS and CY: Conceptualization. XS, LL, FY, and CS: Data curation, Writing-Original draft preparation. YH, MM, and YL: Revising the manuscript critically for important intellectual content. All authors agree with the contents of the manuscript.

Acknowledgments

We thank the survey participants and all members involved in this study for their painstaking efforts in conducting the data collection. All authors gave informed consent prior to the start of the study and agreed with the contents of the manuscript.

Conflict of interest

The authors declare that the research was conducted in the absence of any commercial or financial relationships that could be construed as a potential conflict of interest.

Publisher's note

References

1. Mascarenhas MN, Flaxman SR, Boerma T, Vanderpoel S, Stevens GA. National, regional, and global trends in infertility prevalence since 1990: a systematic analysis of 277 health surveys. *PloS Med* (2012) 9(12):e1001356. doi: 10.1371/journal.pmed.1001356

2. Sunderam S, Kissin DM, Zhang Y, Jewett A, Boulet SL, Warner L, et al. Assisted reproductive technology surveillance — united states, 2018. *MMWR Surveill Summ* (2022) 71(4):1–19. doi: 10.15585/mmwr.ss7104a1

3. Penzias AS. Improving results with assisted reproductive technologies: individualized patient-tailored strategies for ovulation induction. *Reprod BioMed Online* (2011) 22 Suppl 1:S83–6. doi: 10.1016/S1472-6483(11)60013-8

4. Chalumeau C, Moreau J, Gatimel N, Cohade C, Lesourd F, Parinaud J, et al. Establishment and validation of a score to predict ovarian response to stimulation in IVF. *Reprod BioMed Online* (2018) 36(1):26–31. doi: 10.1016/j.rbmo.2017.09.011

5. Kim SW, Kim YJ, Shin JH, Kim H, Ku SY, Suh CS, et al. Correlation between ovarian reserve and incidence of ectopic pregnancy after *in vitro* fertilization and embryo transfer. *Yonsei Med J* (2019) 60(3):285–90. doi: 10.3349/ymj.2019.60.3.285

6. Saleh BO, Ibraheem WF, Ameen NS. The role of anti-mullerian hormone and inhibin b in the assessment of metformin therapy in women with polycystic ovarian syndrome. *Saudi Med J* (2015) 36(5):562–7. doi: 10.15537/smj.2015.5.11112

7. Josso N. WOMEN IN REPRODUCTIVE SCIENCE: anti-müllerian hormone: a look back and ahead. *Reproduction* (2019) 158(6):F81–9. doi: 10.1530/REP-18-0602

8. Brodin T, Hadziosmanovic N, Berglund L, Olovsson M, Holte J. Comparing four ovarian reserve markers–associations with ovarian response and live births after assisted reproduction. *Acta Obstet Gynecol Scand* (2015) 94(10):1056–63. doi: 10.1111/aogs.12710

9. Du YY, Guo N, Wang YX, Hua X, Deng TR, Teng XM, et al. Urinary phthalate metabolites in relation to serum anti-müllerian hormone and inhibin b levels among women from a fertility center: a retrospective analysis. *Reprod Health* (2018) 15(1):33. doi: 10.1186/s12978-018-0469-8

10. Alvin C, Conforti A, Esteves SC, Vallone R, Venturella R, Staiano S, et al. Understanding ovarian hypo-response to exogenous gonadotropin in ovarian stimulation and its new proposed marker-the follicle-To-Oocyte (FOI) index. *Front Endocrinol (Lausanne)* (2018) 9:589. doi: 10.3389/fendo.2018.00589

11. Conforti A, Esteves SC, Di Rella F, Strina I, De Rosa P, Fiorenza A, et al. The role of recombinant LH in women with hypo-response to controlled ovarian stimulation: a systematic review and meta-analysis. *Reprod Biol Endocrinol* (2019) 17(1):18. doi: 10.1186/s12958-019-0460-4

12. Alvin C, Conforti A, Santi D, Esteves SC, Andersen CY, Humaidan P, et al. Clinical relevance of genetic variants of gonadotropins and their receptors in controlled ovarian stimulation: a systematic review and meta-analysis. *Hum Reprod Update* (2018) 24(5):599–614. doi: 10.1093/humupd/dmy019

13. Prasad S, Gupta T, Divya A. Correlation of the day 3 FSH/LH ratio and LH concentration in predicting IVF outcome. *J Reprod Infertil* (2013) 14(1):23–8.

14. Biasoni V, Patriarca A, Dalmasso P, Bertagna A, Manieri C, Benedetto C, et al. Ovarian sensitivity index is strongly related to circulating AMH and may be used to predict ovarian response to exogenous gonadotropins in IVF. *Reprod Biol Endocrinol* (2011) 9:112. doi: 10.1186/1477-7827-9-112

15. Broer SL, Mol BW, Hendriks D, Broekmans FJ. The role of antimullerian hormone in prediction of outcome after IVF: comparison with the antral follicle count. *Fertil Steril* (2009) 91(3):705–14. doi: 10.1016/j.fertnstert.2007.12.013

16. Broer SL, Dólleman M, Opmeer BC, Fauser BC, Mol BW, Broekmans FJ. AMH and AFC as predictors of excessive response in controlled ovarian hyperstimulation: a meta-analysis. *Hum Reprod Update* (2011) 17(1):46–54. doi: 10.1093/humupd/dmq034

17. Pan W, Tu H, Jin L, Hu C, Xiong J, Pan W, et al. Comparison of recombinant and urinary follicle-stimulating hormones over 2000 gonadotropin-releasing hormone antagonist cycles: a retrospective study. *Sci Rep* (2019) 9(1):5329. doi: 10.1038/s41598-019-41846-2

18. Huber M, Hadziosmanovic N, Berglund L, Holte J. Using the ovarian sensitivity index to define poor, normal, and high response after controlled ovarian hyperstimulation in the long gonadotropin-releasing hormone agonist protocol: suggestions for a new principle to solve an old problem. *Fertil Steril* (2013) 100 (5):1270–6. doi: 10.1016/j.fertnstert.2013.06.049

19. van Hoogenhuijze NE, Torrance HL, Mol F, Laven JSE, Scheenjes E, Laven MAF, et al. Endometrial scratching in women with implantation failure after a first IVF/ICSI cycle; does it lead to a higher live birth rate? the SCRaTCH study: a randomized controlled trial (NTR 5342). *BMC Women's Health* (2017) 17(1):47. doi: 10.1186/s12905-017-0378-y

20. Gingold JA, Lee JA, Whitehouse MC, Rodriguez-Purata J, Sandler B, Grunfeld L, et al. Maximum basal FSH predicts reproductive outcome better than cycle-specific basal FSH levels: waiting for a "better" month conveys limited retrieval benefits. *Reprod Biol Endocrinol* (2015) 13:91. doi: 10.1186/s12958-015-0078-0

21. Özkan ZS. Ovarian stimulation modalities in poor responders. *Turk J Med Sci* (2019) 49(4):959–62. doi: 10.3906/sag-1905-179

22. Sun YF, Zhang J, Xu YM, Luo ZY, Sun Y, Hao GM, et al. Effects of age on pregnancy outcomes in patients with simple tubal factor infertility receiving frozen-thawed embryo transfer. *Sci Rep* (2020) 10(1):18121. doi: 10.1038/s41598-020-75124-3

23. Arat Ö, Deveci D, Özkan ZS, Tuncer Can S. What is the effect of the early follicular phase FSH/LH ratio on the number of mature oocytes and embryo development? *Turk J Med Sci* (2020) 50(2):420–5. doi: 10.3906/sag-1910-234

24. Zhou SJ, Zhao MJ, Li C, Su X. The comparison of evaluative effectiveness between antral follicle count/age ratio and ovarian response prediction index for the ovarian reserve and response functions in infertile women. *Med (Baltimore)* (2020) 99 (36):e21979. doi: 10.1097/MD.0000000000021979

25. Scheinhardt MO, Lerman T, König IR, Griesinger G. Performance of prognostic modelling of high and low ovarian response to ovarian stimulation for IVF. *Hum Reprod* (2018) 33(8):1499–505. doi: 10.1093/humrep/dey236

26. Kumba B, Oral E, Kahraman S, Karlikaya G, Karagozoglu H. Young patients with diminished ovarian reserve undergoing assisted reproductive treatments: a preliminary report. *Reprod BioMed Online* (2005) 11(3):294–9. doi: 10.1016/s1472-6483(10)60836-x

27. Polyzos NP, Tournaye H, Guzman L, Camus M, Nelson SM. Predictors of ovarian response in women treated with corifollitropin alfa for *in vitro* fertilization/ intracytoplasmic sperm injection. *Fertil Steril* (2013) 100(2):430–7. doi: 10.1016/ j.fertnstert.2013.04.029

28. Mutlu MF, Erdem M, Erdem A, Yildiz S, Mutlu I, Arisoy O, et al. Antral follicle count determines poor ovarian response better than anti-müllerian hormone but age is the only predictor for live birth in *in vitro* fertilization cycles. *J Assist Reprod Genet* (2013) 30(5):657–65. doi: 10.1007/s10815-013-9975-3

29. Brodin T, Bergh T, Berglund L, Hadziosmanovic N, Holte J. Menstrual cycle length is an age-independent marker of female fertility: results from 6271 treatment cycles of *in vitro* fertilization. *Fertil Steril* (2008) 90(5):1656–61. doi: 10.1016/ j.fertnstert.2007.09.036

30. Kofinas JD, Elias RT. Follicle-stimulating hormone/luteinizing hormone ratio as an independent predictor of response to controlled ovarian stimulation. *Women's Health (Lond)* (2014) 10(5):505–9. doi: 10.2217/whe.14.31

31. Seckin B, Turkcapar F, Ozaksit G. Elevated day 3 FSH/LH ratio: a marker to predict IVF outcome in young and older women. *J Assist Reprod Genet* (2012) 29 (3):231–6. doi: 10.1007/s10815-011-9695-5

32. Vivian K, Isik AZ. Low day 3 luteinizing hormone values are predictive of reduced response to ovarian stimulation. *Hum Reprod* (1999) 14(3):863–4. doi: 10.1093/humrep/14.3.863

33. Mature A, Tenino I, Varik I, Kruse S, Tiido T, Kristjuhan A, et al. FSH/LH-dependent upregulation of ahr in murine granulosa cells is controlled by PKA signaling and involves epigenetic regulation. *Int J Mol Sci* (2019) 20(12):3068. doi: 10.3390/ijms20123068

34. Noel SD, Kaiser UB. G Protein-coupled receptors involved in GnRH regulation: molecular insights from human disease. *Mol Cell Endocrinol* (2011) 346(1-2):91–101. doi: 10.1016/j.mce.2011.06.022

35. Olszewska M, Kordyl O, Kamieniczna M, Fraczek M, Jędrzejczak P, Kurpisz M. Global 5mC and 5hmC DNA levels in human sperm subpopulations with differentially protaminated chromatin in normo- and oligoasthenozoospermic males. *Int J Mol Sci* (2022) 23(9):4516. doi: 10.3390/ijms23094516

36. Giebler M, Greither T, Handke D, Seliger G, Behre HM. Lower spermatozoal PIWI-LIKE 1 and 2 transcript levels are significantly associated with higher fertilization rates in IVF. *Int J Mol Sci* (2021) 22(21):11320. doi: 10.3390/ijms222111320

frontiers | Frontiers in Endocrinology

TYPE Original Research
PUBLISHED 28 July 2023
DOI 10.3389/fendo.2023.1124143

OPEN ACCESS

EDITED BY
Osamu Hiraike,
The University of Tokyo, Japan

REVIEWED BY
Pietro Serra,
University of Palermo, Italy
Kazuki Kurimoto,
Nara Medical University, Japan
Sherman Silber,
Infertility Center of St. Louis, United States

*CORRESPONDENCE
Qing-Yun Mai
maiqy@mail.sysu.edu.cn
Can-Quan Zhou
zhoucanquan@mail.sysu.edu.cn

RECEIVED 14 December 2022
ACCEPTED 14 April 2023
PUBLISHED 28 July 2023

CITATION
Luo Y-Y, Jie H-Y, Huang K-J, Cai B, Zhou X, Liang M-Y, Zhou C-Q and Mai Q-Y (2023) The dynamic expression of SOX17 in germ cells from human female foetus and adult ovaries after specification. *Front. Endocrinol.* 14:1124143. doi: 10.3389/fendo.2023.1124143

The dynamic expression of SOX17 in germ cells from human female foetus and adult ovaries after specification

Ying-Yi Luo[1,2], Hui-Ying Jie[1], Ke-Jun Huang[1,3], Bing Cai[1], Xiu Zhou[1], Ming-Yi Liang[1], Can-Quan Zhou[1*] and Qing-Yun Mai[1*]

[1]Reproductive Medicine Center, The First Affiliated Hospital, Sun Yat-sen University, Guangzhou, China, [2]Reproductive Medicine Center, The First People's Hospital of Foshan, Foshan, China, [3]Department of Obstetrics & Gynaecology, Guangzhou Women and Children's Medical Center, Guangzhou, China

Background: SOX17 has been identified as a critical factor in specification of human primordial germ cells, but whether SOX17 regulates development of germ cells after sex differentiation is poorly understood.

Methods: We collected specimens of gonadal ridge from an embryo (n=1), and ovaries of foetuses (n=23) and adults (n=3). Germ cells were labelled with SOX17, VASA (classic germ cells marker), phosphohistone H3 (PHH3, mitosis marker) and synaptonemal complex protein 3 (SCP3, meiosis marker).

Results: SOX17 was detected in both cytoplasm and nucleus of oogonia and oocytes of primordial and primary follicles from 15 to 28 gestational weeks (GW). However, it was exclusively expressed in cytoplasm of oogonia at 7 GW, and in nucleus of oocytes in secondary follicles. Co-expression rates of SOX17 in $VASA^+$ germ cells ranged from 81.29% to 97.81% in foetuses. Co-staining rates of SOX17 and PHH3 or SCP3 were 0%-34% and 0%-57%, respectively. Interestingly, we distinguished a subpopulation of $SOX17^+VASA^-$ germ cells in fetal ovaries. These cells clustered in the cortex and could be co-stained with the mitosis marker PHH3 but not the meiosis marker SCP3.

Conclusions: The dynamic expression of SOX17 was detected in human female germ cells. We discovered a population of $SOX17^+$ $VASA^-$ germ cells clustering at the cortex of ovaries. We could not find a relationship between mitosis or meiosis and SOX17 or VASA staining in germ cells. Our findings provide insight into the potential role of SOX17 involving germ cells maturation after specification, although the mechanism is unclear and needs further investigation.

KEYWORDS

SOX17, germ cells, VASA, mitosis, meiosis

1 Introduction

Currently, the timeline of key events in human female germ cells is well-defined. Female germ cells, including primordial germ cells (PGCs), oogonia, and oocytes, play a critical role in genetic material transfer across a generation (1). Human PGCs first appear in the posterior epiblast of embryos around 4 gestational weeks (GW), although the origin of PGCs is still unclear. Approximately at 6 GW, human PGCs migrate to genital ridges and differentiate into oogonia with the interaction of gonadal somatic cells. After passing through leptotene, zygotene, and pachytene diplotene stages of meiosis prophase I, oogonia arrest at the dictyate stage to become primary oocytes. Then single-layer pre–granulosa cells surround primary oocytes to form primordial follicles. Primordial follicles further develop into primary, secondary and antral follicles during puberty accompanied by oocyte differentiation. Primordial follicles develop into primary follicles and secondary follicles through activation. After puberty, ovulated oocytes mature after completing meiosis. The process by which a primary oocyte completes the secondary meiotic division is termed oocyte nuclear maturation (2, 3).

Studies involving later stages of human germ cell development are difficult to carry out due to the limited availability of foetal ovarian tissue and ethical constraints. Various gene markers of germ cells at different developmental stages, such as OCT4, DAZL and VASA, have been described (4). Among these markers, VASA (also called DDX4), a member of the DEAD box family, was first identified to be critical in Drosophila oogenesis in 1988 and recognized as a relatively specific marker of human germ cells (5, 6). In addition, germ cells undergoing mitosis or meiosis can be labelled for phosphohistone H3 (PHH3) or synaptonemal complex protein 3 (SCP3). PPH3 is considered a classical mitosis marker. In mitotic cells, histone H3 is phosphorylated at serine 10 and serine 28. When serine 28 is phosphorylated, PHH3 is specifically detected (7). Synaptonemal complex, consisting of SCP1, SCP2 and SCP3, is critical to chromosome segregation during meiosis (8). Studies reported that SCP3 is expressed in human ovaries (9) and is widely used as a meiosis marker (10, 11).

Remarkable progress in inducing human PGCs *in vitro* has been made in recent years (12–15). In 2015, Irie et al. successfully developed human PGC-like cells (hPGCLCs) from differentiated embryonic stem cells (ESCs) and induced pluripotent stem cells (iPSCs). They first demonstrated the critical role of SOX17 in regulating hPGCLC specification (12). SOX17 belongs to the SRY-related box (SOX) family, located on human chromosome 8q11.23 (16). In 1996, two mRNA isoforms of the SOX17 gene were first isolated from the mouse testis cDNA library (17). Similar to other orthologous pairs of SOX genes, SOX17 is characterized by a high mobility group (HMG) box domain, which enables SOX17 to specifically combine with DNA (18). SOX17 is critical in the specification of mammalian embryo primitive endoderm (19) and regulates developmental processes in various organ systems (20–24). In addition, SOX17 might be a tumour suppressor of endometrial cancer, cholangiocarcinoma, colon carcinoma cells, and breast cancer by antagonizing the effect of the canonical Wnt/beta-catenin signalling pathway (19, 25–27).

SOX17 is pivotal for hPGCLC specification, although the molecular mechanisms are still not fully elucidated (28). Studies involving whether SOX17 regulates germ cells maturation after the specification period have rarely been reported. Herein, we describe the expression pattern of the SOX17 protein in different-stage germ cells in human foetal and adult ovaries and analyse the relationship between SOX17 expression and proliferation or first meiosis of human oogonia, which may shed some light on the oogenesis mechanism in human ovaries.

2 Materials and methods

2.1 Collection of human foetal ovaries and adult ovaries

This study was reviewed and approved by the Clinical Research Ethics Committee of the First Affiliated Hospital of Sun Yat-sen University (Ethical approval number (2016): 090) and carried out between 2016 and 2018. Women who participated in this study signed informed consent forms. We collected specimens of gonad ridge of an embryo (n=1), and ovaries of foetuses (n=23) from multiple pregnancy reduction surgery at 7 GW, inevitable spontaneous abortion or induced abortion because of severe malformation of foetus except for urogenital system. The malformations of foetus included cleft lip and palate, Down syndrome, severe thalassemia, ventricular dysplasia syndrome and Cantrell pentalogy. Gestational age was determined by ultrasonography (7 GW) and further confirmed by the foot size of the foetus (15–28 GW). In addition, three adults receiving ovariectomy due to autogenous diseases also gave consent for us to acquire their ovary specimens after surgical removal.

2.2 Histopathologic confirmation of human ovaries

Genital ridges or ovaries were fixed in 10% buffered formalin. After 24–48 hours of fixation, samples were processed for routine paraffin embedding. Embedded samples were serially cut into 4-μm-thick sections, mounted onto cleaned, coated slides and stored at room temperature until use. All samples were examined for tissue integrity and general histology using haematoxylin and eosin staining. These histological sections were all reviewed and confirmed by two pathologists.

2.3 Immunofluorescence

Multiplex immunofluorescence was performed on fixed sections of ovaries described above. Four-μm-thick sections of paraffin-embedded tissues were dried overnight, dewaxed, and rehydrated through xylene and a graded alcohol series [100% (1 min), 95% (1 min), 80% (1 min), and 70% (1 min)]. Antigen retrieval was performed by Pressure-cooking in citrate buffer (#AR0024, BOSTER, China) for 3 minutes, followed by incubation with 0.2% Triton X (#T8200, Solarbio, China)

for 15 minutes. The sections were blocked in 5% donkey serum (#SL050, Solarbio) for 30 mins at room temperature and then incubated with primary antibodies (1:1) at 4 degrees centigrade for 12–14 hours. Primary antibody dilutions were as follows: SOX17 (1:20; #AF1924, R&D, USA), VASA (1:100; #AB27591, Abcam, USA), PHH3 (1:800; #AB47297, Abcam), and SCP3 (1:2000; #AB150292, Abcam). On Day 2, sections were incubated with secondary antibodies for 1 hour at room temperature. Secondary antibody dilutions were as follows: donkey anti-goat (1:400; #AB175704, Alexa Fluor 568, Abcam), donkey anti-mouse (1:400; #AB150105, Alexa Fluor 488, Abcam), and donkey anti-rabbit (1:400; #AB150075, Alexa Fluor 647, Abcam). The sections were then stained with Prolong Gold Antifade Reagent with DAPI (#8961, CST, USA). Fluorescent images were captured using a Leica TCS-SP8 laser scanning confocal microscope (Olympus Ltd.). To obtain a distinct colour contrast, we regulated the yellow signal of SOX17 from the 568 channel to the red signal.

To assess the colocalization of SOX17 and VASA and the trends of mitosis and meiosis in SOX17 positive cells, Leica TCS-SP8 counting frames were used to count the number of germ cells with positive signals. Four frames were entirely counted per section in all cases for each time point. Counting was performed by three independent observers who were unaware of the gestational age at the time-point of the investigation, and the numbers were reviewed by ImageJ software. The results are expressed as the mean value of the absolute number for each time point.

2.4 Statistical analysis

Statistical analysis was performed with IBM SPSS Statistics 25. Pearson correlation analysis was used for statistical analysis. Differences were considered statistically significant when P was less than 0.05.

3 Results

3.1 Collection and Confirmation of human female ovaries

We collected one genital ridge from multifoetal pregnancy reduction surgery and twenty-three ovaries of human foetuses (15 to 28 GW) from inevitable spontaneous abortion or induced abortion because of severe malformation of the foetus except for the urogenital system, and 3 ovarian specimens of adults undergoing ovariectomy due to autogenous diseases. We applied copy number variation sequencing (CNV-seq) to identify the ovary collected from the 7 GW embryo that was female (Supplementary Image 1).

Typical oogonia and different developmental-stage follicles of sections were observed (Figure 1), confirming that the specimens collected were ovaries. Oogonia and primordial follicles were observed in sections from 15 GW. In the ovarian section from 28 GW, primary follicles were observed. In ovarian sections from adults, follicles appeared at different developmental stages, and oogonia were not observed.

3.2 The subcellular localization of SOX17 during the development process of human ovaries

Germ cells from foetuses and adults both expressed SOX17 protein, and the subcellular localization of SOX17 was variable in different developmental stages of germ cells. SOX17 can be expressed not only in the cytoplasm but also in the nuclei. The expression of SOX17 in cytoplasm and nuclei seemed to be related to the maturation of germ cells. In the genital ridge of 7 GW, SOX17 was expressed exclusively in the cytoplasm of oogonia. SOX17 could only be detected in the oocyte nucleus of secondary follicles in adults. SOX17 expression could be detected both in cytoplasm and the nuclei of germ cells from 15 GW to 28 GW (Figure 2A).

For further exploration of the relationship between subcellular localization of SOX17 and the developmental stage of germ cells, the proportion of germ cells with different subcellular localizations of SOX17 was calculated (Figure 2B). In female germ cells, the percentages of cytoplasmic SOX17 expression showed a declining trend with the increase of gestational age, decreasing from 100% at 7 GW to 20% at 28 GW. The percentages of nuclear SOX17 expression showed an increasing trend, elevating from 0% at 7 GW to 80% at 28 GW. In addition, SOX17 was mainly localized in the nuclei of oocytes within primordial follicles (62.9%–91.2%) and primary follicles (66.7%–94.4%) (Supplementary Table 1).

3.3 Co-expression of SOX17 and VASA in the developing female genital glands

For the purpose of investigating the co-expression pattern of SOX17 and the classic germ cell marker VASA in female germ cells during ovarian development, we co-stained human ovarian sections with antibodies of SOX17 and VASA. With the use of the double staining method, we showed the co-expression patterns of SOX17 protein and VASA protein in human female germ cells (Figure 3). The expression of VASA was detected in the cytoplasm of germ cells from 7 GW to adult.

Furthermore, we calculated the percentages of $VASA^{+}$ germ cells positive for SOX17 in different developmental stages (Figure 4 and Supplementary Table 2). The percentage fluctuated from 81.29%–97.81% in foetal ovaries (Figure 4). Pearson correlation analysis showed that co-expression rates of SOX17 and VASA in germ cells did not correlate with gestational weeks ($r = 0.064$, $P = 0.835$).

Interestingly, we observed a subpopulation of germ cells that are immunopositive for SOX17 but not for VASA, clustering in the cortex of foetal ovaries (Figure 3). In these $SOX17^{+}VASA^{-}$ germ cells, the SOX17 signal was only detected in the nuclei. Representative images of these germ cells were shown (Figure 3).

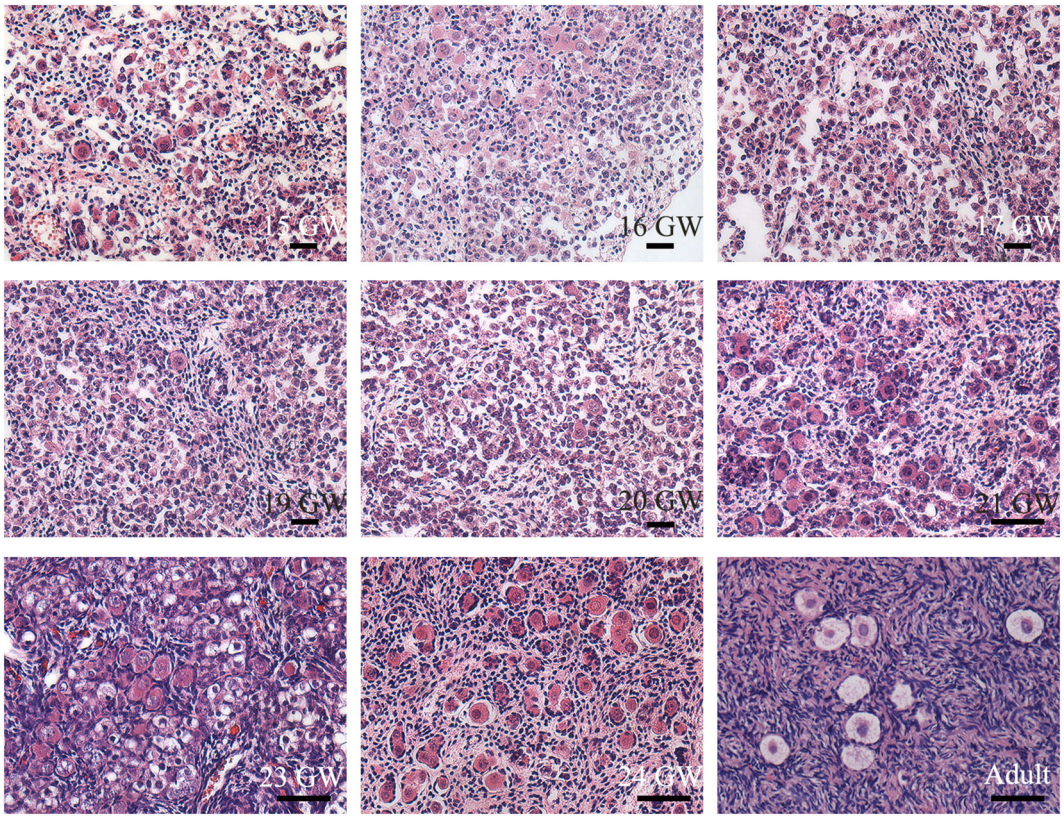

FIGURE 1
Histological sections of ovarian specimens. Representative pictures were shown. One genital ridge and ovarian specimens of foetuses (n=23) and adults (n=3) were collected. Typical oogonia (round or oval shape, chromatin was evenly distributed, and the nucleus was larger than the surrounding somatic cells) were observed in the specimens from 15 GW to 28 GW but disappeared in the adult ovary. Primordial follicles, characterized by single-layer pre–granulosa cells, were also present in ovarian sections after 15 GW. In adult ovarian sections, follicles at different stages are observed. Scale bars, 50 μm.

3.4 The percentage of mitosis or meiosis in SOX17 immunopositive germ cells

We tried to clarify the relationship between the cell division pattern and SOX17 expression in female germ cells. In $SOX17^+$ germ cells, we could detect the expression of mitotic marker PHH3 or meiosis marker SCP3 independently (Figure 5A). PHH3 was highly expressed in $SOX17^+$ germ cells at 7 GW. However, the expression percentage of PHH3 decreased significantly after 15 GW. At 7 GW, we could not observe the expression of meiotic marker SCP3 in SOX17-positive germ cells, but after 15 GW, we could see nearly 30%-50% $SOX17^+$ germ cells were marked by SCP3 in foetal gonads.

We further counted the proportions of $PHH3^+SOX17^+$ germ cells and $SCP3^+SOX17^+$ germ cells (Figure 5B). At 7 GW, the percentage of $SOX17^+PHH3^+$ cells accounted for 34% of germ cells, but that of $SOX17^+SCP3^+$ germ cells was 0%. The proportions of $SOX17^+PHH3^+$ cells ranged from 3–9% in germ cells of 15 to 24 GW and were reduced to 0% in germ cells of 26 and 28 GW and adults. In contrast, the proportions of $SOX17^+SCP3^+$ germ cells varied from 31%–57% between 15–28 GW. In addition, PHH3 and SCP3 expression was undetectable in $SOX17^+$ germ cells from adults (Figure 5B).

3.5 The co-expression features of SOX17, VASA and PHH3/SCP3 immunopositive germ cells

In order to figure out whether the co-expression status of SOX17 and VASA is related to mitosis and meiosis in female germ cells, we further co-stained germ cells with SOX17, VASA and mitosis marker PHH3 or meiosis marker SCP3 (Figure 6). We discovered that after 15GW, $SOX17^+VASA^+$ germ cells could appear mitosis state ($PHH3^+$) and meiosis states ($SCP3^+$). In addition, we detected a special population of $SOX17^+VASA^-$ germ cells also showing mitosis status ($PHH3^+$) but not meiosis status ($SCP3^-$). In $SOX17^+$ germ cells from 15 GW to 23 GW, approximately 1.03% of these cells were positive for PHH3 but negative for VASA.

4 Discussion

In this study, we showed that SOX17 was detectable in germ cells from the gonadal ridge of the embryo, the ovaries of foetuses and adults. We further described that the subcellular expression of SOX17 was dynamic in germ cells at different developmental stages.

10.3389/fendo.2023.1124143

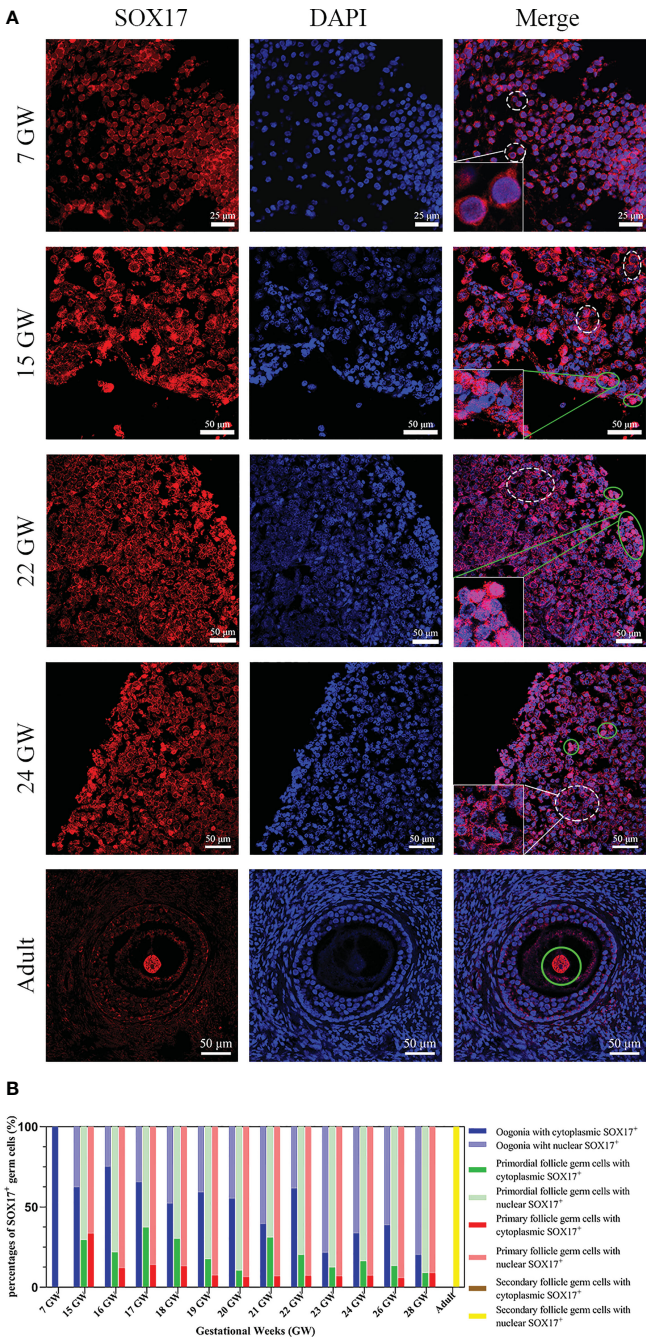

FIGURE 2
The expression pattern of SOX17 in female germ cells. **(A)** Germ cells were stained with SOX17 (red), and DAPI (blue) was used to stain the nucleus. In ovarian sections from 15 and 24 GW, SOX17 was expressed in both the cytoplasm (shown in white dashed line) and nucleus of germ cells (green full line). Signals of SOX17 were only detected in the cytoplasm of the section from 7 GW (white dashed line), and in nucleus from adult (green full line). Scale bars, 25 or 50 μm. **(B)** The percentages of germ cells (including oogonia, primordial follicles, primary follicles, and secondary follicles) with SOX17 expression in nucleus or cytoplasm were calculated. SOX17 was exclusively expressed in the cytoplasm of oogonia at 7 GW and then was detectable in both the nucleus and cytoplasm of oogonia at 15 to 24 GW, 26 GW, and 28 GW. In secondary follicles, SOX17 was only expressed in the nucleus of oocytes.

We determined that there is a subpopulation of germ cells positive for SOX17 in the nucleus but not for VASA which have the potential for mitosis. These findings provide valuable insights for studies of SOX17 and human germ cells.

Müllerian ducts, which are regulated by homeobox genes during differentiation (29), and the ovary together comprise the reproductive system. As the earliest marker of hPGCLCs and a key regulator of hPGCLC fate, SOX17 attracts the interest of researchers (12, 30). In Tang's study (31), the DNA demethylation and chromatin reorganization of human PGCs were mainly governed by a unique transcriptome, which was established by SOX17 and BLIMP1, indicating that SOX17 is critical in the DNA

10.3389/fendo.2023.1124143

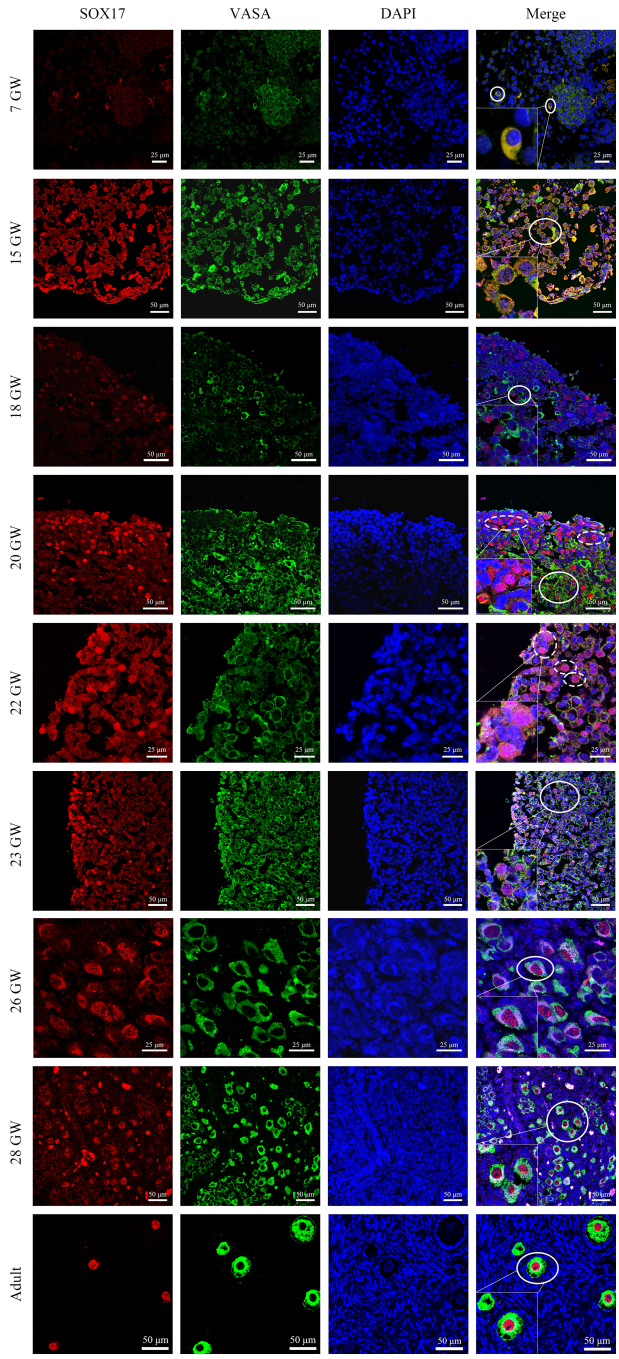

FIGURE 3
Immunolabelling of VASA and SOX17 in germ cells from genital glands during different stages. Representative pictures were shown. Germ cells were stained with SOX17 (red) and VASA (green). DAPI (blue) was used to stain the nucleus. These markers were detected in all stages of germ cells of developing human ovaries. SOX17 was expressed in a majority of germ cells marked by VASA (shown in full line). Some germ cells clustering in the ovarian cortex were positive for SOX17 (red) but not for VASA (green) (shown in dotted line). Scale bars, 25 or 50 μm.

demethylation of PGCs. In addition, Guo et al. analysed the transcriptome and DNA methylome of human PGCs and neighbouring somatic cells from embryos between 4 and 19 GW by a single-cell RNA sequencing method (32). They reported the expression of SOX17 in human germ cells at 4, 8, 10, 11, and 17 GW at the RNA level, but the localization of SOX17 in germ cells has not yet been clarified.

Herein, we described the unique dynamic expression pattern of SOX17 in female germ cells in different developmental stages. In 7 GW, SOX17 was only expressed in the cytoplasm of germ cells. With the increase of gestational weeks, the proportion of SOX17 cytoplasmic expression in human germ cells gradually decreased, but the proportion of SOX17 nuclear expression gradually increased. It indicates that SOX17 is gradually transferred from

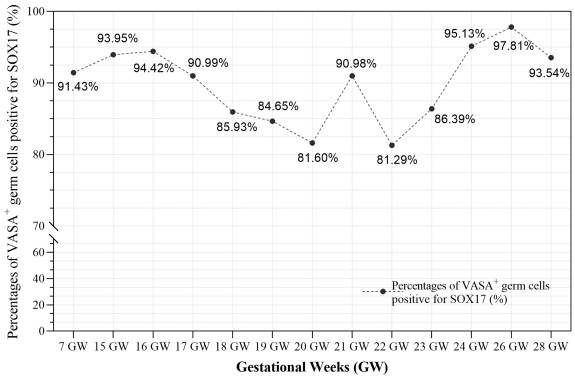

FIGURE 4
The co-expression rates of SOX17 and VASA in germ cells during different gestation ages were calculated. The rates fluctuated from 81.29-97.81% in fetal ovaries. Pearson correlation analysis showed that co-expression rates of SOX17 and VASA did not correlate with gestational weeks (r = 0.064, P = 0.835).

cytoplasm to nucleus with the development and maturity of germ cells. Our study also discovered nearly 60-90% of oocytes of primordial and primary follicles in foetal ovaries expressed SOX17 in the cytoplasm. In the oocytes of secondary follicles, SOX17 was expressed exclusively in the nucleus. Our study confirms for the first time that there are two expression patterns of SOX17 in human female germ cells, and that SOX17 is gradually transferred from the cytoplasm to the nucleus along with the germ cell maturation process.

SOX17 protein was expressed in both the cytoplasm and nucleus of germ cells from foetuses but translocated to the nucleus of an oocyte from secondary follicles in adults. The subcellular localization of SOX17 in germ cells has been reported before. In 1996, Kanai et al. (17) reported two isoforms of SOX17 in mouse testes. One form of SOX17, a specific DNA-binding protein, was detectable in premeiotic germ cells. It transformed into another isoform, losing its DNA-binding ability when spermatogonia entered the pachytene stage. In addition, other research showed that SOX17 exclusively localized in the nucleus of Rhesus PGCLCs (33), or was restricted to the nucleus of Cynomolgus Monkey PGCs at embryonic day 11 (34). However, we showed that there was a nucleus-to-cytoplasm transition of SOX17 in human female germ cells during gonadal differentiation. Whether the nucleus-to-cytoplasm transition of SOX17 only exists in human female germ cells still needs more research. In addition, the specific structural changes of different SOX17 subtypes in human female germ cells still need to be clarified in future studies.

VASA has been regarded as a relatively specific marker of germ cells, especially postmeiotic germ cells (35). And VASA may regulate gonadal development by alternative splicing (36). Parte et al. (37) showed expression characteristics of VASA during ovarian stem cells differentiation and found that VASA was expressed in the cytoplasm of progenitor ovarian stem cells. In this study, we observed that VASA located in the cytoplasm of labelled germ cells from an embryo, foetuses, and adults. With double staining of SOX17 and VASA, we calculated the co-expression rates of SOX17 and VASA in germ cells, which ranged from 81.29%–97.81%. In our study, we discovered a special population of $SOX17^{+}VASA^{-}$ germ cells cluster in the cortex of ovaries. Interestingly, Anderson et al. (38) reported that VASA was detected in germ cells throughout ovaries except in the cortex. They further co-stained germ cells with VASA and OCT4, a pluripotency gene marker of embryonic stem cells and germ cells (39–41). They found that some germ cells were positive for OCT4 in the nucleus but not for VASA in the cortex, similar to germ cells positive for SOX17 but not for VASA that we described. Stoop et al. pointed out that germ cells in the cortex tended to be more proliferative than those in the medulla (35). In addition, in 1986, Konishi et al. (42) observed the ultrastructure of germ cells in foetal ovary specimens by electron microscopy and described that typical germ cells at the premeiotic stage had a 10–15 micron diameter and large, round nuclei. Hence, we hypothesized that these $SOX17^{+}VASA^{-}$ germ cells might be in the early developmental phase.

To determine whether the dynamic expression of SOX17 in germ cells was related to the mitosis and meiosis of female germ cells, we conducted multilabel immunofluorescence staining of germ cells with VASA, SOX17, and PHH3 (a mitotic marker)/ SCP3 (a meiosis marker). We found that the mitotic rate of $SOX17^{+}$ germ cells was highest at 7 GW and then declined with progressing gestational weeks. In $SOX17^{+}$ germ cells, the mitotic rate was the highest at 7 GW (34%) and decreased to 0% after 26 GW. Double-staining germ cells with SCP3 and SOX17 showed that the meiosis rate was 0% at 7 GW, and approximately 43% at 15 GW, indicating that the occurrence of germ cell meiosis was not earlier than 7 GW and no later than 15 GW. But we could not explore the time of meiosis onset in germ cells in this study.

With immunohistochemistry techniques, Fulton et al. (43) calculated the percentage of $PHH3^{+}$ germ cells in foetal ovaries from 14 GW to 20 GW. The percentage was approximately 1%, which was comparable to our findings. We observed that the mitosis rate of germ cells in the human female genital ridge is around 35%, which provides evidence of a large amount of $SOX17^{+}$ germ cells undergoing proliferation at 7 GW. However, the mitosis rate of $SOX17^{+}$ germ cells remained at about 5% and declined to 0% at 26-28 GW, which was consistent with the conclusion drawn by Kurilo et al. (44) and Baker et al. (45). We also detected the first meiosis rate of germ cells in the genital ridge and ovary of 15-28 GW. We could not observe the meiosis factor SCP3 positive in

10.3389/fendo.2023.1124143

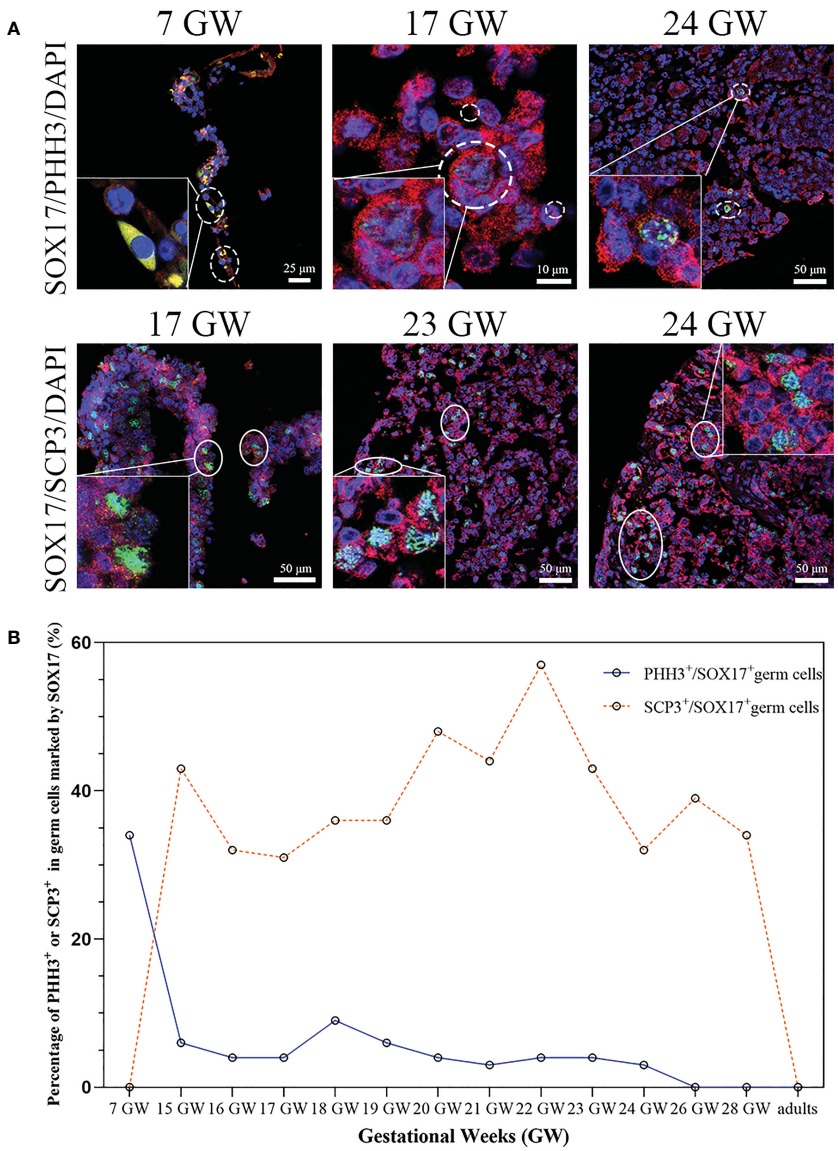

FIGURE 5
The percentage of mitosis or meiosis in SOX17 (red) immunopositive germ cells. **(A)** Representative pictures were shown. A proportion of SOX17$^+$ germ cells were marked by PHH3 (shown in dashed line) or SCP3 (shown in full line). Scale bars, 10, 25, or 50 μm. **(B)** The percentages of PHH$^+$ in germ cells positive for SOX17 decreased along with increasing gestational weeks. The percentage of germ cells immunopositive for both SCP3 and SOX17 was 43% in 15 GW and decreased to 0% in 28 GW and adults.

SOX17$^+$ germ cells from 7 GW genital ridge, though the meiosis rate increased to around 40% in SOX17$^+$ germ cells population from 15GW to 28 GW. Our results indicated that the first meiosis is quite common for SOX17$^+$ germ cells population at 15 GW-28 GW. Our finding is consistent with the classic theory of human germ cells development, but we further provided the detailed proportion of germ cells that underwent mitosis and meiosis during the development of the ovary in the foetus.

In adults, the rates of mitosis and meiosis were 0% in SOX17$^+$ germ cells positive, indicating that germ cells undergoing mitosis or meiosis in prophase I were absent and that neo-oogenesis may not occur in adults. This conclusion was consistent with other studies (44, 46), but further studies are needed to investigate whether there are stem cells in adult ovaries undergo mitosis.

To explore the relationship between the cell division pattern and SOX17/VASA staining in germ cells, with the triple-staining method, we showed the colocalization of VASA, SOX17, and PHH3/SCP3 in germ cells from foetal ovarian specimens. The SOX17$^+$VASA$^-$ germ cells population was co-stained with a mitosis marker but not with meiosis marker. However, due to the scarcity of human female gonad specimens, it is unclear whether the mitosis rate and meiosis rate differ between SOX17$^+$VASA$^+$ and SOX17$^+$VASA$^-$ germ cell population and further validation is needed.

In conclusion, we first described the relatively continuous and dynamic expression of SOX17 in different stages of germ cells from human foetuses and adults and investigated the relationship between the SOX17 dynamic expression and germ cell maturation

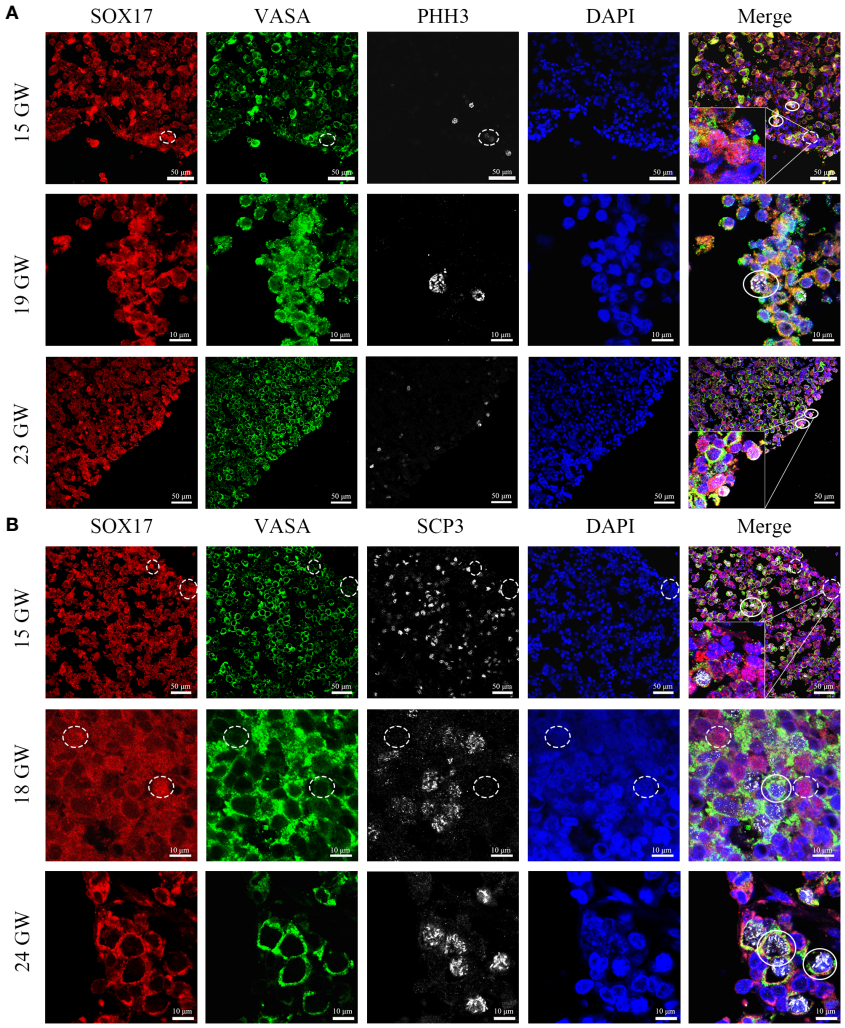

FIGURE 6
Coexpression pattern of SOX17 (red), VASA (green), and PHH3/SCP3 (silver grey) immunopositive germ cells. Representative pictures were shown. **(A)** In 15, 19 and 23 GW ovarian sections, $SOX17^{+}VASA^{+}$ germ cells were co-stained with PHH3 (white full line). In the cortex of the ovary, a small proportion of $SOX17^{+}VASA^{-}$ germ cells were also co-stained with PHH3 (white dashed line). **(B)** In 15, 18, and 24 GW ovarian sections, $SOX17^{+}VASA^{+}$ germ cells were co-stained with SCP3 (white full line). $SOX17^{+}VASA^{-}$ germ cells were not co-stained with SCP3 (shown in white dashed line). The nuclei were stained by DAPI (blue). Scale bars, 10 or 50 μm.

during the development of human ovaries. The dynamic expression of SOX17 was detected in human female germ cells. Cytoplasmic SOX17 transferred into the nucleus during the process of germ cell maturation. We found that the co-expression rate of SOX17 and VASA was relatively high, while a small portion of germ cells positive for SOX17 but not for VASA was found gathering around the ovarian cortex. We described the detailed rate of mitosis and meiosis in the $SOX17^{+}$ germ cell subpopulation. And we found out $SOX17^{+}$ $VASA^{-}$ germ cells subpopulation was co-stained with mitosis marker but not with meiosis marker, although we could not confirm whether mitosis rate and meiosis rate differ between $SOX17^{+}$ $VASA^{+}$ and $SOX17^{+}$ $VASA^{-}$ germ cell populations. This is the first study to depict the expression pattern of SOX17 in human germ cells of foetal and adult genital organs. This study explores the relationship between SOX17 and the proliferation and differentiation of human germ cells, to provide a theoretical basis for the treatment of patients suffering from premature ovarian failure and patients with cancer needing ovarian fertility preservation (47).

The limitations of this observational study were as follows. Due to the scarcity of human female gonad specimens, the expression of SOX17 in germ cells from 8 GW to 14 GW was deficient. The molecular mechanism of SOX17 involved in germ cell maturation during foetal ovarian development needs to be explored in future studies.

Data availability statement

The original contributions presented in the study are included in the article/Supplementary Material. Further inquiries can be directed to the corresponding authors.

Ethics statement

The studies involving human participants were reviewed and approved by the Clinical Research Ethics Committee of the First Affiliated Hospital of Sun Yat-sen University. Written informed consent to participate in this study was provided by the participants' legal guardian/next of kin.

Author contributions

Q-YM and C-QZ designed the study and revised this paper. Y-YL drafted this manuscript. H-YJ and M-YL contributed discussion and helped with manuscript revision. Y-YL and K-JH collected study samples. Y-YL, H-YJ, BC and XZ analyzed the data. All authors contributed to the article and approved the submitted version.

Funding

Clinical Medical Research of China Medical Sciences - Stem Cell Basic Research Project [No:19020010780]; National Natural Science Foundation of China [No: 81270750]; Natural Science Foundation of Guangdong China [No: 2019A1515011845].

Acknowledgments

The authors thank the professional manuscript services of American Journal Experts.

Conflict of interest

The authors declare that the research was conducted in the absence of any commercial or financial relationships that could be construed as a potential conflict of interest.

Publisher's note

Supplementary material

The Supplementary Material for this article can be found online at: https://www.frontiersin.org/articles/10.3389/fendo.2023.1124143/full#supplementary-material

References

1. Gulimiheranmu M, Wang X, Zhou J. Advances in female germ cell induction from pluripotent stem cells. *Stem Cells Int* (2021) 2021:8849230. doi: 10.1155/2021/8849230

2. Laisk T, Tšuiko O, Jatsenko T, Hõrak P, Otala M, Lahdenperä M, et al. Demographic and evolutionary trends in ovarian function and aging. *Hum Reprod Update.* (2019) 25:34–50. doi: 10.1093/humupd/dmy031

3. Larose H, Shami AN, Abbott H, Manske G, Lei L, Hammoud SS. Gametogenesis: a journey from inception to conception. *Curr Top Dev Biol* (2019) 132:257–310. doi: 10.1016/bs.ctdb.2018.12.006

4. Li L, Yang R, Yin C, Kee K. Studying human reproductive biology through single-cell analysis and *in vitro* differentiation of stem cells into germ cell-like cells. *Hum Reprod Update.* (2020) 26:670–88. doi: 10.1093/humupd/dmaa021

5. Lasko PF, Ashburner M. The product of the drosophila gene vasa is very similar to eukaryotic initiation factor-4A. *Nature* (1988) 335:611–7. doi: 10.1038/335611a0

6. Castrillon DH, Quade BJ, Wang TY, Quigley C, Crum CP. The human VASA gene is specifically expressed in the germ cell lineage. *Proc Natl Acad Sci U S A.* (2000) 97:9585–90. doi: 10.1073/pnas.160274797

7. Veras E, Malpica A, Deavers MT, Silva EG. Mitosis-specific marker phospho-histone H3 in the assessment of mitotic index in uterine smooth muscle tumors: a pilot study. *Int J Gynecol Pathol* (2009) 28:316–21. doi: 10.1097/PGP.0b013e318193df97

8. Page SL, Hawley RS. The genetics and molecular biology of the synaptonemal complex. *Annu Rev Cell Dev Biol* (2004) 20:525–58. doi: 10.1146/annurev.cellbio.19.111301.155141

9. Bukovsky A, Caudle MR, Gupta SK, Svetlikova M, Selleck-White R, Ayala AM, et al. Mammalian neo-oogenesis and expression of meiosis-specific protein SCP3 in adult human and monkey ovaries. *Cell Cycle* (2008) 7:683–6. doi: 10.4161/cc.7.5.5453

10. Bhartiya D, Sriraman K, Gunjal P, Modak H. Gonadotropin treatment augments postnatal oogenesis and primordial follicle assembly in adult mouse ovaries? *J Ovarian Res* (2012) 5:32. doi: 10.1186/1757-2215-5-32

11. Liang GJ, Zhang XF, Wang JJ, Sun YC, Sun XF, Cheng SF, et al. Activin a accelerates the progression of fetal oocytes throughout meiosis and early oogenesis in the mouse. *Stem Cells Dev* (2015) 24:2455–65. doi: 10.1089/scd.2015.0068

12. Irie N, Weinberger L, Tang WW, Kobayashi T, Viukov S, Manor YS, et al. SOX17 is a critical specifier of human primordial germ cell fate. *Cell* (2015) 160:253–68. doi: 10.1016/j.cell.2014.12.013

13. Yamashiro C, Sasaki K, Yabuta Y, Kojima Y, Nakamura T, Okamoto I, et al. Generation of human oogonia from induced pluripotent stem cells in vitro. *Science* (2018) 362:356–60. doi: 10.1126/science.aat1674

14. Hamazaki N, Kyogoku H, Araki H, Miura F, Horikawa C, Hamada N, et al. Reconstitution of the oocyte transcriptional network with transcription factors. *Nature* (2021) 589:264–9. doi: 10.1038/s41586-020-3027-9

15. Yamashiro C, Sasaki K, Yokobayashi S, Kojima Y, Saitou M. Generation of human oogonia from induced pluripotent stem cells in culture. *Nat Protoc* (2020) 15:1560–83. doi: 10.1038/s41596-020-0297-5

16. Tam PP, Kanai-Azuma M, Kanai Y. Early endoderm development in vertebrates: lineage differentiation and morphogenetic function. *Curr Opin Genet Dev* (2003) 13:393–400. doi: 10.1016/S0959-437X(03)00085-6

17. Kanai Y, Kanai-Azuma M, Noce T, Saido TC, Shiroishi T, Hayashi Y, et al. Identification of two Sox17 messenger RNA isoforms, with and without the high mobility group box region, and their differential expression in mouse spermatogenesis. *J Cell Biol* (1996) 133:667–81. doi: 10.1083/jcb.133.3.667

18. Schepers GE, Teasdale RD, Koopman P. Twenty pairs of sox: extent, homology, and nomenclature of the mouse and human sox transcription factor gene families. *Dev Cell* (2002) 3:167–70. doi: 10.1016/S1534-5807(02)00223-X

19. Tan DS, Holzner M, Weng M, Srivastava Y, Jauch R. SOX17 in cellular reprogramming and cancer. *Semin Cancer Biol* (2020) 67:65–73. doi: 10.1016/j.semcancer.2019.08.008

20. Kim I, Saunders TL, Morrison SJ. Sox17 dependence distinguishes the transcriptional regulation of fetal from adult hematopoietic stem cells. *Cell* (2007) 130:470–83. doi: 10.1016/j.cell.2007.06.011

21. Sakamoto Y, Hara K, Kanai-Azuma M, Matsui T, Miura Y, Tsunekawa N, et al. Redundant roles of Sox17 and Sox18 in early cardiovascular development of mouse embryos. *Biochem Biophys Res Commun* (2007) 360:539–44. doi: 10.1016/j.bbrc.2007.06.093

22. Tanaka A, Watanabe S. Can cytoplasmic donation rescue aged oocytes? *Reprod Med Biol* (2018) 18:128–39. doi: 10.1002/rmb2.12252

23. Clarke RL, Yzaguirre AD, Yashiro-Ohtani Y, Bondue A, Blanpain C, Pear WS, et al. The expression of Sox17 identifies and regulates haemogenic endothelium. *Nat Cell Biol* (2013) 15:502–10. doi: 10.1038/ncb2724

24. Francois M, Koopman P, Beltrame M. SoxF genes: key players in the development of the cardio-vascular system. *Int J Biochem Cell Biol* (2010) 42:445–8. doi: 10.1016/j.biocel.2009.08.017

25. Sinner D, Kordich JJ, Spence JR, Opoka R, Rankin S, Lin SC, et al. Sox17 and Sox4 differentially regulate beta-catenin/T-cell factor activity and proliferation of colon carcinoma cells. *Mol Cell Biol* (2007) 27:7802–15. doi: 10.1128/MCB.02179-06

26. Fu DY, Wang ZM, Li-Chen, Wang BL, Shen ZZ, Huang W, Shao ZM. Sox17, the canonical wnt antagonist, is epigenetically inactivated by promoter methylation in human breast cancer. *Breast Cancer Res Treat* (2010) 119:601–12. doi: 10.1007/s10549-009-0339-8

27. Merino-Azpitarte M, Lozano E, Perugorria MJ, Esparza-Baquer A, Erice O, Santos-Laso Á, et al. SOX17 regulates cholangiocyte differentiation and acts as a tumor suppressor in cholangiocarcinoma. *J Hepatol* (2017) 67:72–83. doi: 10.1016/j.jhep.2017.02.017

28. Pierson Smela M, Sybirna A, Wong FCK, Surani MA. Testing the role of SOX15 in human primordial germ cell fate. *Wellcome Open Res* (2019) 4:122. doi: 10.12688/wellcomeopenres.15381.1

29. Maniglio P, Ricciardi E, Laganà AS, Triolo O, Caserta D. Epigenetic modifications of primordial reproductive tract: a common etiologic pathway for Mayer-Rokitansky-Kuster-Hauser syndrome and endometriosis? *Med Hypotheses.* (2016) 90:4–5. doi: 10.1016/j.mehy.2016.02.015

30. Chen D, Sun N, Hou L, Kim R, Faith J, Aslanyan M, et al. Human primordial germ cells are specified from lineage-primed progenitors. *Cell Rep* (2019) 29:4568–4582.e5. doi: 10.1016/j.celrep.2019.11.083

31. Tang WW, Dietmann S, Irie N, Leitch HG, Floros VI, Bradshaw CR, et al. A unique gene regulatory network resets the human germline epigenome for development. *Cell* (2015) 161:1453–67. doi: 10.1016/j.cell.2015.04.053

32. Guo F, Yan L, Guo H, Li L, Hu B, Zhao Y, et al. The transcriptome and DNA methylome landscapes of human primordial germ cells. *Cell* (2015) 161:1437–52. doi: 10.1016/j.cell.2015.05.015

33. Sosa E, Chen D, Rojas EJ, Hennebold JD, Peters KA, Wu Z, et al. Differentiation of primate primordial germ cell-like cells following transplantation into the adult gonadal niche. *Nat Commun* (2018) 9:5339. doi: 10.1038/s41467-018-07740-7

34. Sasaki K, Nakamura T, Okamoto I, Yabuta Y, Iwatani C, Tsuchiya H, et al. The germ cell fate of cynomolgus monkeys is specified in the nascent amnion. *Dev Cell* (2016) 39:169–85. doi: 10.1016/j.devcel.2016.09.007

35. Stoop H, Honecker F, Cools M, de Krijger R, Bokemeyer C, Looijenga LH. Differentiation and development of human female germ cells during prenatal gonadogenesis: an immunohistochemical study. *Hum Reprod* (2005) 20:1466–76. doi: 10.1093/humrep/deh800

36. Yang GC, Wang RR, Liu ZQ, Ma KY, Feng JB, Qiu GF. Alternative splice variants and differential relative abundance patterns of vasa mRNAs during gonadal development in the Chinese mitten crab eriocheir sinensis. *Anim Reprod Sci* (2019) 208:106131. doi: 10.1016/j.anireprosci.2019.106131

37. Parte S, Bhartiya D, Patel H, Daithankar V, Chauhan A, Zaveri K, et al. Dynamics associated with spontaneous differentiation of ovarian stem cells in vitro. *J Ovarian Res* (2014) 7:25. doi: 10.1186/1757-2215-7-25

38. Anderson RA, Fulton N, Cowan G, Coutts S, Saunders PT. Conserved and divergent patterns of expression of DAZL, VASA and OCT4 in the germ cells of the human fetal ovary and testis. *BMC Dev Biol* (2007) 7:136. doi: 10.1186/1471-213X-7-136

39. Sybirna A, Wong FCK, Surani MA. Genetic basis for primordial germ cells specification in mouse and human: conserved and divergent roles of PRDM and SOX transcription factors. *Curr Top Dev Biol* (2019) 135:35–89. doi: 10.1016/bs.ctdb.2019.04.004

40. Stefanovic S, Abboud N, Désilets S, Nury D, Cowan C, Pucéat M. Interplay of Oct4 with Sox2 and Sox17: a molecular switch from stem cell pluripotency to specifying a cardiac fate. *J Cell Biol* (2009) 186:665–73. doi: 10.1083/jcb.200901040

41. Aksoy I, Jauch R, Chen J, Dyla M, Divakar U, Bogu GK, et al. Oct4 switches partnering from Sox2 to Sox17 to reinterpret the enhancer code and specify endoderm. *EMBO J* (2013) 32:938–53. doi: 10.1038/emboj.2013.31

42. Konishi I, Fujii S, Okamura H, Parmley T, Mori T. Development of interstitial cells and ovigerous cords in the human fetal ovary: an ultrastructural study. *J Anat.* (1986) 148:121–35.

43. Fulton N, Martins da Silva SJ, Bayne RA, Anderson RA. Germ cell proliferation and apoptosis in the developing human ovary. *J Clin Endocrinol Metab* (2005) 90:4664–70. doi: 10.1210/jc.2005-0219

44. Kurilo LF. Oogenesis in antenatal development in man. *Hum Genet* (1981) 57:86–92. doi: 10.1007/BF00271175

45. Baker TG. A quantitative and cytological study of germ cells in human ovaries. *Proc R Soc Lond B Biol Sci* (1963) 158:417–33. doi: 10.1098/rspb.1963.0055

46. Liu Y, Wu C, Lyu Q, Yang D, Albertini DF, Keefe DL, et al. Germline stem cells and neo-oogenesis in the adult human ovary. *Dev Biol* (2007) 306:112–20. doi: 10.1016/j.ydbio.2007.03.006

47. Vitale SG, La Rosa VL, Rapisarda AMC, Laganà AS. Fertility preservation in women with gynaecologic cancer: the impact on quality of life and psychological well-being. *Hum Fertil (Camb).* (2018) 21(1):35–8. doi: 10.1080/14647273.2017.1339365

frontiers | Frontiers in Endocrinology

TYPE Original Research
PUBLISHED 28 November 2023
DOI 10.3389/fendo.2023.1293358

OPEN ACCESS

EDITED BY
Akira Iwase,
Gunma University, Japan

REVIEWED BY
Emerson Oliveira,
Faculdade de Medicina do ABC, Brazil
Victor Manuel Pulgar,
Campbell University, United States

*CORRESPONDENCE
Weiwei Zhang
sxbqeyyzww@163.com
Xiaochun Liu
tyxchliu@163.com

†These authors have contributed equally to this work

RECEIVED 13 September 2023
ACCEPTED 07 November 2023
PUBLISHED 28 November 2023

CITATION
Li Y, Chang J, Shi G, Zhang W, Wang H, Wei L, Liu X and Zhang W (2023) Effects of stellate ganglion block on perimenopausal hot flashes: a randomized controlled trial. *Front. Endocrinol.* 14:1293358. doi: 10.3389/fendo.2023.1293358

Effects of stellate ganglion block on perimenopausal hot flashes: a randomized controlled trial

Ying Li[1†], Jia Chang[2†], Gaoxiang Shi[1], Wenjing Zhang[1], Hui Wang[1], Lingyun Wei[1], Xiaochun Liu[1*] and Weiwei Zhang[1*]

[1]Third Hospital of Shanxi Medical University, Shanxi Bethune Hospital, Shanxi Academy of Medical Sciences, Tongji Shanxi Hospital, Taiyuan, China, [2]School of Nursing, Shanxi Medical University, Taiyuan, China

Background: Hot flashes are common symptoms afflicting perimenopausal women. A stellate ganglion block (SGB) is believed to be an effective treatment for hot flashes; however, more evidence is needed to evaluate its safety and efficacy in relieving perimenopausal hot flashes.

Objective: To investigate the efficacy and safety of SGB for the treatment of perimenopausal hot flashes.

Methods: A randomized controlled trial was conducted at Shanxi Bethune Hospital. Forty perimenopausal women with hot flashes were recruited from April 2022 to November 2022 and randomly assigned to receive either 6 consecutive SGB treatments or 6 consecutive saline placebo treatments. The primary outcome was the change in hot flash symptom score from baseline to 12 weeks after treatment. The secondary outcomes were the change in hot flash symptom score from baseline to 12 weeks after treatment and the post-treatment Kupperman Index (KI) and Pittsburgh Sleep Quality Index (PSQI) scores.

Results: Of the 40 randomized subjects, 35 completed the study. All the variables were significantly improved. During 12 weeks of follow-up, the hot flash scores, Kupperman Menopause Scale scores, and Pittsburgh Sleep Quality Scale scores decreased significantly. Two subjects in the SGB treatment group experienced transient hoarseness, and the incidence of related adverse events was 10%. No related adverse events occurred in the control group.

Conclusion: Compared to the control treatment, SGB treatment was a safe and effective nonhormone replacement therapy that significantly relieved perimenopausal hot flashes and effectively improved sleep quality. Additional studies are needed to assess the long-term efficacy of this therapy.

KEYWORDS

stellate ganglion block, perimenopause, hot flashes, sleep quality, Kupperman Index and Pittsburgh Sleep Quality Index

1 Introduction

Hot flashes, the most common symptoms of perimenopause, are characterized by sudden fluctuations in body temperature, as well as redness and profuse sweating of the face and neck, sometimes accompanied by chills (1). Although vasomotor disturbances, such as hot flashes, are not an organic impairment, severe hot flashes can significantly impact quality of life by increasing the risk of disrupted sleep, depression and anxiety, cognitive changes, and other serious illnesses. The incidence of hot flashes increases significantly during menopause, peaking in late perimenopause or early menopause, with approximately 80% of postmenopausal women experiencing hot flashes (2, 3). It has been reported that the incidence of hot flashes in sexually mature, perimenopausal, and menopausal women is as high as 21%, 30%, and 36%, respectively (4). It is extremely important to identify effective treatments to relieve the symptoms or reduce the incidence of hot flashes in perimenopausal and postmenopausal women.

Hormone replacement therapy is by far the most effective treatment for hot flashes(5), with an efficiency rate of 80-90% (6), but the frequency of replacement therapy is greatly limited by complications, such as headaches, premenstrual irritability and vaginal bleeding (7, 8), and contraindications, such as high risks of breast cancer, chronic heart disease, stroke or venous thromboembolism (9), and the possible risk of cancer due to hormones.

Some nonhormone replacement therapies or drug therapies are currently available. Paroxetine, a selective 5-hydroxytryptamine reuptake inhibitor (SSRI), is an effective and safe drug that has been approved for the relief of hot flashes as it significantly reduces hot flash scores despite being less effective than hormone replacement therapy (10). Venlafaxine, a selective norepinephrine reuptake inhibitor (SNRI), has also been shown to improve vasomotor symptoms, but there have been reports of interruption of treatment due to complications such as acute anemia (11). In addition, the effects of more moderate drugs, such as phytoestrogens and vitamin E, on hot flashes have been studied, and the results have been less than satisfactory[12]. It is necessary to look for a more effective and safer nonhormone replacement therapy to manage hot flashes in perimenopausal women.

A stellate ganglion block (SGB) is a well-established technique that is widely used to relieve sympathetic-mediated pain and improve vasomotor dysfunction by blocking the sympathetic ganglia in the lower cervical and upper thoracic spine with local anesthetic agents (12). Due to equipment improvements and technological innovations, SGB technology has evolved from blind puncture to precise puncture under guidance of X-rays and ultrasound. Ultrasound during SGB displays important anatomical structures such as blood vessels, thus greatly reducing the possibility of causing damage to important structures such as blood vessels, and significantly improving the safety of the procedure (13).

The exact mechanism by which SGB relieves hot flashes has not yet been clarified. It is hypothesized that SGB may relieve hot flashes by temporarily blocking the central temperature regulation mechanism (14). The effectiveness of SGB for hot flashes has been explored in breast cancer survivors. The results of previous experimental studies have shown good efficacy of SGB for hot flashes with relatively low rates of complications (15). The aim of our current study was to evaluate the safety and efficacy of SGB for the treatment of hot flashes in perimenopausal women through a prospective randomized controlled trial.

2 Methods

2.1 Participant

This was a single-blind randomized controlled trial with a follow-up period of three months that was conducted in Shanxi Bethune Hospital. Forty women who were aged 48-52 years with a gynecologic diagnosis of perimenopausal hot flashes were included in this study. The women had regular menstruation in the past. Women with acute infection, cardiorespiratory dysfunction, hepatic and renal insufficiency, neuropsychiatric disease, communication difficulties, coagulation disorders, who had undergone anticoagulant therapy, or were unable to be followed up were excluded from the study. The clinical trial protocol of this study was reviewed and approved by the Medical Ethics Committee of Shanxi Bethune Hospital (YXLL-2021-083), and registered in the Chinese Clinical Trials Registry (ChiCTR2300070017). All subjects signed the "Informed Consent" form before participating in this study, and all injections were performed by the same experienced anesthesiologist.

2.2 Randomization and blinding

The random number table method was used to achieve random grouping. Forty subjects were numbered from 1 to 40 in the order of their visit. Starting from any number in the random number table, a random number was assigned to each subject in turn. The 40 random numbers were arranged from small to large; odd random numbers were included in the experimental group, and even random numbers were included in the control group.

Double-blinding was impossible for this study because the presence of prominent Horner's syndrome (ptosis, miosis, conjunctival hyperemia facial anhidrosis) on the same side was a sign of successful SGB block. Therefore, this was a single-blind trial, that is, the subjects were not informed of their grouping.

2.3 Operating procedure

The SGB procedures were performed under ultrasound guidance, and the operation was as follows. The patients were placed in the supine position, with their head turned to one side. A GE-LOGIQ5 ultrasonic diagnostic instrument was used for scanning, and the frequency of the ultrasonic probe was set to 10 MHz. Ultrasonic imaging was performed on the axial plane at the level of the cricoid cartilage, and the internal carotid artery and

internal jugular vein were carefully distinguished. The stellate ganglion was located on the surface of the longus carotid muscle below the oblique internal carotid artery, and the 6th cervical vertebral body and the pretransverse tubercle stellate ganglion were punctured to a depth of 3.0-3.5 cm under ultrasound guidance, ensuring that no blood, cerebrospinal fluid or gas leaked, and 5 ml of 0.5% ropivacaine was infused slowly (Figure 1A). The needle tip was adjusted appropriately during the injection process so that the liquid could fully infiltrate the internal carotid artery, the cervical transverse process, and the entire stellate ganglion tissue. After the injection was completed (Figure 1B), the puncture point was compressed to stop bleeding for 5 minutes and the patient was changed to an upright sitting position. The anesthesiologist evaluated the patient for Horner syndrome and other adverse effects within 30 minutes (16). SGB treatment was performed once a day, alternating between the left and right side, for a total of 6 times. The saline control group was treated by the same operator in the same way, and 5 ml of 0.9% saline was used for the injection. In each group, the anesthesia machine, monitor, auxiliary ventilation equipment and other rescue equipment were in a standby state and equipped with necessary first aid drugs. The patients' vital signs were monitored throughout the operation, and whether there was any abnormality in the patients' consciousness or breathing were assessed. After the operation, the subjects were called back every week to ask whether there were any adverse reactions, and the subjects were reminded to follow up at the hospital on time.

SCMM, sternocleidomastoid muscle; IJV, internal jugular vein; ICA, internal carotid artery; LCM, longus collimuscle.

2.4 Observed indicators

Hot flashes were quantified using a hot flash score for patients at baseline (one week before operation) and during follow-up. The hot flash score was obtained by multiplying the severity of hot flashes and the frequency of daily hot flashes (17). The severity of hot flashes was assessed using the scale reported in the Gwen Finck study, and the severity of hot flashes was divided into five grades (none= 0, mild=1, moderate=2, severe=3, very severe=4) (18).

Menopausal symptoms and sleep quality were quantified at baseline and during follow-up using the Kupperman Self-Rating Scale for Female Menopause and the Pittsburgh Sleep Quality Scale for further evaluation and analysis. The Kupperman self-rating scale is used to assess common symptoms of menopause, such as hot flashes, sweating, insomnia, etc., and assigns different weighting coefficients and adds them one by one to obtain the final Kupperman score (perimenopausal syndrome: mild: 15-20, moderate: 20-35, severe: > 35) (19). The Pittsburgh Sleep Quality Scale consists of 19 self-rated items grouped into 7 categories: subjective sleep quality, sleep latency, sleep duration, habitual sleep efficiency, cumulative sleep disturbance problems, sleep medication use, and daytime dysfunction. The scores from each category are added to obtain the final score (0-5: good sleep quality; 6-10: OK sleep quality; 11-15: average sleep quality; 16-20: poor sleep quality) (20). Lower scores indicate better relief of hot flashes and menopausal symptoms and improved sleep quality.

2.5 Statistical analysis

The sample size was estimated based on data from previous studies in the literature (21), assuming a one-sided significance level of 0.05 and a test efficacy of 90%, and 20 cases per group were required with an estimated 20% loss to follow-up. The flow chart of this study is shown in Figure 2.

Quantitative data are described as the mean ± standard deviation. For those with a normal distribution, one-way ANOVA was used to analyze the differences in each indicator at the four specified time points. The data of the two groups at the 4 specified

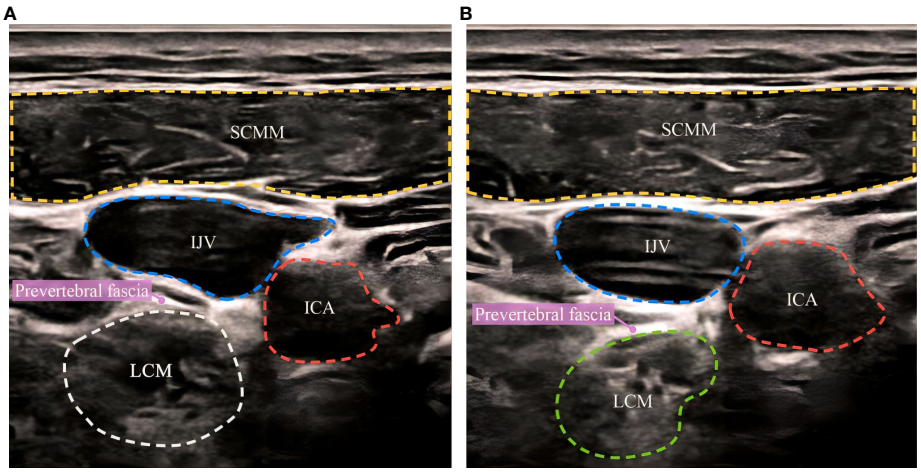

FIGURE 1
Ultrasound-guided stellate ganglion block before and after. **(A)** before SGB, **(B)** after SGB. SCMM, sternocleidomastoid muscle; IJV, internal jugular vein; ICA, internal carotid artery; LCM, longus collimuscle.

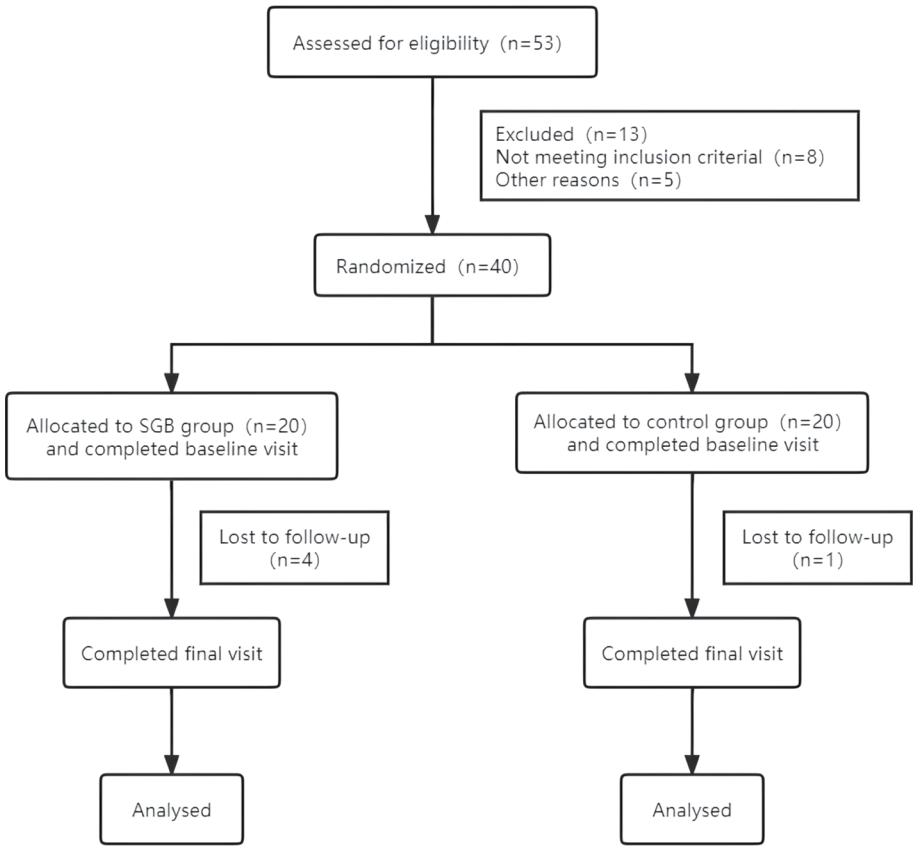

FIGURE 2
Flowchart for participant selection.

time points were compared between the groups. Homogenous and unequal variances were analyzed with t tests. Those nonnormally distributed were tested by the Wilcoxon rank sum test. The chi-square test was used to compare the differences in the incidence of adverse events between the two groups.

IBM SPSS 26.0 was used for statistical analysis, and a P value < 0.05 was considered statistically significant.

3 Results

3.1 General characteristics

Forty women with a gynaecologic diagnosis of perimenopausal hot flashes underwent a three-month intervention and follow-up (Figure 2); 20 were included in the SGB treatment group and 20 were included in the saline control group. During the follow-up period, five patients were lost to follow-up, four of whom were in the SGB group (one patient was not followed up due to postoperative hoarseness, two patients did not participate in follow-up beyond 8 weeks due to unknown reasons, and one patient did not undergo the operation due to the impact of the COVID-19 pandemic). There was one case in the control group (the follow-up at the 12th week after the operation was not performed due to ineffective treatment).

Table 1 shows the population and basic clinical characteristics of the SGB group and control group, and no statistically significant differences were observed between the two groups. There was no significant difference in hot flash score, hot flash frequency,

TABLE 1 Demographic and clinical characteristics of the treatment group at baseline.

	treatment group		P
	SGB(n=20)	control(n=20)	
age(y)	49.60 ± 1.43	49.75 ± 1.37	0.737
BMI(kg/m2)	23.47 ± 2.02	22.58 ± 1.67	0.134
Menstrual disorder how long(m)	5.65 ± 1.46	5.85 ± 1.42	0.664
KI score	28.90 ± 8.71	26.85 ± 12.64	0.554
PSQI score	10.80 ± 1.89	11.20 ± 2.82	0.601
hot flash score	15.55 ± 14.72	15.15 ± 5.37	0.910
diary flush frequency	10.15 ± 6.80	10.55 ± 3.44	0.816

The general data of the subjects in the two groups are presented as the mean ± standard deviation. SGB, stellate ganglion block; BMI, body mass index; KI, Kupperman index; PSQI, Pittsburgh Sleep Quality Index. There were no statistically significant differences in the general data between the two groups.

Kupperman score, or Pittsburgh sleep quality score between the two groups before the intervention (at baseline), and they were comparable.

3.2 Main results

The subjects' hot flash scores and hot flash frequency data are shown in Table 2. At baseline, the mean hot flash score in the SGB group was 15.55 (95% CI, 8.66-22.44), of which 55% were mild and 45% were moderate. The mean hot flash score in the saline group was 15.15 (95% CI, 12.64-17.66), with 50% being mild and 50% being moderate. The statistical analysis of hot flash score and hot flash frequency showed that in the 12th week, hot flash symptoms were significantly relieved in the SGB group, with an average difference of 13.92 and 8.52, respectively. The difference was statistically significant. The control group showed no statistically significant change from baseline.

As shown in Figure 3, the SGB group had the greatest relief of hot flashes during the first 4 weeks of follow-up, with a reduction of 10.1 and 4.7 in hot flash score and hot flash frequency, respectively, when compared with the baseline.

Data points represent the mean value for each time point.

3.3 Secondary results

As shown in Figure 4, compared with that in the control group, the Kupperman Menopause Scale score in the SGB group was more greatly decreased from the baseline. The mean decrease was 17.90 in the 4th week, 21.79 in the 8th week, and 22.15 in the 12th week. The Kupperman scores during the follow-up period were significantly different in the between-group analysis (Table 3).

Data points represent the mean value for each time point.

Changes in Pittsburgh Sleep Scale scores from baseline to the 12th week were similar to changes in the Kupperman Menopause Scale scores.

3.4 Safety evaluation

Only 2 participants in the SGB group had transient hoarseness, a treatment-related adverse event, that did not recur during the follow-up period. No adverse events unrelated to treatment occurred. Participants in the control group did not report any adverse reactions (Table 4).

4 Discussion

SGB is widely used in the treatment of chronic pain and complex regional localized pain syndrome (22–24) as it improves the prognosis of drug-refractory ventricular arrhythmias (25) and posttraumatic stress disorders (PTSD) (26). Currently, the impact of SGB on vasodilatory symptoms, such as hot flashes and night sweats, has been studied in depth (27).

The clinical data related to the effect of SGB on hot flash treatment are limited, and most are case reports, so the level of evidence is not high (28). Due to its invasive nature and lack of evidence from large, long-term randomized controlled trials, the North American Menopause Society classified SGB as a cautionary recommendation, and more trials are needed to demonstrate its safety and efficacy[12]. This is the first randomized controlled trial to study the effect of SGB on hot flashes in normal perimenopausal women.

SGB is considered a relatively safe clinical procedure, with a serious adverse reaction rate of 1.7/1000 as reported by Wulf and

TABLE 2 Comparison of hot flash indicators between the two groups of subjects at different time points.

		baseline	4 weeks	8 weeks	12 weeks
		n = 20	n_{SGB} = 16, n_{cont} = 19		
hot flash score	SGB	15.55 ± 14.72	5.45 ± 3.55[a]	3.85 ± 2.60[b]	1.63 ± 0.74[c]
	control	15.15 ± 5.37	13.95 ± 4.39[a]*	15.00 ± 5.76[b]*	15.30 ± 5.48[c]*
	P value	0.910	<0.001	<0.001	<0.001
diary flush frequency	SGB	10.15 ± 6.80	5.45 ± 3.55[a]	3.85 ± 2.60[b]	1.63 ± 0.74[c]
	control	10.55 ± 3.44	9.70 ± 2.56[a]*	10.25 ± 2.88[b]*	10.70 ± 3.54[c]*
	P value	0.816	<0.001	<0.001	<0.001
Hot flash severity	SGB	1.45 ± 0.51	1.00 ± 0.00[a]	0.80 ± 0.41[b]	0.63 ± 0.49[c]
	control	1.50 ± 0.51	1.50 ± 0.51[a]*	1.50 ± 0.51[b]*	1.50 ± 0.51[c]*
	P value	0.759	<0.001	<0.001	<0.001

[a]compared to the baseline, P<0.05.
[b]compared to the baseline, P<0.05.
[c]compared to the baseline, P<0.05.
*compared to the SGB group, P<0.001.

10.3389/fendo.2023.1293358

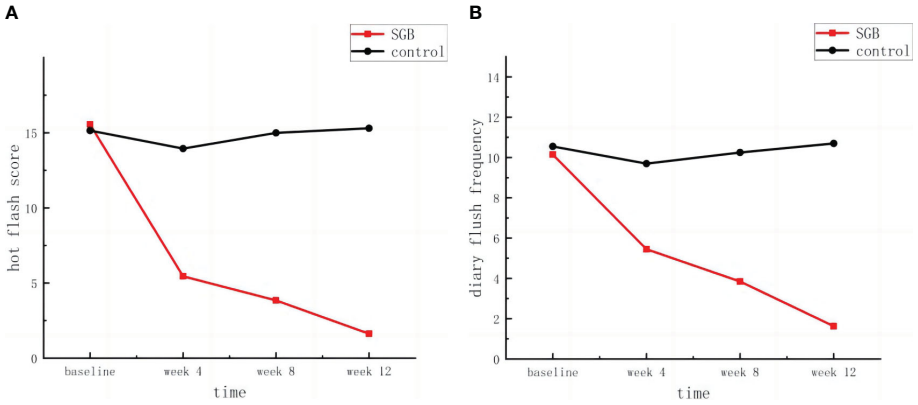

FIGURE 3
(A) Hot flash score and, **(B)** diary flush frequency.

Maier (29). Most complications are temporary and mostly found during or shortly after the procedure; the most common adverse events are hoarseness and dizziness (30). During the three-month follow-up of the subjects in this study, only 2 showed temporary hoarseness within a few hours after SGB, but no adverse reactions recurred during the follow-up period. In addition, there were no reports of serious adverse reactions or events unrelated to treatment. This study provides additional clinical evidence for the safety of SGB.

The mechanism of SGB in preventing and treating hot flashes has not yet been elucidated as it is a block of sympathetic nerve conduction. Lipov believes that the therapeutic effect is based on interrupting the connection between the central nervous system and the sympathetic nervous system (31). Freedman proposed that the thermoneutral zone is narrowed, that the caudate nucleus may be stimulated by environmental stress in a state of sympathetic excitation and that SGB can reduce the stress of sympathetic stimulation and restore the normal state (5). In addition, the therapeutic effect of SGB may also involve the reduction of nerve growth factor levels (32).

SGB was initially used in the treatment of hyperhidrosis, which has similarities to hot flashes in terms of symptom presentation (33). Walega's study showed that SGB treatment can significantly reduce vasomotor symptoms in postmenopausal women (34). In our study, improvement in hot flash symptoms was observed according to the hot flash score, similar to the results of a previous study (15). Consistent with the results of Walega's study, subjects treated with SGB had significantly less severe and less frequent hot flashes over the 12-week follow-up period, with a 13.92 reduction in hot flash scores and an 8.52 reduction in hot flash frequency after SGB treatment. Additionally, we found that the effect was most pronounced in the first 4 weeks after treatment, which is consistent with the findings reported by Haest (15). However, Rahimzadeh found that the greatest degree of remission was observed at 2 weeks postoperatively, and we were unable perform a comparison with this result due to the relatively long

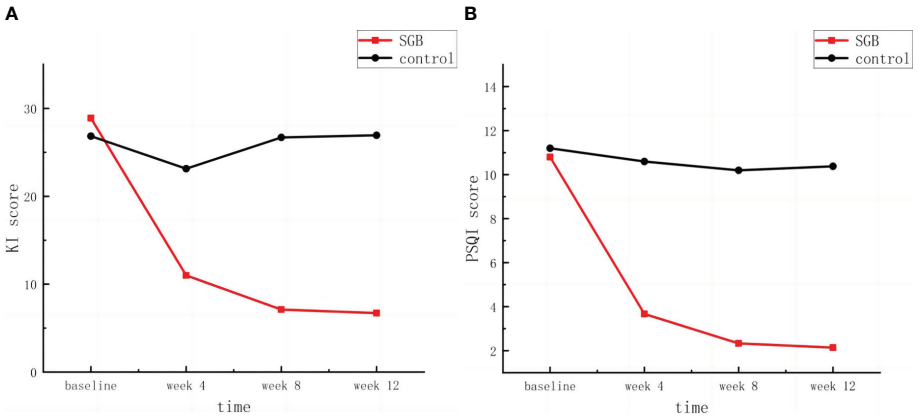

FIGURE 4
(A) Kupperman index score and **(B)** Pittsburgh sleep quality index score.

TABLE 3 Comparison of the Kupperman index score and Pittsburgh sleep quality index score between the two groups of subjects at different time points.

		baseline	4 weeks	8 weeks	12 weeks
		n = 20	n_{SGB} = 16, n_{cont} = 19		
KI score	SGB	28.90 ± 8.71	11.00 ± 4.06[a]	7.11 ± 2.93[b]	6.71 ± 3.63[c]
	control	26.85 ± 12.64	23.15 ± 9.79[a]*	26.70 ± 12.01[b]*	26.95 ± 13.19[c]*
	P value	0.554	<0.001	<0.001	<0.001
PSQI score	SGB	10.80 ± 1.88	3.67 ± 1.53a	2.33 ± 1.61b	2.14 ± 1.87c
	control	11.20 ± 2.82	10.60 ± 2.60[a]*	10.20 ± 2.14[b]*	10.38 ± 2.58[c]*
	P value	0.601	<0.001	<0.001	<0.001

KI, Kupperman index; PSQI, Pittsburgh Sleep Quality Index.
[a]compared to the baseline, P<0.05.
[b]compared to the baseline, P<0.05.
[c]compared to the baseline, P<0.05.
*compared to the SGB group, P<0.001.

TABLE 4 The incidence of adverse events in the two groups.

	hoarseness	dizziness	cough	upper limb numbness	pneumothorax	infections at the puncture site	haematoma at the puncture site	total
SGB	2(10%)	0(0)	0(0)	0(0)	0(0)	0(0)	0(0)	2 (10%)
Control	0(0)	0(0)	0(0)	0(0)	0(0)	0(0)	0(0)	0(0)
χ^2 value	0.526							
P value	0.468							

There were no statistically significant differences in the safety evaluation between the two groups.

follow-up interval (35). However, Othman's study showed a statistically significant increase in hot flash frequency at 4 weeks postoperatively (36). This suggests that additional randomized controlled trials are needed to verify changes in the frequency of hot flashes after 4 weeks of treatment. The hot flash scores were further decreased at the two-month follow-up, but the downwards trend gradually slowed. Our findings support the feasibility of SGB for the treatment of hot flashes in perimenopausal women.

Sleep disturbance is another major concern for perimenopausal women and is often accompanied by hot flashes (37). In the current study, sleep quality improved as the severity and frequency of hot flashes were reduced. That is, there was a significant improvement in the first 4 weeks, and the improvement in sleep quality was relatively slight after 4 weeks. Similarly, other perimenopausal symptoms (such as irritability, dyspareunia, dizziness, fatigue, etc.) were significantly improved along with the improvement of hot flashes and sleep quality.

This study has certain limitations. First, the patients who underwent SGB treatment exhibited significant Horner syndrome, which prevented double-blinding between the investigator and the study subjects and caused possible subjective information bias of the investigator. Second, the sample size of this study was relatively small, not a multicentre, large-sample clinical study with good representation, and PP analysis may have caused overestimation of the treatment effect and reduced the reliability of the experimental results. Third, the goal of this trial is to seek a long-term effective method to alleviate hot flashes in perimenopausal or even postmenopausal women, and the follow-up period of this trial is far from adequate due to research funding constraints and other reasons. Fourth, the time interval between the subjects' visits to the hospital and the evaluation was too long, and our trial indicators, including hot flash score, hot flash frequency, Kupperman scale, and Pittsburgh sleep scale, originated from subjects' subjective evaluation. Fifth, in our trial, we only compared the efficacy of SGB with that of saline and did not compare the difference between hormone replacement therapy, paroxetine, or any other pharmacological treatments. A comparison of the safety and efficacy of several therapies would have revealed the best recommendation for hot flash relief.

5 Conclusion

A SGB was safe and effective for relieving hot flashes and improving sleep quality in perimenopausal women in a 3-month

study. Larger sample sizes, longer follow-up times, and more frequent follow-up are needed to further understand the long-term efficacy and mechanism of action of this treatment modality.

Data availability statement

The raw data supporting the conclusions of this article will be made available by the authors, without undue reservation.

Ethics statement

The studies involving humans were approved by Medical Ethics Committee, Shanxi Academy of Medical Sciences, Shanxi Bethune Hospital. The studies were conducted in accordance with the local legislation and institutional requirements. The participants provided their written informed consent to participate in this study. Written informed consent was obtained from the individual(s) for the publication of any potentially identifiable images or data included in this article.

Author contributions

YL: Writing – original draft. JC: Writing – original draft. GS: Writing – review & editing. WJZ: Writing – review & editing. HW: Writing – review & editing. LW: Writing – review & editing. XL: Writing – review & editing. WWZ: Writing – review & editing.

Funding

The author(s) declare financial support was received for the research, authorship, and/or publication of this article. The Scientific research project of Shanxi Provincial Health Commission 253 (#2022068 to WWZ), The National Natural Science Foundation of China (#81971365 to XL), The Key Research and Development Program of Shanxi Province (International Scientific and Technological Cooperation) (#201903D421060 to XL), The basic research general project of Shanxi Provincial Department of Science and Technology (#202203021221245 to WWZ), China Zhongguancun Precision Medicine Science and Technology Foundation (#Z-2021-002 to WWZ).

Conflict of interest

The authors declare that the research was conducted in the absence of any commercial or financial relationships that could be construed as a potential conflict of interest.

Publisher's note

All claims expressed in this article are solely those of the authors and do not necessarily represent those of their affiliated organizations, or those of the publisher, the editors and the reviewers. Any product that may be evaluated in this article, or claim that may be made by its manufacturer, is not guaranteed or endorsed by the publisher.

References

1. Monteleone P, Mascagni G, Giannini A, Genazzani AR, Simoncini T. Symptoms of menopause - global prevalence, physiology and implications. *Nat Rev Endocrinol* (2018) 14(4):199–215. doi: 10.1038/nrendo.2017.180

2. Woods NF, Mitchell ES. Symptoms during the perimenopause: prevalence, severity, trajectory, and significance in women's lives. *Am J Med* (2005) 118 Suppl 12B:14–24. doi: 10.1016/j.amjmed.2005.09.031

3. Gold EB, Colvin A, Avis N, Bromberger J, Greendale GA, Powell L, et al. Longitudinal analysis of the association between vasomotor symptoms and race/ethnicity across the menopausal transition: study of women's health across the nation. *Am J Public Health* (2006) 96(7):1226–35. doi: 10.2105/AJPH.2005.066936

4. O'Bryant SE, Palav A, McCaffrey RJ. A review of symptoms commonly associated with menopause: implications for clinical neuropsychologists and other health care providers. *Neuropsychol Rev* (2003) 13(3):145–52. doi: 10.1023/a:1025573529407

5. Freedman RR. Menopausal hot flashes: mechanisms, endocrinology, treatment. *J Steroid Biochem Mol Biol* (2014) 142:115–20. doi: 10.1016/j.jsbmb.2013.08.010

6. Maclennan AH, Broadbent JL, Lester S, Moore V. Oral oestrogen and combined oestrogen/progestogen therapy versus placebo for hot flushes. *Cochrane Database system Rev* (2004) 2004(4):Cd002978. doi: 10.1002/14651858.CD002978.pub2

7. Bjorn I, Backsrom T. Drug related negative side-effects is a common reason for poor compliance in hormone replacement therapy. *Maturitas* (1999) 32(2):77–86. doi: 10.1016/s0378-5122(99)00018-3

8. Bakken K, Eggen AE, Lund E. Side-effects of hormone replacement therapy and influence on pattern of use among women aged 45-64 years. The Norwegian Women and Cancer (NOWAC) study 1997. *Acta obstet gynecol Scandinavica* (2004) 83(9):850–6. doi: 10.1111/j.0001-6349.2004.00560.x

9. Rossouw JE, Anderson GL, Prentice RL, LaCroix AZ, Kooperberg C, Stefanick ML, et al. Writing Group for the Women's Health Initiative, I., Risks and benefits of estrogen plus progestin in healthy postmenopausal women: principal results From the Women's Health Initiative randomized controlled trial. *Jama* (2002) 288(3):321–33. doi: 10.1001/jama.288.3.321

10. Hill DA, Crider M, Hill SR. Hormone therapy and other treatments for symptoms of menopause. *Am Family phys* (2016) 94(11):884–9.

11. Ballon JS, Schulman MC. Venlafaxine and the rapid development of anasarca. *J Clin Psychopharmacol* (2006) 26(1):97–8. doi: 10.1097/01.jcp.0000195910.06246.aa

12. Gofeld M, Bhatia A, Abbas S, Ganapathy S, Johnson M. Development and validation of a new technique for ultrasound-guided stellate ganglion block. *Region Anesth Pain Med* (2009) 34(5):475–9. doi: 10.1097/AAP.0b013e3181b494de

13. Narouze S. Ultrasound-guided stellate ganglion block: safety and efficacy. *Curr Pain headache Rep* (2014) 18(6):424. doi: 10.1007/s11916-014-0424-5

14. Lipov EG, Joshi JR, Sanders S, Wilcox K, Lipov S, Xie H, et al. Effects of stellate-ganglion block on hot flushes and night awakenings in survivors of breast cancer: a pilot study. *Lancet Oncol* (2008) 9(6):523–32. doi: 10.1016/S1470-2045(08)70131-1

15. Haest K, Kumar A, Van Calster B, Leunen K, Smeets A, Amant F, et al. Stellate ganglion block for the management of hot flashes and sleep disturbances in breast cancer survivors: an uncontrolled experimental study with 24 weeks of follow-up. *Ann Oncol* (2012) 23(6):1449–54. doi: 10.1093/annonc/mdr478

16. Yan M, Liu X, Wang L, Tao W, Zhang X, Wang S, et al. Chinese expert consensus on stellate ganglion block therapy, (2022 edition). *Chin J Painol* (2022) 18(03):293–301.

17. Loprinzi CL, Barton DL, Rhodes D. Management of hot flashes in breast-cancer survivors. *Lancet Oncol* (2001) 2(4):199–204. doi: 10.1016/S1470-2045(00)00289-8

18. Finck G, Barton DL, Loprinzi CL, Quella SK, Sloan JA. Definitions of hot flashes in breast cancer survivors. *J Pain symp Manage* (1998) 16(5):327–33. doi: 10.1016/s0885-3924(98)00090-6

19. Szadowska-Szlachetka ZC, Stasiak E, Leziak A, Irzmańska-Hudziak A, Łuczyk M, Stanisławek A, et al. Intensity of menopausal symptoms and quality of life in

climacteric women. *Przeglad menopauzalny = Menopause Rev* (2019) 18(4):217–21. doi: 10.5114/pm.2019.93113

20. Buysse DJ, Reynolds CF 3rd, Monk TH, Berman SR, Kupfer DJ. The Pittsburgh Sleep Quality Index: a new instrument for psychiatric practice and research. *Psychiatry Res* (1989) 28(2):193–213. doi: 10.1016/0165-1781(89)90047-4

21. Guttuso T Jr. Stellate ganglion block for treating hot flashes: a viable treatment option or sham procedure? *Maturitas* (2013) 76(3):221–4. doi: 10.1016/j.maturitas.2013.08.001

22. Jeon Y. Therapeutic potential of stellate ganglion block in orofacial pain: a mini review. *J Dental Anesth Pain Med* (2016) 16(3):159–63. doi: 10.17245/jdapm.2016.16.3.159

23. Wie C, Gupta R, Maloney J, Pew S, Freeman J, Strand N. Interventional modalities to treat complex regional pain syndrome. *Curr Pain headache Rep* (2021) 25(2):10. doi: 10.1007/s11916-020-00904-5

24. Sousa LHA, de O Costa C, Novak EM, Giostri GS. Complex regional pain syndrome after carpal tunnel syndrome surgery: A systematic review. *Neurol India* (2022) 70(2):491–503. doi: 10.4103/0028-3886.344616

25. Wen S, Chen L, Wang TH, Dong L, Zhu ZQ, Xiong LL. The efficacy of ultrasound-guided stellate ganglion block in alleviating postoperative pain and ventricular arrhythmias and its application prospects. *Neurol Sci* (2021) 42(8):3121–33. doi: 10.1007/s10072-021-05300-4

26. Summers MR, Nevin RL. Stellate ganglion block in the treatment of post-traumatic stress disorder: A review of historical and recent literature. *Pain Pract* (2017) 17(4):546–53. doi: 10.1111/papr.12503

27. Maki PM, Rubin LH, Savarese A, Drogos L, Shulman LP, Banuvar S, et al. Stellate ganglion blockade and verbal memory in midlife women: Evidence from a randomized trial. *Maturitas* (2016) 92:123–9. doi: 10.1016/j.maturitas.2016.07.009

28. Guirguis M, Abdelmalak J, Jusino E, Hansen MR, Girgis GE. Stellate ganglion block for the treatment of hot flashes in patients with breast cancer: A literature review. *Ochsner J* (2015) 15(2):162–9.

29. Wulf H, Maier C. Complications and side effects of stellate ganglion blockade. Results of a questionnaire survey. *Anaesthesist* (1992) 41(3):146–51.

30. Goel V, Patwardhan AM, Ibrahim M, Howe CL, Schultz DM, Shankar H. Complications associated with stellate ganglion nerve block: a systematic review. *Region Anesth Pain Med* (2019) 44(6):rapm-2018-10012744(6):rapm-2018-100127. doi: 10.1136/rapm-2018-100127

31. Lipov EG, Lipov S, Joshi JR, Santucci VD, Slavin KV, Beck Vigue SG. Stellate ganglion block may relieve hot flashes by interrupting the sympathetic nervous system. *Med Hypotheses* (2007) 69(4):758–63. doi: 10.1016/j.mehy.2007.01.082

32. Lipov EG, Joshi JR, Sanders S, Slavin KV. A unifying theory linking the prolonged efficacy of the stellate ganglion block for the treatment of chronic regional pain syndrome (CRPS), hot flashes, and posttraumatic stress disorder (PTSD). *Med Hypotheses* (2009) 72(6):657–61. doi: 10.1016/j.mehy.2009.01.009

33. Sankstone A, Cornbleet T. Facial hyperhidrosis interruption with stellate ganglion block. *Jama* (1962) 179(7):571–1. doi: 10.1001/jama.1962.03050070077019a

34. Walega DR, Rubin LH, Banuvar S, Shulman LP, Maki PM. Effects of stellate ganglion block on vasomotor symptoms: findings from a randomized, controlled clinical trial in postmenopausal women. *Menopause (New York NY)* (2014) 21(8):807. doi: 10.1097/GME.0000000000000194

35. Rahimzadeh P, Imani F, Nafissi N, Ebrahimi B, Faiz SHR. Comparison of the effects of stellate ganglion block and paroxetine on hot flashes and sleep disturbance in breast cancer survivors. *Cancer Manage Res* (2018) 10:4831–7. doi: 10.2147/CMAR.S173511

36. Othman AH, Zaky AH. Management of hot flushes in breast cancer survivors: comparison between stellate ganglion block and pregabalin. *Pain Med (Malden Mass.)* (2014) 15(3):410–7. doi: 10.1111/pme.12331

37. Freedman RR, Roehrs TA. Lack of sleep disturbance from menopausal hot flashes. *Fertil steril* (2004) 82(1):138–44. doi: 10.1016/j.fertnstert.2003.12.029

frontiers | Frontiers in Endocrinology

TYPE Original Research
PUBLISHED 23 February 2024
DOI 10.3389/fendo.2024.1325386

OPEN ACCESS

EDITED BY
Akira Iwase,
Gunma University, Japan

REVIEWED BY
Eman Gohar,
Vanderbilt University Medical Center, United States
Trudy Ana Kohout,
Organon, United States

*CORRESPONDENCE
Sarah K. Schröder
saschroeder@ukaachen.de
Ralf Weiskirchen
rweiskirchen@ukaachen.de

RECEIVED 21 October 2023
ACCEPTED 06 February 2024
PUBLISHED 23 February 2024

CITATION
Schröder SK, Krizanac M, Kim P, Kessel JC and Weiskirchen R (2024) Ovaries of estrogen receptor 1-deficient mice show iron overload and signs of aging. *Front. Endocrinol.* 15:1325386. doi: 10.3389/fendo.2024.1325386

Ovaries of estrogen receptor 1-deficient mice show iron overload and signs of aging

Sarah K. Schröder*, Marinela Krizanac, Philipp Kim, Jan C. Kessel and Ralf Weiskirchen*

Institute of Molecular Pathobiochemistry, Experimental Gene Therapy and Clinical Chemistry (IFMPEGKC), Rheinisch-Westfälische Technische Hochschule (RWTH) University Hospital Aachen, Aachen, Germany

Introduction: Estrogens are crucial regulators of ovarian function, mediating their signaling through binding to estrogen receptors. The disruption of the estrogen receptor 1 (*Esr1*) provokes infertility associated with a hemorrhagic, cystic phenotype similar to that seen in diseased or aged ovaries. Our previous study indicated the possibility of altered iron metabolism in *Esr1*-deficient ovaries showing massive expression of lipocalin 2, a regulator of iron homeostasis.

Methods: Therefore, we examined the consequences of depleting *Esr1* in mouse ovaries, focusing on iron metabolism. For that reason, we compared ovaries of adult *Esr1*-deficient animals and age-matched wild type littermates.

Results and discussion: We found increased iron accumulation in *Esr1*-deficient animals by using laser ablation inductively coupled plasma mass spectrometry. Western blot analysis and RT-qPCR confirmed that iron overload alters iron transport, storage and regulation. In addition, trivalent iron deposits in form of hemosiderin were detected in *Esr1*-deficient ovarian stroma. The depletion of *Esr1* was further associated with an aberrant immune cell landscape characterized by the appearance of macrophage-derived multinucleated giant cells (MNGCs) and increased quantities of macrophages, particularly M2-like macrophages. Similar to reproductively aged animals, MNGCs in *Esr1*-deficient ovaries were characterized by iron accumulation and strong autofluorescence. Finally, deletion of *Esr1* led to a significant increase in ovarian mast cells, involved in iron-mediated foam cell formation. Given that these findings are characteristics of ovarian aging, our data suggest that *Esr1* deficiency triggers mechanisms similar to those associated with aging.

KEYWORDS

estrogen receptor alpha, ERα, *Esr1*, ovary, iron, macrophage, multinucleated giant cells, aging

1 Introduction

Estrogens, especially 17β-Estradiol (E2), play an essential role in a variety of biological processes within the female reproductive system. They control growth and differentiation of uterine tissue and successful ovulation (1). E2 exerts its functions by binding to specific estrogen receptors in the cytoplasm, which are subsequently translocated to the nucleus and initiate signaling via binding to estrogen response elements (2, 3).

The rodent ovary, which is an important E2 producing organ, expresses all three known estrogen receptors (3). However, their expression differs between functional compartments of the ovary. While estrogen receptor beta (ERβ, *Esr2*) is strongly expressed by granulosa cells in growing follicles (4–7), estrogen receptor alpha (ERα, *Esr1*) is more diffusely expressed in interstitial and thecal cells (6–8). It is therefore not surprising that misregulation or depletion of these receptors has severe effects on physiological processes and impairs fertility (9). The lack of these receptors leads in each case to quite different phenotypic characteristics (3, 10–13). The most severe phenotype occurs when *Esr1* is disrupted, resulting in infertility in both female and male mice (14), while depletion of *Esr2* is associated with sub-fertility and comparatively normal gross morphology (9, 15). The third receptor through which E2 can signal is G-protein coupled estrogen receptor 1 (GPER1). Interestingly, although GPER1 is expressed in the ovary and uterus, *Gper1*-deficient mice do not exhibit any reproductive defects (16).

For about 30 years, mice deficient in *Esr1* have been to study the molecular mechanisms responsible for infertility, and to link them to various ovarian diseases (9, 14, 17). Although *Esr1*-deficient females show follicular maturation up to the antral follicle stage, they do not ovulate (17). Therefore, no *corpora lutea* are formed in the ovaries of these animals, and instead follicular atresia or enlarged hemorrhagic cysts are formed (10, 17). A similar infertile phenotype was observed in mice lacking aromatase (*Cyp19*), the essential enzyme, which converts androgens to estrogens (18, 19). Recently, abnormal iron accumulation was reported in the ovarian stroma of young *Cyp19*-depleted females, indicating impaired iron homeostasis in context of endocrine disruption (20). Interestingly, physiological aging of the ovaries, which is associated with natural decline in fertility is also characterized by elevated iron levels (21–23). Similar findings have been noted in women with infertility-associated endocrine ovarian disorders such as polycystic ovary syndrome (PCOS) or endometriosis (24–26).

Iron is an important element that the body needs for a variety of processes, including physiological functions in female reproductive tract (27). An imbalance in iron homeostasis leads to tissue iron overload that in turn is capable to catalyze redox reactions, resulting in accumulation of toxic lipid peroxides that negatively affect folliculogenesis (28, 29). In general, iron can be present as ferrous (Fe^{2+}) or in the oxidized ferric (Fe^{3+}) state. Ferrous iron is mainly produced transiently because of its higher cellular toxcity, whereas ferric iron is the stable form (30). In the cell, trivalent iron is mainly transported by transferrin and stored in form of ferritin or hemosiderin (30). While ferritin is a physiological bioavailable intracellular storage protein, hemosiderin is an iron-storage aggregate consisting of partially degenerated ferritin and lysosomes, that are often formed after bleeding (31, 32). Hemosiderin accumulation has been observed in different tissues and within the ovaries where it is associated with natural aging, nulliparity and endocrine disease (21, 22, 33, 34). However, the exact function of hemosiderin and the consequences of its deposition in various body systems have not yet been conclusively clarified.

The balance of iron metabolism is ensured by a complex network of cells and proteins involved in transport, export, and import (30). In general, macrophages are described as important players in regulation of iron metabolism through their involvement in import/export, recycling and storage of iron (35). Ovarian macrophages show high levels of heterogenicity, having diverse functions in health and disease (36, 37). In naturally aging murine ovaries, these phagocytic cells are associated with iron accumulation (21, 23). In addition, aging triggers the differentiation of residential ovarian macrophages, leading to increased M2 polarization of macrophages (anti-infammatory) and the appearance of so-called marcophage-derived multinucleated giant cells (MNGCs) (22, 34, 38). Whether endocrine disorders such as the depletion of *Esr1* have similar effects on the ovary has only been speculated (34).

Recently, we reported that *Esr1*-deficient female mice show dramatically increased levels of Lipocalin 2 (LCN2) in ovarian tissue (8). LCN2, originally described as a neutrophil gelatinase-associated lipocalin, is a 25-kDa protein glycoprotein with diverse immunological and metabolic functions including iron transport (39–41). Although LCN2 cannot bind iron directly, it has the ability to chelate Fe^{3+} bound to siderophores. LCN2 uses bacterial siderophores as cofactors to form a complex, thereby limiting bacterial growth and infections by sequestering iron (42, 43). In addition, mammalian siderophores have been discovered that are potential ligands for LCN2 (44). Therefore, we speculate that the strong ovarian LCN2 expression in *Esr1*-deficient females (8) indicates altered iron homeostasis in these animals. To the best of our knowledge, there are currently no studies on whether or in what way iron homeostasis is affected by depletion of *Esr1* in the ovary. In this scenario, a change in iron metabolism is conceivable because an association between a hemorrhagic or cystic phenotype and iron excess has been noted in other ovarian disorders such as PCOS or endometriosis. Although these disorders are formed by different pathomechanisms, they are also related to infertility (24, 45–47). Similarly, natural aging of the ovaries is accompanied by a steady decline in fertility and impaired iron metabolism (21–23).

The aim of the present study was to investigate the consequences of depletion of *Esr1* on iron homeostasis. Therefore, we analyzed the ovaries of adult *Esr1*-deficient animals and aged-matched wild type animals with respect to iron regulation. In addition, we are speculating about the potential link between the depletion of *Esr1* and the early indicatiors of ovarian aging. The results of the present study highlight that endocrine dysfunction is associated with common signs of ovarian aging, such as significant accumulation of iron, the influx of macrophages and the presence of MNGCs.

2 Material and methods

2.1 Animal housing and tissue collection

Homozygote female and male *Esr1*-deficient mice are infertile (48). Therefore, *Esr1*$^{-/-}$ animals were obtained by mating heterozygote *Esr1*$^{+/-}$ (B6N(Cg)-*Esr1*$^{tm4.2Ksk}$/J) males and females, purchased from The Jackson Laboratory (JAX stock #026176, The Jackson Laboratory, Bar Harbor, ME, USA). The handling of the animals was carried out in accordance with the German animal welfare law (Tierschutzgesetz, TSchG) and the Directive 2010/63/EU. All experiments involving animal sacrifice and subsequent tissue dissection were approved by the internal Review Board of the RWTH University Hospital Aachen (permit no.: TV40138). Animal housing and care was carried out as previously described in (8), with mice maintained in a 12 h light/12 h dark cycle. The mice used in this study were between 12- and 22-weeks-old (or reproductively old between 77 and 79 weeks-old, cf. Section 3.5) at sacrifice that was carried out by cervical dislocation with prior isoflurane sedation. The freshly removed female reproductive organs (as well as liver and spleen tissues) were rinsed in phosphate-buffered saline (PBS) and then either fixed for histological analysis (24 h, 4°C in 4% neutral buffered formaldehyde, stabilized with methanol), or snap-frozen in liquid nitrogen and then stored at -80°C for further processing. Since the aim of this study was to compare the female reproductive tract of *Esr1*-deficient animals with that of wild type mice, only female animals were used. In the present study, we included wild-type females in all estrus phases to eliminate the possibility that the reported results are simply due to hormonal fluctuations. The corresponding males were used in the previous study (8), which provides additional information such as the specific genotyping protocol and analysis of the animals total body weights.

2.2 Histological analysis of tissue sections

For all histological procedures described in the following section, the tissue was treated equally. First, the tissue was fixed for 24 h, dehydrated, and then embedded in paraffin. The formaldehyde-fixated paraffin-embedded tissue blocks were stored at room temperature (RT) until sectioning. From the tissue, 3-µm thick sections were prepared and deparaffinized in xylene and subjected for rehydration to decreasing graded ethanol. In order to compare the different histological stains, consecutive sections were made. Unless otherwise stated, all further steps were performed at RT.

2.2.1 Hematoxylin and eosin stain

The tissues were stained for 5 min in Mayers Hematoxylin (Liliess Modification, #S3309, Agilent Technologies, Inc., Santa Clara, CA, USA) diluted 1:3 in dH_2O. Afterwards the tissues were washed under running tap water for 10 min. Cytoplasmic staining was done by placing the slides in Eosin pH 4.5 (#HT110216, Sigma-Aldrich, Taufkirchen, Germany) for 15 sec. The samples were dehydrated (in increasingly graded ethanol and xylene) and subsequently mounted in DPX mounting medium (#06522, Sigma-Aldrich). Hematoxylin and eosin (HE) staining was used for histological analysis of tissue structure and to determine the estrous phase of the wild type females. Details of the assessment and specific histological characteristics can be found in our previous study (8).

2.2.2 Perls Prussian Blue staining

The Perls Prussian Blue (PPB) method, known as Berlin Blue Reaction, is a histochemical method for the detection of trivalent iron associated with hemosiderin in tissue sections (49). To identify iron deposits in reproductive tracts of *Esr1*-deficient and wild type females, Prussian Blue [Iron (III) Detection] staining kit (#11097, MORPHISTO, Offenbach am Main, Germany) was used according to manufacturers instructions. Briefly, after rehydration (see Section 2.2), the tissue samples were incubated for 5 min at 40°C in 5% potassium ferrocyanide (II) and subsequently in freshly prepared working solution of 5% potassium ferrocyanide (II) in hydrochloric acid solution (1:1) for 30 min at 40°C. After washing the section for 5 min in dH_2O, counterstaining for 10 min with 0.1% Seed red (nuclear red) was performed. The tissue samples were dehydrated and mounted with DPX as previously described (see Section 2.2.1). The reaction product of the ferric iron with the potassium hexacyanoferrate (II) in hydrochloric acid solution precipitates as an insoluble blue complex salt, which is clearly distinguishable from pale pink stained tissue structures (49).

2.2.3 Immunohistochemical detection with Perls Prussian Blue staining

To investigate whether the iron deposits co-localize with lipocalin 2 (LCN2), PPB was performed combined with immunohistochemical staining for LCN2. Therefore, the tissue sections were first treated as described in Section 2.2. Afterwards, antigen retrieval was done by heating the slices in sodium citrate buffer (10 mM, 0.05% Tween 20, pH 6.0) in a steamer for 30 min, followed by cooling on ice for 20 min). Next, the samples were washed in PBS and PBS supplemented with 0.1% Tween® 20 (PBS-T). Then, Avidin/Biotin Blocking Kit (#SP-2001, Vector Laboratories, Newark, CA, USA) was used essentially as described in the manufacturers instructions. To block non-specific antibody binding sites, tissue sections were incubated in 5% normal rabbit serum (#X0902, Agilent Technologies) in blocking solution (1% BSA, 0.1% cold fish gelatin, 0.1% Triton-X-100, 0.05% Tween® 20 in PBS) for 90 min. Primary anti-LCN2 Antibody (#AF3508, R&D Systems, Minneapolis, MN, USA) was diluted 1:40 in blocking solution and incubated on slides at 4°C overnight. Normal goat IgG (#AB-108-C, R&D Systems) were used at the same concentration as the primary antibody and served as a negative control. Next day, endogenous peroxidase was blocked by incubating the tissue slices in 3% hydrogen peroxide (#31642, Sigma-Aldrich) in dH_2O. Tissue was then washed in dH_2O and PBS-T and incubated with a biotinylated rabbit polyclonal anti-goat secondary antibody (#E0466, Agilent Technologies, diluted 1:300 in PBS), for 1 h. After washing in PBS-T, the slices were incubated in ABC-

Complex solution (#PK-6100, VECTASTAIN® Elite® ABC-HRP-Kit, Vector Laboratories) according to manufacturers instructions for 1 h in RT. The chromogen 3,3-diaminobenzidine tetrahydrochloride (DAB, SIGMAFAST, #D9292, Sigma-Aldrich) was used to visualize LCN2 expression. Subsequently, the PPB staining kit was used as described above (Section 2.2.2). In brief, tissue sections were first incubated for 5 min at 40°C in 5% potassium ferrocyanide (II) and then for 30 min at 40°C in freshly prepared working solution of 5% potassium ferrocyanide (II) in hydrochloric acid solution (1:1). Tissue sections were washed for 5 min in dH_2O and counterstained in 0.1% Seed red (nuclear red) for 5 min. Finally, samples were dehydrated and mounted with DPX as previously described (see Section 2.2.1).

2.2.4 Periodic Acid-Schiff reaction

The Periodic Acid-Schiff (PAS) reaction is a histochemical staining technique to detect carbohydrate-containing components like glycogen which are typical for macrophages (50). To visualize polysaccharide-enriched phagocytic cells in the female reproductive tract, we used a PAS reaction staining kit (#12153, MORPHISTO) according to manufacturers instructions. In brief, after the rehydration steps (see Section 2.2), tissue sections were incubated in 1% periodic acid for 20 min, washed with H_2O, and the Schiffs reagent was applied on the sections for 10 min. Finally, the tissue was counterstained with hematoxylin for 2.5 min, followed by 'blueing under running tap water for 3 min. The tissue sections were dehydrated and mounted in DPX mounting medium as previously described (see Section 2.2.1).

2.2.5 Toluidine blue staining

Toluidine blue (TB) is a dye for metachromatic staining of mast cells in tissues, which stains mast cell granules in purple and the background in blue (51). A standard protocol was used with a 1% Toluidine blue (#89640-25G, Sigma-Aldrich) stock solution in 70% ethanol. In brief, after the rehydration steps (see Section 2.2), sections were stained with 0.1% toluidine blue working solution in 1% sodium chloride for 5 min. After several immersions in distilled H_2O, the tissue sections were dehydrated in ethanol and xylene and mounted in DPX as previously described (see Section 2.2.1). The number of mast cells per mm^2 was determined by counting the positive (purple stained) mast cells in the ovary. For this purpose, the stained tissue sections were scanned and NDP.view2 software (see Section 2.2.8) was used to determine the areas of the ovaries.

2.2.6 Detection of autofluorescence

Autofluorescence of tissues may be due to the accumulation of lipofuscin, an aging pigment that is stored in phagocytic cells (22, 23). For visualization of autofluorescence in reproductive tissue section, slices were deparaffinized, rehydrated and embedded in aqueous PermaFluor™ mounting medium (#TA-030-FM, Thermo Fisher Scientific Inc., Waltham, MA, USA) with or without nuclear counterstaining in 4,6-diamidino-2-phenylindole dihydrochloride (DAPI) solution (#D1306, Thermo Fisher Scientific).

2.2.7 Immunofluorescence staining

Formalin-fixed, paraffin-embedded tissue sections with a thickness of 3 µm were used for immunofluorescence staining and were deparaffinized and prepared as described above (see Section 2.2). Subsequently, heat-induced antigen retrieval was done in a steamer by placing the slides in citrate buffer (10 mM, pH 6.0, 0.05% Tween® 20) for 30 min, followed by cooling on ice for 20 min. Next, samples were rinsed with PBS and PBS-T. Non-specific binding sites were blocked with 5% normal donkey serum (#ab7475, Abcam, Cambridge, UK) in PBS supplemented with blocking solution (0.1% cold fish skin gelatine, 1% bovine serum albumin, 0.1% Triton X-100, and 0.05% Tween® 20) for 90 min. Tissue sections were incubated with primary antibodies against F4/80 (1:50, #MCA497G, Bio-Rad Laboratories GmbH, Dusseldorf, Germany) and LCN2 (1:40, #AF3508 R&D Systems) or with IgG controls (normal rat IgG_{2b},#65211-1-Ig, Proteintech, Planegg-Martinsried, Germany; normal goat IgG, #AB-108-C, R&D Systems) in blocking buffer overnight at 4°C. IgG controls were used at the same concentration as the primary antibodies. All the following steps were carried out under exclusion of light. The next day, the sections were washed and incubated simultaneously with two fluorescently-labeled secondary antibodies (donkey anti-goat Alexa Fluor Plus 555, #A32816, Thermo Fisher Scientific and donkey anti-rat Alexa Fluor Plus 488, #A11208, Thermo Fisher Scientific), diluted 1:300 in PBS for 1 h. The TrueBlack® Lipofuscin autofluorescence quencher solution (#23007, Biotium, Fremont, CA, USA) was used to quench autofluorescence in reproductive tissue samples (52). For this purpose, the sections were incubated for 3 min in the TrueBlack® solution freshly diluted (1:20) in 70% ethanol. Thereafter, the tissue sections were washed with PBS and nuclear counterstaining was performed for 30 min using a 200 ng/ml DAPI solution in PBS. Finally, tissue slices were mounted with aqueous PermaFluor™ mounting medium and stored in the dark at 4°C until fluorescence microscopic evaluation.

2.2.8 Imaging

Images were taken with a Nikon Eclipse E80i fluorescence microscope, equipped with the NIS-element Vis software (Version 3.22.01, Nikon, Tokio, Japan). In addition, selected tissue slides were scanned using a NanoZoomer (#C13220-04, Hamamatsu, Naka-ku, Japan), viewed using NDP.view2 software (version U12388-01, Hamamatsu), and exported to create final images.

2.3 Laser Ablation Inductively Coupled Plasma Mass Spectrometry (LA-ICP-MS)

Ovarian tissues of female animals (Wild type: n=5, *Esr1*$^{-/-}$: n=5) aged 12-15 weeks were used for laser ablation inductively coupled plasma mass spectrometry (LA-ICP MS) measurement.

2.3.1 Tissue preparation for LA-ICP-MS

Protocols for standardized quantitative LA-ICP-MS analysis with liver tissue were previously established by us (53). In these protocols,

it is necessary to flush the tissue prior measurement with saline buffer for detection of proper endogenous iron concentrations. In unflushed liver, the majority of the measured iron concentration results from the blood and thus can lead to massive misinterpretations (54). Therefore, sacrificed animals were immediately transcardially perfused. For this purpose, a 26G needle was inserted from the tip of the heart about 5 mm into the left ventricle and fixed by means of hemostatic forceps ('Mathieu needle holder). Then a small incision was made in the right atrium with fine scissors and the perfusion with sterile PBS was carefully started and continued until the liver turned pale. Afterwards the tissues were carefully dissected and frozen at -80° C. For preparing slides for LA-ICP-MS analysis, the samples were cut into 30 µm thick slices using a cryomicrotome (#CM3050S, Leica Biosystems, Wetzlar, Germany), in which the temperature of the cryo-chamber was set to -27°C and the object area temperature to -24°C. The slices were mounted on StarFrost® self-adhesive microscope slides (B4 0303, Knittel Glass, Braunschweig, Germany) and stored at -80°C until analysis. Before the sections were subjected to LA-ICP-MS measurement, the cryosections were scanned with a slide scanner (see Section 2.2.8) to obtain a light microscopic overview. Microscopic images were viewed and analyzed using the NDP.view2 software.

2.3.2 LA-ICP-MS measurement and analysis

The LA-ICP-MS technology consists of a line-by-line ablation of tissue material with a fine, focused laser beam. The ablated tissue is then transferred into the inductively coupled plasma source of a mass spectrometer using an inert carrier gas stream (*e.g.*, argon). After being vaporized, atomized and ionized, the molecules are split according to its mass-to-charge ratio (55, 56). In our study, trace element measurements were done in a quadrupole-based inductively coupled plasma mass spectrometer (8900 ICP-MS, Agilent Technologies) that was linked to a laser ablation system (New Wave NWR213; Elemental Scientific, Omaha, NE, USA). In addition to ^{56}Fe, the following isotopes were routinely monitored and quantified as part of the established LA-ICP-MS analysis: ^{13}C, ^{23}Na, ^{24}Mg, ^{31}P, ^{34}M, ^{39}K, ^{44}Cr, ^{55}Mn, ^{63}Cu and ^{64}Zn. Generation, analysis and visualization of LA-ICP-MS data to obtain metal distribution in the tissues was done with the Excel-based Laser-Ablation Imaging (ELAI) program, consisting of Microsoft Excel with Visual Basic for Application (VBA), as described elsewhere (57, 58). For the determination of the elemental concentrations in µg/g tissue, standards including different well-defined concentrations of each element have been prepared from homogenized liver tissues. The concentration of each isotope was normalized to the mean intensity of ^{13}C ion intensity per tissue as an alternative marker for sample thickness. More detailed information regarding experimental set up during LA-ICP-MS measurement, calibration and standard preparation are described elsewhere (53, 56, 57, 59, 60).

2.4 RNA analysis

Parts of snap-frozen female tissue were placed in RNA lysis buffer with DTT and homogenized as described previously (4). Protocols for RNA extraction and purification including DNase digestion followed by reverse transcription and quantitative real-time PCR (RT-qPCR), and evaluation were previously published (8). A list of all primers used in this study is given in Supplementary Table 1.

2.5 Protein analysis by Western blot

Female tissues were placed in RIPA buffer (on ice) containing 20 mM Tris-HCl (pH 7.2), 150 nM NaCl, 2% (*w*/*v*) NP-40, 0.1% (*w*/*v*) SDS, and 0.5% (*w*/*v*) sodium deoxycholate supplemented with the Complete™ mixture of phosphatase inhibitors (#P5726-1ML, Sigma-Aldrich). For ovarian protein analysis, both ovaries of each female were pooled. Tissue homogenization was performed with a mixer mill and protein extraction and Western blot analysis was performed as described elsewhere (8). 70 µg protein samples per lane were loaded for liver and spleen tissue analysis and 60 µg for ovaries. An overview of the antibodies used in this study is given in Supplementary Table 2.

2.6 Data analysis

All calculations were done in Excel v16 (Microsoft Corporation, Redmond, WA, USA). Statistical analysis was performed with GraphPad Prism v.8.0 (GraphPad Software, Inc., La Jolla, CA). Gaussian distribution was tested with Shapiro-Wilk Tests. Subsequently, Students *t*-test was used if normality could be assumed, while otherwise a non-parametric Mann-Whitney Test was applied. All data in this study is shown as mean ± standard deviation (SD). Statistical significance between groups was assumed when probability values were below 0.05 ($p < 0.05$). Significant differences are indicated by asterisks: * $p < 0.05$, ** $p < 0.01$, *** $p < 0.001$.

3 Results

3.1 LA-ICP-MS analysis of murine ovaries

In reproductive organs, especially in the ovary, studies have shown that unbalanced iron homeostasis, is associated with unexplained infertility (61, 62). Therefore, we speculated that depletion of *Esr1*, which leads to infertility, may be associated with imbalance in iron homeostasis. To test our hypothesis, we used the LA-ICP-MS technology that represents a powerful imaging technique that can be used to determine the distribution of iron (isotopes) in biological tissue in health and disease (55, 57).

To determine whether the absence of *Esr1* affects iron load in murine ovaries, we subjected cryosections of *Esr1*-deficient and wild type (WT) animals to LA-ICP-MS imaging. In total 12 different isotopes were measured (57, 58). The calculated concentrations of the individual isotopes refer in each case to the total ovarian tissue shown and are given in µg/g tissue (Supplementary Table 3). The LA-ICP-MS analysis of the ovarian tissue of *Esr1*-deficient and WT animals showed no differences in the majority of the studied isotopes. Only ^{52}Cr (higher in WTs), ^{23}Na and ^{56}Fe (both

10.3389/fendo.2024.1325386

increased in *Esr1*-deficient) showed significant differences between the two groups (Figure 1A; Supplementary Table 3). Interestingly, statistical analysis revealed significantly higher ^{56}Fe iron content in *Esr1*-deficient ovaries (Figure 1B). These animals had approximately 4-fold higher iron concentration in the ovary (595 ± 189 µg/g) compared to WTs (148 ± 63 µg/g). The increased iron concentration (^{56}Fe) is clearly evident when the concentration-based scale (usually 0-1,000 µg/g) was expanded to 0-3,000 µg/g (Figure 1C). Defined areas of high iron content in the *Esr1*-deficient ovary are marked by red color. The light microscopic analysis further revealed that increased iron content in *Esr1*-deficient animals is most likely localized to the ovarian stroma.

From the LA-ICP-MS analysis, we concluded that *Esr1*-deficient animals had significantly higher amount of iron in the ovaries compared to WT animals. However, these measurements do not allow the determination of exact form of iron present, and therefore the iron metabolism of the animals was further investigated.

3.2 Analysis of different iron-regulators in *Esr1*-deficient ovaries and liver

Considering the increase in iron in murine ovaries of *Esr1*$^{-/-}$ mice, we speculated that proteins and genes associated with iron metabolism might be altered in these animals. Therefore, we next investigated the expression of key mediators involved in cellular handling of iron, including iron storage (ferritin, transferrin), iron export/import (ferroportin, divalent metal transporter 1) and iron regulation (iron regulatory protein 1/2) proteins. Importantly, we detected significantly enhanced expression of ferritin heavy chain 1

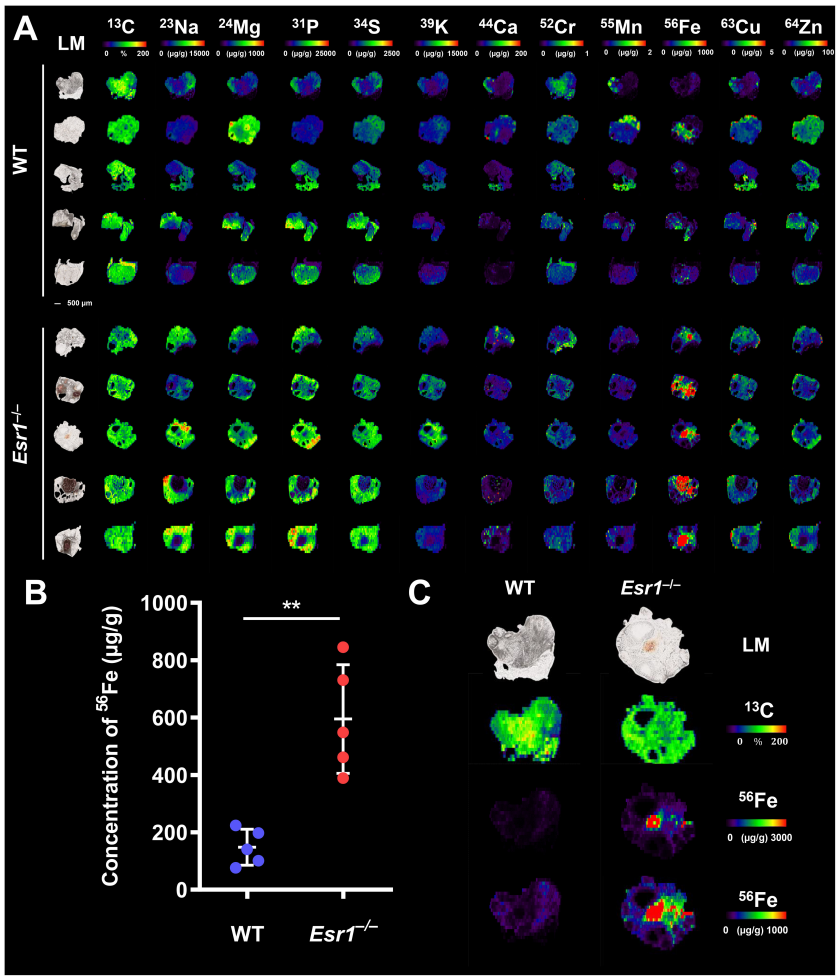

FIGURE 1
Laser ablation inductively coupled plasma mass spectrometry (LA-ICP-MS) imaging of wild type (WT) and *Esr1*-deficient ovaries. LA-ICP-MS imaging was performed on 30 µm-thick cryosections and the distribution of different isotopes was determined. Details are described in the Material and Methods section. **(A)** Overview of all analyzed isotopes in ovaries of WT (n=5) and *Esr1*-deficient (n=5) animals. Individual images were generated with the ELAI software tool. Light microscopy (LM) images of the cryosections of the individual ovaries are shown on the left side. Scale bar represents 500 µm. The content of ^{13}C used for normalization is presented in %, while other isotope concentrations are shown in µg/g tissue. **(B)** The concentration of ^{56}Fe (in µg/g) is significantly higher in *Esr1*-deficient ovaries compared to WT controls. For statistical analysis a Students *t*-test was performed. The significant difference between both groups is indicated by asterisks: $^{**}p<0.01$. **(C)** Images of ^{56}Fe distribution are shown at different concentration-based scales for a representative WT and *Esr1*-deficient ovary. The ^{56}Fe isotope concentration-based scale was lowered from 0-3,000 µg/g to 0-1,000 µg/g to highlight ^{56}Fe accumulation in *Esr1*-deficient animals.

10.3389/fendo.2024.1325386

(*Fth1)* and a trend to higher ferritin light chain (*Ftl1*) in *Esr1*-deficient ovaries at the mRNA level (Figure 2A). In addition, significantly increased expression of transferrin (*Tf*) was detected in these animals. In line, Western blot analysis revealed significantly higher ovarian transferrin protein in *Esr1*-depleted mice than in WT controls (Figure 2B). Furthermore, solute carrier family 11 member 2 (*Slc11a2*), a metal importer, was significantly enhanced in *Esr1*-deficient ovaries compared with WT animals (Figure 2C). However, there was no change in ferroportin (*Fpn1*) expression, which is an important iron exporter/efflux pump. Moreover, we found significantly higher expression of iron responsive element binding protein 2 (*Ireb2)*, but lower levels of aconitase *(Aco1)* in *Esr1*-deficient compared to WT ovaries.

Increased iron deposition and altered iron metabolism are signs of stress to which cells react by upregulating critical adaptive response mechanisms such as heme oxygenase 1 (HMOX1) (63). Interestingly, we detected significantly higher mRNA expression of *Hmox1* in *Esr1*-deficient ovaries compared to WT animals, which was reflected by a slight but not significant increase of HMOX1 protein (Supplementary Figures 1A, B). Iron overload can drive cellular death (known as ferroptosis), which is prevented by *e.g.*, the glutathione peroxidase signaling (GPX4) pathway (64). However, no differences in *Gpx4* mRNA or protein expression was detected between WT and *Esr1*-deficient ovaries (Supplementary Figures 1C, D).

Since our results indicated enhanced iron storage and transport in the *Esr1*-deficient ovary, the question arose about whether this is a local occurrence limited to ovaries or is also systemically reflected in these animals. To address this issue, we next analyzed the expression of iron in the liver as the site of iron synthesis and the spleen as an iron recycling organ (35). To do so, liver tissue slices from female WT and *Esr1* null mice were subjected to Perls Prussian blue (PPB) staining. Since PPB exclusively stains the non-heme iron in the cells, the ferric Fe^{3+}-positive cells (stained blue) can be clearly distinguished in the staining from erythrocytes present in the blood (stained red) (49). This analysis revealed a very low overall positive staining for iron in parenchymal liver cells (Figure 3A). Several PPB-positive cells were detected in the *Esr1*-null livers, whereas positive cells were only rarely found in the WT livers (Figure 3A). In line, LA-ICP-MS imaging (Figure 3B) revealed that livers of WT animals have significantly higher amounts of isotope ^{56}Fe (196.5 ± 17.6 µg/g) compared to *Esr1*-deficient animals

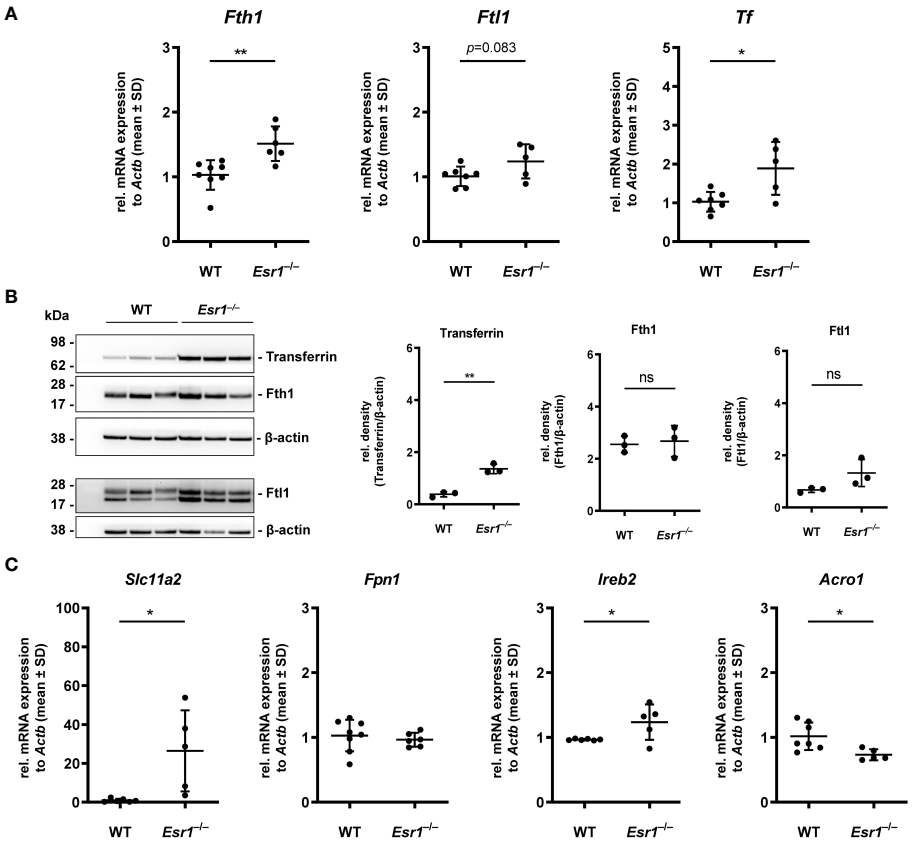

FIGURE 2
Analysis of key players in cellular iron metabolism handling in ovarian tissue. Wild type (WT) and *Esr1*-deficient ovarian tissues were either used for mRNA (WT, n=7; $Esr1^{-/-}$, n=5) or protein analysis (WT, n=3; $Esr1^{-/-}$, n=3). Relative mRNA expression of *Fth1*, *Ftl1* and *Tf* were measured by RT-qPCR and validated by **(B)** Western blot analysis. Protein expressions of Transferrin, Fth1 and Ftl1 were quantified densitometrically and plotted relative to β-actin expression. **(C)** mRNA expression of *Slc11a2*, *Fpn1*, *Ireb2* and *Aco1* were detected by RT-qPCR. All data **(A-C)** are displayed as mean ± SD. For statistical analysis a Students *t*-test was performed. Significant differences between groups are marked with asterisks: *p<0.05, **p<0.01, ns = not significant.

(377.3 ± 36.11 µg/g). Western blot analysis of Fth1 and transferrin further showed significantly lower expression of these iron storage proteins in *Esr1*-deficient livers (Figure 3C). However, at mRNA level, there were no significant differences in hepatic expression of key players in iron metabolism (*Fth1, Ftl1, Tf, Slc11a2, Hamp1*) between WT and *Esr1*-deficent animals (Figure 3D). Only the expression of *Fpn1* was significantly decreased in *Esr1*-deficient livers.

To confirm that there was no systemic iron overload, splenic tissue of *Esr1*-deficent and WT mice were stained with PPB to visualize location of iron deposits. This analysis revealed iron-laden cells predominantly in the red pulp and occasionally in the white pulp of the spleen (Supplementary Figure 2A). Strikingly, *Esr1*-deficient animals showed no excess but even quite in opposite a lower amount of iron compared to the WTs. This corresponds to the similar Fth1 and transferrin expression in both groups as determined by Western blot analysis (Supplementary Figure 2B).

In conclusion, we found that different players of iron homeostasis are altered in *Esr1*-deficient ovaries, which are associated with iron overload conditions. Our data further indicate that there is no systematic iron overload in other organs involved in iron regulation (*i.e.*, liver and spleen).

3.3 Ovaries of *Esr1*-knockout mice show iron accumulation and LCN2 upregulation

Hemosiderin, an iron storage aggregate with poor accessibility, can be formed during iron overload when cells reach their capacity to bind iron to ferritin, such as during hemorrhages (65). This can be easily analyzed in routine hematoxylin and eosin (HE) staining in which hemosiderin appears as golden-brown aggregates (21).

Since iron transport and storage is increased in *Esr1*-deficient ovaries (c.f. Figure 2), we next investigated whether hemosiderin is present in ovarian tissue. Therefore, ovarian tissue sections of adult *Esr1*-deficient and WT animals were initially stained with HE and serial sections were stained with Perls Prussian Blue (PPB) to confirm the ferric Fe^{3+} deposition (hemosiderin) (Figures 4A, B, *upper panels*). Interestingly, large amounts of golden-brown deposits were evident in the ovaries of *Esr1*-deficient animals throughout the tissue section, while in contrast no deposits were seen in the WT animals. These accumulations were preferentially located in the interstitial ovarian stroma (Figure 4B) or in close proximity to hemorrhagic cysts (Figure 4C, *upper panel*). PPB staining confirmed that the golden-brown deposits were hemosiderin accumulations (Figures 4A, C, *lower panels*). While

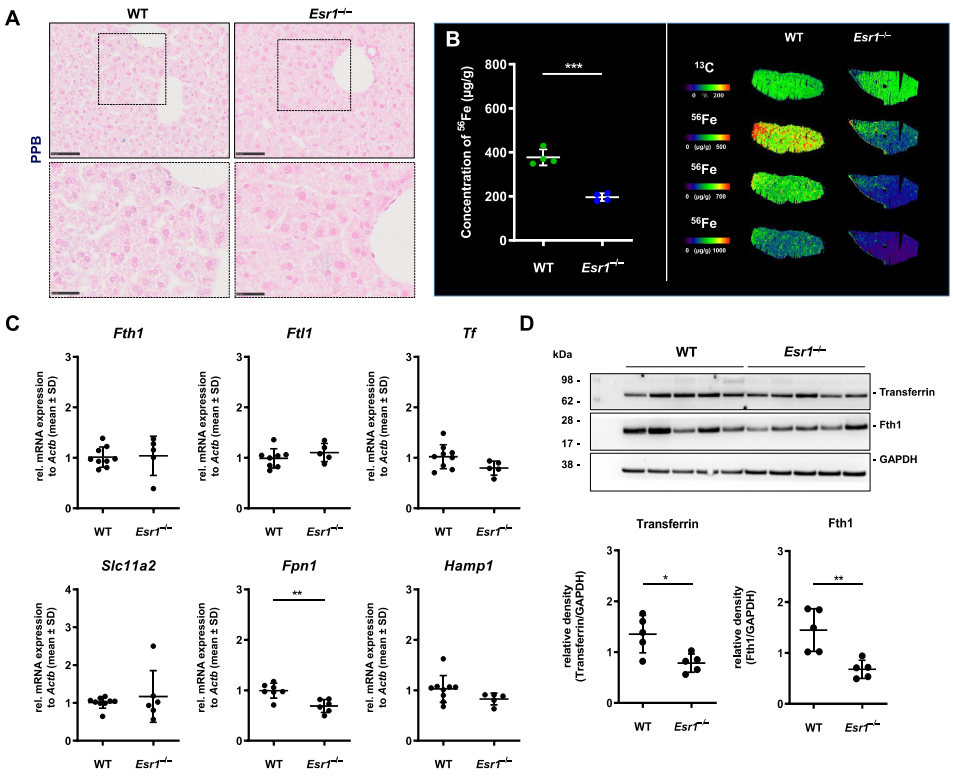

FIGURE 3
Analysis of cellular iron metabolism in liver tissue. Wild type (WT) and *Esr1*-deficient liver tissues were used for different analysis. **(A)** Formalin-fixated paraffin-embedded liver tissues sections (WT, n=4; $Esr1^{-/-}$, n=4) were stained for iron using Perls Prussian Blue (PPB). The scale bars equal to 50 µm (solid boarder) or 25 µm (dashed border). **(B)** Liver cryosections were subjected to LA-ICP-MS imaging. Concentration of elemental iron isotope (^{56}Fe) (µg/g) is significantly lower in *Esr1*-deficient livers compared to WTs (left panel). ^{56}Fe distribution is shown for both genotypes at different concentration-based scales for a representative WT and *Esr1*-deficient liver (left panel). **(C)** Regulators of cellular iron metabolism (*Fth1, Ftl1, Tf, Dmt1, Fpn1*, and *Hamp1*) were analyzed by RT-qPCR. **(D)** Protein expression of transferrin and Fth1 was investigated by Western blot analysis. Expression levels were quantified densitometrically and plotted relative to GAPDH expression. All data **(B–D)** are displayed as mean ± SD. For statistical analysis a Students *t*-test was done. Significant differences between groups are marked with asterisks: *p<0.05, **p<0.01, ***p<0.001.

the WT ovaries showed only sporadic, blue-stained cells, the ovaries of *Esr1*-deficient animals exhibited many dark, blue-stained areas that coincided with the deposits occurring in HE staining. In addition to the dark blue stains, the ovaries of *Esr1*-depleted mice also contained light-blue colored cell clusters (see Section 3.5).

In our previous study we demonstrated dramatically increased lipocalin-2 (LCN2) expression in female *Esr1*-deficient ovaries (8). Since this protein is an important player in iron homeostasis (44), we investigated in the following whether the same cells are responsible for both producing LCN2 and accumulating iron. Therefore, we combined immunohistochemical detection of LCN2 with subsequent PPB staining. Ovarian tissues of WT and *Esr1*-deficient animals were stained according to the described method (Figure 4D). In agreement with our previous report, WT ovaries contained only few LCN2-positive cells. In addition, we found no double-positive cells in WT ovaries. However, *Esr1*-deficient ovaries showed many cells that were positive for LCN2 and iron. Normal goat IgG that were used as a negative control showed no brownish stain that were observed after staining with the LCN2 specific antibody. Importantly, the results show that the vast majority of LCN2-positive cells do not coincide with the iron-loaded cells.

Taken together, staining with PPB revealed dramatically increased hemosiderin quantities in *Esr1*-deficient ovaries. The data further indicate that cells that are strongly positive for LCN2 are different than those in which iron is deposited. Nevertheless, it is conceivable that the high expression of LCN2 affects the iron deposition and metabolism. Possibly the iron is associated with phagocytic cell types and other immune cells, as it is the case in a different hemorrhagic disease model (66).

3.4 Macrophages in *Esr1*-deficient ovaries

Ovarian macrophages are an essential cell type for ovarian iron metabolism (37). Therefore, we hypothesize that the severe iron accumulation in the *Esr1*-deficient animals is linked to macrophage influx in these tissue. To test this hypothesis, we first performed RT-qPCR to investigate whether WT and *Esr1*-deficient animals differ in terms of ovarian macrophage expression. We found significantly higher expression of pan-macrophage markers *Cd68* (known as well as macrosialin) and *Adgre1* (encoding F4/80 protein) in *Esr1*-depleted ovaries when compared to WTs (Figure 5A). Moreover, Western blot analysis showed a clear trend of higher CD68 protein

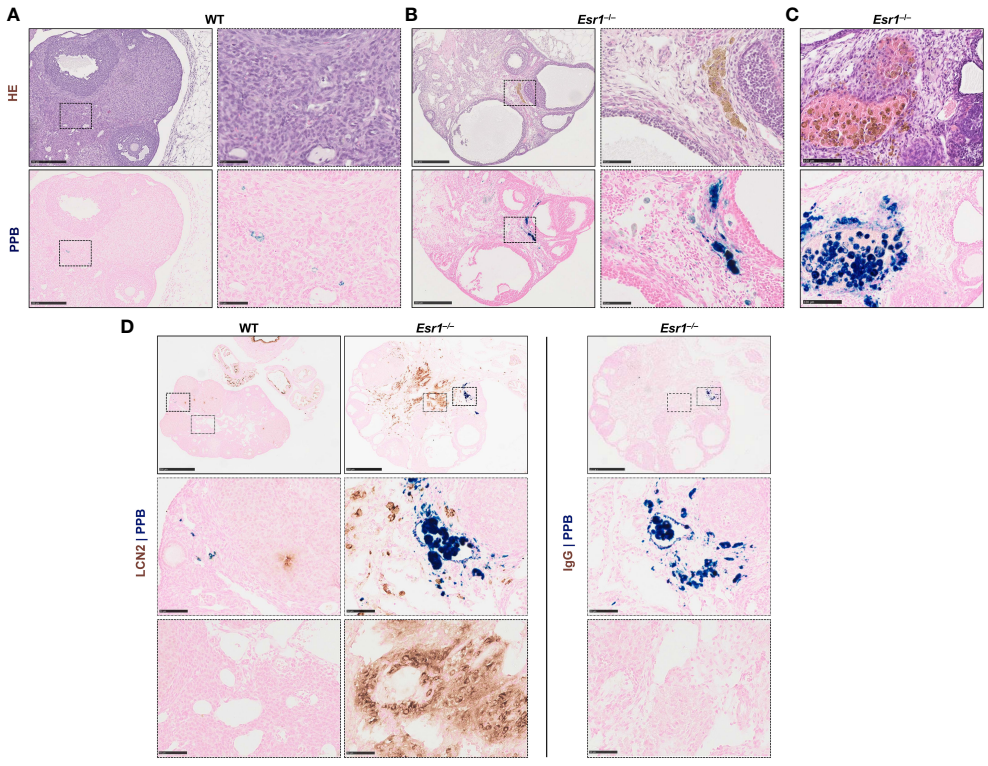

FIGURE 4
Hemosiderin deposits in ovarian tissues. Formalin-fixated paraffin-embedded ovarian tissues section of wild type (WT, n=8) and *Esr1*-deficient (n=8) animals were used for staining. Serial tissue slices of WT **(A)** and *Esr1*-deficient **(B)** ovaries were stained with Hematoxylin-Eosin (HE) or Perls Prussian Blue (PPB) to detect iron in form of hemosiderin. Hemosiderin can be seen in HE staining as brown-gold deposits and turns blue with PPB. The scale bars equal to 250 µm (solid boarder) or 50 µm (dashed border). Hemosiderin accumulations were found in ovarian stroma of *Esr1*-deficient animals but not in WTs and were localized around hemorrhagic cysts **(C)**. The scale bars equal to 100 µm. **(D)** Immunohistochemical localization of lipocalin 2 (LCN2) was combined with PPB staining to examine whether iron-positive cells co-localize with LCN2-positive cells. WT (n=3) and *Esr1*-deficient (n=4) ovaries were stained, showing no co-localization of iron and LCN2. Normal goat IgG was used as a negative control instead of the primary antibody. The scale bars equal to 500 µm (solid boarder) or 50 µm (dotted boarder and dashed border).

expression in *Esr1*-deficient animals (Figure 5B). The mRNA analysis was in line with results from immunohistochemical detection of F4/80 in the ovaries showing no- to low-numbers of F4/80-positive macrophages in the WT ovaries (Figure 5C). In WT ovaries, these cells were found in atretic follicles and regressing *corpus luteum*. Interestingly, the number of F4/80-positive cells were increased in ovaries of *Esr1*-deficient animals, which were located in the ovarian stroma (Figure 5D). Co-staining with LCN2 demonstrated no co-localization of F4/80-positive macrophages with LCN2-positive cells in either WT or *Esr1*-deficient ovaries (Figures 5C, D). As negative controls for immunofluorescence staining normal rat and goat IgGs instead of primary antibodies have been used, showing only a low background staining (Figure 5E). Furthermore, we investigated whether the increase in macrophages was predominantly due to M1-like (pro-inflammatory) or M2-like (anti-inflammatory) macrophages. Based on our previous findings of significantly elevated *Tnf* expression in *Esr1*-deficient ovaries, we anticipated an increase in pro-inflammatory macrophages. However, we observed no disparity in *Nos2* or *Il1r1* mRNA expression between WT and *Esr1*-deficient ovaries, which commonly used markers for M1-like macrophages (Figure 5F). In sharp contrast, there was a significant increase in all analyzed M2-like macrophage markers (*Arg1, Cd163, Mrc*) in *Esr1*-deficient compared with WT ovaries (Figure 5G).

Overall, our results demonstrate a strong increase in phagocytic cells in the *Esr1*-deficient ovary. Interestingly, we found significantly higher expressions of different M2-like macrophage markers in these animals, most likely indicating enhanced remodeling and tissue repair activity.

3.5 *Esr1*-deficient ovaries exhibit multinucleated giant cells

In the last decade, a unique ovarian macrophage-derived multinucleated giant cell population (termed as multinucleated giant cell, MNGC) has been exclusively found in aged murine ovaries (22, 23, 34), but speculated to be affected by altered endocrine processes. Therefore, we next examined *Esr1*-deficient and WT ovaries for the presence of MNGCs. Interestingly, in HE staining, we detected several clusters of pale brownish cells in ovaries of *Esr1*-depleted mice (Figure 6A), which most likely represent MNGCs. Higher magnification of these clusters showed that the cells appeared foamy and contained multiple nuclei (Figure 6A, I-IV). By phagocytosis, MNGCs engulf and store diverse products, including polysaccharides, which can be positively stained by Periodic Acid Schiff (PAS) reaction (22, 50). To verify these characteristic, serial sections of ovarian tissue from *Esr1*-deficient animals were stained with HE and PAS, revealing that the MNGC clusters which appeared pale brownish in HE (Figure 6B, *left panels*) were strongly positive (stained pinkish) in PAS reaction Figure 6B, *right panels*). In addition, we could confirm that these MNGCs contained iron, as they appeared colored light blue in PPB staining (Figure 6C). Another characteristic of MNGCs is their strong autofluorescence compared with the surrounding ovarian tissue (22). Observation of the PPB-stained *Esr1*-deficient ovary slices under a fluorescence microscope revealed that foamy ovarian MNGCs exhibited strong autofluorescence (Figure 6D). Finally, we found that MNGCs are present in aged ovaries, as we detected small numbers of these cells in old animals of all groups (WT, $Esr1^{-/-}$ and $Esr1^{+/-}$). These cell clusters are visible in HE staining, are PAS reaction positive, contain iron accumulations, and exhibit strong autofluorescence (Supplementary Figures 3A–D).

In conclusion, we detected several clusters of MNGCs in the ovaries of 3-month-old *Esr1*-deficient mice, but not age-matched WT controls. These findings indicate that disruption of *Esr1* leads to signs of reproductive aging, confirming altered endocrinology as an underlying cause of MNGCs formation.

3.6 *Esr1*-deficient ovaries show high number of mast cells

Mast cells are present in the ovary at all stages of rodent estrous cycle and human ovaries and can release various mediators such as tumor necrosis factor alpha (13, 67–70). In addition, mast cells are involved in iron-induced conversion of macrophages to foam cells during hemorrhage (66). In the last part of this study, we determined the number of mast cells in ovaries of female WT and *Esr1*-deficient mice by toluidine blue (TB) staining. We found numerous mast cells in the *Esr1*-deficient ovary in the interstitial area, whereas only singular mast cells were observed in WT ovaries (Figure 7A). This observation was reflected in the calculated number of mast cells (per mm^2) in the ovaries. The mean calculated number of mast cells in 38.6 ± 11.5 mast cells per mm^2 in *Esr1*-deficient ovary was significantly higher than those observed in WT ovaries (2.8 ± 4.3 mast cells per mm^2) (Figure 7B). In addition, TB staining in *Esr1*-deficient ovaries showed yellow deposits that were located at the same sides of iron deposits found in PPB staining (Figure 7C). Interestingly, we observed some degranulated mast cells in the *Esr1*-deficient ovaries, indicated by purple-stained granules that were released in the surrounding ovarian tissue (Figure 7D). In line, RT-qPCR revealed significantly higher levels of mast cell protease 6 and 2 (*Mcpt6, Mcpt2)* in *Esr1*-depleted ovaries (Figure 7E).

Overall, the number of mast cells is increased in *Esr1*-deficient ovaries compared with WT animals, suggesting that ovarian mast cells play an active role in the hemorrhagic cystic *Esr1*-knockout phenotype and might be involved in the formation of MNGCs.

4 Discussion

Estradiol (E2) and estrogen receptor alpha (ERα, *Esr1*) are essential for the maintenance of normal ovarian function and development in mammals. Consequently, *Esr1*-deficient animals are infertile (1, 14, 17, 48). The role of ERα in aging, particularly in ovarian aging is poorly understood. A recent study gave evidence that hormonal imbalance leads to increased iron deposition and altered iron homeostasis (20).

Overall, our data show that *Esr1*-deficient ovaries exhibit signs that are comparable to those seen in ovarian aging. Most interesting

10.3389/fendo.2024.1325386

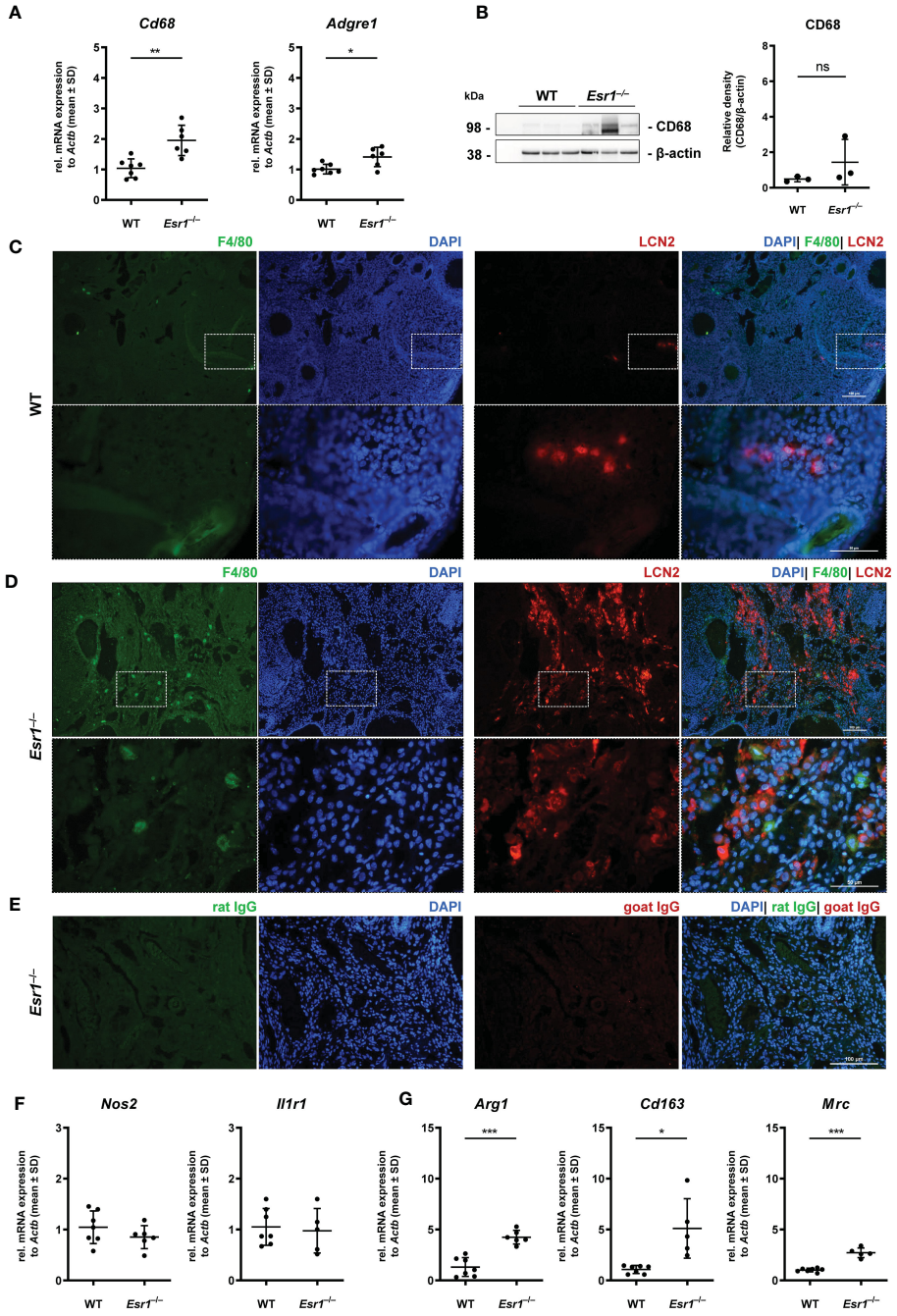

FIGURE 5
Macrophages in ovarian tissues. Wild type (WT) and *Esr1*-deficient ovarian tissues were either used for mRNA (WT, n=7; $Esr1^{-/-}$, n=5-6), protein analysis (WT, n=3; $Esr1^{-/-}$, n=3) or immunofluorescence staining (WT, n=3; $Esr1^{-/-}$, n=3). **(A)** Relative mRNA expression of pan-macrophage markers *Cd68* and *Adgre* were detected by RT-qPCR. **(B)** Western blot analysis was used to detect CD68 protein expression, which was quantified densitometrically and plotted relative to β-actin expression. F4/80 (green) and LCN2 (red) protein expression was visualized by immunofluorescence staining with nuclear DAPI counterstaining in **(C)** WT and *Esr1*-deficient **(D)** ovaries. **(E)** Normal rat and goat IgG were used as a negative control instead of the primary antibodies. The scale bars equal to 100 µm (solid boarder) or 50 µm (dashed border). **(F)** Relative mRNA expression of *Nos2* and *Il1r1*, as well as *Arg1*, *Cd163* and *Mrc* **(G)** were determined by RT-qPCR. All data **(A-B, F-G)** are displayed as mean ± SD. For statistical analysis, Students *t*-test was done. Significant differences between groups are marked with asterisks: *$p<0.05$, **$p<0.01$, ***$p<0.001$, ns =not significant.

is the massive iron overload in the *Esr1*-deficient ovaries, whereas only very small amounts are found in WT ovaries. The ovarian iron overload was confirmed by different techniques. We first demonstrated it by LA-ICP-MS imaging technique, which has already been established in hepatic metal bio-imaging for diagnostics (53, 71). LA-ICP-MS imaging revealed that *Esr1*-deficient ovaries had approximately 4-fold higher quanties of iron compared with WTs. Based on the light microscopy images of the native preparations and the LA-ICP-MS images that provided precise iron distribution within the tissue, we conclude that large

10.3389/fendo.2024.1325386

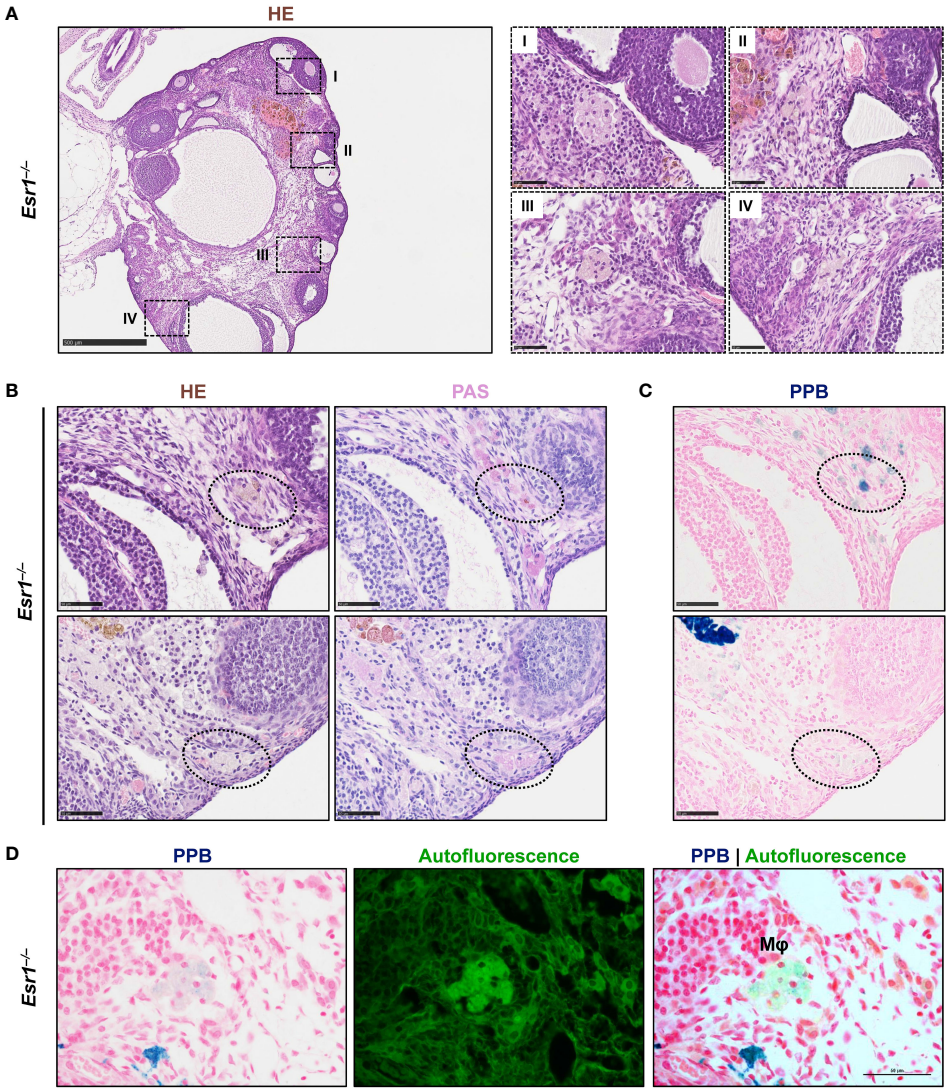

FIGURE 6
Multinucleated giant cells (MNGCs) are present in ovarian stroma of *Esr1*-deficient mice. Formaldehyde-fixated, paraffin-embedded serial ovarian tissue sections from *Esr1*-deficient mice (n=7) were used for different histological stainings. **(A)** Hematoxylin-Eosin (HE) staining shows pale cell clusters with a foamy appearance and multiple nuclei (I-IV) throughout the section of the *Esr1*-deficient ovary. **(B)** Cell clusters were identified as MNGCs by positive Periodic Acid-Schiff (PAS) reaction. **(C)** Perls Prussian Blue (PPB) staining revealed iron inclusions in the MNGCs. **(D)** PPB-stained MNGCs show strong autofluorescence. Scale bar equals 500 µm (solid boarder in **(A)**) or 50 µm (dashed boarder in **(A)** and in **(B–D)**).
Mφ, macrophage.

iron deposits are localized in the ovarian stroma of the animals, which is in contrast to the normal ovary where it is present within the atrectic follicles or regressing *corpora lutea*. Due to anovulation, infertile *Esr1*-deficient mice develop large cysts in the ovaries, which are mainly hemorrhagic (14, 17, 48), suggesting a link or a cause for elevated iron. Since iron is required for a variety of physiological prcoesses, but toxic in free form, precise balance of iron metabolism is mandatory (28). However, LA-ICP-MS analysis is limited to the determination of the elemental content of biometals and not suitable to assess the electron configation of measured iron. Therefore, it was necessary to investigate the form of the severe iron excess in *Esr1*-deficient ovaries and how this affects the iron metabolism of the animals. Our data demonstrate that ovarian iron deposition in *Esr1*-deficient animals was a local and not a systemic condition, due to the fact that liver and spleen (which act as important organs for iron storage and recycling) (35) were similar in control and *Esr1*-deficient animals. For a more detailed analysis of the systemic effects of iron, it would be useful to perform a comprehensive serum analysis. This analysis should include measuring typical iron-related parameters such as unsaturated iron binding capacity, transferrin saturation, and hemoglobin.

In a previous study we demonstrated that *Esr1* deletion dramatically increases expression of lipocalin 2 (LCN2), which acts as an alternative iron transporter (8). In line, we here found that *Esr1*-deficient ovaries had significantly increased transferrin mRNA and protein expression whem compared to WT ovaries, which indicates enhanced iron transport, possibly due to the hemorrhaghic phenotype of the animals. The iron storage protein

10.3389/fendo.2024.1325386

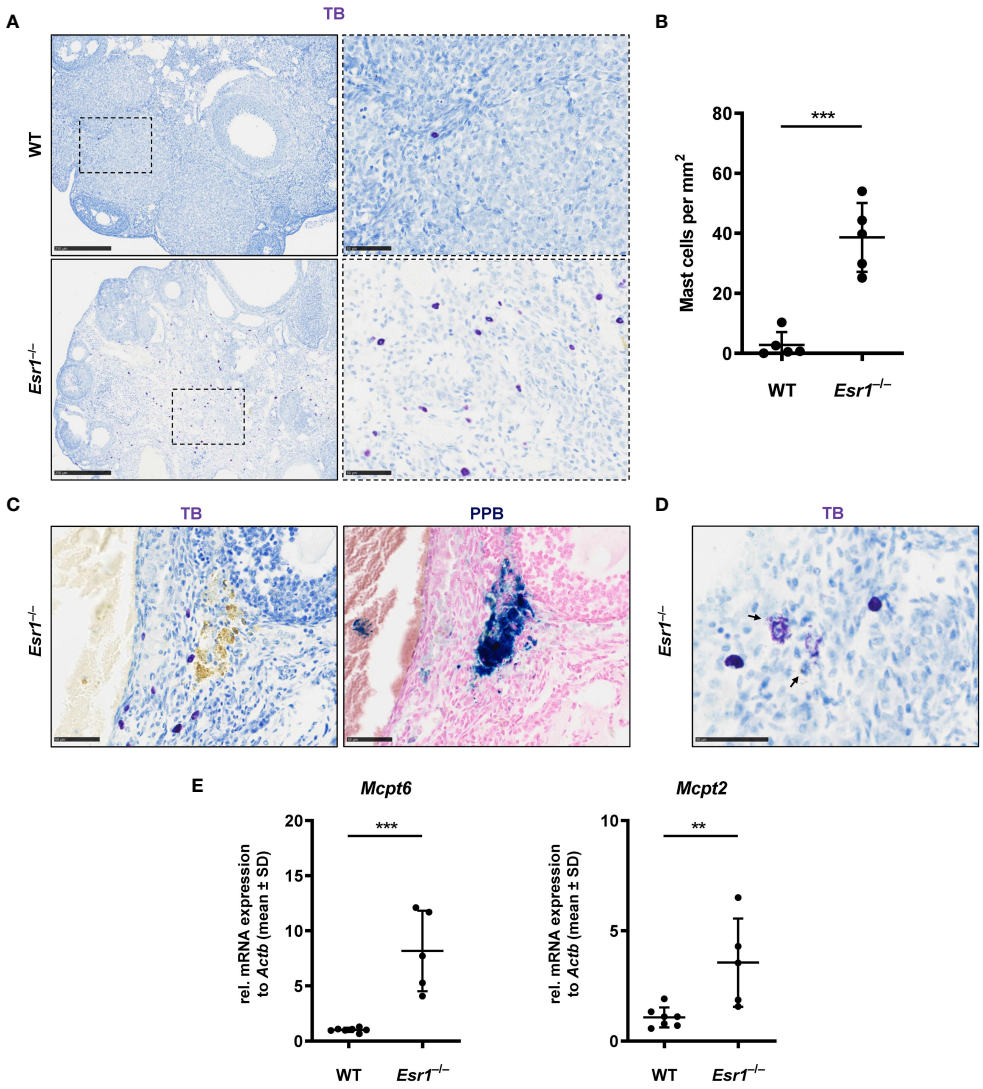

FIGURE 7
Increased number of mast cells in *Esr1*-deficient ovaries. Ovaries from wild type (WT, n=5) and *Esr1*-deficient mice ($Esr1^{-/-}$, n=5) were dissected and formalin-fixed paraffin-embedded tissue section were prepared. Toluidine blue (TB) staining was performed on ovarian tissue sections to detect mast cells. **(A)** WT animals demonstrate lower number of (purple stained) mast cells in the ovary than $Esr1^{-/-}$ animals. Scale bar correspond to 250 µm (solid boarder) or 50 µm (dashed boarder). **(B)** Evaluation of all female mice shows that $Esr1^{-/-}$ animals have significantly more mast cells per mm^2 in the ovary compared to WT controls. Each dot represents an individual mouse and horizontal lines indicate the mean (± SD). **(C)** Serial sections either stained with TB or Perls Prussian Blue (PPB) demonstrate that some mast cells in $Esr1^{-/-}$ animals reside in the vicinity of iron-accumulated areas (blue precipitates). Scale bar corresponds to 50 µm. **(D)** Occasionally, degranulated mast cells were found in the $Esr1^{-/-}$ ovary. Arrows indicate release of mast cell granules into surrounding ovarian tissue. Scale bar equals 50 µm. **(E)** RT-qPCR was performed to evaluate relative mRNA levels of mast cell specific markers (*Mcpt6, Mcpt2*). **(B, D)** Students *t*-test was used for statistical analysis. Significant differences between groups are marked with asterisks: $^{**}p<0.01$,$^{***}p<0.001$.

ferritin that exists either as heavy (Fth1) or as light chain (Ftl1), was strongly expressed by the murine ovaries, but only *Fth1* mRNA was significantly enhanced in *Esr1*-deficient ovaries. In addition, we found significantly higher expression of *Slc11a2*, a metal importer that is resposible for uptake of Fe^{2+} (72), in *Esr1*-depleted ovaries. Comparable, *Slc11a2* expression is elevated in ovarian endometriosis, a disease of the female reproductive tract associated with iron and related ovarian carcinogenesis (73). This suggests that the hemorrhagic iron-overload phenotype of *Esr1*-deficient ovaries has certain parallels with these diseases that are influenced by hormones. That only *Fth1* is strongly elevated in *Esr1*-deficient ovaries, might be explained by the functional difference between *Fth1* and *Ftl1*. It is known that only Fth1 has the ability to oxidize Fe^{2+} to Fe^{3+} (74). Considering that Slc11a2 mediates the uptake of iron as Fe^{2+}, thereby leading to increase iron levels, enhanced *Fth*1 expression could be essential in protecting against iron-induced oxidative stress.

Iron-regulatory proteins such as IRP2 regulate iron metabolism post-transcriptionally. When iron is present, IRP2 loses its high affinity for RNA, leading to an increase ferritin to prevent cellular damage (74). In contrast, we observed increased *Ireb2* expression in *Esr1*-deficient ovaries compared to WT controls. An abberrant

expression of IRPs, especially upregulation of IRP2, has been observed in aging rat ovaries and endometrial cysts (64, 75). These and our results underline that certain conditions, such as excess iron, upset the regulation of iron metabolism, which presumably leads to cellular damage in the long term.

Using PPB staining, we detected a tremendous accumulation of hemosiderin in *Esr1*-deficient ovaries, closely resembling the characteristics of aged ovaries (21, 23) In naturally aged murine ovaries, these deposits are stored in macrophages (so called hemosiderin-laden macrophages) as a consequence of red blood cell phagocytosis (21). It is likely that these cells are also present in *Esr1*-deficient ovary, as the hemorrhagic phenotype of these animals is clearly a source of these cells. However, it is still not clear what function and effect can be attributed to this deposition of hemosiderin in the tissue. Since hemosiderin is composed in part of degraded ferritin, it is postulated that hemosiderin acts as a protective factor in the cell by reducing the ability of iron to promote oxidative stress (33). On the other hand, it is assumed that decreased stability of hemosiderin deposits may lead to iron-induced lipid peroxidation in disease and aging (76). In addition, intramyocardial hemorrhages was shown to recruit iron-laden marcrophages in an animal model of myocardial infarction, which provokes foam cell formation and lipid peroxidation (66). Therefore, we concluded that the hemosiderin deposition in the ovaries is most likely due to the hemorrhagic phenotype of the *Esr1*-deficient animals and could probably be cell-damaging.

Iron overload with increased lipid peroxidation can lead to tissue damage resulting in ferroptosis, a form of oxidative damage-related cell death (77). However, there are a variety of mechanisms that can be activated to reduce severe cellular damage caused by *e.g.* excess iron. Interestingly, Fths function is not only limited to iron storage. It further has essential roles in the detoxification capacity of macrophages (78). Ferroptosis (iron-induced cell death) is characterized by ferritinophagy, the degradation of ferritins. However, expression of genes associated with ferroptosis were not found different in *Esr1*-deficient and WT ovaries. Another defense mechanism of ferroptosis is the expression of glutathione peroxidase 4 (GPX4) (79). The strong expression of *Gpx4* mRNA and protein in WT and *Esr1*-depleted ovaries suggests that antioxidant activity is not altered in ovaries lacking *Esr1*. In addition, we found that *Esr1*-deficient animals show significantly enhanced *Hmox1* mRNA expression. In general, activation cytoprotective enzymes such as heme oxygenase-1 (HMOX1, *Hmox1*) is a mechanism to handle iron overload conditions (35, 80). In aging female mice, HMOX1 expression was found around atrectic follicles in macrophages, indicating degeneration of engulfed heme (23). Overall, we can conclude from our data that defense mechanisms against oxidative stress are activated in the *Esr1*-deficient animals, while we observed no alterations in iron-driven cell death associated with the lack of *Esr1*. Since there are a large number of parameters associated with iron-induced cell damage, it is advisable to comprehensively investigate these in future studies. It would be suitable to examine the amount of 4-hydroxynonenal as a marker of lipid peroxidation and analyze the Nrf2-Keap1 axis, which is one of the most important signaling pathways in the control of oxidative and electrophilic stress. Additionally, it is important to not only focus on protein expression, but also on its localization in the tissue.

Since macrophages are recruited in hemorrhage conditions and are key players in iron metabolism, we investigated whether these are aberrant in the *Esr1*-deficient ovaries. Indeed, we found signifcantly higher expression of *Cd68* and *Adgre* representin important pan-macrophage markers. In line, immunofluoresence detection of F4/80 verified these findings. Interestingly, we found no co-localization of F4/80 and the iron regulator LCN2. LCN2 that plays a pleiotropic role in relation to macrophages and inflammation, depends on various factors (81, 82). Our results show significantly higher expression of M2-like macrophage markers (*Arg1*, *Cd163*, *Mrc*) in *Esr1*-deficient ovaries when compared to WT animals, whereas, contrary to expectations, there was no significant difference in M1-like markers (*Il1r*, *Nos2*). These results suggest that despite the intense iron accumulation, the ovary of *Esr1*-knockout animals express anti-inflammatory markers, which are indicative for remodeling and tissue repair, similar to characteristics foun during ovarian aging (38). Further studies should investigate systemic levels of inflammatory markers and clearly identify whether these ovarian immune cells are resident or infiltrating.

In the last decade, a unique type of ovarian macrophage found exclusively in reproductively old animals was discovered (21–23, 34). Based on the typical appearance of this cell type, these cells are referred as MNGCs. These cells are likely the result of a disruption in normal physiology that is caused by altered endocrinology as one possible cause (34). Our data provides the first evidence that endocrine dysfunction indeed causes formation of MNGCs, as these cells are present in the aged ovaries of *Esr1*-deficient animals but not in WT littermates. Considering that their appearance correlates with a strong increase in classical M2-like macrophage markers, they may play a role in remodeling and tissue repair. In addition, we found that iron storage seems to play a role in these cells, as we confirmed iron deposition in the MNGCs by PPB staining. These foam cell clusters in *Esr1*-deficient ovaries exhibit strong autofluroresence, likely due to accumulation of lipofuscin, an 'aging-pigment observed in ovarian aging and disease (21–23, 83). Lipofuscin and iron storage are associated with oxidative DNA damage and ovarian disease (21). Although our limited results suggest that adult *Esr1*-deficient animals have not higher tendency to induce ferroptosis than WT animals, it is possible that this changes after futher aging. This is supported by preliminary data of a small number of older *Esr1*-deficient animals that we have analyzed, showing strong accumulation of lipofuscin and massive iron deposits in the aged organs (cf. Supplementary Figure 3). Interestingly, preliminary (unpublished) results using Oil Red staining show that the MNGCs in *Esr1*-deficient ovaries and aged WT ovaries contain numerous lipid droplets. Further analysis of these specific MNGCs, which are formed in both the aged WT animals and after *Esr1* depletion, will shed light on the potential link between aging processes and *Esr1* signaling.

Studies outside the ovary have shown that iron-induced macrophage influx and foam cell formation in a hemorrhage lesion are associated with increased mast cell activity (66). In fact, our results confirm a similar finding in the hemorrhagic ovary as

there is a significantly higher number of mast cells in *Esr1*-deficient than in WT ovaries. This is consistent with the results of another *Esr1* depletion model, in which the PCOS phenotype is associated with enhanced mast cells (13). Interestingly, release of granules from mast cells is mediated by hormones such as luteinizing hormone (84). As suggested previously by others (13), high quantities of serum luteinizing hormone in the *Esr1*-deficient ovary (48) may lead to mast cell activity.

5 Conclusion

In the study presented, we have demonstrated that disruption of *Esr1* in the mouse ovary leads to changes in iron metabolism. Specifically, we report for the first time an iron overload phenotype in the *Esr1*-deficient ovary, accompanied by abnormal iron metabolism. In addition, these animals showed increased numbers of ovarian macrophages and mast cells. Notably, we observed an influx of M2-like macrophages and formation of foam macrophages, which are considered hallmarks of ovarian aging. Therefore, our results suggest that there may be similar underlying mechanisms involved in ovarian aging. However, further studies, including age-dependent observation of *Esr1*-deficient animals are required to understand the role and potential consequences of these MNGCs in the ovary. In this context, it is also important to determine whether tissue architecture remodeling is abnormal in *Esr1*-deficient ovaries, as is seen in aging (22, 85). A better understanding of the aging processes in the ovaries could therefore lead to the development of therapies that curb oocyte damage and age-related infertility.

Data availability statement

The raw data supporting the conclusions of this article will be made available by the authors, without undue reservation.

Ethics statement

The animal study was approved by internal Review Board of the RWTH University Hospital Aachen. The study was conducted in accordance with the local legislation and institutional requirements.

Author contributions

SKS: Conceptualization, Formal analysis, Investigation, Methodology, Project administration, Validation, Visualization, Writing – original draft. MK: Formal analysis, Investigation, Methodology, Validation, Visualization, Writing – review & editing. PK: Formal analysis, Methodology, Visualization, Writing – review & editing. JCK: Formal analysis, Methodology, Writing – review & editing. RW: Conceptualization, Data curation, Funding acquisition, Investigation, Project administration, Resources, Supervision, Visualization, Writing – review & editing.

Funding

The author(s) declare financial support was received for the research, authorship, and/or publication of this article. RW is supported by grants from the German Research Foundation (grants WE2554/13-1, WE2554/15-1, and WE 2554/17-1), the Deutsche Krebshilfe (grant 70115581), and the Interdisciplinary Centre for Clinical Research within the faculty of Medicine at the RWTH Aachen University (grant PTD 1-5). The funders had no role in the design of this article or in the decision to publish it.

Acknowledgments

This work was supported by the Immunohistochemistry Facility, a core facility of the Interdisciplinary Center for Clinical Research (IZKF) Aachen within the Faculty of Medicine at RWTH Aachen University. The authors are grateful to Carmen G. Tag (IFMPEGKC, Aachen, Germany) for excellent technical assistance with animal tissue dissection, genotyping and staining and to Sabine Weiskirchen (IFMPEGKC, Aachen, Germany) for preparing the cryosections and technical support in using the NanoZoomer SQ digital slide scanner. The authors thank Manuela Pinoe-Schmidt (IFMPEGKC, Aachen, Germany) for technical assistance in molecular biology and Sven Thoroe-Boveleth (Institute for Occupational, Social and Environmental Medicine, RWTH Aachen University) for performing the LA-ICP-MS measurements.

Conflict of interest

The authors declare that the research was conducted in the absence of any commercial or financial relationships that could be construed as a potential conflict of interest.

The author(s) declared that they were an editorial board member of Frontiers, at the time of submission. This had no impact on the peer review process and the final decision.

Publisher's note

Supplementary material

The Supplementary Material for this article can be found online at: https://www.frontiersin.org/articles/10.3389/fendo.2024.1325386/full#supplementary-material

References

1. Hamilton KJ, Hewitt SC, Arao Y, Korach KS. Estrogen hormone biology. *Curr Top Dev Biol* (2017) 125:109–46. doi: 10.1016/bs.ctdb.2016.12.005

2. Mahboobifard F, Pourgholami MH, Jorjani M, Dargahi L, Amiri M, Sadeghi S, et al. Estrogen as a key regulator of energy homeostasis and metabolic health. *BioMed Pharmacother* (2022) 156:113808. doi: 10.1016/j.biopha.2022.113808

3. Hewitt SC, Korach KS. Estrogen receptors: new directions in the new millennium. *Endocrine Rev* (2018) 39:664–75. doi: 10.1210/er.2018-00087

4. Schroder SK, Tag CG, Kessel JC, Antonson P, Weiskirchen R. Immunohistochemical detection of estrogen receptor-beta (ERβ) with PPZ0506 antibody in murine tissue: from pitfalls to optimization. *Biomedicines* (2022) 10:3100. doi: 10.3390/biomedicines10123100

5. Kuiper GG, Enmark E, Pelto-Huikko M, Nilsson S, Gustafsson JA. Cloning of a novel receptor expressed in rat prostate and ovary. *Proc Natl Acad Sci U S A* (1996) 93:5925–30. doi: 10.1073/pnas.93.12.5925

6. Hiroi H, Inoue S, Watanabe T, Goto W, Orimo A, Momoeda M, et al. Differential immunolocalization of estrogen receptor alpha and beta in rat ovary and uterus. *J Mol Endocrinology* (1999) 22:37–44. doi: 10.1677/jme.0.0220037

7. Sar M, Welsch F. Differential expression of estrogen receptor-β and estrogen receptor-α in the rat ovary. *Endocrinology* (1999) 140:963–71. doi: 10.1210/endo.140.2.6533

8. Kessel JC, Weiskirchen R, Schroder SK. Expression analysis of lipocalin 2 (LCN2) in reproductive and non-reproductive tissues of esr1-deficient mice. *Int J Mol Sci* (2023) 24:9280. doi: 10.3390/ijms24119280

9. Nalvarte I, Antonson P. Estrogen receptor knockout mice and their effects on fertility. *Receptors* (2023) 2:116–26. doi: 10.3390/receptors2010007

10. Couse JF, Korach KS. Estrogen receptor null mice: what have we learned and where will they lead us? *Endocrine Rev* (1999) 20:358–417. doi: 10.1210/edrv.20.3.0370

11. Hamilton KJ, Arao Y, Korach KS. Estrogen hormone physiology: reproductive findings from estrogen receptor mutant mice. *Reprod Biol* (2014) 14:3–8. doi: 10.1016/j.repbio.2013.12.002

12. Hewitt SC, Couse JF, Korach KS. Estrogen receptor transcription and transactivation: Estrogen receptor knockout mice: what their phenotypes reveal about mechanisms of estrogen action. *Breast Cancer Res* (2000) 2:345–52. doi: 10.1186/bcr79

13. Dupont S, Krust A, Gansmuller A, Dierich A, Chambon P, Mark M. Effect of single and compound knockouts of estrogen receptors alpha (ERalpha) and beta (ERbeta) on mouse reproductive phenotypes. *Development* (2000) 127:4277–91. doi: 10.1242/dev.127.19.4277

14. Lubahn DB, Moyer JS, Golding TS, Couse JF, Korach KS, Smithies O. Alteration of reproductive function but not prenatal sexual development after insertional disruption of the mouse estrogen receptor gene. *Proc Natl Acad Sci United States America* (1993) 90:11162–6. doi: 10.1073/pnas.90.23.11162

15. Antonson P, Apolinario LM, Shamekh MM, Humire P, Poutanen M, Ohlsson C, et al. Generation of an all-exon Esr2 deleted mouse line: Effects on fertility. *Biochem Biophys Res Commun* (2020) 529:231–7. doi: 10.1016/j.bbrc.2020.06.063

16. Prossnitz ER, Hathaway HJ. What have we learned about GPER function in physiology and disease from knockout mice? *J Steroid Biochem Mol Biol* (2015) 153:114–26. doi: 10.1016/j.jsbmb.2015.06.014

17. Schomberg DW, Couse JF, Mukherjee A, Lubahn DB, Sar M, Mayo KE, et al. Targeted disruption of the estrogen receptor-alpha gene in female mice: characterization of ovarian responses and phenotype in the adult. *Endocrinology* (1999) 140:2733–44. doi: 10.1210/endo.140.6.6823

18. Britt KL, Drummond AE, Dyson M, Wreford NG, Jones ME, Simpson ER, et al. The ovarian phenotype of the aromatase knockout (ArKO) mouse. *J Steroid Biochem Mol Biol* (2001) 79:181–5. doi: 10.1016/S0960-0760(01)00158-3

19. Britt KL, Drummond AE, Cox VA, Dyson M, Wreford NG, Jones ME, et al. An age-related ovarian phenotype in mice with targeted disruption of the Cyp 19 (aromatase) gene. *Endocrinology* (2000) 141:2614–23. doi: 10.1210/endo.141.7.7578

20. Toothaker JM, Roosa K, Voss A, Getman SM, Pepling ME. Oocyte survival and development during follicle formation and folliculogenesis in mice lacking aromatase. *Endocrine Res* (2022) 47:45–55. doi: 10.1080/07435800.2021.2011907

21. Urzua U, Chacon C, Espinoza R, Martinez S, Hernandez N. Parity-dependent hemosiderin and lipofuscin accumulation in the reproductively aged mouse ovary. *Anal Cell Pathol (Amst)* (2018) 2018:1289103. doi: 10.1155/2018/1289103

22. Briley SM, Jasti S, McCracken JM, Hornick JE, Fegley B, Pritchard MT, et al. Reproductive age-associated fibrosis in the stroma of the mammalian ovary. *Reproduction* (2016) 152:245–60. doi: 10.1530/REP-16-0129

23. Asano Y. Age-related accumulation of non-heme ferric and ferrous iron in mouse ovarian stroma visualized by sensitive non-heme iron histochemistry. *J Histochem Cytochem* (2012) 60:229–42. doi: 10.1369/0022155411431734

24. Mathew M, Sivaprakasam S, Phy JL, Bhutia YD, Ganapathy V. Polycystic ovary syndrome and iron overload: biochemical link and underlying mechanisms with potential novel therapeutic avenues. *Biosci Rep* (2023) 43:BSR20212234. doi: 10.1042/BSR20212234

25. Escobar-Morreale HF. Iron metabolism and the polycystic ovary syndrome. *Trends Endocrinol Metab* (2012) 23:509–15. doi: 10.1016/j.tem.2012.04.003

26. Sanchez AM, Papaleo E, Corti L, Santambrogio P, Levi S, Vigano P, et al. Iron availability is increased in individual human ovarian follicles in close proximity to an endometrioma compared with distal ones. *Hum Reprod* (2014) 29:577–83. doi: 10.1093/humrep/det466

27. Miller EM. The reproductive ecology of iron in women. *Am J Phys Anthropol* (2016) 159:S172–95. doi: 10.1002/ajpa.22907

28. Galaris D, Pantopoulos K. Oxidative stress and iron homeostasis: mechanistic and health aspects. *Crit Rev Clin Lab Sci* (2008) 45:1–23. doi: 10.1080/10408360701713104

29. Xia L, Shen Y, Liu S, Du J. Iron overload triggering ECM-mediated Hippo/YAP pathway in follicle development: a hypothetical model endowed with therapeutic implications. *Front Endocrinol (Lausanne)* (2023) 14:1174817. doi: 10.3389/fendo.2023.1174817

30. Anderson GJ, McLaren GD. *Iron Physiology and Pathophysiology in Humans* Humana Press, Springer New York, Dordrecht, Heidelberg, London (2012). doi: 10.1007/978-1-60327-485-2

31. Cook SF. The structure and composition of hemosiderin. *J Biol Chem* (1929) 82:595–609. doi: 10.1016/S0021-9258(18)77144-5

32. Saito H. Metabolism of iron stores. *Nagoya J Med science* (2014) 76:235–54.

33. Iancu TC. Ferritin and hemosiderin in pathological tissues. *Electron microscopy Rev* (1992) 5:209–29. doi: 10.1016/0892-0354(92)90011-E

34. Foley KG, Pritchard MT, Duncan FE. Macrophage-derived multinucleated giant cells: hallmarks of the aging ovary. *Reproduction* (2021) 161:V5–9. doi: 10.1530/REP-20-0489

35. Sukhbaatar N, Weichhart T. Iron regulation: macrophages in control. *Pharm (Basel)* (2018) 11:137. doi: 10.3390/ph11040137

36. Zhang D, Yu Y, Duan T, Zhou Q. The role of macrophages in reproductive-related diseases. *Heliyon* (2022) 8:e11686. doi: 10.1016/j.heliyon.2022.e11686

37. Zhang Z, Huang L, Brayboy L. Macrophages: an indispensable piece of ovarian health. *Biol Reprod* (2021) 104:527–38. doi: 10.1093/biolre/ioaa219

38. Zhang Z, Schlamp F, Huang L, Clark H, Brayboy L. Inflammaging is associated with shifted macrophage ontogeny and polarization in the aging mouse ovary. *Reproduction* (2020) 159:325–37. doi: 10.1530/REP-19-0330

39. Berger T, Togawa A, Duncan GS, Elia AJ, You-Ten A, Wakeham A, et al. Lipocalin 2-deficient mice exhibit increased sensitivity to Escherichia coli infection but not to ischemia-reperfusion injury. *Proc Natl Acad Sci United States America* (2006) 103:1834–9. doi: 10.1073/pnas.0510847103

40. Mosialou I, Shikhel S, Luo N, Petropoulou PI, Panitsas K, Bisikirska B, et al. Lipocalin-2 counteracts metabolic dysregulation in obesity and diabetes. *J Exp Med* (2020) 217:e20191261. doi: 10.1084/jem.20191261

41. Kjeldsen L, Johnsen AH, Sengelov H, Borregaard N. Isolation and primary structure of NGAL, a novel protein associated with human neutrophil gelatinase. *J Biol Chem* (1993) 268:10425–32. doi: 10.1016/S0021-9258(18)82217-7

42. Goetz DH, Holmes MA, Borregaard N, Bluhm ME, Raymond KN, Strong RK. The neutrophil lipocalin NGAL is a bacteriostatic agent that interferes with siderophore-mediated iron acquisition. *Mol Cell* (2002) 10:1033–43. doi: 10.1016/S1097-2765(02)00708-6

43. Flo TH, Smith KD, Sato S, Rodriguez DJ, Holmes MA, Strong RK, et al. Lipocalin 2 mediates an innate immune response to bacterial infection by sequestrating iron. *Nature* (2004) 432:917–21. doi: 10.1038/nature03104

44. Xiao X, Yeoh BS, Vijay-Kumar M. Lipocalin 2: an emerging player in iron homeostasis and inflammation. *Annu Rev Nutr* (2017) 37:103–30. doi: 10.1146/annurev-nutr-071816-064559

45. Rockfield S, Raffel J, Mehta R, Rehman N, Nanjundan M. Iron overload and altered iron metabolism in ovarian cancer. *Biol Chem* (2017) 398:995–1007. doi: 10.1515/hsz-2016-0336

46. Li A, Ni Z, Zhang J, Cai Z, Kuang Y, Yu C. Transferrin insufficiency and iron overload in follicular fluid contribute to oocyte dysmaturity in infertile women with advanced endometriosis. *Front Endocrinol (Lausanne)* (2020) 11:391. doi: 10.3389/fendo.2020.00391

47. Zhang J, Liu Y, Yao W, Li Q, Liu H, Pan Z. Initiation of follicular atresia: gene networks during early atresia in pig ovaries. *J Reproduction* (2018) 156:23–33. doi: 10.1530/REP-18-0058

48. Hewitt SC, Kissling GE, Fieselman KE, Jayes FL, Gerrish KE, Korach KS. Biological and biochemical consequences of global deletion of exon 3 from the ER alpha gene. *FASEB J* (2010) 24:4660–7. doi: 10.1096/fj.10.163428

49. Meguro R, Asano Y, Odagiri S, Li C, Iwatsuki H, Shoumura K. Nonheme-iron histochemistry for light and electron microscopy: a historical, theoretical and technical review. *Arch Histol cytology* (2007) 70:1–19. doi: 10.1679/aohc.70.1

50. Sobolev SM. Result of histochemical studies on certain PAS-positive substances in macrophages. *Biulleten' eksperimental'noi biologii i meditsiny* (1959) 47:104–9. doi: 10.1007/BF00779693

51. Grigorev IP, Korzhevskii DE. Modern imaging technologies of mast cells for biology and medicine (Review). *Sovremennye tekhnologii v meditsine* (2021) 13:93–107. doi: 10.17691/stm2021.13.4.10

52. Whittington NC, Wray S. Suppression of red blood cell autofluorescence for immunocytochemistry on fixed embryonic mouse tissue. *Curr Protoc Neurosci* (2017) 81:2.28.1–2.12. doi: 10.1002/cpns.35

53. Kim P, Weiskirchen S, Uerlings R, Kueppers A, Stellmacher F, Viveiros A, et al. Quantification of liver iron overload disease with laser ablation inductively coupled plasma mass spectrometry. *BMC Med Imaging* (2018) 18:51. doi: 10.1186/s12880-018-0291-3

54. Chakrabarti M, Cockrell AL, Park J, McCormick SP, Lindahl LS, Lindahl PA. Speciation of iron in mouse liver during development, iron deficiency, IRP2 deletion and inflammatory hepatitis. *Metallomics* (2015) 7:93–101. doi: 10.1039/C4MT00215F

55. Becker JS. Imaging of metals in biological tissue by laser ablation inductively coupled plasma mass spectrometry (LA-ICP-MS): state of the art and future developments. *J Mass Spectrom* (2013) 48:255–68. doi: 10.1002/jms.3168.

56. Weiskirchen R, Uerlings R. Laser ablation inductively coupled plasma mass spectrometry in biomedicine and clinical diagnosis. *Cell Mol Medicine: Open access* (2015) 01:1. doi: 10.21767/2573-5365

57. Uerlings R, Matusch A. Reconstruction of laser ablation inductively coupled plasma mass spectrometry (LA-ICP-MS) spatial distribution images in Microsoft Excel 2007. *Int Journals Mass Spectrometry* (2016) 395:27–35. doi: 10.1016/j.ijms.2015.11.010

58. Weiskirchen R, Weiskirchen S, Kim P, Winkler R. Software solutions for evaluation and visualization of laser ablation inductively coupled plasma mass spectrometry imaging (LA-ICP-MSI) data: a short overview. *J Cheminform* (2019) 11:16. doi: 10.1186/s13321-019-0338-7

59. Boaru SG, Merle U, Uerlings R, Zimmermann A, Flechtenmacher C, Willheim C, et al. Laser ablation inductively coupled plasma mass spectrometry imaging of metals in experimental and clinical Wilson's disease. *J Cell Mol Med* (2015) 19:806–14. doi: 10.1111/jcmm.12497

60. Kim P, Zhang CC, Thoroe-Boveleth S, Buhl EM, Weiskirchen S, Stremmel W, et al. Analyzing the therapeutic efficacy of bis-choline-tetrathiomolybdate in the atp7b (-/-) copper overload mouse model. *Biomedicines* (2021) 9:1861. doi: 10.3390/biomedicines9121861

61. Pathak P, Kapil U. Role of trace elements zinc, copper and magnesium during pregnancy and its outcome. *Indian J pediatrics* (2004) 71:1003–5. doi: 10.1007/BF02828116

62. Ceko MJ, O'Leary S, Harris HH, Hummitzsch K, Rodgers RJ. Trace elements in ovaries: measurement and physiology. *Biol Reprod* (2016) 94:86. doi: 10.1095/biolreprod.115.137240

63. Kovtunovych G, Eckhaus MA, Ghosh MC, Ollivierre-Wilson H, Rouault TA. Dysfunction of the heme recycling system in heme oxygenase 1-deficient mice: effects on macrophage viability and tissue iron distribution. *Blood* (2010) 116:6054–62. doi: 10.1182/blood-2010-03-272138

64. Sze SCW, Zhang L, Zhang S, Lin K, Ng TB, Ng ML, et al. Aberrant transferrin and ferritin upregulation elicits iron accumulation and oxidative inflammaging causing ferroptosis and undermines estradiol biosynthesis in aging rat ovaries by upregulating NF-kappab-activated inducible nitric oxide synthase: first demonstration of an intricate mechanism. *Int J Mol Sci* (2022) 23:12689. doi: 10.3390/ijms232012689

65. Kasztura M, Kiczak L, Paslawska U, Bania J, Janiszewski A, Tomaszek A, et al. Hemosiderin accumulation in liver decreases iron availability in tachycardia-induced porcine congestive heart failure model. *Int J Mol Sci* (2022) 23:1026. doi: 10.3390/ijms23031026

66. Cokic I, Chan SF, Guan X, Nair AR, Yang HJ, Liu T, et al. Intramyocardial hemorrhage drives fatty degeneration of infarcted myocardium. *Nat Commun* (2022) 13:6394. doi: 10.1038/s41467-022-33776-x

67. Zhang Y, Ramos BF, Jakschik BA. Neutrophil recruitment by tumor necrosis factor from mast cells in immune complex peritonitis. *Sci (New York NY)* (1992) 258:1957–9. doi: 10.1126/science.1470922

68. Batth BK, Parshad RK. Mast cell dynamics in the house rat (Rattus rattus) ovary during estrus cycle, pregnancy and lactation. *Eur J morphology* (2000) 38:17–23. doi: 10.1076/0924-3860(200002)38:01;1-#;FT017

69. Karaca T, Yoruk M, Uslu S. Distribution and quantitative patterns of mast cells in ovary and uterus of rat. *Archivos medicina veterinaria* (2007) 39:135-39. doi: 10.4067/S0301-732X2007000200006

70. Atiakshin D, Patsap O, Kostin A, Mikhalyova L, Buchwalow I, Tiemann M. Mast cell tryptase and carboxypeptidase A3 in the formation of ovarian endometrioid cysts. *Int J Mol Sci* (2023) 24:6498. doi: 10.3390/ijms24076498

71. Weiskirchen S, Kim P, Weiskirchen R. Determination of copper poisoning in Wilson's disease using laser ablation inductively coupled plasma mass spectrometry. *Ann Transl Med* (2019) 7:S72. doi: 10.21037/atm

72. Vogt AS, Arsiwala T, Mohsen M, Vogel M, Manolova V, Bachmann MF. On iron metabolism and its regulation. *Int J Mol Sci* (2021) 22:4591. doi: 10.3390/ijms22094591

73. Akashi K, Nagashima Y, Tabata T, Oda H. Immunochemical analysis of iron transporters and M2 macrophages in ovarian endometrioma and clear cell adenocarcinoma. *Mol Clin Oncol* (2021) 15:159. doi: 10.3892/mco

74. Wallander ML, Leibold EA, Eisenstein RS. Molecular control of vertebrate iron homeostasis by iron regulatory proteins. *Biochim Biophys Acta* (2006) 1763:668–89. doi: 10.1016/j.bbamcr.2006.05.004

75. Takenaka M, Suzuki N, Mori M, Hirayama T, Nagasawa H, Morishige KI. Iron regulatory protein 2 in ovarian endometrial cysts. *Biochem Biophys Res Commun* (2017) 487:789–94. doi: 10.1016/j.bbrc.2017.04.115

76. Tian Y, Tian Y, Yuan Z, Zeng Y, Wang S, Fan X, et al. Iron metabolism in aging and age-related diseases. *Int J Mol Sci* (2022) 23:3612. doi: 10.3390/ijms23073612

77. Chen X, Comish PB, Tang D, Kang R. Characteristics and biomarkers of ferroptosis. *Front Cell Dev Biol* (2021) 9:637162. doi: 10.3389/fcell.2021.637162

78. Mesquita G, Silva T, Gomes AC, Oliveira PF, Alves MG, Fernandes R, et al. H-Ferritin is essential for macrophages' capacity to store or detoxify exogenously added iron. *Sci Rep* (2020) 10:3061. doi: 10.1038/s41598-020-59898-0

79. Zhang LL, Tang RJ, Yang YJ. The underlying pathological mechanism of ferroptosis in the development of cardiovascular disease. *Front Cardiovasc Med* (2022) 9:964034. doi: 10.3389/fcvm.2022.964034

80. Recalcati S, Cairo G. Macrophages and iron: a special relationship. *Biomedicines* (2021) 9:1585. doi: 10.3390/biomedicines9111585

81. An HS, Yoo JW, Jeong JH, Heo M, Hwang SH, Jang HM, et al. Lipocalin-2 promotes acute lung inflammation and oxidative stress by enhancing macrophage iron accumulation. *Int J Biol Sci* (2023) 19:1163–77. doi: 10.7150/ijbs.79915

82. Jung M, Brune B, Hotter G, Sola A. Macrophage-derived Lipocalin-2 contributes to ischemic resistance mechanisms by protecting from renal injury. *Sci Rep* (2016) 6:21950. doi: 10.1038/srep21950

83. Watson JM, Marion SL, Rice PF, Utzinger U, Brewer MA, Hoyer PB, et al. Two-photon excited fluorescence imaging of endogenous contrast in a mouse model of ovarian cancer. *Lasers Surg Med* (2013) 45:155–66. doi: 10.1002/lsm.22115

84. Norman RJ, Brannstrom M. White cells and the ovaryincidental invaders or essential effectors? *J Endocrinol* (1994) 140:333–6. doi: 10.1677/joe.0.1400333

85. Amargant F, Manuel SL, Tu Q, Parkes WS, Rivas F, Zhou LT, et al. Ovarian stiffness increases with age in the mammalian ovary and depends on collagen and hyaluronan matrices. *Aging Cell* (2020) 19:e13259. doi: 10.1111/acel.13259

Glossary

Aco1	Aconitase 1
Adgre	Adhesion G protein-coupled receptor
Arg1	Arginase 1
Cd	Cluster of differentiation
E2	17β-Estradiol
ER, Esr	Estrogen receptor
Fpn	Ferroportin
Fth1	Ferritin heavy chain 1
Ftl1	Ferritin light chain 1
GPER1	G-protein coupled estrogen receptor 1
Hamp1	Hepcidin antimicrobial peptide 1
HE	Hematoxylin-eosin
Il1r1	Interleukin 1 receptor type 1
IRP	Iron regulatory protein
LA-ICP-MS	laser ablation inductively coupled plasma mass spectrometry
LCN2	Lipocalin 2
Mcpt	Mast cell protease
MNGC	Macrophage-derived multinucleated giant cell
Mrc	Mannose receptor
Nos2	Nitric oxide synthase 2
PAS	Periodic acid-Schiff
PBS	Phosphate-buffered saline
PBS-T	PBS supplemented with 0.1% Tween® 20
PCOS	Polycystic ovary syndrome
PPB	Perls Prussian Blue
RT	Room temperature
RT-qPCR	reverse transcription and quantitative real-time polymerase chain reaction
Slc11a2	Solute carrier family 11 member 2
TB	Toluidine Blue
Tf	Transferrin

frontiers | Frontiers in Endocrinology

TYPE Original Research
PUBLISHED 26 February 2024
DOI 10.3389/fendo.2024.1280760

OPEN ACCESS

EDITED BY
Osamu Hiraike,
The University of Tokyo, Japan

REVIEWED BY
Arindam Dhali,
National Institute of Animal Nutrition and Physiology (ICAR), India
Marianna Santonastaso,
Universitàdegli Studi della Campania "Luigi Vanvitelli", Italy
Waleed Fawzy Marei,
University of Antwerp, Belgium

*CORRESPONDENCE
Jia-ping Yu
m17790992792@163.com

RECEIVED 21 August 2023
ACCEPTED 31 January 2024
PUBLISHED 26 February 2024

CITATION
Chu Q, Yu Y-x, Zhang J-z, Zhang Y-t and Yu J-p (2024) Effects of flaxseed oil supplementation on metaphase II oocyte rates in IVF cycles with decreased ovarian reserve: a randomized controlled trial. *Front. Endocrinol.* 15:1280760. doi: 10.3389/fendo.2024.1280760

Effects of flaxseed oil supplementation on metaphase II oocyte rates in IVF cycles with decreased ovarian reserve: a randomized controlled trial

Qi Chu, Yue-xin Yu, Jing-zi Zhang, Yi-tong Zhang and Jia-ping Yu*

Department of Reproductive Medicine, General Hospital of Northern Theater Command, Shenyang, Liaoning, China

Background: This study was designed to explore the effects of flaxseed oil on the metaphase II (MII) oocyte rates in women with decreased ovarian reserve (DOR).

Methods: The women with DOR were divided into a study group (n = 108, flaxseed oil treatment) and a control group (n = 110, no treatment). All patients were treated with assisted reproductive technology (ART). Subsequently, the ART stimulation cycle parameters, embryo transfer (ET) results, and clinical reproductive outcomes were recorded. The influencing factors affecting the MII oocyte rate were analyzed using univariate analysis and multivariate analysis.

Results: Flaxseed oil reduced the recombinant human follicle-stimulating hormone (r-hFSH) dosage and stimulation time and increased the peak estradiol (E2) concentration in DOR women during ART treatment. The MII oocyte rate, fertilization rate, cleavage rate, high-quality embryo rate, and blastocyst formation rate were increased after flaxseed oil intervention. The embryo implantation rate of the study group was higher than that of the control group (p = 0.05). Additionally, the female age [odds ratio (OR): 0.609, 95% confidence interval (CI): 0.52–0.72, p < 0.01] was the hindering factor of MII oocyte rate, while anti-Müllerian hormone (AMH; OR: 100, 95% CI: 20.31–495, p < 0.01), peak E2 concentration (OR: 1.00, 95% CI: 1.00–1.00, p = 0.01), and the intake of flaxseed oil (OR: 2.51, 95% CI: 1.06–5.93, p = 0.04) were the promoting factors for MII oocyte rate.

Conclusion: Flaxseed oil improved ovarian response and the quality of oocytes and embryos, thereby increasing the fertilization rate and high-quality embryo rate in DOR patients. The use of flaxseed oil was positively correlated with MII oocyte rate in women with DOR.

Clinical trial number: https://www.chictr.org.cn/, identifier ChiCTR2300073785

KEYWORDS

decreased ovarian reserve, flaxseed oil, metaphase II oocyte rates, omega-3 fatty acids, human follicle-stimulating hormone

Introduction

The ovarian reserve reflects the sum of follicles in the ovary. With the increase in women's age, their fertility decreases, as well as their ovarian reserve function and the number and quality of oocytes (1, 2). Compared with women of the same age, women with decreased ovarian reserve (DOR) have lower fecundity and responsiveness to exogenous ovarian hormone stimulation, resulting in less oocyte retrieval, poorer embryo quality, and lower implantation rate and pregnancy rate (2, 3). Additionally, DOR patients may be also characterized by perimenopausal symptoms, such as irregular menstruation, sleep disorder, and mood fluctuations (3). Currently, DOR is one of the most important therapeutic challenges in assisted reproduction (4, 5).

The decline in fertility caused by DOR has attracted attention. A woman with DOR may suffer from ovarian hypo-response, increased use of ovulation stimulants, and a high miscarriage rate after receiving assisted reproductive technology (ART) (6). These difficulties increase the psychological burden on patients and reduce the possibility of achieving parenthood. A previous study reported that DOR affected the quantity and number of metaphase II (MII) oocytes during ART treatment (7). Therefore, it is necessary to explore the treatment methods to improve the pregnancy outcomes of DOR patients.

Flax is a traditional plant, and flaxseed oil is extracted from the seeds of plant flax. Flaxseed oil is rich in omega-3 fatty acids required for human health, of which α-linolenic acid (ALA) is the most abundant (8, 9). As confirmed by previous studies, flaxseed oil plays a role in the human reproductive system, such as promoting follicular development, improving oocyte quality, and even improving oocyte fertilization rate (10, 11). Animal researchers have reported that flaxseed oil can be used as a supplement to improve reproductive processes (12, 13). However, the effects of flaxseed oil on the MII oocytes in DOR patients have not been reported yet. Therefore, this study focused on the investigation of the influence of flaxseed oil on the MII oocyte rates of women with DOR in *in vitro* fertilization (IVF)-assisted pregnancy.

Materials and methods

Study design and randomization

This was a prospective, randomized controlled study conducted at the Reproductive Medical Center of General Hospital of Northern Theater Command from April 1, 2021, and June 30, 2022. The experimental flow in this study is presented in Figure 1.

All participants were randomized 1:1 to either the study group or the control group. The randomization was performed over the period of 14 months (between April 1, 2021, and June 30, 2022) using computer-generated randomization codes. The study participants and the investigators were not blinded to the patient grouping. Additionally, this study was approved by the Ethics Committee of the General Hospital of Northern Theater Command (Y(2021)-089). All procedures were in accordance with the ethical guidelines and the Declaration of Helsinki. Informed consent was obtained from all patients.

Participants

Inclusion criteria were shown as follows: 1) women aged ≤40 years; 2) anti-Müllerian hormone (AMH) <1.2 ng/ml; 3) antral follicle count (AFC) <7; 4) follicle-stimulating hormone (FSH) greater than 10 and less than 25.

Exclusion criteria were as follows: 1) women aged >40 years; 2) suffering from gynecological diseases of the ovaries (ovarian tumors, ovarian cysts, and endometriosis); 3) having taken ovarian stimulation drugs or received controlled hyperovulation therapy within 6 months; 4) with history of ovarian surgery; 5) with endocrine or autoimmune disease (e.g., diabetes, thyroid disease, and polycystic ovary syndrome); 6) having taken drugs affecting the metabolism of macro- and micronutrients within 3 months including hypoglycemic and lipid-lowering drugs; 7) receiving prior antioxidant treatment or known allergy to flaxseed oil in the past 1 year.

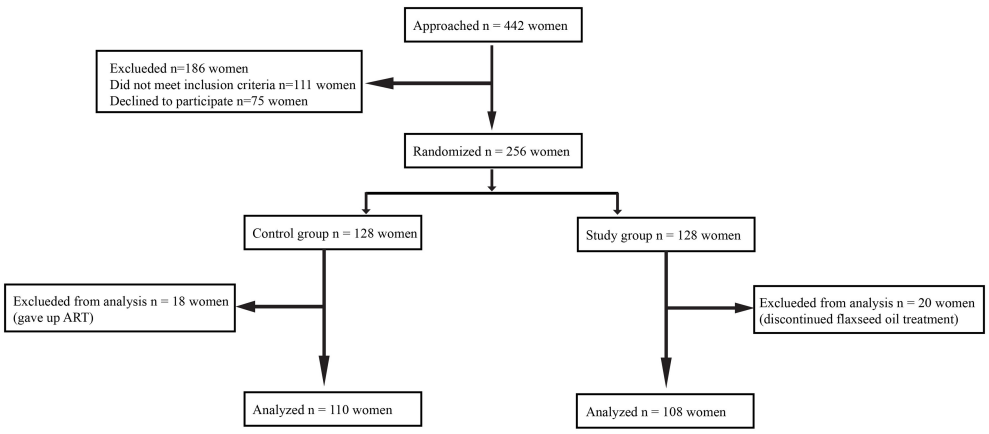

FIGURE 1
The chart of experimental flow.

Treatment protocols

The patients in the study group were given oral flaxseed oil (ALA 500 mg/pill, Kings Healthbay, Walnut, CA, USA) twice a day for 30 days before receiving ART treatment. During ART treatment, oral drug doses were maintained until a clinical pregnancy was established. The subjects in the control group received ART before and after IVF or intracytoplasmic sperm injection (ICSI), without any additional treatment.

Ovarian stimulation

On the second or third day of menstruation, recombinant human follicle-stimulating hormone (r-hFSH; Jinsai, China) was given at an initiative dose ranging from 150 to 225 U. The late dose of r-hFSH was adjusted according to the size and counts of the follicles and hormone levels. When the diameter of dominant follicles was ≥12–14 mm, gonadotropin-releasing hormone (GnRH) antagonist (Cetrorelix, 250 μg/day; Merck Serono, Darmstadt, Germany) was administered until the follicles were mature. After that, recombinant human chorionic gonadotrophin (hCG) (Ovidrel, 250 μg; Merck Serono S.p.A, Rome, Italy) was used to trigger ovulation. Thirty-six hours later, ovulation was triggered, and oocytes were extracted (14).

Embryo culture

Oocytes were fertilized by conventional IVF or ICSI depending on sperm quality (15, 16). Embryos were evaluated 16–18 hours after IVF or ICSI fertilization, and zygotes normally fertilized were cultured in an embryo incubator for 3–5 days (17).

Embryo transfer

The embryos were graded according to the consensus of the laboratory group of the Reproductive Medicine Branch of the Chinese Medical Association and the Istanbul consensus (18). All subjects selected the best morphologically graded embryos for fresh or frozen embryo transfer (ET) on the third day (19, 20). If the subjects were eligible for fresh transplantation, 40 mg of progesterone was injected intramuscularly from the day of oocyte extraction, 200-mg oral progesterone capsules were given per day, and luteal support was given until 14 days after ET (17). For subjects with a positive pregnancy, luteal support was provided until 8 weeks of gestation.

Those who failed to undergo fresh transfer were subjected to a frozen ET cycle at a later stage. Patients with a regular menstrual cycle and normal ovulation underwent the natural cycle program, and their ovulation status was tracked using transvaginal ultrasound. Meanwhile, blood luteinizing hormone (LH), estradiol (E2), and progesterone were monitored. The patients were given progesterone 20 mg/day of intramuscular injection on ovulation day and a progesterone capsule 200 mg/day orally to transform the endometrium. ET was performed 3 days after ovulation with luteal support until 8 weeks of gestation.

As for menstrual irregularities, artificial cycles were applied in the endometrium of subjects with ovulatory disorders. From the fifth day of the menstrual cycle, 2-mg fenmoton white tablets (E2 tablets) were orally given to patients twice a day, and their endometrial thickness was monitored by transvaginal ultrasonography. When the endometrial thickness exceeded 8 mm, luteal support (ketone injection 40 mg combined with oral progesterone capsules 200 mg/day) was given, and ET was performed 5 days later. Hormone therapy was discontinued if the pregnancy test result was negative. A positive pregnancy test resulted in luteal support up to 11 weeks of gestation and tapering after 10 weeks.

Outcome measures

The primary outcome measure was the MII oocyte rate for one stimulation cycle. The MII oocyte rate was defined as the ratio of the total number of MII oocytes to the total number of oocytes extracted.

The secondary outcomes included stimulation cycle parameters, embryology-related parameters, and clinical reproductive outcome parameters. Specifically, stimulation cycle parameters consisted of the total dose of r-hFSH, duration of stimulation, peak E2 concentration, LH concentration on the day of the hCG trigger, endometrial thickness on the day of the hCG trigger, duration between the day of the hCG trigger and oocyte collection, and canceled cycles. Embryology-related parameters were composed of the percentage of ICSI, fertilization rate, cleavage rate, day 3 high-quality embryo rate, and blastocyst development rate. Clinical reproductive outcome parameters were composed of the number of fresh or frozen ET cycles, clinical pregnancy rate per fresh ET, implantation rate, cumulative clinical pregnancy rate, multiple pregnancy, and spontaneous miscarriage.

The fertilization rate was defined as the number of fertilized oocytes developed by the number of MII oocytes. Cleavage rate was defined as the number of fertilized oocytes divided into embryos divided by the total number of fertilized oocytes. Day 3 high-quality embryo rate was defined as the number of good-quality embryos divided by the number of all embryos. Clinical pregnancy was defined as the presence of an intrauterine gestational sac observed on ultrasound after ET. The cumulative clinical pregnancy rate was defined as the number of clinical pregnancies resulting from the index ART cycle following fresh or frozen ET divided by the number of all women who received treatment. Multiple pregnancy was defined as the simultaneous presence of two or more gestational sacs in the uterine cavity after a single transplant. Spontaneous miscarriage was defined as a loss of clinical pregnancy before 24 weeks of gestation.

Statistical analysis

Continuous variables were expressed as mean ± standard deviation (SD) (normal distribution) or median (quartile) (skewed distribution). Categorical variables were expressed in frequency or as a percentage. For normally distributed variables, a t-test was used to compare differences between groups. For non-normally distributed variables, differences between groups were compared using the Mann–Whitney U test. The chi-squared test was employed for comparisons of categorical variables. Univariate and multivariate

logistic regression analyses were performed, and MII oocyte rates ≥50% were defined as a positive event. Univariate logistic regression analyses were performed to assess potential predictors associated with MII oocyte rates. The influence factors with statistical differences ($p < 0.05$) in univariate analyses were subject to multivariate logistic regression analyses. All analyses were performed using SPSS 22.0 software. $p < 0.05$ indicated significant differences.

Results

Overall conditions and baseline characteristics of patients

A total of 442 women were recruited. Subsequently, 186 women were excluded because they failed to meet the inclusion criteria (n = 111) or declined to participate (n = 75). The remaining 256 women agreed to participate in the study, and they were randomly assigned to a study group (n = 128) or a control group (n = 128). Additionally, 38 subjects were excluded from the analysis for the following reasons: 18 women changed their minds and gave up ART, and 20 women discontinued flaxseed oil treatment due to adherence problems. Finally, 108 women were retained in the study group and 110 in the control group. Baseline characteristics of the two groups were comparable in terms of age, body mass index (BMI), duration of infertility, type of infertility, other causes of infertility, and ovarian reserve (AMH, AFC, and day 3 FSH). The baseline characteristics of the two groups are displayed in Table 1.

TABLE 1 Baseline characteristics of two groups.

Variables	Study group (n = 108)	Control group (n = 110)	*p*
Female age (years)	35 ± 2.54	34.4 ± 3.02	0.15
BMI (kg/m^2)	23.9 ± 4.24	23.5 ± 3.47	0.41
Infertility duration (years)	3.97 ± 3.23	4.17 ± 3.46	0.66
Primary infertility, n (%)	45 (41.7%)	51 (49.1%)	0.48
Diagnosis of infertility in addition to DOR, n (%)			
Male factor	22 (20.4%)	26 (23.6%)	0.56
Tubal factor	38 (35.2%)	45 (41.0%)	0.38
Adverse pregnancy and birth history, n (%)	15/108	14/110 (12.7%)	0.80
Ovarian reserve markers			
AMH (ng/ml)	0.66 ± 0.31	0.60 ± 0.32	0.42
AFC (number)	3 (2,4)	3 (2,4)	0.08
Day 3 FSH (IU/ml)	16.2 ± 2.50	16.2 ± 2.56	0.96

Data are expressed as mean ± SD, n (%), or median (IQR).
BMI, body mass index; DOR, decreased ovarian reserve; AMH, anti-Müllerian hormone; AFC, antral follicle count; FSH, follicle-stimulating hormone.

TABLE 2 ART cycle stimulation parameters and embryology outcomes of two groups.

Variables	Study group (n = 108)	Control group (n = 110)	*p*
Cycle stimulation			
Total dose of r-hFSH (IU)	2,111 ± 788	2,233 ± 900	0.04
Duration of stimulation (days)	9.34 ± 2.96	9.78 ± 3.04	0.03
Peak E2 concentration (pmol/L)	1,212 ± 792	1,026 ± 1,114	0.01
Endometrial thickness on the day of hCG trigger (mm)	0.98 ± 0.25	1.02 ± 0.21	0.11
Duration between the day of hCG trigger and oocyte collection (hours)	36.2 ± 0.65	36.1 ± 0.66	0.19
Embryology outcomes			
MII oocyte rate (%)	287/339 (84.6%)	292/370 (78.9%)	0.05
ICSI (%)	68/108 (63.0%)	59/110 (53.6%)	0.16
Fertilization rate (%)	221/287 (76.9%)	207/292 (70.9%)	0.02
Cleavage rate (%)	141/221 (63.8%)	107/207 (51.7%)	0.01
Day 3 high-quality embryo rate (%)	155/287 (54.0%)	133/292 (45.6%)	0.04
Blastocyst development rate (%)	67/117 (57.3%)	50/114 (43.9%)	0.04

Data are expressed as mean ± SD or n (%).
r-hFSH, recombinant human follicle-stimulating hormone; E2, estradiol; hCG, human chorionic gonadotrophin; MII, metaphase II; ICSI, intracytoplasmic sperm injection.

Comparison of ART stimulation cycle parameters and embryological results between two groups

ART stimulation cycle parameters and embryological results are summarized in Table 2. The total dose and the duration of stimulation of r-hFSH in the study group were lower than those in the control group ($p = 0.04$ and 0.03). The peak E2 concentration in the study group was significantly higher than that in the control group ($p = 0.01$). There was no significant difference between the two groups in terms of endometrial thickness on the day of the hCG trigger ($p = 0.11$) and the interval between the day of the hCG trigger and oocyte retrieval ($p = 0.19$).

There was no statistical difference in fertilization method between the two groups, and the proportions of ICSI in the two groups were 64.0% and 53.6%, respectively ($p = 0.16$). Although not statistically significant, the MII oocyte rate was greater in the study group (84.6%) compared to the control group (78.9%). The fertilization rate (76.9% vs. 70.9%) and cleavage rate (63.8% vs. 51.7%) in the study group

10.3389/fendo.2024.1280760

TABLE 3 Clinical reproductive outcomes of two groups.

Variables	Study group (n = 108)	Control group (n = 110)	*p*
Canceled cycles (%)	6/108 (5.56)	7/110 (6.36)	0.80
Number of fresh ET cycles (%)	32/108 (29.6)	26/110 (23.6)	0.32
Number of frozen ET cycles (%)	70/108 (64.8)	67/110 (60.9)	0.55
Implantation rate (%)	56/108 (51.9)	50/110 (45.5)	0.04
Cumulative clinical pregnancy rate (%)	41/108 (38.0)	40/110 (36.4)	0.81
Multiple pregnancy (%)	11/108 (10.2)	13/110 (11.8)	0.70
Spontaneous miscarriage (%)	12/108 (11.1)	14/110 (12.7)	0.71

ET, embryo transfer.

were higher than those in the control group, and there was a statistical difference. In addition, the day 3 high-quality embryo rate and blastocyst formation rate in the study group were higher than those in the control group. Furthermore, flaxseed oil intervention not only improved oocyte quality and embryo quality but also increased MII oocyte rate, fertilization rate, cleavage rate, high-quality embryo rate, and blastocyst formation rate.

Comparison of clinical reproductive outcomes between two groups

The clinical reproductive outcomes of the two groups of subjects are summarized in Table 3. The cycle cancellation rate was not statistically different between the two groups ($p = 0.80$). In the study group, 32 subjects received fresh transfer, and 70 received frozen ET. In the control group, 26 subjects received fresh transfer, and 67 subjects received frozen ET. The fresh transfer cycle of the two groups was less than the frozen ET cycle, and there was no statistical difference. However, the embryo implantation rate of the study group (51.9%) was higher than that of the control group (45.5%, $p = 0.04$). Although the cumulative clinical pregnancy rate of the study group was higher than that of the control group, there was no significant difference ($p = 0.81$). In addition, there was no significant difference in the rates of multiple pregnancy and early miscarriage between the two groups.

Multivariate regression analysis for factors influencing MII oocyte rates

An analysis was performed on the influencing factors for MII oocyte rates. The results of the univariate analysis showed that the influencing factors for MII oocyte rates included female age, AMH, AFC, peak E2 concentration, and use of flaxseed oil (Table 4). Female age was significantly negatively correlated with MII oocyte rate ($p = 0.01$), while AMH ($p = 0.05$), AFC ($p = 0.03$), peak E2 concentration ($p = 0.01$), and flaxseed oil intake ($p = 0.05$) were positively correlated with MII oocyte rate.

TABLE 4 Univariate analysis of MII oocyte rate.

Variables	OR (95% CI)	*p*
Female age (years)	1.81 (1.15–2.85)	0.01
BMI (kg/m^2)	0.97 (0.93–1.00)	0.56
Infertility duration (years)	1.00 (0.97–1.04)	0.96
Types of infertility	0.77 (0.58–1.02)	0.06
Infertility factor	0.93 (0.66–1.30)	0.66
AMH (ng/ml)	1.59 (1.00–2.51)	0.05
AFC (number)	1.12 (1.01–1.23)	0.03
Day 3 FSH (IU/ml)	1.02 (0.98–1.07)	0.38
Total dose of r-hFSH (IU)	1.00 (1.00–1.00)	0.56
Duration of stimulation (days)	1.00 (0.97–1.04)	0.91
Peak E2 concentration (pmol/L)	1.00 (1.00–1.00)	0.01
Endometrial thickness on the day of hCG trigger (mm)	0.88 (0.54–1.43)	0.62
Duration between the day of hCG trigger and oocyte collection (hour)	0.96 (0.89–1.04)	0.32
Flaxseed oil intake	1.33 (1.01–1.75)	0.05

OR, odds ratio; CI, confidence interval; BMI, body mass index; AMH, anti-Müllerian hormone; AFC, antral follicle count; FSH, follicle-stimulating hormone; r-hFSH, recombinant human follicle-stimulating hormone; E2, estradiol; hCG, human chorionic gonadotrophin.

TABLE 5 Multivariate analysis of MII oocyte rate.

	Multivariate analysis	
Variables	OR (95% CI)	*p*
Female age (years)	0.61 (0.52–0.72)	<0.01
AMH (ng/ml)	100 (20.3–495)	<0.01
AFC (number)	1.25 (0.94–1.67)	0.13
Peak E2 concentration (pmol/L)	1.00 (1.00–1.00)	0.01
Flaxseed oil intake	2.51 (1.06–5.93)	0.04

OR, odds ratio; CI, confidence interval; AMH, anti-Müllerian hormone; AFC, antral follicle count.

We further analyzed the association between MII oocyte rate and these influencing factors using multiple-factor analysis (Table 5). Briefly, the female age [odds ratio (OR): 0.61, 95% confidence interval (CI): 0.52–0.72, $p < 0.01$] was the hindering factor, while AMH (OR: 100, 95% CI: 20.3–495, $p < 0.01$), peak E2

concentration (OR: 1.00, 95% CI: 1.00–1.00, p = 0.01), and the intake of flaxseed oil (OR: 2.51, 95% CI: 1.06–5.93, p = 0.04) were the promoting factors for MII oocyte rate. These results indicated that the increase in female age was related to the decrease in MII oocyte rate. Additionally, high AMH and E2 levels and flaxseed oil treatment contributed to the high MII oocyte rate.

Discussion

DOR is characterized by a decrease in the quality and quantity of oocytes (1, 2). It has seriously affected the fertility of women and is progressively worse with the delay of childbearing age (2). The prevalence of DOR is approximately 10% among infertile women (21). Previous studies have shown that flaxseed oil can improve fertility (10, 11). In this study, we demonstrated the potential benefits of flaxseed oil treatment in improving oocyte quality and ovarian response in women with DOR. Our results showed that the flaxseed oil intervention could improve ovarian response, reduce r-hFSH dosage, shorten r-hFSH stimulation time, and increase E2 peak concentration. Furthermore, flaxseed oil intervention could improve oocyte quality and embryo quality and increase the rate of mature oocyte acquisition, fertilization rate, cleavage rate, high-quality embryo rate, and blastocyst formation rate. Additionally, the embryo implantation rate after flaxseed oil treatment was higher than that of the control group. The cumulative clinical pregnancy rate was higher after flaxseed oil treatment, but there was no significant difference, probably due to insufficient sample size. In conclusion, flaxseed oil administration enhanced ovarian response to stimulation and improved oocyte and embryo quality. The results of this study are generally consistent with those of some previous studies.

The intake of linseed oil can increase the levels of ALA and eicosapentaenoic acid in the body (22). These two substances are very important for germ cell development. Specifically, they play a role in maintaining the structure and function of cell membranes, enhancing immune function, promoting growth and development, and regulating lipid metabolism and related gene expression (23, 24). A study of 235 women who underwent IVF/ICSI revealed that a high intake of ALA was associated with a higher baseline E2 level. They also showed positive associations between ALA intake and embryo morphology (25). Another study pointed out that total oocyte volume and MII oocyte volume were positively correlated with ALA intake, and a higher intake of linseed oil increased the oocyte fertilization rate (11). The beneficial effect of flaxseed oil on the fertility of women may be related to omega-3 fatty acids. A randomized controlled study of 110 participants proposed that dietary intervention with omega-3 fatty acids could significantly improve embryo development through morphodynamic markers improving embryo quality (26). In a randomized controlled trial of 27 participants, dietary supplementation with omega-3 fatty acids reduced serum FSH levels in normal-weight women (27). This is consistent with the direction of data in mice that higher dietary omega-3 fatty acids can increase reproductive lifespan (27, 28). In addition, it was reported that the combination of flaxseed oil and vitamin E increased semen quality and sperm motility, prevented sperm lipid peroxidation, and increased blastocyst rate (29). Although our study did not pay attention to the effect of flaxseed oil on sperm, our results demonstrated the beneficial effects of flaxseed oil on reproduction and were not limited to a single gender.

In our study, flaxseed oil intervention increased the rate of mature oocyte acquisition and follicle formation. This may be related to the effects of omega-3 fatty acids. Evans et al. and Mossa et al. suggested that dietary omega-3 fatty acids increased ovarian follicle production, which may have a positive effect on fertility performance (30, 31). Studies in cattle have shown that omega-3 fatty acids promote follicle growth in the ovaries, in addition to shortening the interval between first ovulation after delivery (32). The possible mechanism is that high omega-3 fatty acid levels increase arachidonic acid (AA) in the phospholipid of follicular granulosa cells. Under the stimulation of gonadotrophin, AA is released from the phospholipid and metabolized through the cyclooxygenase pathway to produce prostaglandins. Prostaglandin E2 stimulates ovarian hormone production and then increases follicles (33–35). It also may be associated with the antioxidant capacity of omega-3 fatty acids (36).

Omega-3 fatty acids may influence many factors related to the synthesis and metabolism of important reproductive hormones, such as steroid hormones, progesterone, and E2 (37, 38). It was found that the follicular fluid progesterone concentration of ewes fed with the omega-3 fatty acids diet was significantly higher than that of the control group (39). Diets rich in omega-3 fatty acids promote early embryonic development and progesterone secretion, suggesting that sex steroid metabolism may be affected by regulating omega-3 fatty acids intake (40). To be specific, inhibition of prostaglandin-endoperoxide synthase 2 (PTGS2) activity can promote cAMP-induced steroidogenesis in mouse Leydig tumor cells by increasing the expression of steroidogenic acute regulatory (STAR) protein, and omega-3 fatty acids are effective inhibitors of PTGS2 activity (41). In this study, the E2 peak level was associated with the MII oocyte rate, and flaxseed oil increased the peak E2 concentration in DOR women.

Our study showed that flaxseed oil intervention improved the quality of oocytes and embryos and increased fertilization rate, high-quality embryo rate, and blastocyst formation rate. Additionally, omega-3 fatty acids could increase fertilization rate and promote embryo development. Notably, high levels of omega-3 fatty acids improve membrane fluidity, reduce embryo fragmentation, and make blastocyst division more (42) symmetrical; all of these are associated with increased implantation, high live birth rates, and improved blastocyst development (25, 43). It has also been suggested that omega-3 fatty acids increase insulin-like growth factor-I (IGF-I) gene expression in granulosa cells (44, 45), thereby improving fertilization rates and embryonic development. IGF-1 is a key regulator of follicular differentiation and other reproductive functions (42, 46, 47). Our study did not analyze the outcomes of fresh or frozen ET with flaxseed oil. We suspected that flaxseed oil may have no effect on the method of transplantation (fresh or frozen). Previous studies have stated that omega-3 fatty acids affect oocyte development mainly through antioxidants, steroid metabolism, gene expression, and other mechanisms (48–50). Therefore, it is speculated that flaxseed oil may mainly function by targeting the effect of ovulation induction on the oocytes of

subjects. However, some studies have stated that the pregnancy outcome of fresh and frozen ET cycles may be mainly related to the quality of transplanted embryos and the endometrial environment (51, 52). Perhaps, more clinical and basic studies are needed in the future to confirm the effects of linseed oil omega-3 fatty acids on the endometrial environment and embryo quality.

The main strength of this study is that the impact of flaxseed oil on MII oocyte rate in patients with DOR has not been reported yet. Our study population was focused on a specific population of women with DOR, applying the same clinical treatment protocol and laboratory testing methods and using a prospective design of an unbiased randomization process to eliminate bias.

There are several limitations in this study. First of all, the sample size in this study was small, so a larger sample size may be required to account for significant clinical differences. Second, the pregnancy outcomes related to live births were not tracked in this study. The pregnancy outcomes related to live births are the final outcome of IVF treatment, and a longer follow-up may be needed to evaluate patients. Furthermore, the effect of other lifestyle factors that may have put women at higher risk was not assessed in this study, and these factors need to be considered in subsequent studies. Finally, the optimal time and duration of flaxseed oil supplementation in this study were unclear. Considering the patient's need for pregnancy assistance, lengthy intervention may not be accepted by patients, so the non-intervention time of 1 month was selected. In future research, the intervention time can be explored by further grouping. In other words, future research can explore the optimal intervention program for flaxseed oil by adjusting the intervention time and duration.

Conclusion

Flaxseed oil improved ovarian response and the quality of oocytes and embryos, thereby increasing the fertilization rate and high-quality embryo rate in DOR patients. Furthermore, the use of flaxseed oil was positively correlated with MII oocyte rate in women with DOR.

Data availability statement

The original contributions presented in the study are included in the article/supplementary material. Further inquiries can be directed to the corresponding author.

Ethics statement

The studies involving humans were approved by General Hospital of Northern Theater Command (Y(2021)-089). The studies were conducted in accordance with the local legislation and institutional requirements. Written informed consent for participation in this study was provided by the participants' legal guardians/next of kin.

Author contributions

QC: Conceptualization, Investigation, Writing – review & editing. YY: Data curation, Formal analysis, Writing – original draft. JZ: Data curation, Formal analysis, Writing – original draft. YZ: Data curation, Formal analysis, Writing – original draft. JY: Conceptualization, Methodology, Writing – review & editing.

Funding

The author(s) declare financial support was received for the research, authorship, and/or publication of this article. This study was supported by Liaoning Provincial Science and Technology Plan Project (2020JH2/10300118).

Conflict of interest

The authors declare that the research was conducted in the absence of any commercial or financial relationships that could be construed as a potential conflict of interest.

Publisher's note

References

1. Richardson MC, Guo M, Fauser BC, Macklon NS. Environmental and developmental origins of ovarian reserve. *Hum Reprod Update*. (2014) 20:353–69. doi: 10.1093/humupd/dmt057

2. Practice Committee of the American Society for Reproductive Medicine. Testing and interpreting measures of ovarian reserve: a committee opinion. *Fertil Steril*. (2020) 103(3):E9–E17. doi: 10.1016/j.fertnstert.2014.12.093

3. Scantamburlo VM, Linsingen RV, Centa LJR, Toso KFD, Scaraboto D, Araujo Júnior E, et al. Association between decreased ovarian reserve and poor oocyte quality. *Obstet Gynecol Sci*. (2021) 64:532–9. doi: 10.5468/ogs.20168

4. Wallace WH, Kelsey TW. Human ovarian reserve from conception to the menopause. *PloS One*. (2010) 5:e8772. doi: 10.1371/journal.pone.0008772

5. Tal R, Tal O, Seifer BJ, Seifer DB. Antimüllerian hormone as predictor of implantation and clinical pregnancy after assisted conception: a systematic review and meta-analysis. *Fertil Steril*. (2015) 103:119–30.e3. doi: 10.1016/j.fertnstert.2014.09.041

6. Chang Y, Li J, Li X, Liu H, Liang X. Egg quality and pregnancy outcome in young infertile women with diminished ovarian reserve. *Med Sci Monit*. (2018) 24:7279–84. doi: 10.12659/MSM.910410

7. Jahromi BN, Sadeghi S, Alipour S, Parsanezhad ME, Alamdarloo SM. Effect of melatonin on the outcome of assisted reproductive technique cycles in women with diminished ovarian reserve: A double-blinded randomized clinical trial. *Iran J Med Sci*. (2017) 42:73–8. doi: 10.23880/whsj-16000158

8. Simopoulos AP. Omega-3 fatty acids in health and disease and in growth and development. *Am J Clin Nutr*. (1991) 54:438–63. doi: 10.1093/ajcn/54.3.438

9. Tasneem R, Khan HMS, Rasool F, Khan KU, Umair M, Esatbeyoglu T, et al. Development of phytocosmeceutical microemulgel containing flaxseed extract and its *in vitro* and *in vivo* characterization. *Pharmaceutics*. (2022) 14:1656. doi: 10.3390/pharmaceutics14081656

10. Mirabi P, Chaichi MJ, Esmaeilzadeh S, Ali Jorsaraei SG, Bijani A, Ehsani M, et al. The role of fatty acids on ICSI outcomes: a prospective cohort study. *Lipids Health Dis*. (2017) 16:18. doi: 10.1186/s12944-016-0396-z

11. Jahangirifar M, Taebi M, Nasr-Esfahani MH, Heidari-Beni M, Asgari GH. Dietary fatty acid intakes and the outcomes of assisted reproductive technique in infertile women. *J Reprod Infertil*. (2021) 22:173–83. doi: 10.18502/jri.v22i3.6718

12. El-Tarabany MS, Atta MA, Emara SS, Mostafa MM. Folic acid and flaxseed oil supplements in Ossimi ewes: effect on body weight changes, progesterone profile, blood chemistry, and litter traits. *Trop Anim Health Prod*. (2020) 52:301–8. doi: 10.1007/s11250-019-02017-7

13. Castro T, Martinez D, Isabel B, Cabezas A, Jimeno V. Vegetable oils rich in polyunsaturated fatty acids supplementation of dairy cows' Diets: effects on productive and reproductive performance. *Anim (Basel)*. (2019) 9:205. doi: 10.3390/ani9050205

14. ART EWGoUi, D'Angelo A, Panayotidis C, Amso N, Marci R, Matorras R, et al. Recommendations for good practice in ultrasound: oocyte pick up(dagger). *Hum Reprod Open*. (2019) 2019:hoz025. doi: 10.1093/hropen/hoz025

15. Palermo G, Joris H, Devroey P, Van Steirteghem AC. Pregnancies after intracytoplasmic injection of single spermatozoon into an oocyte. *Lancet*. (1992) 340:17–8. doi: 10.1016/0140-6736(92)92425-F

16. Orvieto R, Venetis CA, Fatemi HM, D'Hooghe T, Fischer R, Koloda Y, et al. Optimising follicular development, pituitary suppression, triggering and luteal phase support during assisted reproductive technology: A Delphi consensus. *Front Endocrinol (Lausanne)*. (2021) 12:675670. doi: 10.3389/fendo.2021.675670

17. Practice Committee of the American Society for Reproductive Medicine. Performing the embryo transfer: a guideline. *Fertil Steril*. (2017) 107:882–96. doi: 10.1016/j.fertnstert.2017.01.025

18. Alpha Scientists in Reproductive Medicine and ESHRE Special Interest Group of Embryology. The Istanbul consensus workshop on embryo assessment: proceedings of an expert meeting. *Hum Reprod*. (2011) 26:1270–83. doi: 10.1093/humrep/der037

19. Medicine, Reproductive ASI. The Alpha consensus meeting on cryopreservation key performance indicators and benchmarks: proceedings of an expert meeting. *J Reprod Biomed Online*. (2012) 25:146–67. doi: 10.1016/j.rbmo.2012.05.006

20. Practice Committee of American Society for Reproductive Medicine and Practice Committee of Society for Assisted Reproductive Technology. Revised guidelines for human embryology and andrology laboratories. *Fertil Steril*. (2008) 90:S45–59. doi: 10.1016/j.fertnstert.2008.08.099

21. Lin S, Yang R, Chi H, Lian Y, Wang J, Huang S, et al. Increased incidence of ectopic pregnancy after in *vitro* fertilization in women with decreased ovarian reserve. *Oncotarget*. (2017) 8:14570–5. doi: 10.18632/oncotarget.v8i9

22. Kalo D, Reches D, Netta N, Komsky-Elbaz A, Zeron Y, Moallem U, et al. Carryover effects of feeding bulls with an omega-3-enriched-diet-From spermatozoa to developed embryos. *PloS One*. (2022) 17:e0265650. doi: 10.1371/journal.pone.0265650

23. Van Tran L, Malla BA, Kumar S, Tyagi AK. Polyunsaturated fatty acids in male ruminant reproduction - A review. *Asian-Australas J Anim Sci*. (2017) 30:622–37. doi: 10.5713/ajas.15.1034

24. Wang T, Sha L, Li Y, Zhu L, Wang Z, Li K, et al. Dietary α-linolenic acid-rich flaxseed oil exerts beneficial effects on polycystic ovary syndrome through sex steroid hormones-microbiota-inflammation axis in rats. *Front Endocrinol (Lausanne)*. (2020) 11:284. doi: 10.3389/fendo.2020.00284

25. Hammiche F, Vujkovic M, Wijburg W, de Vries JH, Macklon NS, Laven JS, et al. Increased preconception omega-3 polyunsaturated fatty acid intake improves embryo morphology. *Fertil Steril*. (2011) 95:1820–3. doi: 10.1016/j.fertnstert.2010.11.021

26. Kermack AJ, Calder PC, Houghton FD, Godfrey KM, Macklon NS. A randomised controlled trial of a preconceptional dietary intervention in women undergoing IVF treatment (PREPARE trial). *BMC Womens Health*. (2014) 14:130. doi: 10.1186/1472-6874-14-130

27. Al-Safi ZA, Liu H, Carlson NE, Chosich J, Harris M, Bradford AP, et al. Omega-3 fatty acid supplementation lowers serum FSH in normal weight but not obese women. *J Clin Endocrinol Metab*. (2016) 101:324–33. doi: 10.1210/jc.2015-2913

28. Nehra D, Le HD, Fallon EM, Carlson SJ, Woods D, White YA, et al. Prolonging the female reproductive lifespan and improving egg quality with dietary omega-3 fatty acids. *Aging Cell*. (2012) 11:1046–54. doi: 10.1111/acel.12006

29. Yuan C, Zhang K, Wang Z, Ma X, Liu H, Zhao J, et al. Dietary flaxseed oil and vitamin E improve semen quality *via* propionic acid metabolism. *Front Endocrinol (Lausanne)*. (2023) 14:1139725. doi: 10.3389/fendo.2023.1139725

30. Evans AC, Mossa F, Walsh SW, Scheetz D, Jimenez-Krassel F, Ireland JL, et al. Effects of maternal environment during gestation on ovarian folliculogenesis and consequences for fertility in bovine offspring. *Reprod Domest Ani*. (2012) 47 Suppl 4:31–7. doi: 10.1111/j.1439-0531.2012.02052.x

31. Mossa F, Walsh SW, Butler ST, Berry DP, Carter F, Lonergan P, et al. Low numbers of ovarian follicles ≥3 mm in diameter are associated with low fertility in dairy cows. *J Dairy Sci*. (2012) 95:2355–61. doi: 10.3168/jds.2011-4325

32. Moallem U, Shafran A, Zachut M, Dekel I, Portnick Y, Arieli A. Dietary α-linolenic acid from flaxseed oil improved folliculogenesis and IVF performance in dairy cows, similar to eicosapentaenoic and docosahexaenoic acids from fish oil. *Reproduction*. (2013) 146:603–14. doi: 10.1530/REP-13-0244

33. Cooke BA, Dirami G, Chaudry L, Choi MS, Abayasekara DR, Phipp L. Release of arachidonic acid and the effects of corticosteroids on steroidogenesis in rat testis Leydig cells. *J Steroid Biochem Mol Biol*. (1991) 40:465–71. doi: 10.1016/0960-0760(91)90216-R

34. Van der Kraak G, Chang JP. Arachidonic acid stimulates steroidogenesis in goldfish preovulatory ovarian follicles. *Gen Comp Endocrinol*. (1990) 77:221–8. doi: 10.1016/0016-6480(90)90306-7

35. Johnson AL, Tilly JL. Arachidonic acid inhibits luteinizing hormone-stimulated progesterone production in hen granulosa cells. *Biol Reprod*. (1990) 42:458–64. doi: 10.1095/biolreprod42.3.458

36. Wu A, Ying Z, Gomez-Pinilla F. Dietary omega-3 fatty acids normalize BDNF levels, reduce oxidative damage, and counteract learning disability after traumatic brain injury in rats. *J Neurotrauma*. (2004) 21:1457–67. doi: 10.1089/neu.2004.21.1457

37. Stanhiser J, Jukic AMZ, Steiner AZ. Serum omega-3 and omega-6 fatty acid concentrations and natural fertility. *Hum Reprod*. (2020) 35:950–7. doi: 10.1093/humrep/dez305

38. Teymouri Zadeh Z, Shariatmadari F, Sharafi M, Karimi Torshizi MA. Amelioration effects of n-3, n-6 sources of fatty acids and rosemary leaves powder on the semen parameters, reproductive hormones, and fatty acid analysis of sperm in aged Ross broiler breeder roosters. *Poult Sci*. (2020) 99:708–18. doi: 10.1016/j.psj.2019.12.031

39. Abayasekara DR, Wathes DC. Effects of altering dietary fatty acid composition on prostaglandin synthesis and fertility. *Prostaglandins Leukot Essent Fatty Acids*. (1999) 61:275–87. doi: 10.1054/plef.1999.0101

40. Wang X, Dyson MT, Jo Y, Stocco DM. Inhibition of cyclooxygenase-2 activity enhances steroidogenesis and steroidogenic acute regulatory gene expression in MA-10 mouse Leydig cells. *Endocrinology*. (2003) 144:3368–75. doi: 10.1210/en.2002-0081

41. Ringbom T, Huss U, Stenholm A, Flock S, Skattebøl L, Perera P, et al. Cox-2 inhibitory effects of naturally occurring and modified fatty acids. *J Nat Prod*. (2001) 64:745–9. doi: 10.1021/np000620d

42. Javvaji PK, Dhali A, Francis JR, Kolte AP, Roy SC, Selvaraju S, et al. IGF-1 treatment during in *vitro* maturation improves developmental potential of ovine oocytes through the regulation of PI3K/Akt and apoptosis signaling. *Anim Biotechnol*. (2021) 32:798–805. doi: 10.1080/10495398.2020.1752703

43. Norwitz ER, Schust DJ, Fisher SJ. Implantation and the survival of early pregnancy. *N Engl J Med*. (2001) 345:1400–8. doi: 10.1056/NEJMra000763

44. Shahnazi V, Zaree M, Nouri M, Mehrzad-Sadaghiani M, Fayezi S, Darabi M, et al. Influence of ω-3 fatty acid eicosapentaenoic acid on IGF-1 and COX-2 gene expression in granulosa cells of PCOS women. *Iran J Reprod Med*. (2015) 13:71–8. doi: 10.26226/morressier.59a6b34cd462b80290b55c0e

45. Han Y, Chen Y, Yang F, Sun X, Zeng S. Mechanism underlying the stimulation by IGF-1 of LHCGR expression in porcine granulosa cells. *Theriogenology*. (2021) 169:56–64. doi: 10.1016/j.theriogenology.2021.04.011

46. Toori MA, Mosavi E, Nikseresht M, Barmak MJ, Mahmoudi R. Influence of insulin-like growth factor-I on maturation and fertilization rate of immature oocyte and embryo development in NMRI mouse with TCM199 and α-MEM medium. *J Clin Diagn Res*. (2014) 8:Ac05–8. doi: 10.7860/JCDR/2014/9129.5242

47. Daftary SS, Gore AC. IGF-1 in the brain as a regulator of reproductive neuroendocrine function. *Exp Biol Med (Maywood)*. (2005) 230:292–306. doi: 10.1177/153537020523000503

48. Bo L, Jiang S, Xie Y, Kan H, Song W, Zhao J. Effect of vitamin E and omega-3 fatty acids on protecting ambient PM2.5-induced inflammatory response and oxidative stress in vascular endothelial cells. *PloS One*. (2016) 11:e0152216. doi: 10.1371/journal.pone.0152216

49. Wathes DC, Abayasekara DR, Aitken RJ. Polyunsaturated fatty acids in male and female reproduction. *Biol Reprod*. (2007) 77:190–201. doi: 10.1095/biolreprod.107.060558

50. Hohos NM, Elliott EM, Cho KJ, Lin IS, Rudolph MC, Skaznik-Wikiel ME. High-fat diet-induced dysregulation of ovarian gene expression is restored with chronic omega-3 fatty acid supplementation. *Mol Cell Endocrinol*. (2020) 499:110615. doi: 10.1016/j.mce.2019.110615

51. Zaat T, Zagers M, Mol F, Goddijn M, van Wely M, Mastenbroek S. Fresh versus frozen embryo transfers in assisted reproduction. *Cochrane Database Syst Rev*. (2021) 2:CD011184. doi: 10.1002/14651858.CD011184.pub3

52. Maheshwari A, Bell JL, Bhide P, Brison D, Child T, Chong HY, et al. Elective freezing of embryos versus fresh embryo transfer in IVF: a multicentre randomized controlled trial in the UK (E-Freeze). *Hum Reprod*. (2022) 37:476–87. doi: 10.1093/humrep/deab279

frontiers | Frontiers in Endocrinology

TYPE Review
PUBLISHED 17 April 2024
DOI 10.3389/fendo.2024.1361289

OPEN ACCESS

EDITED BY
Akira Iwase,
Gunma University, Japan

REVIEWED BY
Chiara Papulino,
University of Campania Luigi Vanvitelli, Italy
Juan Antonio Fafian Labora,
University of A Coruña, Spain

*CORRESPONDENCE
Shan Xiang
axiangshan@163.com
Fang Lian
lianfangbangong@163.com

†These authors have contributed equally to this work and share first authorship

RECEIVED 25 December 2023
ACCEPTED 22 March 2024
PUBLISHED 17 April 2024

CITATION
Ju W, Zhao Y, Yu Y, Zhao S, Xiang S and Lian F (2024) Mechanisms of mitochondrial dysfunction in ovarian aging and potential interventions.
Front. Endocrinol. 15:1361289.
doi: 10.3389/fendo.2024.1361289

Mechanisms of mitochondrial dysfunction in ovarian aging and potential interventions

Wenhan Ju[1†], Yuewen Zhao[2†], Yi Yu[3], Shuai Zhao[1], Shan Xiang[1*] and Fang Lian[3*]

[1]The First Clinical Medical College, Shandong University of Traditional Chinese Medicine, Jinan, China, [2]CReATe Fertility Centre, Toronto, ON, Canada, [3]Department of Reproduction and Genetics, Affiliated Hospital of Shandong University of Traditional Chinese Medicine, Jinan, China

Mitochondria plays an essential role in regulating cellular metabolic homeostasis, proliferation/differentiation, and cell death. Mitochondrial dysfunction is implicated in many age-related pathologies. Evidence supports that the dysfunction of mitochondria and the decline of mitochondrial DNA copy number negatively affect ovarian aging. However, the mechanism of ovarian aging is still unclear. Treatment methods, including antioxidant applications, mitochondrial transplantation, emerging biomaterials, and advanced technologies, are being used to improve mitochondrial function and restore oocyte quality. This article reviews key evidence and research updates on mitochondrial damage in the pathogenesis of ovarian aging, emphasizing that mitochondrial damage may accelerate and lead to cellular senescence and ovarian aging, as well as exploring potential methods for using mitochondrial mechanisms to slow down aging and improve oocyte quality.

KEYWORDS

oocyte, aging, mitochondria, fertility preservation, mechanism

1 Introduction

The average age of primiparous women has been gradually increasing since the 21st century, which is known to be negatively associated with reproductive outcomes (1–3). The advancement of assisted reproductive technology can compensate for the age-related decline in fertility, but evidence suggests that stopping or reversing the biological aging process is impossible (4, 5). Patients with certain genetic and autoimmune diseases, or women with excessive dieting, long-term radiation interference, or postoperative chemotherapy for cancer, may experience a premature decline in ovarian function (6), resulting in early-onset ovarian dysfunction, also called premature ovarian insufficiency (POI). Age-related infertility is mainly related to the decreased quantity and quality of oocyte that limit a woman's ability to conceive. Studies using animal models revealed several cellular and genetic dysfunctions are causally related or correlated with aging.

Although the mechanism of ovarian aging remains unclear, possible explanations for female ovarian aging are summarized in Figure 1.

Mitochondrial dysfunction provides a clue for explaining ovarian aging. Mitochondria is a kind of organelle with a double membrane structure and a diameter of 0.5~1.0 μm, containing limited Genetic material. Mitochondria is controlled by the mitochondrial and nuclear genomes. Human mitochondrial DNA (mtDNA) is a circular DNA molecule containing 16569 base pairs. All 13 proteins encoded by mtDNA are structural components of the electron transport chain (ETC), which assemble with nuclear-encoded proteins and become crucial components of the oxidative phosphorylation(OXPHOS) process. Mitochondria is the sites for oxidative metabolism in eukaryotes, and is the sites where sugars, fats, and amino acids ultimately oxidize and release energy. The common pathway responsible for the final oxidation of mitochondria is the tricarboxylic acid (TCA) cycle and OXPHOS, which correspond to the second and third stages of aerobic respiration, respectively. The glycolysis completed in the cytoplasmic matrix and the TCA cycle completed in the mitochondrial matrix produce high-energy molecules such as reduced nicotinamide adenine dinucleotide (NADH) and reduced flavin adenine dinucleotide (FADH2). The role of OXPHOS in this step is to use these substances to reduce oxygen and release energy to synthesize adenosine triphosphate (ATP).

A big difference from somatic cells is that the number of mitochondria and the copy number of mtDNA in human mature oocyte are very high (6). These mitochondria are produced during the oogenesis stage, and the mitochondrial replication is believed to remain quiescent until the embryo reaches the blastocyst stage (25, 26). Using transcriptome sequencing, differential expression of mitochondrial-related genes was found by comparing the oocyte of young women and women with advanced age (27–30). It is reported that the increase in maternal age significantly decreased the number and quality of mitochondria in aging oocyte (31, 32). After ovarian aging, the morphology of mitochondria changed significantly, showing an increase in the number of swollen and vacuolated mitochondria (33–37). But ovarian functions can be partially restored by supplementing healthy mitochondria or

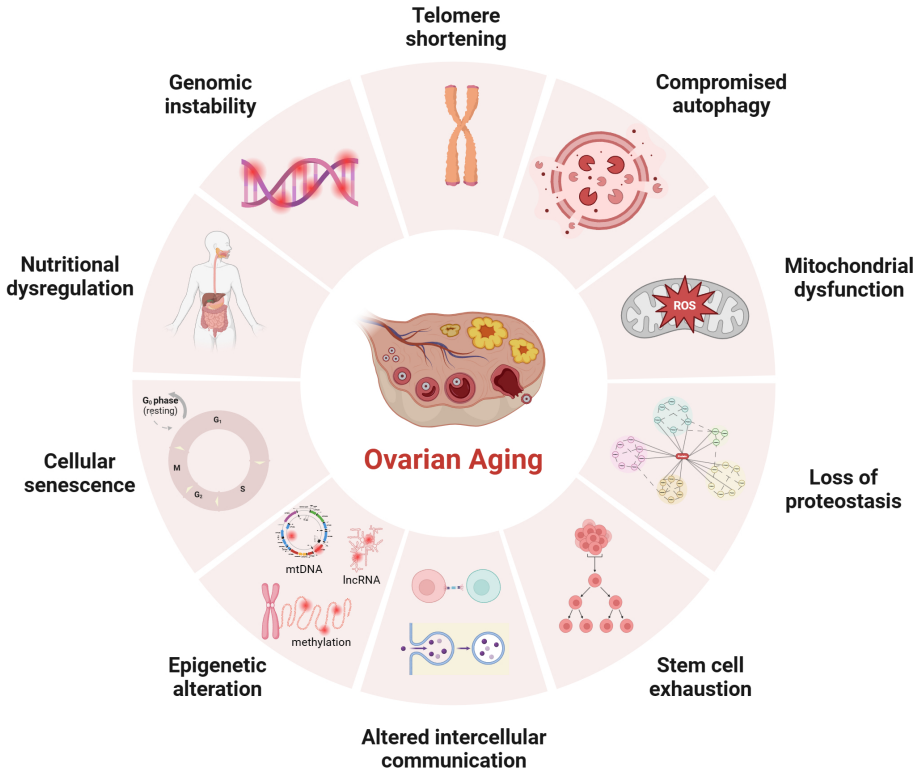

FIGURE 1
Potential mechanisms of ovarian aging (the figure was created with BioRender.com) Telomere shortening: Once telomere length becomes critically short, cellular senescence and apoptosis may occur during ovarian aging in mammals (7, 8); Compromised autophagy: The decrease of autophagic activity with age, likely leads to the accumulation of damaged macromolecules and organelles (9, 10); Mitochondial dysfunction: Mitochondial factors are explained further under subheadings in the text; Loss of proteostasis: Loss of proteostasis may damage the stability of microtubules and the integrity of meiosis in naturally aged mice oocyte (11); Stem cell exhaustion: Due to germ-line stem cells do not exist post-natally in female mammals (12–14), the reproductive potential of the ovaries will continue to decline after birth; Altered intercellular communication: There is an Increase In preantral follicles atresia in mice with suppression of intercellular junctions, which may be the cause of premature ovarian failure (15, 16); Epigenetic alteration: Studies have revealed the occurrence of epigenetic changes in the cells within the ovaries as age increases, including abnormal DNA methylation (17), histone modifications (18), and non-coding RNA-regulated modifications (19, 20); Cellular senescence: With the dysfunction of senescent cell, limited mitochondrial energy production, increased apoptosis of ovarian granulosa cells (21), increased inflammatory cytokines secretion (22) etc., would alter the microenvironment of follicle growth and affecting the quality and quantity of oocyte; Nutritional dysregulation: Dietary factors (23), low energy availability and high fat diet can increase the risk of POI; Genomic instability: In aging oocyte deceased efficacy of DNA repair mechanisms could cause low potentiation of anti-oxidant buffering and promote cell death (24).

improving mitochondrial function (38, 39), such as reducing the risk of mitochondrial oxidative damage caused by free radicals, reducing the expression of mitochondrial apoptosis-related proteins (40), and stimulating mitochondrial autophagy enhancers (41). The current manuscript reviews and summarizes the mechanism of mitochondrial damage in ovarian aging to explore possible intervention measures for improving and protecting the fertility of women with advanced age of childbearing age.

2 Mitochondrial dysfunction leads to ovarian aging

2.1 The key role of mitochondrial oxidative stress damage in ovarian aging

The disruption of oxidative and antioxidant balance leads to excessive oxidative stress(OS), resulting in irreversible damage of ovarian. Reactive oxygen species (ROS) are byproducts resulting from energy production in the mitochondrial electron transfer chain to generate ATP. When the human body ages or is subjected to various harmful stimuli, excessive production of ROS and reactive nitrogen species (RNS) can disrupt the antioxidant defense barrier, trigger cellular OS response. The emergence of mitochondrial OS may be a mechanism leading to infertility, which is not unfamiliar to us. The high OS level detected in the human ovary is associated with follicular atresia, low fertilization potential of oocyte, the risk of aneuploidy, and sub-fertility (42, 43). Numerous studies have shown that during ovarian aging, the antioxidant enzymes in granulosa cells(GCs), and follicular fluid, such as superoxide dismutase (SOD), catalase (CAT), and Glutathione peroxidase (GSH-Px), were significantly reduced (44, 45). OS reaction is regarded as a specific initiator for oocyte aging (46), directly attacking the mitochondrial membrane and destroying the mitochondrial OXPHOS, resulting in reduced ATP production. Excessive ROS production directly affecting the target of the signaling pathway and acting as a second messenger interacting with intermediate reaction steps (47). ROS reduces the expression of isocitrate dehydrogenase 1 (IDH1) by activating the mitogen-activated protein kinase (MAPK) signaling pathway (48), activates the p53-SIAH1-TRF2 axis to induce telomere shortening (49), and promotes the aging of GCs. In addition to aging, GCs apoptosis is related to follicular atresia, which is an important mechanism of ovarian aging. Research has found that the strong oxidant H_2O_2 passes through HIF-1α signaling pathway to stimulates apoptosis of GCs (50). Peroxiredoxin 2(PRX2) deficiency accelerated age-related ovarian failure through the ROS-mediated JNK pathway in mice, and increased numbers of apoptotic cells (51). Another study showed that Ginsenoside Rb1 inhibits age-related GCs oxidative damage by activating Akt phosphorylation at Ser473 and by further interaction with FOXO1 (44). Therefore, the increase of OS plays an important role in the development of ovarian aging. The use of antioxidants to minimize OS may affect improving ovarian function women with advanced age (41, 43).

It is worth noting that when OS occurs, mitochondria will respond. Nuclear respiratory factors (NRF) can sense OS in the mitochondrial matrix and be activated. NRF1/2 can regulate the formation of mitochondrial respiratory chain complexes, transcription and replication of mtDNA. Loss of full-length NRF1 led to a dramatic increase in ROS and oxidative damages (52). In addition, SIRT1/3 also acts as a sensor by activating PGC1α- NRF1 promotes mitochondrial synthesis and coordinates cellular defense against ROS invasion (53, 54). Unfortunately, current research has found that NRF1, SIRT1, and SIRT3 are all downregulated in the ovaries of reproductive aging (55–57), indicating a decrease in the ability of mtDNA transcription and replication (mitochondrial synthesis). The antagonist response orchestrated by SIRT1 in oocyte seems to decrease with aging (53). When ROS accumulation exceeds the critical point, OS will further induce cell aging or apoptosis, affecting oocyte quality.

In summary, the increase of OS plays an important role in the development of ovarian aging by disrupting OXPHOS, inducing telomere shortening, and stimulating cell apoptosis (46–48). At the same time, the expression of molecules that receive ROS signals to activate mitochondrial synthesis is downregulated in the aging ovaries (55–57). The insufficient transcription and replication ability(mitochondrial synthesis) of mtDNA leads to a decreased ability to resist ROS in the cells.

2.2 Changes in mitochondrial genome during ovarian aging

2.2.1 The decrease in mtDNA quantity leads to a decrease in the quality of aging oocyte

When OS occurs within cells, mtDNA transcription and replication are driven to synthesize new mitochondria. Unfortunately, it has been found that mtDNA copy number decreases with ovarian aging (58, 59). The mtDNA is compacted into dense mitochondrial nucleoids. The mitochondrial transcription factor A (TFAM) binds to mtDNA and regulates mtDNA transcription activation *in vivo* by recruiting mitochondrial RNA polymerase (POLRMT) and mitochondrial transcription factor B (TFBM) for mtDNA replication (58). Current research has found that female individuals with TFAM recessive missense mutation showed the clinical phenotype of POI (59). Evidence up to date indicated the decreasing pattern of mitochondrial quantity and mtDNA content in mammalian oocyte with aging (31, 60, 61). In addition, a significant decrease in the copy number of mtDNA was found in unfertilized and degenerated oocyte of women with advanced age, with a notable positive correlation existing between the cytoplasmic volume of blastomeres from embryos and the mtDNA copy number (35). The decrease in mtDNA copy number is consistent with the difficulty in conceiving in patients with reproductive aging. The mtDNA copy number is an indicator of oocyte maturation and fertilization potential (62). The optimal mtDNA copy number and sufficient ATP level (at least 2pMol) are prerequisites for normal follicular development and maturation to ensure the good developmental potential of the fertilized blastocyst (63, 64).

On the other hand, the quality of oocyte is regulated by GCs (65). GCs include two types: mural granulosa cells(MGCs) and cumulus cells (CCs). Current research has found that, women with moderate expression of TFAM in the cytoplasm of human follicular fluid GCs exhibit better results in IVF (66). The mtDNA content of CCs and oocyte in women with diminished ovarian reserve (DOR) significantly decreased, while the quality of oocyte was positively correlated with the expression of TFAM mRNA in CCs (60). The copy number of mtDNA in GCs in POI patients and low prognosis in patients classified by POSEIDON negatively correlate with age (67). Due to the crucial importance of maintaining stable mtDNA copy number for maintaining mitochondrial function and cell growth (68), the decrease in mtDNA copy number in GCs is closely related to the occurrence of excessive cell apoptosis (69). Excessive apoptosis of GCs can lead to follicular atresia and decreased oocyte quality.

In summary, a significant decrease in the copy number of mtDNA in oocyte and GCs was found in individuals with reproductive aging (35, 60, 67). The decrease in mtDNA copy number is associated with a decrease in oocyte fertilization potential. In this context, some researchers have carried out mitochondrial transplantation techniques with the aim of increasing the number of healthy mitochondria in the cells, resulting in improved oocyte quality and pregnancy rates (70, 71). However, due to the small sample size of the study, further expansion is still needed to confirm the findings. Due to the high number of mitochondria and copy number of mtDNA in mature human oocyte (6). The decrease in mtDNA copy number may only affect one aspect of oocyte quality, and mtDNA mutations cannot be ignored.

2.2.2 The significant increase in mtDNA instability leads to a decrease in the quality of aging oocyte

The “mitochondrial aging theory” hypothesizes that mtDNA undergoes sustained oxidative damage, leading to the accumulation of harmful mutations (72). ROS formation takes place in close proximity to mtDNA, which lacks the protective measures of histone complexes and efficient DNA repair mechanisms, in contrast to nuclear DNA. Consequently, this vulnerability results in a heightened mutation rate (73). In situations such as aging, obesity, or chronic inflammatory stimulation, ROS production escalates, which renders mtDNA more susceptible to mutations (74, 75). The instability of mtDNA is manifested in various means, including mutations, base oxidation modifications, single-strand breaks, and so on. It has been found that harmful mtDNA mutations gradually accumulate in aging human tissues (76, 77). In addition, multiple studies have demonstrated that mutations in mtDNA encoding genes may lead to mitochondrial dysfunction and play a positive role in the pathogenesis of POI (28–30).

However, a few studies found no correlation between mtDNA deletion, rearrangement, and mutations of human oocyte and maternal age (75, 78–80). In their studies, the mtDNA mutation rate of oocyte was as high as 28~50.5%, and that of CCs was as high as 66% (78–80). The heteroplasmy created by mtDNA mutations are common in oocyte. The mtDNA bottleneck genetic mechanism during generational transmission is predicted to filter out the mitochondria population with mtDNA mutations effectively (81, 82). The difference in representative phenotypes and lower recurrence risk among women carrying heterogeneous mtDNA mutations demonstrate the effectiveness of the bottleneck theory (83, 84). Additionally, the number of primordial follicles in female mammals is fixed at birth, and there is no regeneration or renewal of the follicular pool after birth. It is unclear whether the prolonged quiescent stage before the resumption of meiosis could be affected by a hypoxic environment to undergo mtDNA mutations. In addition, during the oocyte’s maturation, there is a surge in mtDNA quantity and redox reactions (6), due to excessive ROS can also lead to mtDNA mutations, making it difficult to evaluate the occurrence time of mtDNA mutations.

Besides, nuclear encoded mitochondrial Helicase Twinkle (TWNK) and mitochondrial DNA polymerase γ (POLG) are essential proteins for mtDNA proofreading and fidelity (85–87). In humans, individuals with TWNK mutations exhibit Perrault syndrome (ovarian hypoplasia) (88), individuals with POLG mutations exhibit premature aging (89), genome wide association studies(GWAS) has found that POLG is associated with female menopause (89), and individuals with DOR have decreased POLG mRNA expression in CCs (90). POLG mutant mice showed a decrease in the number of mitochondria, abnormal mitochondrial distribution (aggregation and clustering), lower NADH/NAD+ redox ratio and weaker energy production, and a corresponding decrease in fertility (91, 92). The above research highlights the insight that mutations in nuclear coding genes lead to ovarian aging by affecting the stability of mtDNA.

In summary, many studies on mitochondrial gene expression have shown a link between decreased mtDNA copy number, accumulated mtDNA mutations, and ovarian failure. Genes are internal factors that determine the normal operation of mitochondria. The instability of the mtDNA genome will lead to dysfunction of executing proteins within mitochondria, which in turn will lead to a decrease in mitochondrial function. In fact, there is an endogenous protective mechanism within cells that is responsible for monitoring mitochondrial mass to maintain mitochondrial balance. Will the negative effects caused by mtDNA instability be recognized and eliminated? Therefore, it is necessary to further elucidate the relationship between mitochondrial quality testing and ovarian aging.

2.3 Disorder of mitochondrial quality monitoring mechanism in ovarian aging

2.3.1 Mutation of the key gene CLPP in mitochondrial unfolded protein response leads to depletion of ovarian reserve

Mitochondrial unfolded protein response (UPRmt), as a typical mitochondrial nuclear signal transduction process, promotes the high expression of nuclear-encoded mitochondrial stress proteins by transmitting mitochondrial damage signals to the nucleus (93, 94), helping to restore mitochondrial protein balance, thereby protecting electron transport chain complexes to avoid proteotoxicity. The maintenance of mitochondrial protein function, including correct folding, aggregation, and necessary degradation, requires the

involvement of proteolytic enzymes and molecular chaperones. It is known that caseinolytic peptidase P(CLPP) is a highly conserved serine proteolytic enzyme and a key enzyme in UPRmt (95). Currently, it is reported that human *CLPP* gene mutation has a clinical phenotype of Perrault syndrome or POI (96, 97). In animal experiments, *CLPP*-/- mice showed auditory defects and complete infertility (98), and the ovarian reserve in mice showed an accelerated state of depletion with age (99, 100). The reason maybe that *CLPP*-/- mice activate the Sirolimus target (mTOR) pathway *in vivo* (99), affecting the degradation of aggregated or misfolded cytochrome oxidase subunit 5A(COX5A) (97), blocking UPRmt, thus affecting the content and activity of complex IV in ETC, accumulating ROS and reducing mitochondrial membrane potential (MMP), and finally activating the internal apoptosis pathway. It follows that mutations in the key gene CLPP, where UPRmt is affected, will lead to ovarian reserve depletion in mice and humans. Therefore, we hypothesize that ovarian aging may be associated with differential expression of the CLPP gene, but providing a definitive conclusion is challenging due to the paucity of studies on ovarian aging-associated UPRmt. The inhibition of UPRmt process means a decrease in the genes driving mtDNA replication and transcription in the nucleus, and a limitation in the synthesis of new mitochondrial proteins.

2.3.2 Obstacles in mitochondrial biogenesis in aging ovary

Mitochondrial biogenesis is a strict regulatory process that activates signaling molecules such as NRF1/2, TFAM, and TFBM through peroxisome proliferator-activated receptor-gamma coactivator-1alpha (PGC1α), driving the replication and transcription of mtDNA, translating it into proteins, and assembling it into new mitochondria (101). SIRT1/3 also activates PGC1α-NRF1 promotes mitochondrial synthesis (53, 54). When mitochondria sense the initiation of OS or UPRmt processes, mitochondrial biogenesis is activated to maintain mitochondrial balance. Current research found a significant downregulation of PGC1α expression in the ovaries of cyclophosphamide-induced injury in POI (54, 102). NRF1, SIRT1, and SIRT3 are all downregulated in the ovaries of reproductive aging (55–57). In the ovaries of SIRT3 gene knockout mice, there was a decrease in mitochondrial membrane potential, uneven distribution of mitochondria, and a decrease in mtDNA copy number (56). Ginsenoside Rg1 improves ovarian function by activating SIRT1 and coenzyme Q10 improves ovarian function by increasing the expression of SIRT1 in PGC1α in animal experiments (103, 104). In addition, Adenosine 5'-monophosphate-activated protein kinase (AMPK), which is associated with the onset of POI (105), can activate and interacts with PGC1α through various mechanisms (106). Research has found that exercise can increase intracellular energy metabolism, activate AMPK and PGC1α to increase intracellular calcium concentrations thereby increasing the induction of mitochondrial biogenesis through transcription factors (such as NRFs, TFAM) (101). Inhibition of the AMPK/SIRT3 pathway will induce mitochondrial protein hyperacetylation and mitochondrial dysfunction in pig oocyte (107). In summary, mitochondrial biogenesis is a regeneration process that maintains the number of mitochondria, replacing old and damaged mitochondria with new and healthy mitochondria. Mitochondria with decreased membrane potential will fuse with newly formed mitochondria (one aspect of mitochondrial dynamics), sharing an internal system to restore mitochondrial quality once again. However, the downregulation of key genes involved in mitochondrial biogenesis in aging ovaries may lead to obstacles in the regeneration process (55–57, 60).

2.3.3 Defects in mitochondrial dynamics of aging oocyte

Mitochondria undergo continuous transformation through fusion and division states, which are manifested by morphological remodeling of the mitochondrial cristae and fracturing and lengthening of the tubular network, in order to achieve physiological functions. Mitochondrial fusion protein (MFN) mediate the assembly and fusion of mitochondrial inner and outer membranes to form a homogeneous mitochondrial network to maintain quality. Optic Atrophy 1(OPA1) is a GTPase that promotes fusion of the inner mitochondrial membrane and maintains cristae integrity. Dynamin-related protein 1 (DRP1), as core protein in mitochondrial division, can promote rapid changes in mitochondrial division activity according to cellular needs. Existing studies found that, the absence of MFN1 and MFN2 in mice oocyte resulted in infertility phenotype and loss of follicular reserve (108, 109), and the expression of DRP1 in aging oocyte was reduced (110). Low expression of MFN2 is associated with mitochondrial damage and apoptosis in ovarian tissue in POI model mice (111, 112). Since activated JNK phosphorylates MFN2, causing it to be degraded via the ubiquitin-proteasome system, the expression of MFN2 can be restored after supplementation with hydrogen sulfide or glutathione, antioxidants, or JNK inhibitors, and the improvement of mitochondrial morphology contributes to cell proliferation in ovarian cancer (113). In goat ovarian granulosa cell, Neuromedin S(NMS) treatment upregulates the expression of OPA1, MFN1, and MFN2 in the presence of NMUR2 knockdown, maintains mitochondrial fusion capacity and function, and thus regulates steroidogenesis (114). Therefore, we speculate that there are mitochondrial motility defects in aging oocyte. Due to the ability of mitochondrial fission to separate damaged mitochondria with low membrane potential from the entire mitochondrial network. Damaged mitochondria either fuse with newly formed mitochondria or are cleared through mitochondrial autophagy. The downregulation of mitochondrial fusion and fission ability implies an inevitable decrease in mitochondrial quality.

2.3.4 Downregulation of mitochondrial autophagy in aging ovary

When mitochondrial damage cannot be repaired through fission/fusion, the role of mitochondrial autophagy becomes particularly important. Mitochondrial autophagy is achieved through the phagocytosis of damaged mitochondria by autophagosomes, primarily via the PINK1-Parkin pathway, which removes damaged and membrane potential loss mitochondria, and receptor-dependent mitochondrial autophagy such as BCL2/adenovirus E1B 19 kDa protein-interacting protein 3 (BNIP3), BCL2/E1B 19kDa interacting protein 3-like (BLIP3L or NIX), or FUN14 domain-containing protein

1(FUNDC1) (115). Studies have shown that maintaining mitochondrial autophagy is crucial for prolonging the reproductive capacity and oocyte quality of *C. elegans* and mice (116, 117). In particular, mitophagosome formation defects and accumulated damaged mitochondria were observed in germinal vesicle (GV) oocyte collected from the ovaries of older mice (118), which may be caused by PINK1 and Parkin proteins age-related accumulation and the degradation of ras-related protein rab-7a(RAB7) ubiquitination modification (118, 119). RAB7 is a monomeric guanosine triphosphate (GTP)-binding protein and an essential regulatory factor for the late endosomal/lysosomal network (120). Following treatment with RAB7 activators, the fertility of mice was improved. Therefore, Jin et al. suggested that excessive ubiquitination of RAB7 inhibits mitochondrial autophagy that should have been activated during ovarian aging (118). Another research reported a therapeutic strategy to ameliorate oocyte quality and reproductive outcome by enhancing mitophagy in aged mice (117). CoQ10 significantly increased PINK1 and Parkin proteins and improved embryonic development in postovulatory oocyte of pigs (104). From the above findings, it can be surmised that mitochondrial autophagy is down-regulated in senescent oocyte. Defects in the formation of mitochondrial phagosomes lead to the accumulation of damaged mitochondria and a decrease in mitochondrial quality. The decline in mitochondrial function ultimately leads to ovarian aging. Although the above results are exciting. It should be noted that so far, most of our understanding of mitochondrial autophagy has been through detecting the expression of proteins related to related pathways. However, for some reasons, such as the instantaneous occurrence of mitochondrial autophagy leading to cell apoptosis, it is challenging to measure mitochondrial autophagy accurately (121, 122).

In summary, we have elucidated four aspects of mitochondrial quality monitoring that may be related to ovarian aging (as shown in Figure 2). Current researches indicate that mutations in the key gene CLPP of UPRmt can lead to depletion of ovarian reserves in both mice and humans. The expression of key genes involved in mitochondrial biogenesis, mitochondrial dynamics, and mitochondrial autophagy in aging ovaries has been downregulated. Therefore, various functions of mitochondrial quality monitoring in aging ovaries may have been downregulated to varying degrees. A decrease in mitochondrial quality usually means a decrease in mitochondrial cristae area and enzymes related to aerobic respiration in the matrix, resulting in insufficient mitochondrial energy supply and affecting the function of oocyte.

2.4 Mitochondrial dysfunction disrupts normal physiological function of oocyte

2.4.1 Inadequate mitochondrial energy supply is a factor in meiotic errors

Some scholars have found that euploid oocyte screened from women with advanced age have implantation potential similar to that of young women with *in vitro* fertilization (IVF) (123). The production of aneuploid oocyte is the main reason for the decline in female fertility. The error of MI of female oocyte is considered to be the primary cause of human abortion and congenital defects (124, 125), and oocyte meiotic spindle morphology is a predictive marker of blastocyst ploidy (126), although mechanism of meiosis is complex. During meiosis, mitochondrial dysfunction significantly affects spindle assembly and ratio of kinetochore-microtubule connection (127, 128), and maternal age-related meiotic errors can be attenuated by reducing mitochondrial function (128). In the process of meiosis of mice oocyte, mitochondrial calcium uniporter protein (MCU) mediates the rapid entry of Ca2+ into mitochondria and provides high energy in an instant (129). The specific deletion of MCU leads to a low concentration of Ca2+ in mitochondria, low ATP levels, abnormal spindle assembly, and altered meiosis progression (129). Interestingly, the decrease of mitochondrial ATP concentration activates AMPK signal transduction. However, over-activated AMPK and Ca^{2+} overload result in OS, apoptosis, and meiotic cell cycle arrest and apoptosis in mammalian oocyte (130, 131). Above research demonstrated that precise mitochondrial Ca^{2+} homeostasis mediated by MCU is critical to oocyte meiosis. Moreover, the deletion of spindle defective protein 3 (SPD3) located on the outer membrane of mitochondria directly leads to the abnormal pairing of homologous chromosomes in the meiosis of *Caenorhabditis elegans*, which may be caused by the inhibition of mitochondrial function (132). Other proteins that regulate mitochondrial function, such as multidrug resistance protein 1 (MDR1) (133), regulate ROS efflux from the inner mitochondrial membrane, and RAB7 specific deletion regulates DRP1 phosphorylation (134), resulting in mitochondrial dysfunction, abnormal spindle shape, and increase of oocyte meiosis chromosome errors. In addition, SIRT3-/- mice aging oocyte exhibited spindle assembly interruption (55). These studies together highlighted the importance of mitochondrial energy supply for meiosis (as shown in Figure 3). In aging ovaries, the decline in mtDNA number and mutations, the down-regulation of mitochondrial quality monitoring mechanisms, and insufficient supply of mitochondria may persist, culminating in derangement of spindle assembly and motility, leading to an increase in meiotic chromosome errors in oocyte.

2.4.2 Mitochondrial dysfunction disrupts the oocyte-cumulus cell crosstalk in aging ovaries

In the cumulus oocyte complex (COC), CCs continuously consume glucose to supply metabolic intermediates (such as pyruvic acid) to oocyte, which will be crucial to energy metabolism in the mitochondria of oocyte (135). CCs are GCs surrounding oocyte that participate in the reproductive and maturation processes of oocyte through intercellular communication. MFN1-/- mice oocyte showed DOR phenotype, as well as damaged communication between oocyte and CCs (cadherin and connexin were downregulated), which may be caused by mitochondrial dysfunction and mitochondrial dynamics changes, the accumulation of ceramide in oocyte and the damage of PI3K-AKT signal transduction (109, 136). Ceramide is considered an important inducer of programmed cell death, and ceramide metabolic enzyme therapy can improve the quality of oocyte and embryos and the outcome of IVF (137). The PI3K-AKT pathway is an important signaling pathway for FSH to regulate glucose uptake in GCs and prevent ovarian aging (138). In addition, mitochondrial dysfunction of MII oocyte in AMPK -/- mice increased abnormally, PGC1α level

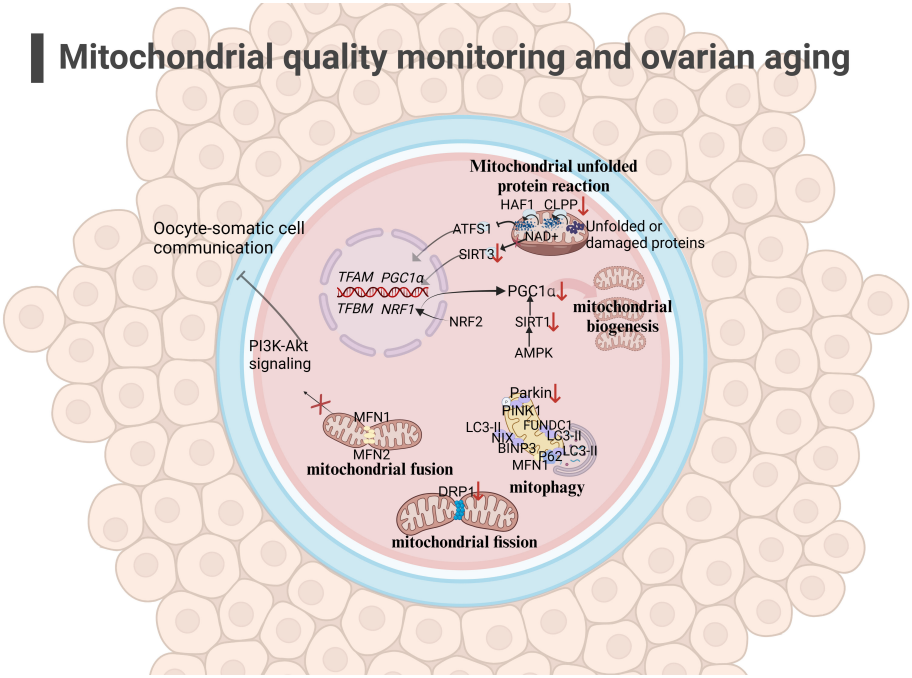

FIGURE 2
Mitochondrial quality monitoring and ovarian aging(the figure was created with BioRender.com) (1)mitochondrial fusion: The low expression of MFN1 ang MFN2 in the outer membrane in aging oocyte may affect mitochondrial fusion and inhibit the PI3K-AKT pathway, affecting oocyte-somatic cell communication (108, 109); (2) mitochondrial fission: The decreased expression of DRP1 in oocyte may affect mitochondrial function, leading to a decrease in oocyte quality (110); (3) mitophagy: Mitochondrial autophagy function decreases during ovarian aging (117, 118); (4) UPRmt: The decreased expression of CLPP and PGC1α in aging oocyte may hinder the occurrence of UPRmt (96, 97).

decreased, ATP concentration decreased from normal, and connexin 37 and n-cadherin, which are involved in connection and communication between oocyte and CCs, were downregulated (139). The emergence of mitochondria-associated gene mutant mice with down-regulated expression of junctional gap junction proteins may have affected the delivery of some small molecules from the colobus cells to the oocyte, which in turn affected the quality of the oocyte. The above research provides evidence for mitochondrial dysfunction leading to abnormal communication between oocyte and CCs, supporting the theory of mitochondrial dysfunction leading to ovarian aging. However, there is a paucity of relevant studies, which need to be further clarified by rigorous experiments.

2.4.3 Hyperactivation of the mitochondrial apoptotic pathway is present during ovarian aging

In addition to energy generation, the important role of mitochondria in cells is also reflected in regulating cell apoptosis. Mitochondria is the central organelle of the apoptosis pathway, having an irreplaceable role in apoptosis. Under physiological conditions, Cytochrome c (Cytc) is the carrier for transferring electrons in ETC, establishing the mitochondrial transmembrane potential and generating ATP. BCL2 and BCL-xL form heterodimers with BCL2-associated X(BAX) and BCL2 homologous antagonist/killer (BAK), maintaining the integrity of the mitochondrial outer membrane and preventing mitochondrial apoptosis response. When stimulated by apoptosis, BAX/BAK forms an oligomer complex and inserts into the outer membrane pores of mitochondria, leading to changes in mitochondrial osmotic pressure, abnormal activation of Cytc release channels, and initiation of downstream caspase cascade reaction to induce apoptosis. Consistent with this, many studies have illustrated upregulated expression of apoptotic protein BAX, Cytc and Caspase 9 in the ovaries of mice with POF and POI animals (140–142), while the expression of anti-apoptotic protein BCL2 was downregulated. After intervention, the expression of these proteins was reversed, partially restoring ovarian function. Gene knockdown experiments have shown that BAX mutations prolong the fertility of female mice and alleviate health issues related to aging (143, 144). In addition, mitochondrial dysfunction and reduced ATP production may disrupt the normal physiological functions of cells (145, 146), leading to cell apoptosis. In summary, mitochondrial dysfunction can disrupt cellular antioxidant capacity and disrupt the OXPHOS process, hindering ATP production. Mitochondria themselves can perceive a decrease in membrane potential, sense apoptotic signals, and initiate the mitochondrial apoptotic pathway. The excessive activation of mitochondrial apoptosis pathway is likely closely related to the occurrence of ovarian aging (as shown in Figure 4). Because there is excessive apoptosis of GCs and increased follicular atresia during ovarian aging.

2.4.4 The link between mitochondrial dysfunction and telomere damage as one of the latest mechanisms of ovarian aging

In addition, the telomere theory is one of the latest mechanisms to explain female reproductive aging (147).Telomeres are

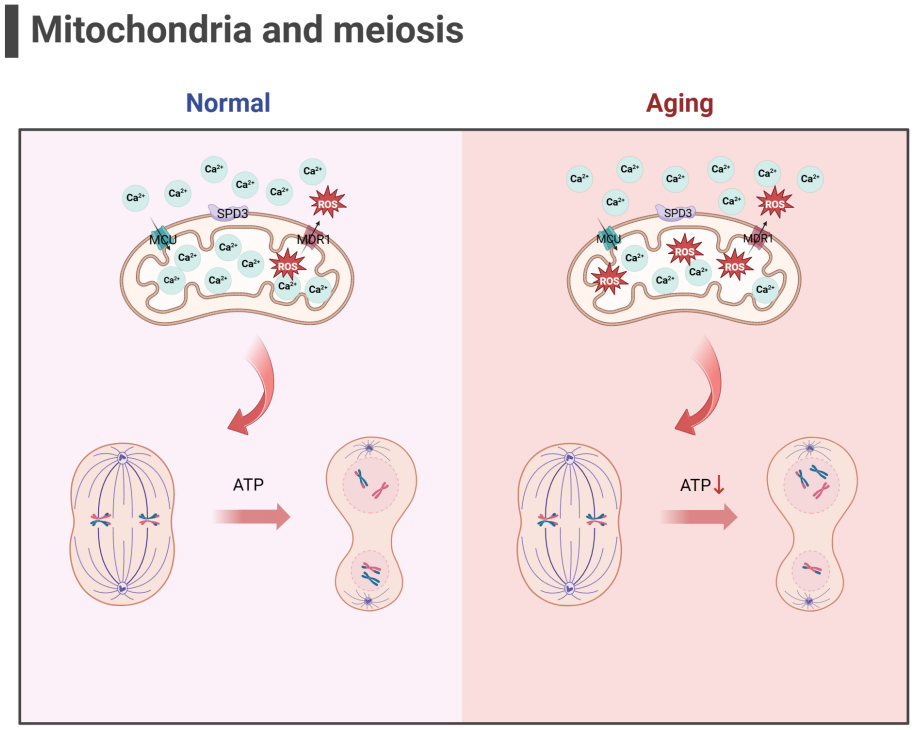

FIGURE 3
Mitochondria and meiosis in the oocyte (the figure was created with BioRender.com) MCU mediates the rapid entry of Ca^{2+} into mitochondria and provides high energy in an instant (129). MDR1 regulate ROS efflux from the inner mitochondrial membrane to maintain mitochondrial function (133). SPD3 may affect the abnormal pairing of homologous chromosomes which may be caused by the inhibition of mitochondrial function (132). Oxidative stress and mitochondrial ATP production disorders in aging oocyte may lead to abnormal spindle shape and increase chromosomal errors during meiosis in oocyte.

nucleoprotein complexes at the end of chromosomes, maintaining the integrity of chromosomes and inhibit DNA damage reactions at the free end of chromosomes (148). It is widely recognized that telomeres are susceptible to oxidative damage, and OS markers have been shown to exhibit a negative correlation with telomere length (149). Due to the significant features of ovarian aging, such as reduced ATP production and increased ROS accumulation (88), telomere loss and telomere-driven replicative senescence caused by OS may be important mechanisms of ovarian aging (150). In addition, there is a link between telomere function and mitochondrial biosynthesis. Existing studies have found decreased telomerase activity in ovarian GCs of POI patients (151, 152). The lack of telomerase activates p53 which in turn binds and represses PGC1α and PGC1β promoters, thereby inhibiting mitochondrial biogenesis (153, 154). The dysfunction of mitochondrial biosynthesis leads to the decline of cell resistance to OS and further accelerates the modification of 8-hydroxy deoxyguanosine on the telomere guanosine base. In addition, the link between telomere shortening and mitochondria is also mediated by NAD +-SIRT1-PGC1α axis establishment (124, 155, 156). The DNA repair process after telomere damage consumes NAD+, and the loss of SIRT1 activity will further affect the mitochondrial biogenesis mediated by PGC1α (155). In aging ovaries, the decrease in SIRT1 expression is a common phenomenon (55). Thus, the excessive occurrence of mitochondrial OS may accelerate telomere shortening at the ends of chromosomes, which in turn can inhibit the expression of the key gene for mitochondrial biosynthesis, PGC1α, through the activation of P53, leading to a decline in intracellular mitochondrial function, which further affects the DNA repair process. Ultimately, this vicious cycle of the above leads to the onset of ovarian senescence (as shown in Figure 5). Given the current research results, it is difficult to explain the sequence between telomere damage and mitochondrial dysfunction. Still, the two seem to interact with each other to lead to ovarian aging in women.

2.4.5 Epigenetic regulation involving mitochondria influences oocyte senescence

Oocyte quality decline during ovarian aging occurs in part through epigenetic regulation. Intermediates generated by metabolic processes within mitochondria can generation and modify nuclear epigenetic marks to achieve important mediators of mitochondrial-nuclear communication (157). Histone methyltransferases (HMTs) and histone demethylases (HDMs) are responsible for histone methylation status. S-adenosyl methionine (SAM) produced by the cytoplasmic methionine homocysteine cycle in the mitochondrial folate cycle is a donor of histone methyltransferases (HMTs) (158). Besides, the acetyl-CoA-producing enzyme ATP-citrate lyase (ACL) also regulates DNA methyltransferase 1 (DNMTl) (159), which affects the level of DNA methylation. Pyruvate, ketones, amino acids, citrate, acetate, and beta oxidation of lipids can produce acetyl-CoA, which is the substrate for

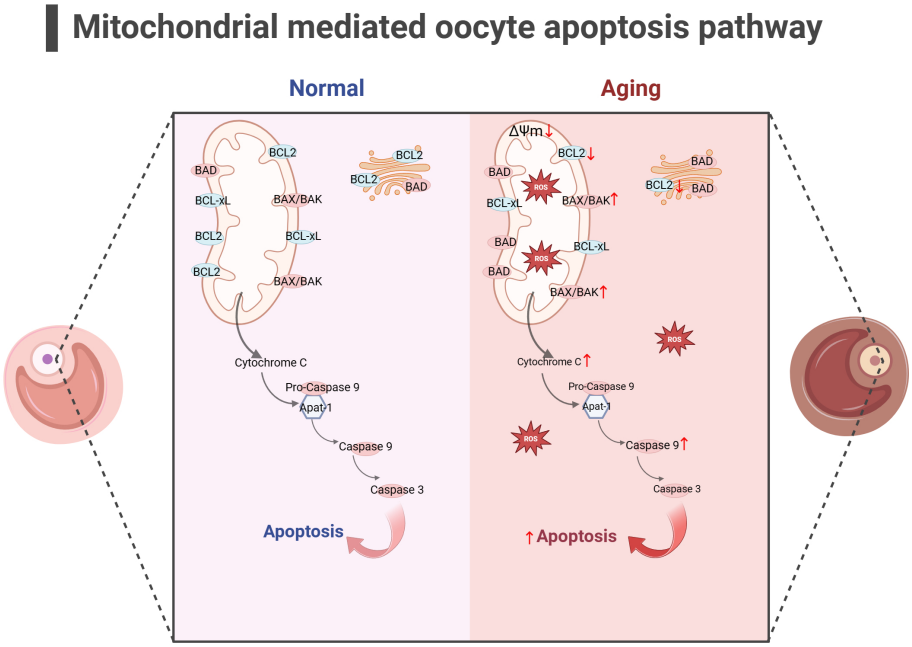

FIGURE 4
Mitochondrial-mediated oocyte apoptosis pathway (the figure was created with BioRender.com) In aging oocyte, excessive cell apoptosis signals are activated under stimuli such as mitochondrial oxidative stress and decreased mitochondrial membrane potential. At the same time, the expression of anti-apoptotic proteins such as BCL2 decreased, while the expression of apoptotic proteins such as BAK, CytC and Caspase9 increased (140–142).

the histone acetyltransferases (HAT) (160). Under conditions of energy and acetyl-CoA enrichment, this leads to histone acetylation and gene transcription. Histone demethylases (HDMs) comprise two major classes: lysine-specific demethylases (LSD) and Jumonji C domain demethylases (JMJD). LSD1 catalyzes the demethylation of mono- or dimethylated H3K4 and H3K9, whereas LSDs act as receptors in the mitochondrial ETC (161). JMJD-mediated demethylation of histones requires α-ketoglutarate (162), a substrate produced mainly by the tricarboxylic acid (TCA) cycle in the mitochondrial matrix. Current research has found that low methylation of DNMT1/DNMT3a/DNMT3b/DNMT3L promotes oocyte aging (17). Specific disruption of LSD1 led to a significant

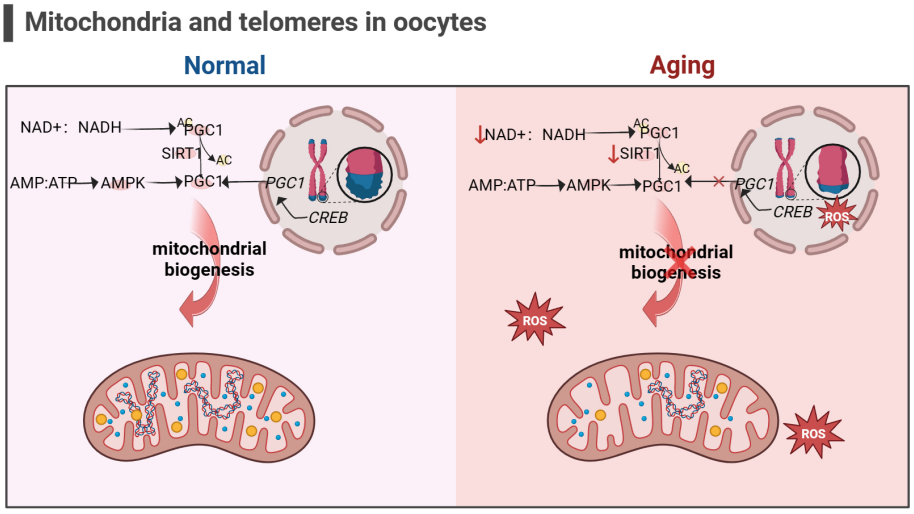

FIGURE 5
Mitochondria and telomeres in the oocyte (the figure was created with BioRender.com) The cAMP response element-binding protein (CREB) is a co-factor for PGC1 expression. Abnormal telomere function can activate p53, thereby inhibiting the expression of PGC1. The decrease in PGC1 expression in turn inhibits mitochondrial biogenesis, leading to a decrease in the ability of cells to resist oxidative stress (156). In addition, increasement in the proportion of intracellular AMP/ATP and NAD+/NADH also promotes PGC1 expression, but this is not suitable for aging cells, as the content of NAD+ and SIRT1 significantly decreases (53, 54).

increase in autophagy through its H3K4me2 demethylase activity and a decrease in the number of oocyte in perinatal mice, leading to depletion of oocyte (163). Epigenetic enzymes recognize, add, and remove epigenetic markers on DNA and histones. Due to the association between the formation of epigenetic enzymes and mitochondrial metabolism, the transmission of mitochondrial metabolite levels or stress signals may lead to various epigenetic changes. Unfortunately, few studies have directly explored the association between mitochondrial epigenetic regulation and ovarian aging.

In summary, mitochondrial dysfunction during cellular aging may lead to spindle assembly and motility during meiosis by affecting energy supply. Both MFN1-/- and AMPK -/- mice showed mitochondrial dysfunction and abnormal communication between oocyte and GCs. In addition, the occurrence of mitochondrial dysfunction may directly initiate the mitochondrial apoptosis pathway, leading to follicular atresia. Excessive OS during aging not only activates the mitochondrial apoptosis pathway, but may also accelerate telomere shortening. Telomere shortening hinders the recovery of mitochondrial function by inhibiting mitochondrial biosynthesis. Finally, mitochondrial metabolites may also affect the expression of epigenetic enzymes and promote ovarian aging.

3 Methods to slow down ovarian aging and prolong reproductive lifespan by intervening in mitochondrial function

At present, there is no effective technology in clinical practice to prevent the occurrence of female reproductive aging, and the current treatment methods are still in the exploratory stage. However, it is worth celebrating that some animal experiments have shown great potential in improving female reproductive function. Below we will discuss each of the currently discovered therapeutic mechanisms of drugs for mitochondrial damage.

3.1 Mitochondrial nutrition therapy

We summarize the therapeutic drugs targeting mitochondria to prevent ovarian aging in Table 1 and classify them according to mitochondrial energy metabolism, quality control, and mitochondrial apoptosis pathways.

3.1.1 Drugs for improving mitochondrial energy metabolism

Research has shown that multiple antioxidants can restore mitochondrial function by reducing ROS production and stimulating antioxidant production. It mainly includes coenzyme Q10 (177), vitamin E (164), vitamin C (164), L-carnitine (165, 166), melatonin (167, 168), quercetin (169), resveratrol (170), astaxanthin (171), and ginsenoside Rb1 (44).

In addition, ginsenoside Rb1 also promotes Akt binding to FOXO1 and inhibits OS occurrence (44). Metformin regulates calcium homeostasis to prevent follicular atresia of aging ovaries of Laying Chickens (40). NAD+/NADH, or coenzyme I, is a redox cofactor and enzyme substrate in mitochondria, critical for energy metabolism, DNA repair, and epigenetic regulation in cells. In the ovaries, the level of NAD+ decreases with age in a dependent manner (172, 173). After supplementing NAD+ precursors (NR or NMN), ovarian function in elderly mice was restored, and the mitochondrial TCA cycle was improved at the micro level (172, 173).

3.1.2 Drugs for coordinating mitochondrial quality control

Normal mitochondrial function and internal environmental homeostasis require close coordination between mitochondrial biogenesis and clearance. Compounds coordinating mitochondrial quality control are expected to become effective therapeutic interventions for ovarian aging. It is reported that ginsenoside Rg1 can increase SOD, CAT levels, and activate SIRT1 in POF

TABLE 1 Drugs that improve mitochondrial function.

Classification	Drug	Mechanism	References
improve mitochondrial energy metabolism	coenzyme Q10, vitamin E, vitamin C, astaxanthin,L-carnitine, melatonin, quercetin, resveratrol, metformin, ginsenoside Rb1	reduce superoxide radicals and scavenge hydrogen peroxide	(40, 44, 164–171)
	ginsenoside Rb1	Akt-FOXO1 interaction	(44)
	metformin	regulation of calcium ion homeostasis	(40)
	NAD+ nucleoside	promotes TCA cycle	(172, 173)
coordinate mitochondrial quality control	ginsenoside Rg1, coenzyme Q10,	SIRT1 or PGC1α activator	(103, 104)
	melatonin, metformin	AMPK activator	(104, 174)
	resveratrol, coenzyme Q10	upregulate Parkin-induced mitochondrial autophagy	(104, 175)
	NAD+ nucleoside	mitochondrial autophagy enhancers	(41)
regulating mitochondrial apoptosis pathway	metformin	inhibit release of BAD and caspase	(40)
	resveratrol	inhibition of caspase 3 and BAX, upregulation of BCL2	(176)

mice model (103). CoQ10 significantly prevented aging-induced oxidative stress, and increased mitochondrial biogenesis (SIRT1 and PGC1α) and mitophagy (PINK1 and Parkin)-related proteins in postovulatory oocyte of pigs (104). Resveratrol can increase the expression of PINK1 and Parkin proteins regulate the autophagy ability of mitochondria, and protect ovarian function (175). Metformin and Melatonin are AMPK activators (105, 174), which could increase intracellular calcium concentrations thereby increasing the induction of mitochondrial biogenesis through transcription factors (such as NRFs, TFAM) (111). After 20 weeks of treatment with NMN in 40-week-old mice (41), mitochondrial biogenesis, autophagy level and protease activity in ovarian GCs were increased, and the ovarian reserve was rescued to some extent.

3.1.3 Drugs that regulate mitochondrial apoptosis pathways

The study found that Resveratrol treatment reduced the expression of mitochondrial apoptosis promoting protein caspase 3 and BAX and upregulated BCL2 expression in POI model mice (176). Metformin can inhibit the release of mitochondrial apoptosis factors (BAD and caspase) in Laying Chickens (40). However, whether these benefits observed in animal models can be replicated in humans remains to be determined.

Currently, various potential drugs targeting mitochondria have been developed (Table 1). However, these drugs are not necessarily suitable for preventing ovarian aging. Various drugs have been found to have positive effects in resisting OS, improving OXPHOS efficiency, promoting mitochondrial occurrence and autophagy, and inhibiting mitochondrial apoptosis in animal experiments. Whether these benefits observed in animal models can be replicated in the human body remains to be determined.

3.2 Mitochondrial replacement therapy

Mitochondrial transplantation was initially primarily used to prevent disease transmission caused by mtDNA mutations, becoming a viable alternative to avoiding damaged mitochondrial offspring inheritance. Subsequently, due to the increasingly important role of mitochondria in human reproduction, people began to think about improving the quality of gametes by enhancing the quality of mitochondria.

3.2.1 Autologous mitochondrial transplantation technology

The autologous mitochondrial transplantation technology (178), focuses on increasing the number of healthy mitochondria in cells while avoiding the introduction of third-party DNA in gametes. It is reported that injection of mitochondrial from oogonial precursor cells(OPCs) while intracytoplasmic sperm injection (ICSI) can improve the quality of oocyte and pregnancy rate in the ICSI cycle of women with multiple IVF failure (70, 71). Unfortunately, a more rigorous tri-blinded, randomized, and single center-controlled study conducted in Spain in 2019 found that mitochondrial transfer of OPCs did not improve embryonic development potential and pregnancy rate in patients with previously IVF failed (179). Recently, it has been confirmed that autologous adipose stem cells (ASCs) mitochondrial transplantation can improve the quality of oocyte in juvenile or aged mice (180–182), while Sheng et al. found negative results (183). It should be noted that the mitochondrial dysfunction of aging oocyte seems to have occurred long ago. Most of the common aneuploid oocyte originate from MI (126, 184). It may be too late to save the quality of MII oocyte by ICSI injection of active mitochondria. Furthermore, the origin of mitochondria is an issue, and whether oogonial stem cells exist and how to obtain them is a highly controversial issue (185, 186). In summary, the efficacy of the above mitochondrial transplantation methods in improving ovarian function is controversial, and they are not considered standard treatments.

Tang et al. have established a noninvasive optimized autologous mitochondrial transplantation technique: inducing mice autologous umbilical cord mesenchymal stem cells into GCs (iGCs) and co-cultured them with weakened zona pellucida GV in growth differentiation factor 9 (GDF9) containing medium for three days. Tang et al. have found that mitochondria migrate from iGCs to GV oocyte through transzonal filopodia, significantly improving these oocyte' maturation rate, quality, and developmental potential (187). The birth rate of aged mice after embryo transfer has also been improved (187). In Table 2, we summarized the mitochondrial transplantation methods of from different sources. Due to its non-invasive and early intervention characteristics, it is worth further research. In the future, we look forward to researching and solving the source of mitochondrial acquisition, achieving timely and non-invasive transplantation as much as possible, and providing promising strategies for improving the quality of oocyte and the fertility of women with advanced age.

3.2.2 Cytoplasmic transfer and germline nuclear transfer

A study in 1998 reported that Cohen et al. injected a small amount of oocyte cytoplasm directly from the donor oocyte into the oocyte of patients with recurrent implantation failure (RIF) through cytoplasmic transfer (CT), and successfully achieved live birth (188). Unfortunately, specific abnormalities (chronic migraine headaches, mild asthma, minor vision and minor skin problems et al.) were found in the investigation of the health status of offspring, and the safety and benefits of CT are still unclear (189), although it is uncertain whether CT causes these abnormalities. However, there are concerns about mtDNA heterogeneity in CT (190), and currently, the US FDA has suspended this study.

Previous nuclear transfer (NT) is used clinically in patients with mtDNA diseases to prevent the transmission of maternal mutated mtDNA to the next generation. The new NT technology can improve embryonic development by transferring nuclear DNA from oocyte with inferior cytoplasm to oocyte with higher fertility potential. NT includes spindle transfer (ST), pronuclear transfer (PNT), and polar body transfer (PBT).

ST refers to the transfer of spindle apparatus from MII oocyte to denucleated MII donor oocyte (191). A pilot study conducted in Europe reported the feasibility of ST technology, targeting 25 couples with recurrent IVF failures and giving birth to 6 newborns over 28 ST

TABLE 2 Comparison of mitochondrial transplantation methods from different sources.

Mitochondrial source	Model	Advantage	Disadvantage	Reference
oogonial precursor cells	human	high homology; mitochondria derived from stem cells	difficulty in obtaining invasive procedures; mitochondrial transplantation during Metaphase II	(70, 71, 179)
adipose-derived stem cells	mice	Rich sources; easy to obtain; low immune rejection	mitochondrial transplantation during Metaphase II	(180–183)
umbilical cord-derived mesenchymal stem cells	mice	non-invasive procedures; mitochondrial transplantation during germinal vesicle	differentiation needs to be induced *in vitro*	(187)

and ICSI cycles (192). However, it is worth noting that one child with the same low mtDNA carryover (0.8%) in the blastocyst stage showed an increase in maternal mtDNA haplotype, accounting for 30% to 60% of the total number at birth (192). The mtDNA haplotype phenomenon may be due to the specific interaction between nuclear and mitochondrial coding genes. Heterogeneous mice model experiment show that one of the mtDNA haplotypes gradually dominates during oogenesis and early embryonic development (193). Therefore, before applying NT to clinical practice, it is necessary to carefully consider the occurrence of mtDNA mutations in patients.

In addition, PNT is a nucleoplasmic replacement technique, which refers to the process of removing the male and female protoplasts together and transplanting them into a new cytoplasm after the oocyte is fertilized. It was found that by replacing the cytoplasm of young mice, the MMP of oocyte from ST or PNT-reconstructed aged mice was increased, the probability of spindle and chromosome misalignment was decreased, and the rate of embryo haploidy and blastocyst formation was improved (194, 195). Several human preclinical studies have also reported the feasibility of the PNT technique in human zygotes (196), where early PNT performed 8 hours after ICSI can achieve blastocyst formation rates at control levels.

PB1T and PB2T also emerged as a strategy to prevent the spread of harmful mtDNA mutations. Unfortunately, the rate of reconstructed PB1T oocyte developing from zygotes to the blastocyst stage (42%) was lower compared to the control (75%) (197). Subsequently, researchers optimized the use of PB2T in human oocyte through new technologies. They found that PB2T embryos produced by *in vitro* maturation (IVM) oocyte exhibited similar development and diploid rates to the ICSI control group (198). It is important to note that more studies are needed to improve the efficiency and safety of the PNT technique and to provide at least evidence of live birth before it can be considered for clinical use.

In Table 3, we summarized the research methods for cytoplasmic transfer and germline nuclear transfer. It is worth noting that CT and NT cannot correct fertility disorders in all women with advanced age by improving receptor mitochondrial function, and the use of PGT to evaluate embryo ploidy remains an important choice. Because if there are genetic abnormalities in the spindle apparatus or polar body of women with advanced age, CT and NT are of little value. In 2015, the UK became the first country to approve the use of mitochondrial donations. More research evaluating the safety of this technology for women with low fertility is warranted.

3.3 Biomaterials and advanced technologies for preventing ovarian aging

Over the years, various strategies have been developed to maintain women's Fertility. Recently, advances in biomaterials and technology have shown the potential to prevent ovarian aging. Exosomes from various sources, such as human umbilical

TABLE 3 Comparison of cytoplasmic transfer and germline nuclear transfer.

Technique	Model	Results	Disadvantage	Reference
cytoplasmic transfer	human	successfully achieved live birth in patients with recurrent implantation failure	concerns about the health status of offspring and mtDNA heterogeneity	(189)
spindle transfer	human	6 newborns in 28 cycles	an increase in maternal mtDNA haplotype	(192)
pronuclear transfer	mice	increased the MMP of oocyte, the rate of embryo haploidy and blastocyst formation; decreased the probability of spindle and chromosome misalignment	species diversity; inability to correct aneuploidies already present in some aged MII oocyte	(194, 195)
pronuclear transfer	human	early PNT performed 8 hours after ICSI can achieve blastocyst formation rates at control levels	unreported pregnancy outcomes	(196)
first polar body transfer	human	the rate of blastocyst (42%) was lower compared to the control (75%)	unreported pregnancy outcomes	(197)
second polar body transfer	human	similar development and diploid rates in IVM compared to ICSI control	unreported pregnancy outcomes	(198)

cord mesenchymal stem cell-derived exosomes (hUCMSC-exos) (199), human amniotic mesenchymal stem cell-derived exosomes (hAMSC-exos) (200), human amniotic epithelial cell-derived mitochondria (hAEC-exos) (201), human amniotic fluid mesenchymal stem cells (AFMSC-exos) can decreased the ROS levels (202), increase the expression of anti-apoptotic genes (such as BAD and BCL2) and reduce the expression of pro-apoptotic genes (such as CPP32 and BAX) by transferring functional miRNAs (such as miR-320a, miR-1246, and miR-21), thereby inhibiting the mitochondrial apoptotic pathway and preventing ovarian GCs apoptosis in POI mice and primitive follicle activation. In mice ovarian experiments, transplantation of platelet-rich fibrin scaffolds indirectly reduced OS, thereby improving ovarian endocrine function and follicle formation (203). The effect of biomaterials on improving ovarian function is mainly based on the results of animal experiments. However, it is necessary to clarify the effectiveness of biomaterials in evaluating and treating ovarian aging, and to use effective preclinical models to accurately predict the therapeutic outcomes of these biomaterials.

In summary, some potential therapeutic drugs or technologies for improving mitochondrial quality have been developed or clinically tested. However, no treatment method is definitely suitable for preventing ovarian aging. Due to the highly complex process of reproduction, some treatment methods that have been introduced into clinical practice need to undergo comprehensive evaluation and be determined to have no side effects before being applied in clinical practice.

4 Focus on mitochondria of human oocyte during assisted reproduction technique

Age related infertility is mainly related to a decrease in the quantity and quality of oocyte, which limits a woman's ability to conceive. Currently, an increasing number of women worldwide are seeking help from ART for conception. The need between mitochondria, infertility, and ovarian aging has attracted people's attention. There is a close relationship between mitochondria and the declining quality of oocyte with age. The instability of mtDNA leads to the accumulation of mtDNA mutations in oocyte, posing a risk of transmitting mitochondrial abnormalities to offspring. Overactivation of OS during ovarian aging disrupts OXPHOS, induces telomere shortening, and stimulates cell apoptosis. However, due to the decrease in mtDNA copy number and the downregulation of mitochondrial quality monitoring ability, mitochondrial homeostasis is difficult to recover. At the cellular level, the mitochondrial apoptosis pathway is overactivated and ATP required for meiosis is lacking. Table 4 summarizes and highlights the findings and links between mitochondrial dysfunction and infertility. During the oocyte developmental maturation stage, there is a process of transmission of damaged mitochondria to the embryo. Studies have shown that abnormalities in mitochondrial structure and function may be responsible for abnormal embryonic development in ART cycles.

4.1 How do abnormal mitochondria in aging oocyte affect ART outcomes?

4.1.1 The mtDNA content of oocytes and cumulus cells affects embryo quality

Prior to oocyte maturation, the mitochondria of the oocyte is virtually quiescent to prevent genetic mtDNA mutations, and the energy to support oocyte maturation is supplied primarily by the surrounding CCs and GCs. This observation is reflected in the fact that the number of oocyte obtained from *in vitro* fertilization (IVF), basal follicle-stimulating hormone (FSH) levels, and anti-Mullerian hormone (AMH) are the determining factors of mtDNA content (209), and the copy number of mtDNA in CCs can positively predict embryo quality and developmental outcomes (204–207). In addition, a significant reduction in mtDNA copy number was found in unfertilized oocyte from women with advanced age, and there was a significant positive correlation between cytoplasmic volume of the cleavage sphere of uncleaved embryos and mtDNA copy number (35). In addition, oocyte from women with advanced age had higher mtDNA copy numbers after IVM than younger women, which may be related to spindle abnormalities and increased oxidative stress in IVM (210).

It has been suggested that the survival rate of early mammalian embryos is related to their quiet metabolism (211). Research indicates that the mitochondrial oxygen consumption rate of morula embryos is linked to maternal age rather than mtDNA content (212, 213). However, by the blastocyst stage, as differentiation occurs within the embryo, mtDNA replication rapidly recovers, and the TCA cycle becomes widely activated, leading to a more efficient ATP generation method (214). Consequently, low oxygen consumption is observed in undifferentiated stem cells in the inner cell mass, while the mtDNA copy number in trophoblast cells and mitochondrial aerobic metabolism increases (213). Interestingly, Fragouli et al.'s have shown that the mtDNA level in blastocysts significantly increases with female age, with high mtDNA levels present in 30% of non-implanting euploid embryos (215). These studies suggest that the elevated mtDNA content in blastocyst embryos of women with advanced maternal age could be driven by a compensatory mechanism (as shown in Table 5). This abnormal increase in mtDNA content appears to compensate for the low energy generation efficiency and diminished developmental potential observed in non-implanting euploid embryos.

4.1.2 Abnormal distribution patterns of mitochondria and increased mitochondrial vesicle complex *in vitro* matured oocytes affect development and fertilization potential

Despite the tremendous advances that have been made in IVF techniques, infertility outcomes continue to correlate strongly with the age of the patient. To date, very few clinical studies have looked at the ultrastructure of oocyte, particularly mitochondria. A study of 158 ICSI cycles evaluated the changes in mitochondrial distribution in human oocyte before and after *in vitro* maturation(IVM) and the effect of IVM on mitochondrial distribution, identifying three

TABLE 4 Link between mitochondrial damage and infertility.

Mechanism	Species	Targets	Results	References
changes in mitochondrial genome	human	TFAM	a recessive variant in TFAM causes mtDNA depletion associated with POI	(59)
	human	TFAM, POLG	a decreased mtDNA content in DOR, and a positively correlation between the quality of oocyte with the expression of TFAM and POLG in cumulus cells	(60)
	human	TFAM	women with moderate TFAM expression in follicular fluid granulosa cells showed better IVF outcomes	(66)
	human		the mtDNA copy number in cumulus cells can positively predict embryo quality and developmental outcome in IVF	(204–207)
	human		the mtDNA copy number in granulosa cells was significantly negatively correlated with age in the POSEIDON low prognosis groups	(67)
	human		a significantly lower mtDNA copy number in unfertilized oocyte and uncleaved embryos in women >40 years age	(35)
	human	POLG	mutations in POLG cause premature aging	(208)
	human	POLG	POLG is associated with female menopause	(89)
	human		there was no correlation between mtDNA deletion, rearrangement, and mutation of human oocyte and maternal age	(75, 77, 79, 80)
oxidative stress	mice, human	IDH1, JNK, p38 MAPK	ROS inhibits proliferation and promotes apoptosis in granulosa cells	(48)
	rat,human	SIAH1,TRF2	ROS promotes telomere shortening and granulosa cell aging	(49)
	human	H202, HIF-1α,VEGF	H_2O_2 stimulated oxidative injury and apoptosis in GCs	(50)
	human	SOD, CAT, GSHPx	decreased expression of antioxidant enzymes in follicular fluid of women with advanced age	(44, 45)
	mice	SIRT1	SIRT1 signaling protects mice oocyte against oxidative stress and is deregulated during aging	(53)
	mice	PRX2, JNK	ROS accelerates ovarian failure	(51)
	mice, human		an increase in ROS and a decrease in MMP may lead to spindle and chromosomal abnormalities in aging oocyte	(42)
	human		the assessment of the oxidative stress rate may be helpful in evaluating *in vitro* fertilization potential	(43)
mitochondrial dynamics	mice	MFN1, MFN2	lack of MFN1 and MFN2 in oocyte resulted in accelerated follicular depletion and impaired oocyte quality	(108)
	mice	MFN1	absence of MFN1 and resulting apoptotic cell loss caused depletion of ovarian follicular reserve	(109, 136)
	mice	MFN2	low expression of MFN2 was associated with mitochondrial damage and apoptosis of ovarian tissues in the POI mice	(111)
	human	MFN2	MFN2 expression was remarkably lower in granulosa cells from the DOR patients and decreased as age increased	(112)
	mice	DRP1	DRP1 deficiency affected follicle maturation and ovulation	(110)

(Continued)

TABLE 4 Continued

Mechanism	Species	Targets	Results	References
mitochondrial biogenesis	mice	PGC1α	the expression of PGC1 in the ovaries of POI mice induced by cyclophosphamide was significantly downregulated, and mitochondrial damage occurred	(54, 102)
	mice	SIRT1	SIRT1 deficiency led to a decrease in the number of oocyte and premature infertility	(55)
	mice	SIRT3	SIRT3 deficiency accelerated ovarian reserve depletion	(56)
	human	SIRT3	decreased SIRT3 mRNA in granulosa cells of DOR and women with advanced age	(57)
mitochondrial autophagy	Caenorhabditis elegans	PINK1	the absence of PINK1 shortened the reproductive span of C.elegans	(116)
	mice		polyamine metabolite spermidine restored oocyte quality by enhancing mitochondrial autophagy in elderly female mice	(117)
	mice	RAB7, PINK1, PRKN	the regulation of mitophagy affected oocyte meiosis and oocyte quality control during ovarian aging	(118)
mitochondrial unfolded protein response	human	CLPP	mutations in CLPP cause Perrault syndrome and POI	(96, 97)
	mice	CLPP	mutations in CLPP cause complete sterility	(98)
	mice	CLPP, mTOR, COX5A	CLPP deficiency accelerated the depletion of ovarian follicle reserves	(99, 100)
mitochondrial apoptotic	mice, rat	BAX, CytC, Caspase9, BCL2	excessive occurrence of mitochondrial apoptosis in POF and POI	(140)
	mice	BAX	absence of BAX protein extends fertility and alleviates age-related health complications	(143, 144)
mitochondrial dysfunction and telomere damage	human		reduced telomerase activity in granulosa cells of POI patients	(151, 152)
Inadequate mitochondrial energy supply and meiotic errors	mice	MCU	oocyte of MCU knockdown failed to correctly assemble the spindle during meiosis	(129)
	Caenorhabditis elegans	SPD3	the absence of SPD3 can lead to homologous chromosome pairing defects	(132)
	mice	MDR1	MDR1 mutation leads to abnormal meiosis and decreased oocyte quality	(133)
	mice	RAB7, DRP1	RAB7 GTPase regulates actin dynamics for DRP1-mediated mitochondria function and spindle migration in oocyte meiosis	(134)
mitochondrial dysfunction and abnormal intercellular communication	mice	AMPK	lack of AMPK can alter oocyte quality through energy processes and oocyte-somatic communication	(139)

patterns of mitochondrial distribution: peripheral, semi-peripheral, and uniformly diffuse (221). The 64.1% of GV-stage oocyte showed a peripheral distribution, compared with 45.2% of MI oocyte, but after IVM 75.5% (80/106) of oocyte showed a uniformly spread distribution, which may explain part of the reduced developmental potential of oocyte matured *in vitro* (221).

Bianchi et al. in 2015 evaluated the ultrastructure of oocyte from patients of different ages (<35 years old and ≥35 years old, n = 36) undergoing *in vitro* aging (IVA) (due to extended culture), showing that significant decrease of mitochondria-smooth endoplasmic reticulum (M-SER) aggregates, increase of mitochondrial vesicle (MV) complexes size and amount, decrease of cortical granules and microvilli, and alterations of the spindle structure characterized both reproductive aging and IVA oocyte, these changes were significantly more evident in the reproductive aging oocyte submitted to IVA (222). M-SER aggregates are considered to be precursors of MV complexes,

TABLE 5 Prediction of embryonic developmental potential by detection of embryonic mtDNA quantity.

Patients	Number	Protocol	Technique	Results	Reference
infertile women	275 patients and 716 blastocysts	PGT-A	mtDNA copy number detection	higher mtDNA copy number in aneuploid embryos than in euploid embryos, whereas no statistically significant differences in ability to implant	(216)
infertile women	490 patients and 1505 euploid blastocysts	PGT	mtDNA copy number detection	increased implantation rates for embryos with normal and elevated mtDNA levels	(217)
infertile women	174 patients and 199 blastocysts	PGT-A	mtDNA copy number detection	increased ongoing pregnancy rate for morphologically good, euploid blastocysts, with normal/low levels of mtDNA	(218)
infertile women	829 D5 and 472 D6 blastocysts from 460 patients	PGT-A	mtDNA copy number detection	higher mean mtDNA levels in D5 than their D6 counterparts	(219)
infertile women	61 patients and 287 blastocysts	PGT-A	mtDNA copy number detection	lower mtDNA content in euploid blastocysts compared to aneuploid blastocysts	(220)

and they play an important role in making oocyte fertile and facilitating the formation of preimplantation embryonic developmental membranes (223). Therefore, the presence of a greater number of MV complexes in reproductively senescent oocyte is considered to be an aberration. In addition, dysregulation of the M-SER/MV ratio may also lead to disturbances in calcium homeostasis known as a cause of low fertilizing capacity of oocyte (224). Another study demonstrated that MII oocyte from IVA exhibited a low-frequency, short-duration pattern of calcium oscillations within the matrix. In human oocyte (225), oocyte with dark zona pellucida have more MVs than normal oocyte, and dark zona pellucida has been associated with reduced fertilization, implantation and pregnancy rates (226). The above studies suggest that the abnormal mitochondrial distribution pattern and increased MV complexes in our *in vitro* matured oocyte may affect fertilization capacity, but the limited number of *in vivo* matured MII oocyte in humans donated for research and ethical issues have prevented extensive studies.

In summary, limited clinical studies have shown that the copy number of oocyte and CCs mtDNA during ART can positively predict embryo quality. But the abnormal increase in mtDNA content in embryos seems to be a compensatory response to low-quality embryos. In addition, mitochondria exhibit a more peripheral distribution state, and the imbalance of M-SER/MV ratio may affect the fertilization ability of oocyte. However, due to the extremely small number of MII oocyte obtained in current clinical studies, further research is needed to confirm the above findings.

4.2 Aging and mitochondrial disorders affect the developmental potential of oocytes and embryos: can we intervene?

4.2.1 Detection of mtDNA quantity in embryos for embryo selection

In clinical application, PGT or prenatal testing can be used to evaluate the mtDNA heterogeneity of embryos to prevent the occurrence of mitochondrial genetic diseases. According to a study, the mtDNA mutation rate of embryos should be less than 18% if they can be used for transplantation (227). However, it should be noted that PGT is not always effective, because patients carrying homoplasmic mtDNA mutations cannot be screened through PGT and mtDNA in embryos may undergo mutations during development due to environmental influences.

Practically, the assessment of mtDNA quantity accompanying the preimplantation genetic testing for aneuploidy (PGT-A) of the trophectoderm biopsy has been used to predict embryo implantation potential. Studies in multiple clinics found that high mtDNA levels in blastocysts were related to aneuploidy embryos and implantation failure (216–218). The latest retrospective investigation analyzed the transfer cycle of frozen single euploid embryos, and the results showed that no correlation was observed between mtDNA content and blastocyst morphology grades or pregnancy outcomes (219, 220). Still, lower mtDNA content was associated with delayed blastocyst development (219). It should be noted that there is currently no consensus on the threshold for the mtDNA copy number of blastocysts, and the accuracy of using mtDNA copy number as a single predictive biomarker for embryo selection and developmental potential remains low (216–220).

4.2.2 Adding antioxidants to IVF or IVM culture medium to prevent oxidative stress

Some clinical trials have added compounds targeting mitochondrial function to IVF culture media in an attempt to evaluate whether they can enhance mitochondrial dysfunction caused by advanced maternal age, but it is currently unclear.

According to a report, the level of melatonin in follicular fluid is related to the quantity and quality of oocyte, and can predict the outcome of IVF (228). A clinical trial has shown that supplementing with melatonin in the IVM culture system can enhance the reactive oxygen species and Ca^{2+} levels and decrease the mitochondrial membrane potential compared to *in vivo* maturation IVF oocyte (229). In addition, compared to the control group, adding melatonin to the embryo culture medium can improve the rate of high-quality embryos on the third day in patients with repetitive

low-quality embryos and the blastocyst development rate in FET patients (230). At the same time, it can increase the expression of CAT gene in blastocysts, but there is no significant statistical difference in ROS level and clinical pregnancy rate between the two groups. Another human study showed that compared to the control group, melatonin supplements increased the fertilization rate, high-quality embryo rate, and high-quality blastocyst development rate of patients with previous IVF/ICSI failures, and significantly increased the implantation rate and clinical pregnancy rate of this group of patients during FET (231).

A study demonstrated that the addition of Coenzyme Q10 supplement (MitoQ) culture during IVM of human GV-stage oocyte significantly promoted nuclear maturation and had a similar positive effect in preventing chromosomal misalignment (52).

A trial was conducted on 38 thawed embryos from 6-11 cell stages provided to 19 couples (232). Two embryos from each couple were randomly divided into two groups and cultured in a medium containing or without 1 mM L-carnitine. The results showed that adding L-carnitine to the medium significantly increased the oxygen consumption rate of morula and the formation rate of blastocysts.

Overall, current research supports the discovery that antioxidants that improve mitochondrial function may enhance pre-implantation embryo development and implantation success rates, as demonstrated by human clinical and animal studies (as shown in Table 6). However, since these antioxidants are not the main essential factors for pregnancy, it is even more necessary to determine whether adding them to the culture medium will have any negative effects on fetal and perinatal outcomes.

4.2.3 Oral antioxidant pretreatment to improve mitochondrial function before starting IVF treatment

In IVF treatment, clinical workers have been committed to studying how to improve the quality of oocyte in order to produce more high-quality embryos for transfer to the uterus. In addition to being applied to IVF culture media, some clinical trials have used antioxidants in women with poor IVF prognosis to observe whether treatment for mitochondrial damage can improve the quality of embryos obtained.

A randomized controlled trial enrolling 169 patients in POSEIDON classification group 3 (age < 35 years, poor ovarian reserve parameters), in which participants were randomly assigned to coenzyme Q10 pretreatment or no pretreatment 60 days prior to the IVF-ICSI cycle, demonstrated that women treated with coenzyme Q10 had more high-quality embryos, usable frozen embryos, and significantly fewer women cancelled embryo transfers due to poor embryo development than the control group (233). Additional clinical trials have shown that the use of coenzyme Q10 prior to and during IVF treatment in women 31 years of age and older resulted in significant reductions in levels of follicular fluid total antioxidant capacity of mature oocyte (234).

115 patients who failed to conceive due to low fertilization rate (≤50%) in the previous IVF-ET cycle were divided into two groups in the next IVF-ET cycle: 56 patients who received melatonin treatment (3 mg/day) and 59 patients who did not receive melatonin treatment. Compared with the previous IVF-ET cycle, melatonin treatment increased fertilization rate, and the concentrations of 8-hydroxy-2'- deoxyguanosine (8-OHdG) and hexanoyl-lysine adduct in follicles were significantly reduced, which suggests that melatonin treatment can protect oocyte from free radical damage, improve mitochondria, and increase fertilization rate (235). Another clinical trial showed that supplementing with melatonin did not increase the mRNA level of the MT-ATP6 gene in CCs of ovarian follicles, as well as the likelihood of clinical pregnancy and the number of retrieved mature oocyte, but significantly reduced the number of low-quality embryos (236).

Furthermore, 214 patients who underwent previous IVF-ET and were unable to conceive received IVF-ET again after an average of 82 days of treatment with L-carnitine, and results showed that the quality of embryo on Days 3 and 5 after implantation was improved (237).

In a clinical trial of DOR patients with advanced age given resveratrol supplementation three months prior to an IVF cycle, follicular fluid was tested for 13 differentially expressed microRNAs compared to women not receiving supplementation, specifically miR-125b-5p, miR-132-3p, miR-19a-3p, miR-30a-5p and miR-660-5p, and functional predictions of these microRNAs indicate possible regulation of mitochondrial proteins thereby controlling metabolism and mitochondrial biogenesis (238). On the contrary, a retrospective study compared the pregnancy outcomes of consecutive recipients of resveratrol supplements (200 mg/day) and a control group, showing that the clinical pregnancy rate was reduced and the risk of miscarriage was increased in the resveratrol supplemented group (239).

Table 7 summarizes the application of oral antioxidants in the IVF/ICSI cycles. In summary, it is necessary to further study downstream signaling pathways to accurately understand how these antioxidants affect embryonic development. These molecules may not act in isolation, but rather form complex interactions. Therefore, a comprehensive approach that includes different perspectives is essential for its thorough research and application. These antioxidants are expected to be beneficial supplements to IVF treatment, especially when research evidence with larger sample sizes, multi center participation, and comprehensive long-term follow-up (including birth outcomes) is obtained.

4.2.4 Improving embryonic development potential through mitochondrial transfer technology

Mitochondrial transplantation techniques, including autologous mitochondrial transplantation, ST, and PNT, have been applied on a small scale in assisted reproductive clinical practice and live births have been reported using autologous mitochondrial transplantation and ST (70, 71, 179, 195, 196) (as shown in Table 8). However, mitochondrial transplantation technology still needs further optimization and development. Currently, it cannot correct fertility disorders in all elderly

TABLE 6 Comparison of antioxidants added in IVF or IVM culture medium.

Patients	Number	Protocol	Treatment	Results	Reference
infertile women	22 patients (15 IVF vs.15 IVM/ IVF oocyte)	IVF, ICSI	a melatonin-supplemented IVM/ IVF system	increased the cleavage rate in the IVF versus IVM group, increased reactive oxygen species and Ca^{2+} levels, decreased mitochondrial membrane potential in IVM compared with IVF oocyte.	(229)
experiment 1:repeated-poor-quality-embryo patients; experiment 2: non-repeated-poor-quality-embryo patients	experiment 1:42 patients (48 melatonin cycles vs. 133 non-melatonin cycles); experiment 2:143 supernumerary human cleavage-stage embryos(71 in melatonin group vs. 72 in control group)	IVF	10^{-7} M melatonin added to the culture medium	increased 3 high-quality embryos in melatonin cycles, the rate of available blastocysts and clinical pregnancy rate in experiment 1; increased the expression of CAT in experiment 2	(230)
patients with repeated cycles after IVF/ ICSI failure	140 patients (140 melatonin culture cycles vs. previous failed cycles)	IVF, ICSI	10^{-9} M melatonin added to the culture medium	increased the fertilization rate, cleavage rate, high-quality embryo rate, blastocyst rate, high-quality blastocyst rate, biochemical pregnancy rate and clinical pregnancy rate	(231)
infertile women	89 GV oocytes (44 in MitoQ group vs. 45 in control group)	IVM	50nM MitoQ added to the culture medium	a similar positive effect in protecting against chromosomal misalignments	(52)
infertile women	38 vitrified–thawed morulae after ICSI from 19 couples (1:1matched)	ICSI	1 mM l-carnitine added to the culture medium	increased the oxygen consumption rates of morula and the morphologically-good blastocyst formation rate	(232)

TABLE 7 Comparison of oral antioxidants in IVF/ICSI cycles.

Patients	Number	Protocol	Treatment	Results	Reference
poor ovarian reserve women with age < 35 years old	169 patients (76 treated with CoQ10 vs. 93 controls)	IVF, ICSI	oral 200 mg CoQ10 three times a day, for a period of 60 days	increased number of retrieved oocyte, fertilization rate, high-quality embryos, available cryopreserved embryos and decreased cancelled embryo transfer rate	(233)
infertile women aged 31-46 years old	30 patients (15 treated with CoQ10 vs. 15 controls)	IVF	200 mg/day oral CoQ10	decreased follicular fluid total antioxidant capacity	(234)
infertile women with a low fertilization rate (< or =50%) in the previous IVF-ET cycle	115 patients (56 treated with melatonin vs. 59 controls)	IVF, ICSI	melatonin 3 mg/day	decreased 8-OHdG and hexanoyl-lysine adduct, increased fertilization rate	(235)
infertile women	90 patients(45 treated with melatonin vs. 45 controls)	IVF	melatonin 3 mg/day	decreased the number of low-quality embryos	(236)
patients with IVF-ET failure	214 patients(treated with l-carnitine vs. previous failed controls)	IVF, ICSI	1000 mg/day l-carnitine for 82 days on average	increased quality of embryos on Days 3 and 5	(237)
poor ovarian reserve women with advanced age	12 patients (6 treated with resveratrol vs. 6 controls)	IVF	150 mg resveratrol	increased number of fertilized good quality oocyte, decreased the level of miR-125b-5p, miR-132-3p, miR-19a-3p, miR-30a-5p and miR-660-5p	(238)
infertile women	7277 cycles (204 treated with resveratrol vs. 7073 controls)	IVF	200 mg/day resveratrol supplementation	decrease clinical pregnancy rate, increased risk of miscarriage	(239)

TABLE 8 Mitochondrial transplantation techniques in ICSI cycles.

Patients	Number	Protocol	Treatment	Result	Reference
women with multiple IVF failures	10 patients	ICSI	OPCs-derived autologous mitochondrial injection	increased fertilization rate	(70)
patients with a poor prognosis for success with standard IVF	94 patients (106 ICSI-only cycles vs. 171 AUGMENT cycles)	ICSI	OPCs-derived autologous mitochondrial injection	increased oocyte, embryo transfers, and pregnancy rate	(71)
patients with previously IVF failures	57 patients (250 ICSI-only MII vs. 253 AUGMENT MIIs)	ICSI	OPCs-derived autologous mitochondrial injection	decreased Day 5 blastocyst formation rate	(179)
women with multiple IVF failures	25 patients (28 ST cycles)	ICSI	ST	19 embryo transfers, 7 clinical pregnancies	(190)
healthy women aged 25-31 years old	32 PB1T oocytes vs. 21 control oocytes	ICSI	PB1T	decreased blastocysts rate, but similar DNA methylation and transcriptome profiles	(195)
infertile women with aged <37 years old	139 PB2T oocytes vs. 77 control oocytes	IVM, ICSI	PB2T	similar 2PN zygotes rate, cleavage embryo rate, and blastocysts rate	(196)

women by improving receptor mitochondrial function. Before considering its clinical application, more evidence is needed to demonstrate its efficiency and safety.

In summary, we summarized the close relationship between oocyte quality and mitochondria during human IVF. A certain number of mitochondria allows for normal early embryonic development and avoids untimely activation of mitochondrial biogenesis, and thus abnormalities in mtDNA content have been linked to a reduced developmental potential of the oocyte and embryo. In addition, abnormal mitochondrial distribution patterns, and abnormal structure may affect the fertilizing ability of the oocyte. A small number of clinical trials are currently attempting to measure mtDNA levels to predict embryonic developmental potential or to explore ways to improve maternal oocyte quality for better IVF outcomes through modified IVF/IVM media, oral antioxidants, and mitochondrial transplantation techniques. All of the above explorations are of great interest, and a more comprehensive understanding of the role of mitochondria in clinical cases of infertility associated with ovarian senescence will contribute to better management of this disease in the future.

5 Outlook

The postponement of childbirth due to the advancement of the economy and society has emerged as a worldwide concern. Maternal and fetal health risks, such as infertility, elevated miscarriage rates, birth defects, and pregnancy complications, have become significant challenges (226, 240–242). Mitochondrial function plays an important role in maintaining the physiological state of the human body, and mitochondrial damage at any stage may lead to a decrease in oocyte quality.

In this manuscript, we summarize the insights between mammalian models and human senescent oocyte and mitochondrial damage. Quantitatively, mitochondrial biogenesis is critical during oocyte maturation and fertilization. The mtDNA of the oocyte and the surrounding granulosa cells needs to be maintained at a certain quantity, and a decline in mtDNA quantity predicts a decline in ovarian reserve. Senescence-associated mtDNA instability leads to the accumulation of mtDNA mutations in oocyte, which may carry the risk of passing on abnormal mitochondria to the offspring and thus play a key role in the deterioration of oocyte quality. Excessive OS occurs in the aging ovary, and impairment of mitochondrial function is difficult to recover from by autophagy, biogenesis. The link between telomere shortening, meiotic abnormalities, apoptosis and mitochondria has also been tentatively revealed. In addition, mitochondrial dysfunction may also affect cellular communication between oocyte and surrounding GCs. Epigenetic changes also contribute to the decline in oocyte quality during ovarian aging, and the involvement of mitochondrial metabolites in the epigenetic regulation of these processes deserves further investigation. At present, some animal experiments have explored the changes in mitochondrial function during ovarian aging, but most of them have detected changes in mitochondrial related indicators. Lack of more reliable and rigorous experiments to verify the specific roles of mitochondrial related genes. At present, there is a need for more flexible application of cutting-edge molecular and cellular biology technologies to further enhance the coherence, multi-perspective, and depth of research on mitochondrial damage and ovarian aging.

Mitochondria is known as the energy factory of cells and play an important role in the maintenance of human health and the occurrence of diseases. In fact, it is difficult to accurately explain the relationship between mitochondrial damage and disease occurrence. Mitochondrial dysfunction is present in some genetic diseases, such as Perrault syndrome (243), individuals with *POLG* mutations (89, 208), and individuals with *CLPP* mutations (95, 96), all exhibiting clinical phenotypes of ovarian dysfunction and infertility. In addition, the environment in which humans is exposed, including air pollution exposure and chemical exposure, seems to be associated with premature menopause, premature ovarian failure, and low fertility (244–246). Given the sensitivity

of mitochondria to the external environment, environmental pollution is likely to lead to ovarian aging by disrupting mitochondrial function. Unhealthy lifestyles, such as excessive dieting and lack of exercise, also lead to aging by affecting mitochondrial OS, biogenesis, and ATP generation (247, 248). Therefore, the mechanism of mitochondrial damage is most likely a key player in ovarian aging rather than a single pathogenic factor. The relationship between mitochondrial damage and genetics, environment, and diet deserves further research and determination. It is important to use epidemiological methods to investigate the correlation between reproductive health and mitochondrial damage, establish predictive models, and actively develop more accurate preventive measures that include the elderly population.

In addition, given that the current research on the mechanism of mitochondrial damage in ovarian aging is not comprehensive enough, emerging biomarkers that appear to predict ovarian function and embryonic development potential, such as mtDNA, may be valuable. During ART, it was found that abnormal mitochondrial distribution patterns and increased MV complexes in mature oocyte *in vitro* may affect fertilization capacity. It is feasible to predict the developmental potential of embryos by detecting the level of mtDNA in blastocysts (215). However, it should be noted that due to differences in PGT methods, biopsy methods, and techniques, it is not possible to provide standardized decision-making methods for mtDNA for embryo management. In the future, the combination of mtDNA detection with big data, multi-omics technology, and multimodal imaging may contribute to embryo management, birth defect prevention, and other aspects.

Consequently, enhancing the quality of oocyte through the improvement of mitochondrial quality appears to be a novel approach for the management and enhancement of reproductive outcomes in the elderly population. In recent years, the efficacy of targeted treatment of mitochondrial function in ART-assisted pregnancy has been discussed (249), thereby enhancing the success rate of IVF/ICSI. In a limited number of clinical studies, scholars have evaluated methods for improving oocyte energy supply through autologous mitochondrial transplantation from multiple sources (71), and reversing the decline in oocyte quality caused by aging. However, the evidence for high-level randomized controlled trials with large sample sizes from multiple centers is still very limited. We call on clinical researchers to design more rigorous trials to assess the safety and effectiveness of targeted mitochondrial therapies.

In summary, we call for more in-depth research to better understand the mechanisms and consequences of mitochondrial damage in ovarian aging. Mitochondrial targeted therapy is expected to play an important role in delaying female reproductive aging. Incorporating these new technologies and therapies into routine treatment can provide more ideal reproductive outcomes for elderly patients.

Author contributions

WJ: Writing – original draft. YZ: Writing – original draft, Writing – review & editing. YY: Validation, Writing – review & editing. SZ: Validation, Writing – review & editing, Funding acquisition. SX: Funding acquisition, Supervision, Writing – review & editing. FL: Funding acquisition, Supervision, Writing – review & editing.

Funding

The author(s) declare financial support was received for the research, authorship, and/or publication of this article. This study was funded by the Natural Science Foundation of Shandong Province of China(ZR2023MH112), the National Natural Science Foundation of China (82174429, 82104914).

Conflict of interest

The authors declare that the research was conducted in the absence of any commercial or financial relationships that could be construed as a potential conflict of interest.

Publisher's note

References

1. Esencan E, Simsek B, Seli E. Analysis of female demographics in the United States: life expectancy, education, employment, family building decisions, and fertility service utilization. *Curr Opin Obstet Gynecol.* (2021) 33:170–7. doi: 10.1097/GCO.0000000000000704

2. Smock PJ, Schwartz CR. The demography of families: A review of patterns and change. *J Marriage Fam.* (2020) 82:9–34. doi: 10.1111/jomf.12612

3. Cao J, Xu W, Liu Y, Zhang B, Zhang Y, Yu T, et al. Trends in maternal age and the relationship between advanced age and adverse pregnancy outcomes: a population-based register study in Wuhan, China, 2010-2017. *Public Health.* (2022) 206:8–14. doi: 10.1016/j.puhe.2022.02.015

4. Balasch J. Ageing and infertility: an overview. *Gynecol Endocrinol.* (2010) 26:855–60. doi: 10.3109/09513590.2010.501889

5. Colchero F, Aburto JM, Archie EA, Boesch C, Breuer T, Campos FA, et al. The long lives of primates and the 'invariant rate of ageing' hypothesis. *Nat Commun.* (2021) 12:3666. doi: 10.1038/s41467-021-23894-3

6. May-Panloup P, Chretien MF, Malthiery Y, Reynier P. Mitochondrial DNA in the oocyte and the developing embryo. *Curr Top Dev Biol.* (2007) 77:51–83. doi: 10.1016/S0070-2153(06)77003-X

7. Hemann MT, Strong MA, Hao LY, Greider CW. The shortest telomere, not average telomere length, is critical for cell viability and chromosome stability. *Cell*. (2001) 107:67–77. doi: 10.1016/s0092-8674(01)00504-9

8. Kalmbach KH, Fontes Antunes DM, Dracxler RC, Knier TW, Seth-Smith ML, Wang F, et al. Telomeres and human reproduction. *Fertil Steril*. (2013) 99:23–9. doi: 10.1016/j.fertnstert.2012.11.039

9. Peters AE, Mihalas BP, Bromfield EG, Roman SD, Nixon B, Sutherland JM. Autophagy in female fertility: A role in oxidative stress and aging. *Antioxid Redox Signal*. (2020) 32:550–68. doi: 10.1089/ars.2019.7986

10. Peters AE, Caban SJ, McLaughlin EA, Roman SD, Bromfield EG, Nixon B, et al. The impact of aging on macroautophagy in the pre-ovulatory mice oocyte. *Front Cell Dev Biol*. (2021) 9:691826. doi: 10.3389/fcell.2021.691826

11. Mihalas BP, Bromfield EG, Sutherland JM, De Iuliis GN, McLaughlin EA, Aitken RJ, et al. Oxidative damage in naturally aged mice oocyte is exacerbated by dysregulation of proteasomal activity. *J Biol Chem*. (2018) 293:18944–64. doi: 10.1074/jbc.RA118.005751

12. Woods DC, Tilly JL. Isolation, characterization and propagation of mitotically active germ cells from adult mice and human ovaries. *Nat Protoc*. (2013) 8:966–88. doi: 10.1038/nprot.2013.047

13. Li L, Yang R, Yin C, Kee K. Studying human reproductive biology through single-cell analysis and in *vitro* differentiation of stem cells into germ cell-like cells. *Hum Reprod Update*. (2020) 26:670–88. doi: 10.1093/humupd/dmaa021

14. Hainaut M, Clarke HJ. Germ cells of the mammalian female: A limited or renewable resource?†. *Biol Reprod*. (2021) 105:774–88. doi: 10.1093/biolre/ioab115

15. Zhou S, Yan W, Shen W, Cheng J, Xi Y, Yuan S, et al. Low expression of SEMA6C accelerates the primordial follicle activation in the neonatal mice ovary. *J Cell Mol Med*. (2018) 22:486–96. doi: 10.1111/jcmm.13337

16. Yan W, Zhou S, Shen W, Cheng J, Yuan S, Ye S, et al. Suppression of SEMA6C promotes preantral follicles atresia with decreased cell junctions in mice ovaries. *J Cell Physiol*. (2019) 234:4934–43. doi: 10.1002/jcp.27294

17. Yue MX, Fu XW, Zhou GB, Hou YP, Wang L, Zhu SE. Abnormal DNA methylation in oocyte could be associated with a decrease in reproductive potential in old mice. *J Assist Reprod Genet*. (2012) 29:643–50. doi: 10.1007/s10815-012-9780-4

18. De La Fuente R. Chromatin modifications in the germinal vesicle (GV) of mammalian oocyte. *Dev Biol*. (2006) 292:1–12. doi: 10.1016/j.ydbio.2006.01.008

19. Battaglia R, Vento ME, Ragusa M, Barbagallo D, La Ferlita A, Di Emidio G, et al. MicroRNAs are stored in human MII oocyte and their expression profile changes in reproductive aging. *Biol Reprod*. (2016) 95:131. doi: 10.1095/biolreprod.116.142711

20. Colella M, Cuomo D, Peluso T, Falanga I, Mallardo M, De Felice M, et al. Ovarian aging: role of pituitary-ovarian axis hormones and ncRNAs in regulating ovarian mitochondrial activity. *Front Endocrinol (Lausanne)*. (2021) 12:791071. doi: 10.3389/fendo.2021.791071

21. Xing J, Zhang M, Zhao S, Lu M, Lin L, Chen L, et al. EIF4A3-Induced Exosomal circLRRC8A Alleviates Granulosa Cells Senescence Via the miR-125a-3p/NFE2L1 axis. *Stem Cell Rev Rep*. (2023) 19:1994–2012. doi: 10.1007/s12015-023-10564-8

22. Chien Y, Scuoppo C, Wang X, Fang X, Balgley B, Bolden JE, et al. Control of the senescence-associated secretory phenotype by NF-κB promotes senescence and enhances chemosensitivity. *Genes Dev*. (2011) 25:2125–36. doi: 10.1101/gad.17276711

23. Shelling AN, Ahmed Nasef N. The role of lifestyle and dietary factors in the development of premature ovarian insufficiency. *Antioxid (Basel)*. (2023) 12:1601. doi: 10.3390/antiox12081601

24. Zhang D, Zhang X, Zeng M, Yuan J, Liu M, Yin Y, et al. Increased DNA damage and repair deficiency in granulosa cells are associated with ovarian aging in rhesus monkey. *J Assist Reprod Genet*. (2015) 32:1069–78. doi: 10.1007/s10815-015-0483-5

25. St John JC, Facucho-Oliveira J, Jiang Y, Kelly R, Salah R. Mitochondrial DNA transmission, replication and inheritance: a journey from the gamete through the embryo and into offspring and embryonic stem cells. *Hum Reprod Update*. (2010) 16:488–509. doi: 10.1093/humupd/dmq002

26. Eichenlaub-Ritter U, Wieczorek M, Lüke S, Seidel T. Age related changes in mitochondrial function and new approaches to study redox regulation in mammalian oocyte in response to age or maturation conditions. *Mitochondrion*. (2011) 11:783–96. doi: 10.1016/j.mito.2010.08.011

27. Ntostis P, Iles D, Kokkali G, Vaxevanoglou T, Kanavakis E, Pantou A, et al. The impact of maternal age on gene expression during the GV to MII transition in euploid human oocyte. *Hum Reprod*. (2021) 37:80–92. doi: 10.1093/humrep/deab226

28. Kumar M, Pathak D, Kriplani A, Ammini AC, Talwar P, Dada R. Nucleotide variations in mitochondrial DNA and supra-physiological ROS levels in cytogenetically normal cases of premature ovarian insufficiency. *Arch Gynecol Obstet*. (2010) 282:695–705. doi: 10.1007/s00404-010-1623-x

29. Zhen X, Wu B, Wang J, Lu C, Gao H, Qiao J. Increased incidence of mitochondrial cytochrome C oxidase 1 gene mutations in patients with primary ovarian insufficiency. *PloS One*. (2015) 10:e0132610. doi: 10.1371/journal.pone.0132610

30. Ding Y, Xia BH, Zhuo GC, Zhang CJ, Leng JH. Premature ovarian insufficiency may be associated with the mutations in mitochondrial tRNA genes. *Endocr J*. (2019) 66:81–8. doi: 10.1507/endocrj.EJ18-0308

31. Müller-Höcker J, Schäfer S, Weis S, Münscher C, Strowitzki T. Morphological-cytochemical and molecular genetic analyses of mitochondria in isolated human oocyte in the reproductive age. *Mol Hum Reprod*. (1996) 2:951–8. doi: 10.1093/molehr/2.12.951

32. Lu X, Liu Y, Xu J, Cao X, Zhang D, Liu M, et al. Mitochondrial dysfunction in cumulus cells is related to decreased reproductive capacity in advanced-age women. *Fertil Steril*. (2022) 118:393–404. doi: 10.1016/j.fertnstert.2022.04.019

33. Feng P, Xie Q, Liu Z, Guo Z, Tang R, Yu Q. Study on the reparative effect of PEGylated growth hormone on ovarian parameters and mitochondrial function of oocyte from rats with premature ovarian insufficiency. *Front Cell Dev Biol*. (2021) 9:649005. doi: 10.3389/fcell.2021.649005

34. Czajkowska K, Ajduk A. Mitochondrial activity and redox status in oocyte from old mice: The interplay between maternal and postovulatory aging. *Theriogenology*. (2023) 204:18–30. doi: 10.1016/j.theriogenology.2023.03.022

35. Murakoshi Y, Sueoka K, Takahashi K, Sato S, Sakurai T, Tajima H, et al. Embryo developmental capability and pregnancy outcome are related to the mitochondrial DNA copy number and ooplasmic volume. *J Assist Reprod Genet*. (2013) 30:1367–75. doi: 10.1007/s10815-013-0062-6

36. Nagai S, Mabuchi T, Hirata S, Shoda T, Kasai T, Yokota S, et al. Oocyte mitochondria: strategies to improve embryogenesis. *Hum Cell*. (2004) 17:195–201. doi: 10.1111/huc.2004.17.issue-4

37. Nardelli C, Labruna G, Liguori R, Mazzaccara C, Ferrigno M, Capobianco V, et al. Haplogroup T is an obesity risk factor: mitochondrial DNA haplotyping in a morbid obese population from southern Italy. *BioMed Res Int*. (2013) 2013:631082. doi: 10.1155/2013/631082

38. Woods DC, Tilly JL. Autologous germline mitochondrial energy transfer (AUGMENT) in human assisted reproduction. *Semin Reprod Med*. (2015) 33:410–21. doi: 10.1055/s-0035-1567826

39. Song C, Peng W, Yin S, Zhao J, Fu B, Zhang J, et al. Melatonin improves age-induced fertility decline and attenuates ovarian mitochondrial oxidative stress in mice. *Sci Rep*. (2016) 6:352. doi: 10.1038/srep35165

40. Yao J, Ma Y, Zhou S, Bao T, Mi Y, Zeng W, et al. Metformin prevents follicular atresia in aging laying chickens through activation of PI3K/AKT and calcium signaling pathways. *Oxid Med Cell Longev*. (2020) 2020:3648040. doi: 10.1155/2020/3648040

41. Huang P, Zhou Y, Tang W, Ren C, Jiang A, Wang X, et al. Long-term treatment of Nicotinamide mononucleotide improved age-related diminished ovary reserve through enhancing the mitophagy level of granulosa cells in mice. *J Nutr Biochem*. (2022) 101:108911. doi: 10.1016/j.jnutbio.2021.108911

42. Al-Zubaidi U, Adhikari D, Cinar O, Zhang QH, Yuen WS, Murphy MP, et al. Mitochondria-targeted therapeutics, MitoQ and BGP-15, reverse aging-associated meiotic spindle defects in mice and human oocyte. *Hum Reprod*. (2021) 36:771–84. doi: 10.1093/humrep/deaa300

43. Luddi A, Governini L, Capaldo A, Campanella G, De Leo V, Piomboni P, et al. Characterization of the age-dependent changes in antioxidant defenses and protein's sulfhydryl/carbonyl stress in human follicular fluid. *Antioxid (Basel)*. (2020) 9:927. doi: 10.3390/antiox9100927

44. Zhou P, Deng F, Yang Z, Cao C, Zhao H, Liu F, et al. Ginsenoside Rb1 inhibits oxidative stress-induced ovarian granulosa cell injury through Akt-FoxO1 interaction. *Sci China Life Sci*. (2022) 65:2301–15. doi: 10.1007/s11427-021-2080-x

45. Debbarh H, Louanjli N, Aboulmaouahib S, Jamil M, Ahbbas L, Kaarouch I, et al. Antioxidant activities and lipid peroxidation status in human follicular fluid: age-dependent change. *Zygote*. (2021) 29:490–4. doi: 10.1017/S0967199421000241

46. Wang L, Tang J, Wang L, Tan F, Song H, Zhou J, et al. Oxidative stress in oocyte aging and female reproduction. *J Cell Physiol*. (2021) 236:7966–83. doi: 10.1002/jcp.30468

47. Agarwal A, Gupta S, Sekhon L, Shah R. Redox considerations in female reproductive function and assisted reproduction: from molecular mechanisms to health implications. *Antioxid Redox Signal*. (2008) 10:1375–403. doi: 10.1089/ars.2007.1964

48. Sun J, Guo Y, Fan Y, Wang Q, Zhang Q, Lai D. Decreased expression of IDH1 by chronic unpredictable stress suppresses proliferation and accelerates senescence of granulosa cells through ROS activated MAPK signaling pathways. *Free Radic Biol Med*. (2021) 169:122–36. doi: 10.1016/j.freeradbiomed.2021.04.016

49. Lin L, Gao W, Chen Y, Li T, Sha C, Chen L, et al. Reactive oxygen species-induced SIAH1 promotes granulosa cells' senescence in premature ovarian failure. *J Cell Mol Med*. (2022) 26:2417–27. doi: 10.1111/jcmm.17264

50. Yang Z, Hong W, Zheng K, Feng J, Hu C, Tan J, et al. Chitosan oligosaccharides alleviate H2O2-stimulated granulosa cell damage via HIF-1α Signaling pathway. *Oxid Med Cell Longev*. (2022) 2022:4247042. doi: 10.1155/2022/4247042

51. Park SJ, Kim JH, Lee DG, Kim JM, Lee DS. Peroxiredoxin 2 deficiency accelerates age-related ovarian failure through the reactive oxygen species-mediated JNK pathway in mice. *Free Radic Biol Med*. (2018) 123:96–106. doi: 10.1016/j.freeradbiomed.2018.05.059

52. Hu S, Feng J, Wang M, Wufuer R, Liu K, Zhang Z, et al. Nrf1 is an indispensable redox-determining factor for mitochondrial homeostasis by integrating multi-hierarchical regulatory networks. *Redox Biol*. (2022) 57:102470. doi: 10.1016/j.redox.2022.102470

53. Di Emidio G, Falone S, Vitti M, D'Alessandro AM, Vento M, Di Pietro C, et al. SIRT1 signalling protects mice oocyte against oxidative stress and is deregulated during aging. *Hum Reprod*. (2014) 29:2006–17. doi: 10.1093/humrep/deu160

54. Di Emidio G, Rossi G, Bonomo I, Alonso GL, Sferra R, Vetuschi A, et al. The natural carotenoid crocetin and the synthetic tellurium compound AS101 protect the

ovary against cyclophosphamide by modulating SIRT1 and mitochondrial markers. *Oxid Med Cell Longev*. (2017) 2017:8928604. doi: 10.1155/2017/8928604

55. Iljas JD, Wei Z, Homer HA. Sirt1 sustains female fertility by slowing age-related decline in oocyte quality required for post-fertilization embryo development. *Aging Cell*. (2020) 19:e13204. doi: 10.1111/acel.13204

56. Zhu J, Yang Q, Li H, Wang Y, Jiang Y, Wang H, et al. Sirt3 deficiency accelerates ovarian senescence without affecting spermatogenesis in aging mice. *Free Radic Biol Med*. (2022) 193:511–25. doi: 10.1016/j.freeradbiomed.2022.10.324

57. Pacella-Ince L, Zander-Fox DL, Lan M. Mitochondrial SIRT3 and its target glutamate dehydrogenase are altered in follicular cells of women with reduced ovarian reserve or advanced maternal age. *Hum Reprod*. (2014) 29:1490–9. doi: 10.1093/humrep/deu071

58. Bouda E, Stapon A, Garcia-Diaz M. Mechanisms of mammalian mitochondrial transcription. *Protein Sci*. (2019) 28:1594–605. doi: 10.1002/pro.3688

59. Ullah F, Rauf W, Khan K, Khan S, Bell KM, de Oliveira VC, et al. A recessive variant in TFAM causes mtDNA depletion associated with primary ovarian insufficiency, seizures, intellectual disability and hearing loss. *Hum Genet*. (2021) 140:1733–51. doi: 10.1007/s00439-021-02380-2

60. Babayev E, Wang T, Szigeti-Buck K, Lowther K, Taylor HS, Horvath T, et al. Reproductive aging is associated with changes in oocyte mitochondrial dynamics, function, and mtDNA quantity. *Maturitas*. (2016) 93:121–30. doi: 10.1016/j.maturitas.2016.06.015

61. Kushnir VA, Ludaway T, Russ RB, Fields EJ, Koczor C, Lewis W. Reproductive aging is associated with decreased mitochondrial abundance and altered structure in murine oocyte. *J Assist Reprod Genet*. (2012) 29:637–42. doi: 10.1007/s10815-012-9771-5

62. Reynier P, May-Panloup P, Chrétien MF, Morgan CJ, Jean M, Savagner F, et al. Mitochondrial DNA content affects the fertilizability of human oocyte. *Mol Hum Reprod*. (2001) 7:425–9. doi: 10.1093/molehr/7.5.425

63. Van Blerkom J, Davis PW, Lee J. ATP content of human oocyte and developmental potential and outcome after *in-vitro* fertilization and embryo transfer. *Hum Reprod*. (1995) 10:415–24. doi: 10.1093/oxfordjournals.humrep.a135954

64. Takeuchi T, Neri QV, Katagiri Y, Rosenwaks Z, Palermo GD. Effect of treating induced mitochondrial damage on embryonic development and epigenesis. *Biol Reprod*. (2005) 72:584–92. doi: 10.1095/biolreprod.104.032391

65. Alam MH, Miyano T. Interaction between growing oocyte and granulosa cells in *vitro*. *Reprod Med Biol*. (2019) 19:13–23. doi: 10.1002/rmb2.12292

66. Wang CM, Liu CM, Jia XZ, Zhao SB, Nie ZY, Lv CT, et al. Expression of mitochondrial transcription factor A in granulosa cells: implications for oocyte maturation and in vitro fertilization outcomes. *J Assist Reprod Genet*. (2023). doi: 10.1007/s10815-023-03001-9

67. Jiang Z, Shi C, Han H, Wang Y, Liang R, Chen X, et al. Mitochondria-related changes and metabolic dysfunction in low prognosis patients under the POSEIDON classification. *Hum Reprod*. (2021) 36(11):2904–2915. doi: 10.1093/humrep/deab203.

68. Clay Montier LL, Deng JJ, Bai Y. Number matters: control of mammalian mitochondrial DNA copy number. *J Genet Genomics*. (2009) 36:125–31. doi: 10.1016/S1673-8527(08)60099-5

69. Wang J, Wu J, Zhang Y, Zhang J, Xu W, Wu C, et al. Growth hormone protects against ovarian granulosa cell apoptosis: Alleviation oxidative stress and enhancement mitochondrial function. *Reprod Biol*. (2021) 21:100504. doi: 10.1016/j.repbio.2021.100504

70. Oktay K, Baltaci V, Sonmezer M, Turan V, Unsal E, Baltaci A, et al. Oogonial precursor cell-derived autologous mitochondria injection to improve outcomes in women with multiple IVF failures due to low oocyte quality: A clinical translation. *Reprod Sci*. (2015) 22:1612–7. doi: 10.1177/1933719115612137

71. Fakih MH, El Shmoury ME, Szeptycki J, Cruz DD, Lux CR, Verjee S, et al. The AUGMENTSM treatment: physician reported outcomes of the initial global patient experience. *JFIV Reprod Med Genet*. (2015) 3:154. doi: 10.4172/2375-4508

72. Alexeyev MF. Is there more to aging than mitochondrial DNA and reactive oxygen species? *FEBS J*. (2009) 276:5768–87. doi: 10.1111/j.1742-4658.2009.07269.x

73. Wallace DC, Chalkia D. Mitochondrial DNA genetics and the heteroplasmy conundrum in evolution and disease. *Cold Spring Harb Perspect Biol*. (2013) 5:a021220. doi: 10.1101/cshperspect.a021220

74. Wang L, O'Kane AM, Zhang Y, Ren J. Maternal obesity and offspring health: Adapting metabolic changes through autophagy and mitophagy. *Obes Rev*. (2023) 24: e13567. doi: 10.1111/obr.13567

75. Arnheim N, Cortopassi G. Deleterious mitochondrial DNA mutations accumulate in aging human tissues. *Mutat Res*. (1992) 275:157–67. doi: 10.1016/0921-8734(92)90020-P

76. Wang CM, Liu CM, Jia XZ, Zhao SB, Nie ZY, Lv CT, et al. Expression of mitochondrial transcription factor A in granulosa cells: implications for oocyte maturation and in vitro fertilization outcomes. *J Assist Reprod Genet*. (2024). doi: 10.1007/s10815-023-03001-9

77. Ross JM, Stewart JB, Hagström E, Brené S, Mourier A, Coppotelli G, et al. Germline mitochondrial DNA mutations aggravate ageing and can impair brain development. *Nature*. (2013) 501:412–5. doi: 10.1038/nature12474

78. Brenner CA, Wolny YM, Barritt JA, Matt DW, Munné S, Cohen J. Mitochondrial DNA deletion in human oocyte and embryos. *Mol Hum Reprod*. (1998) 4:887–92. doi: 10.1093/molehr/4.9.887

79. Barritt JA, Brenner CA, Cohen J, Matt DW. Mitochondrial DNA rearrangements in human oocyte and embryos. *Mol Hum Reprod*. (1999) 5:927–33. doi: 10.1093/molehr/5.10.927

80. Boucret L, Bris C, Seegers V, Goudenège D, Desquiret-Dumas V, Domin-Bernhard M, et al. Deep sequencing shows that oocyte are not prone to accumulate mtDNA heteroplasmic mutations during ovarian ageing. *Hum Reprod*. (2017) 32:2101–9. doi: 10.1093/humrep/dex268

81. Radzvilavicius AL, Johnston IG. Organelle bottlenecks facilitate evolvability by traversing heteroplasmic fitness valleys. *Front Genet*. (2022) 13:974472. doi: 10.3389/fgene.2022.974472

82. Chinnery PF. Inheritance of mitochondrial disorders. *Mitochondrion*. (2002) 2:149–55. doi: 10.1016/s1567-7249(02)00046-6

83. Poulton J, Finsterer J, Yu-Wai-Man P. Genetic counselling for maternally inherited mitochondrial disorders. *Mol Diagn Ther*. (2017) 21:419–29. doi: 10.1007/s40291-017-0279-7

84. Smeets HJ, Sallevelt SC, Dreesen JC, de Die-Smulders CE, de Coo IF. Preventing the transmission of mitochondrial DNA disorders using prenatal or preimplantation genetic diagnosis. *Ann N Y Acad Sci*. (2015) 1350(1):1350:29–36. doi: 10.1111/nyas.12866

85. Johnson LC, Singh A, Patel SS. The N-terminal domain of human mitochondrial helicase Twinkle has DNA-binding activity crucial for supporting processive DNA synthesis by polymerase γ. *J Biol Chem*. (2023) 299:102797. doi: 10.1016/j.jbc.2022.102797

86. Trombly G, Said AM, Kudin AP, Peeva V, Altmüller J, Becker K, et al. The fate of oxidative strand breaks in mitochondrial DNA. *Antioxid (Basel)*. (2023) 12:1087. doi: 10.3390/antiox12051087

87. Fekete B, Pentelényi K, Rudas G, Gál A, Grosz Z, Illés A, et al. Broadening the phenotype of the TWNK gene associated Perrault syndrome. *BMC Med Genet*. (2019) 20:198. doi: 10.1186/s12881-019-0934-4

88. Gotta F, Lamp M, Geroldi A, Trevisan L, Origone P, Fugazza G, et al. A novel mutation of Twinkle in Perrault syndrome: A not rare diagnosis? *Ann Hum Genet*. (2020) 84:417–22. doi: 10.1111/ahg.12384

89. Day FR, Ruth KS, Thompson DJ, Lunetta KL, Pervjakova N, Chasman DI, et al. Large-scale genomic analyses link reproductive aging to hypothalamic signaling, breast cancer susceptibility and BRCA1-mediated DNA repair. *Nat Genet*. (2015) 47:1294–303. doi: 10.1038/ng.3412

90. Boucret L, Chao de la Barca JM, Morinière C, Desquiret V, Ferré-L'Hôtellier V, Descamps P, et al. Relationship between diminished ovarian reserve and mitochondrial biogenesis in cumulus cells. *Hum Reprod*. (2015) 30(7):1653–64. doi: 10.1093/humrep/dev114

91. Faraci C, Annis S, Jin J, Li H, Khrapko K, Woods DC. Impact of exercise on oocyte quality in the POLG mitochondrial DNA mutator mice. *Reproduction*. (2018) 156:185–94. doi: 10.1530/REP-18-0061

92. Yang L, Lin X, Tang H, Fan Y, Zeng S, Jia L, et al. Mitochondrial DNA mutation exacerbates female reproductive aging via impairment of the NADH/NAD+ redox. *Aging Cell*. (2020) 19:e13206. doi: 10.1111/acel.13206

93. Smyrnias I. The mitochondrial unfolded protein response and its diverse roles in cellular stress. *Int J Biochem Cell Biol*. (2021) 133:105934. doi: 10.1016/j.biocel.2021.105934

94. Richards BJ, Slavin M, Oliveira AN, SanFrancesco VC, Hood DA. Mitochondrial protein import and UPR in skeletal muscle remodeling and adaptation. *Semin Cell Dev Biol*. (2023) 143:28–36. doi: 10.1016/j.semcdb.2022.01.002

95. Sen B, Rastogi A, Nath R, Shasthry SM, Pamecha V, Pandey S, et al. Senescent hepatocytes in decompensated liver show reduced UPRMT and its key player, CLPP, attenuates senescence in vitro. *Cell Mol Gastroenterol Hepatol*. (2019) 8:73–94. doi: 10.1016/j.jcmgh.2019.03.001

96. Jenkinson EM, Rehman AU, Walsh T, Clayton-Smith J, Lee K, Morell RJ, et al. Perrault syndrome is caused by recessive mutations in CLPP, encoding a mitochondrial ATP-dependent chambered protease. *Am J Hum Genet*. (2013) 92:605–13. doi: 10.1016/j.ajhg.2013.02.013

97. Yuan X, Ma W, Chen S, Wang H, Zhong C, Gao L, et al. CLPP inhibition triggers apoptosis in human ovarian granulosa cells via COX5A abnormality-Mediated mitochondrial dysfunction. *Front Genet*. (2023) 14:1141167. doi: 10.3389/fgene.2023.1141167

98. Gispert S, Parganlija D, Klinkenberg M, Dröse S, Wittig I, Mittelbronn M, et al. Loss of mitochondrial peptidase Clpp leads to infertility, hearing loss plus growth retardation via accumulation of CLPX, mtDNA and inflammatory factors. *Hum Mol Genet*. (2013) 22:4871–87. doi: 10.1093/hmg/ddt338

99. Wang T, Babayev E, Jiang Z, Li G, Zhang M, Esencan E, et al. Mitochondrial unfolded protein response gene Clpp is required to maintain ovarian follicular reserve during aging, for oocyte competence, and development of pre-implantation embryos. *Aging Cell*. (2018) 17:e12784. doi: 10.1111/acel.12784

100. Esencan E, Jiang Z, Wang T, Zhang M, Soylemez-Imamoglu G, Seli E. Impaired mitochondrial stress response due to CLPP deletion is associated with altered mitochondrial dynamics and increased apoptosis in cumulus cells. *Reprod Sci*. (2020) 27:621–30. doi: 10.1007/s43032-019-00063-y

101. Alizadeh Pahlavani H, Laher I, Knechtle B, Zouhal H. Exercise and mitochondrial mechanisms in patients with sarcopenia. *Front Physiol*. (2022) 13:1040381. doi: 10.3389/fphys.2022.1040381

102. Chen Y, Zhao Y, Miao C, Yang L, Wang R, Chen B, et al. Quercetin alleviates cyclophosphamide-induced premature ovarian insufficiency in mice by reducing

mitochondrial oxidative stress and pyroptosis in granulosa cells. *J Ovarian Res*. (2022) 15:138. doi: 10.1186/s13048-022-01080-3

103. Liu XH, Cai SZ, Zhou Y, Wang YP, Han YJ, Wang CL, et al. Ginsenoside rg1 attenuates premature ovarian failure of D-gal induced POF mice through downregulating p16INK4a and upregulating SIRT1 expression. *Endocr Metab Immune Disord Drug Targets*. (2022) 22:318–27. doi: 10.2174/1871523020666210830164152

104. Niu YJ, Zhou W, Nie ZW, Zhou D, Xu YN, Ock SA, et al. Ubiquinol-10 delays postovulatory oocyte aging by improving mitochondrial renewal in pigs. *Aging (Albany NY)*. (2020) 12:1256–71. doi: 10.18632/aging.102681

105. Navarro-Pando JM, Bullón P, Cordero MD, Alcocer-Gómez E. Is AMP-activated protein kinase associated to the metabolic changes in primary ovarian insufficiency? *Antioxid Redox Signal*. (2020) 33:1115–21. doi: 10.1089/ars.2020.8144

106. Nemoto S, Fergusson MM, Finkel T. SIRT1 functionally interacts with the metabolic regulator and transcriptional coactivator PGC-1{alpha}. *J Biol Chem*. (2005) 280:16456–60. doi: 10.1074/jbc.M501485200

107. Itami N, Shirasuna K, Kuwayama T, Iwata H. Palmitic acid induces ceramide accumulation, mitochondrial protein hyperacetylation, and mitochondrial dysfunction in porcine oocyte. *Biol Reprod*. (2018) 98:644–53. doi: 10.1093/biolre/ioy023

108. Cozzolino M, Ergun Y, Seli E. Targeted deletion of mitofusin 1 and mitofusin 2 causes female infertility and loss of follicular reserve. *Reprod Sci*. (2023) 30:560–8. doi: 10.1007/s43032-022-01014-w

109. Zhang M, Bener MB, Jiang Z, Wang T, Esencan E, Scott Iii R, et al. Mitofusin 1 is required for female fertility and to maintain ovarian follicular reserve. *Cell Death Dis*. (2019) 10:560. doi: 10.1038/s41419-019-1799-3

110. Udagawa O, Ishihara T, Maeda M, Matsunaga Y, Tsukamoto S, Kawano N, et al. Mitochondrial fission factor Drp1 maintains oocyte quality via dynamic rearrangement of multiple organelles. *Curr Biol*. (2014) 24:2451–8. doi: 10.1016/j.cub.2014.08.060

111. Chen W, Xu X, Wang L, Bai G, Xiang W. Low expression of mfn2 is associated with mitochondrial damage and apoptosis of ovarian tissues in the premature ovarian failure model. *PloS One*. (2015) 10:e0136421. doi: 10.1371/journal.pone.0136421

112. Wang L, Song S, Liu X, Zhang M, Xiang W. Low MFN2 expression related to ageing in granulosa cells is associated with assisted reproductive technology outcome. *Reprod BioMed Online*. (2019) 38:152–8. doi: 10.1016/j.rbmo.2018.10.011

113. Chakraborty PK, Murphy B, Mustafi SB, Dey A, Xiong X, Rao G, et al. Cystathionine β-synthase regulates mitochondrial morphogenesis in ovarian cancer. *FASEB J*. (2018) 32:4145–57. doi: 10.1096/fj.201701095R

114. Sun X, Zeng C, Wang F, Zhang Z, Yang F, Liu ZP, et al. Neuromedin S Regulates Steroidogenesis through Maintaining Mitochondrial Morphology and Function via NMUR2 in Goat Ovarian Granulosa Cells. *Int J Mol Sci*. (2022) 23:13402. doi: 10.3390/ijms232113402

115. Chen G, Kroemer G, Kepp O. Mitophagy: an emerging role in aging and age-associated diseases. *Front Cell Dev Biol*. (2020) 8:200. doi: 10.3389/fcell.2020.00200

116. Cota V, Sohrabi S, Kaletsky R, Murphy CT. Oocyte mitophagy is critical for extended reproductive longevity. *PloS Genet*. (2022) 18:e1010400. doi: 10.1371/journal.pgen.1010400

117. Zhang Y, Bai J, Cui Z, Li Y, Gao Q, Miao Y, et al. Polyamine metabolite spermidine rejuvenates oocyte quality by enhancing mitophagy during female reproductive aging. *Nat Aging*. (2023) 3(11):1372–86. doi: 10.1038/s43587-023-00498-8

118. Jin X, Wang K, Wang L, Liu W, Zhang C, Qiu Y, et al. RAB7 activity is required for the regulation of mitophagy in oocyte meiosis and oocyte quality control during ovarian aging. *Autophagy*. (2022) 18:643–60. doi: 10.1080/15548627.2021.1946739

119. Tan EHN, Tang BL. Rab7a and mitophagosome formation. *Cells*. (2019) 8:224. doi: 10.3390/cells8030224

120. Guerra F, Bucci C. Multiple roles of the small GTPase rab7. *Cells*. (2016) 5:34. doi: 10.3390/cells5030034

121. Diot A, Dombi E, Lodge T, Liao C, Morten K, Carver J, et al. Modulating mitochondrial quality in disease transmission: towards enabling mitochondrial DNA disease carriers to have healthy children. *Biochem Soc Trans*. (2016) 44:1091–100. doi: 10.1042/BST20160095

122. Palozzi JM, Jeedigunta SP, Minenkova AV, Monteiro VL, Thompson ZS, Lieber T, et al. Mitochondrial DNA quality control in the female germline requires a unique programmed mitophagy. *Cell Metab*. (2022) 34:1809–1823.e6. doi: 10.1016/j.cmet.2022.10.005

123. Geraedts J, Montag M, Magli MC, Repping S, Handyside A, Staessen C, et al. Polar body array CGH for prediction of the status of the corresponding oocyte. Part I: clinical results. *Hum Reprod*. (2011) 26:3173–80. doi: 10.1093/humrep/der294

124. Lodge C, Herbert M. Oocyte aneuploidy-more tools to tackle an old problem. *Proc Natl Acad Sci U S A*. (2020) 117:11850–2. doi: 10.1073/pnas.2005739117

125. Greaney J, Wei Z, Homer H. Regulation of chromosome segregation in oocyte and the cellular basis for female meiotic errors. *Hum Reprod Update*. (2018) 24:135–61. doi: 10.1093/humupd/dmx035

126. Tilia L, Chapman M, Kilani S, Cooke S, Venetis C. Oocyte meiotic spindle morphology is a predictive marker of blastocyst ploidy-a prospective cohort study. *Fertil Steril*. (2020) 113:105–113.e1. doi: 10.1016/j.fertnstert.2019.08.070

127. Zhou Q, Xu K, Zhao BW, Qiao JY, Li YY, Lei WL, et al. Mitochondrial E3 ubiquitin ligase MARCH5 is required for mice oocyte meiotic maturation†. *Biol Reprod*. (2023) 108:437–46. doi: 10.1093/biolre/ioac215

128. Kim KH, Kim EY, Lee KA. GAS6 ameliorates advanced age-associated meiotic defects in mice oocyte by modulating mitochondrial function. *Aging (Albany NY)*. (2021) 13:18018–32. doi: 10.18632/aging.203328

129. Zhang LY, Lin M, Qingrui Z, Zichuan W, Junjin L, Kexiong L, et al. Mitochondrial Calcium uniporters are essential for meiotic progression in mice oocyte by controlling Ca2+ entry. *Cell Prolif*. (2021) 54:e13127. doi: 10.1111/cpr.13127

130. Tiwari M, Prasad S, Shrivastav TG, Chaube SK. Calcium signaling during meiotic cell cycle regulation and apoptosis in mammalian oocyte. *J Cell Physiol*. (2017) 232:976–81. doi: 10.1002/jcp.25670

131. Zhang L, Wang Z, Lu T, Meng L, Luo Y, Fu X, et al. Mitochondrial ca2+ Overload leads to mitochondrial oxidative stress and delayed meiotic resumption in mice oocyte. *Front Cell Dev Biol*. (2020) 8:580876. doi: 10.3389/fcell.2020.580876

132. Labrador L, Barroso C, Lightfoot J, Müller-Reichert T, Flibotte S, Taylor J, et al. Chromosome movements promoted by the mitochondrial protein SPD-3 are required for homology search during Caenorhabditis elegans meiosis. *PloS Genet*. (2013) 9:e1003497. doi: 10.1371/journal.pgen.1003497

133. Nabi D, Bosi D, Gupta N, Thaker N, Fissore R, Brayboy LM. Multidrug resistance transporter-1 dysfunction perturbs meiosis and Ca2+ homeostasis in oocyte. *Reproduction*. (2022) 165:79–91. doi: 10.1530/REP-22-0192

134. Pan ZN, Pan MH, Sun MH, Li XH, Zhang Y, Sun SC. RAB7 GTPase regulates actin dynamics for DRP1-mediated mitochondria function and spindle migration in mice oocyte meiosis. *FASEB J*. (2020) 34:9615–27. doi: 10.1096/fj.201903013R

135. Purcell SH, Chi MM, Lanzendorf S, Moley KH. Insulin-stimulated glucose uptake occurs in specialized cells within the cumulus oocyte complex. *Endocrinology*. (2012) 153:2444–54. doi: 10.1210/en.2011-1974

136. Carvalho KF, MaChado TS, Garcia BM, Zangirolamo AF, Macabelli CH, Sugiyama FHC, et al. Mitofusin 1 is required for oocyte growth and communication with follicular somatic cells. *FASEB J*. (2020) 34:7644–60. doi: 10.1096/fj.201901761R

137. Eliyahu E, Shtraizent N, Martinuzzi K, Barritt J, He X, Wei H, et al. Acid ceramidase improves the quality of oocyte and embryos and the outcome of in *vitro* fertilization. *FASEB J*. (2010) 24:1229–38. doi: 10.1096/fj.09-145508

138. Dong J, Guo C, Yang Z, Wu Y, Zhang C. Follicle-stimulating hormone alleviates ovarian aging by modulating mitophagy- and glycophagy-based energy metabolism in hens. *Cells*. (2022) 11:3270. doi: 10.3390/cells11203270

139. Bertoldo MJ, Guibert E, Faure M, Ramé C, Foretz M, Viollet B, et al. Specific deletion of AMP-activated protein kinase (α1) in murine oocyte alters junctional protein expression and mitochondrial physiology. *PloS One*. (2015) 10:e0119680. doi: 10.1371/journal.pone.0119680

140. Luo Q, Tang Y, Jiang Z, Bao H, Fu Q, Zhang H. hUCMSCs reduce theca interstitial cells apoptosis and restore ovarian function in premature ovarian insufficiency rats through regulating NR4A1-mediated mitochondrial mechanisms. *Reprod Biol Endocrinol*. (2022) 20:125. doi: 10.1186/s12958-022-00992-5

141. Jiang XL, Tai H, Kuang JS, Zhang JY, Cui SC, Lu YX, et al. Jian-Pi-Yi-Shen decoction inhibits mitochondria-dependent granulosa cell apoptosis in a rat model of POF. *Aging (Albany NY)*. (2022) 14:8321–45. doi: 10.18632/aging.204320

142. Liu Z, Li F, Xue J, Wang M, Lai S, Bao H, et al. Esculentoside A rescues granulosa cell apoptosis and folliculogenesis in mice with premature ovarian failure. *Aging (Albany NY)*. (2020) 12:16951–62. doi: 10.18632/aging.103609

143. Perez GI, Jurisicova A, Wise L, Lipina T, Kanisek M, Bechard A, et al. Absence of the proapoptotic Bax protein extends fertility and alleviates age-related health complications in female mice. *Proc Natl Acad Sci U S A*. (2007) 104:5229–34. doi: 10.1073/pnas.0608557104

144. Perez GI, Robles R, Knudson CM, Flaws JA, Korsmeyer SJ, Tilly JL. Prolongation of ovarian lifespan into advanced chronological age by Bax-deficiency. *Nat Genet*. (1999) 21:200–3. doi: 10.1038/5985

145. Ayed-Boussema I, Rjiba-Touati K, Hamdi H, Chaabani H, Abid-Essefi S. Oxidative stress-mediated mitochondrial apoptosis induced by the acaricide, fenpyroximate, on cultured human colon cancer HCT 116 cells. *Toxicol In Vitro*. (2023) 89:105587. doi: 10.1016/j.tiv.2023.105587

146. Watabe M, Nakaki T. ATP depletion does not account for apoptosis induced by inhibition of mitochondrial electron transport chain in human dopaminergic cells. *Neuropharmacology*. (2007) 52:536–41. doi: 10.1016/j.neuropharm.2006.07.037

147. Córdova-Oriz I, Chico-Sordo L, Varela E. Telomeres, aging and reproduction. *Curr Opin Obstet Gynecol*. (2022) 34(3):151–8. doi: 10.1097/GCO.0000000000000779

148. Maser RS, DePinho RA. Connecting chromosomes, crisis, and cancer. *Science*. (2002) 297:565–9. doi: 10.1126/science.297.5581.565

149. Phillippe M. Telomeres, oxidative stress, and timing for spontaneous term and preterm labor. *Am J Obstet Gynecol*. (2022) 227:148–62. doi: 10.1016/j.ajog.2022.04.024

150. von Zglinicki T. Oxidative stress shortens telomeres. *Trends Biochem Sci*. (2002) 27:339–44. doi: 10.1016/s0968-0004(02)02110-2

151. Butts S, Riethman H, Ratcliffe S, Shaunik A, Coutifaris C, Barnhart K. Correlation of telomere length and telomerase activity with occult ovarian insufficiency. *J Clin Endocrinol Metab*. (2009) 94:4835–43. doi: 10.1210/jc.2008-2269

152. Xu X, Chen X, Zhang X, Liu Y, Wang Z, Wang P, et al. Impaired telomere length and telomerase activity in peripheral blood leukocytes and granulosa cells in

patients with biochemical primary ovarian insufficiency. *Hum Reprod*. (2017) 32:201–7. doi: 10.1093/humrep/dew283

153. Sahin E, Colla S, Liesa M, Moslehi J, Müller FL, Guo M, et al. Telomere dysfunction induces metabolic and mitochondrial compromise. *Nature*. (2011) 470:359–65. doi: 10.1038/nature09787

154. Park JH, Zhuang J, Li J, Hwang PM. p53 as guardian of the mitochondrial genome. *FEBS Lett*. (2016) 590:924–34. doi: 10.1002/1873-3468.12061

155. Lin J, Epel E. Stress and telomere shortening: Insights from cellular mechanisms. *Ageing Res Rev*. (2022) 73:101507. doi: 10.1016/j.arr.2021.101507

156. Sun C, Wang K, Stock AJ, Gong Y, Demarest TG, Yang B, et al. Re-equilibration of imbalanced NAD metabolism ameliorates the impact of telomere dysfunction. *EMBO J*. (2020) 39:e103420. doi: 10.15252/embj.2019103420

157. Zhu D, Li X, Tian Y. Mitochondrial-to-nuclear communication in aging: an epigenetic perspective. *Trends Biochem Sci*. (2022) 47:645–59. doi: 10.1016/j.tibs.2022.03.008

158. Tang Q, Grathwol CW, Aslan-Üzel AS, Wu S, Link A, Pavlidis IV, et al. Directed evolution of a halide methyltransferase enables biocatalytic synthesis of diverse SAM analogs. *Angew Chem Int Ed Engl*. (2021) 60:1524–7. doi: 10.1002/anie.202013871

159. Londoño Gentile T, Lu C, Lodato PM, Tse S, Olejniczak SH, Witze ES, et al. DNMT1 is regulated by ATP-citrate lyase and maintains methylation patterns during adipocyte differentiation. *Mol Cell Biol*. (2013) 33:3864–78. doi: 10.1128/MCB.01495-12

160. Bradshaw PC. Acetyl-coA metabolism and histone acetylation in the regulation of aging and lifespan. *Antioxid (Basel)*. (2021) 10:572. doi: 10.3390/antiox10040572

161. Carnesecchi J, Forcet C, Zhang L, Tribollet V, Barenton B, Boudra R, et al. ERRα induces H3K9 demethylation by LSD1 to promote cell invasion. *Proc Natl Acad Sci U S A*. (2017) 114:3909–14. doi: 10.1073/pnas.1614664114

162. Huang F, Luo X, Ou Y, Gao Z, Tang Q, Chu Z, et al. Control of histone demethylation by nuclear-localized α-ketoglutarate dehydrogenase. *Science*. (2023) 381:eadf8822. doi: 10.1126/science.adf8822

163. He M, Zhang T, Zhu Z, Qin S, Wang H, Zhao L, et al. LSD1 contributes to programmed oocyte death by regulating the transcription of autophagy adaptor SQSTM1/p62. *Aging Cell*. (2020) 19:e1310. doi: 10.1111/acel.13102

164. Mondal R, Pal P, Biswas S, Chattopadhyay A, Bandyopadhyay A, Mukhopadhyay A, et al. Attenuation of sodium arsenite mediated ovarian DNA damage, follicular atresia, and oxidative injury by combined application of vitamin E and C in post pubertal Wistar rats. *Naunyn Schmiedebergs Arch Pharmacol*. (2023) 396 (10):2701–20. doi: 10.1007/s00210-023-02491-9

165. Jiang WJ, Yao XR, Zhao YH, Gao QS, Jin QG, Li YH, et al. L-carnitine prevents bovine oocyte aging and promotes subsequent embryonic development. *J Reprod Dev*. (2019) 65:499–506. doi: 10.1262/jrd.2019-046

166. Kujjo LL, Acton BM, Perkins GA, Ellisman MH, D'Estaing SG, Casper RF, et al. Ceramide and its transport protein (CERT) contribute to deterioration of mitochondrial structure and function in aging oocyte. *Mech Ageing Dev*. (2013) 134:43–52. doi: 10.1016/j.mad.2012.12.001

167. Cheng J, Mi P, Li Y, Lu Y, Sun F. Melatonin prevents oocyte deterioration due to cotinine exposure in mice†. *Biol Reprod*. (2022) 107:635–49. doi: 10.1093/biolre/ioac043

168. Li XQ, Wang Y, Yang SJ, Liu Y, Ma X, Liu L, et al. Melatonin protects against maternal diabetes-associated meiotic defects by maintaining mitochondrial function. *Free Radic Biol Med*. (2022) 188:386–94. doi: 10.1016/j.freeradbiomed.2022.06.243

169. Jiao Y, Wang Y, Jiang T, Wen K, Cong P, Chen Y, et al. Quercetin protects porcine oocyte from in *vitro* aging by reducing oxidative stress and maintaining the mitochondrial functions. *Front Cell Dev Biol*. (2022) 10:915898. doi: 10.3389/fcell.2022.915898

170. Liang QX, Lin YH, Zhang CH, Sun HM, Zhou L, Schatten H, et al. Resveratrol increases resistance of mice oocyte to postovulatory aging in vivo. *Aging (Albany NY)*. (2018) 10:1586–96. doi: 10.18632/aging.101494

171. He W, Wang H, Tang C, Zhao Q, Zhang J. Dietary supplementation with astaxanthin alleviates ovarian aging in aged laying hens by enhancing antioxidant capacity and increasing reproductive hormones. *Poult Sci*. (2023) 102:102258. doi: 10.1016/j.psj.2022.102258

172. Bertoldo MJ, Listijono DR, Ho WJ, Riepsamen AH, Goss DM, Richani D, et al. NAD+ Repletion rescues female fertility during reproductive aging. *Cell Rep*. (2020) 30:1670–1681.e7. doi: 10.1016/j.celrep.2020.01.058

173. Yang Q, Cong L, Wang Y, Luo X, Li H, Wang H, et al. Increasing ovarian NAD + levels improve mitochondrial functions and reverse ovarian aging. *Free Radic Biol Med*. (2020) 156:1–10. doi: 10.1016/j.freeradbiomed.2020.05.003

174. Zhang L, Zhang Z, Wang J, Lv D, Zhu T, Wang F, et al. Melatonin regulates the activities of ovary and delays the fertility decline in female animals via MT1/AMPK pathway. *J Pineal Res*. (2019) 66:e12550. doi: 10.1111/jpi.12550

175. Xu J, Sun L, He M, Zhang S, Gao J, Wu C, et al. Resveratrol Protects against Zearalenone-Induced Mitochondrial Defects during Porcine Oocyte Maturation via PINK1/Parkin-Mediated Mitophagy. *Toxins (Basel)*. (2022) 14:641. doi: 10.3390/toxins14090641

176. Guo L, Liu X, Chen H, Wang W, Gu C, Li B. Decrease in ovarian reserve through the inhibition of SIRT1-mediated oxidative phosphorylation. *Aging (Albany NY)*. (2022) 14:2335–47. doi: 10.18632/aging.203942

177. Heydarnejad A, Ostadhosseini S, Varnosfaderani SR, Jafarpour F, Moghimi A, Nasr-Esfahani MH. Supplementation of maturation medium with CoQ10 enhances developmental competence of ovine oocytes through improvement of mitochondrial function. *Mol Reprod Dev*. (2019) 86(7):812–824. doi: 10.1002/mrd.23159

178. Rodríguez-Varela C, Labarta E. Role of mitochondria transfer in infertility: A commentary. *Cells*. (2022) 11:1867. doi: 10.3390/cells11121867

179. Labarta E, de Los Santos MJ, Herraiz S, Escribá MJ, Marzal A, Buigues A, et al. Autologous mitochondrial transfer as a complementary technique to intracytoplasmic sperm injection to improve embryo quality in patients undergoing in *vitro* fertilization-a randomized pilot study. *Fertil Steril*. (2019) 111:86–96. doi: 10.1016/j.fertnstert.2018.09.023

180. Wang ZB, Hao JX, Meng TG, Guo L, Dong MZ, Fan LH, et al. Transfer of autologous mitochondria from adipose tissue-derived stem cells rescues oocyte quality and infertility in aged mice. *Aging (Albany NY)*. (2017) 9:2480–8. doi: 10.18632/aging.101332

181. Kankanam Gamage US, Hashimoto S, Miyamoto Y, Nakano T, Yamanaka M, Koike A, et al. Mitochondria transfer from adipose stem cells improves the developmental potential of cryopreserved oocyte. *Biomolecules*. (2022) 12:1008. doi: 10.3390/biom12071008

182. Yang Y, Zhang C, Sheng X. Mitochondrial transfer from mice adipose-derived mesenchymal stem cells into aged mice oocyte. *J Vis Exp*. (2023) 191:e64217. doi: 10.3791/64217

183. Sheng X, Yang Y, Zhou J, Yan G, Liu M, Xu L, et al. Mitochondrial transfer from aged adipose-derived stem cells does not improve the quality of aged oocyte in C57BL/6 mice. *Mol Reprod Dev*. (2019) 86:516–29. doi: 10.1002/mrd.23129

184. Chiang T, Schultz RM, Lampson MA. Meiotic origins of maternal age-related aneuploidy. *Biol Reprod*. (2012) 86:1–7. doi: 10.1095/biolreprod.111.094367

185. Wagner M, Yoshihara M, Douagi I, Damdimopoulos A, Panula S, Petropoulos S, et al. Single-cell analysis of human ovarian cortex identifies distinct cell populations but no oogonial stem cells. *Nat Commun*. (2020) 11:1147. doi: 10.1038/s41467-020-14936-3

186. Bhartiya D, Sharma D. Ovary does harbor stem cells - size of the cells matter! *J Ovarian Res*. (2020) 13:39. doi: 10.1186/s13048-020-00647-2

187. Tang S, Yang N, Yu M, Wang S, Hu X, Ni H, et al. Noninvasive autologous mitochondria transport improves the quality and developmental potential of oocyte from aged mice. *F S Sci*. (2022) 3:310–21. doi: 10.1016/j.xfss.2022.07.004

188. Cohen J, Scott R, Alikani M, Schimmel T, Munné S, Levron J, et al. Ooplasmic transfer in mature human oocyte. *Mol Hum Reprod*. (1998) 4:269–80. doi: 10.1093/molehr/4.3.269

189. Chen SH, Pascale C, Jackson M, Szvetecz MA, Cohen J. A limited survey-based uncontrolled follow-up study of children born after ooplasmic transplantation in a single centre. *Reprod BioMed Online*. (2016) 33:737–44. doi: 10.1016/j.rbmo.2016.10.003

190. Barritt JA, Brenner CA, Malter HE, Cohen J. Mitochondria in human offspring derived from ooplasmic transplantation. *Hum Reprod*. (2001) 16:513–6. doi: 10.1093/humrep/16.3.513

191. Tachibana M, Amato P, Sparman M, Woodward J, Sanchis DM, Ma H, et al. Towards germline gene therapy of inherited mitochondrial diseases. *Nature*. (2013) 493:627–31. doi: 10.1038/nature11647

192. Costa-Borges N, Nikitos E, Späth K, Miguel-Escalada I, Ma H, Rink K, et al. First pilot study of maternal spindle transfer for the treatment of repeated in *vitro* fertilization failures in couples with idiopathic infertility. *Fertil Steril*. (2023) 119:964–73. doi: 10.1016/j.fertnstert.2023.02.008

193. Latorre-Pellicer A, Lechuga-Vieco AV, Johnston IG, Hämäläinen RH, Pellico J, Justo-Méndez R, et al. Regulation of mother-to-offspring transmission of mtDNA heteroplasmy. *Cell Metab*. (2019) 30:1120–1130.e5. doi: 10.1016/j.cmet.2019.09.007

194. Tang M, Popovic M, Stamatiadis P, van der Jeught M, Van Coster R, Deforce D, et al. Germline nuclear transfer in mice may rescue poor embryo development associated with advanced maternal age and early embryo arrest. *Hum Reprod*. (2020) 35:1562–77. doi: 10.1093/humrep/deaa112

195. Costa-Borges N, Spath K, Miguel-Escalada I, Mestres E, Balmaseda R, Serafín A, et al. Maternal spindle transfer overcomes embryo developmental arrest caused by ooplasmic defects in mice. *Elife*. (2020) 9:e48591. doi: 10.7554/eLife.48591

196. Hyslop LA, Blakeley P, Craven L, Richardson J, Fogarty NM, Fragouli E, et al. Towards clinical application of pronuclear transfer to prevent mitochondrial DNA disease. *Nature*. (2016) 534:383–6. doi: 10.1038/nature18303

197. Ma H, O'Neil RC, Marti Gutierrez N, Hariharan M, Zhang ZZ, He Y, et al. Functional human oocyte generated by transfer of polar body genomes. *Cell Stem Cell*. (2017) 20:112–9. doi: 10.1016/j.stem.2016.10.001

198. Tang M, Guggilla RR, Gansemans Y, van der Jeught M, Boel A, Popovic M, et al. Comparative analysis of different nuclear transfer techniques to prevent the transmission of mitochondrial DNA variants. *Mol Hum Reprod*. (2019) 25:797–810. doi: 10.1093/molehr/gaz062

199. Zhang J, Yin H, Jiang H, Du X, Yang Z. The protective effects of human umbilical cord mesenchymal stem cell-derived extracellular vesicles on cisplatin-damaged granulosa cells. *Taiwan J Obstet Gynecol*. (2020) 59:527–33. doi: 10.1016/j.tjog.2020.05.010

200. Ding C, Qian C, Hou S, Lu J, Zou Q, Li H, et al. Exosomal miRNA-320a Is Released from hAMSCs and Regulates SIRT4 to Prevent Reactive Oxygen Species

Generation in POI. *Mol Ther Nucleic Acids*. (2020) 21:37–50. doi: 10.1016/j.omtn.2020.05.013

201. Zhang Q, Sun J, Huang Y, Bu S, Guo Y, Gu T, et al. Human amniotic epithelial cell-derived exosomes restore ovarian function by transferring microRNAs against apoptosis. *Mol Ther Nucleic Acids*. (2019) 16:407–18. doi: 10.1016/j.omtn.2019.03.008

202. Thabet E, Yusuf A, Abdelmonsif DA, Nabil I, Mourad G, Mehanna RA. Extracellular vesicles miRNA-21: a potential therapeutic tool in premature ovarian dysfunction. *Mol Hum Reprod*. (2020) 26:906–19. doi: 10.1093/molehr/gaaa068

203. Shojafar E, Mehranjani MS, Shariatzadeh SM. Utilizing platelet-rich fibrin bioscaffold at the graft site improves the structure and function of mice ovarian grafts. *Regener Med*. (2019) 14:409–22. doi: 10.2217/rme-2018-0050

204. Ogino M, Tsubamoto H, Sakata K, Oohama N, Hayakawa H, Kojima T, et al. Mitochondrial DNA copy number in cumulus cells is a strong predictor of obtaining good-quality embryos after IVF. *J Assist Reprod Genet*. (2016) 33:367–71. doi: 10.1007/s10815-015-0621-0

205. Desquiret-Dumas V, Clément A, Seegers V, Boucret L, Ferré-L'Hotellier V, Bouet PE, et al. The mitochondrial DNA content of cumulus granulosa cells is linked to embryo quality. *Hum Reprod*. (2017) 32:607–14. doi: 10.1093/humrep/dew341

206. Rahmawati P, Wiweko B, Boediono A. Mitochondrial DNA copy number in cumulus granulosa cells as a predictor for embryo morphokinetics and chromosome status. *Syst Biol Reprod Med*. (2023) 69:101–11. doi: 10.1080/19396368.2022.2145248

207. Chuang TH, Chen CY, Kuan CS, Lai HH, Hsieh CL, Lee MJ, et al. Reduced mitochondrial DNA content correlate with poor clinical outcomes in cryotransfers with day 6 single euploid embryos. *Front Endocrinol (Lausanne)*. (2023) 13:1066530. doi: 10.3389/fendo.2022.1066530

208. Trifunovic A, Wredenberg A, Falkenberg M, Spelbrink JN, Rovio AT, Bruder CE, et al. Premature ageing in mice expressing defective mitochondrial DNA polymerase. *Nature*. (2004) 429:417–23. doi: 10.1038/nature02517

209. Bowolaksono A, Sundari AM, Fauzi M, Maidarti M, Wiweko B, Mutia K, et al. Anti-Müllerian hormone independently affect mtDNA copy number in human granulosa cells. *J Ovarian Res*. (2022) 15:111. doi: 10.1186/s13048-022-01047-4

210. Pasquariello R, Ermisch AF, Silva E, McCormick S, Logsdon D, Barfield JP, et al. Alterations in oocyte mitochondrial number and function are related to spindle defects and occur with maternal aging in mice and humans†. *Biol Reprod*. (2019) 100:971–81. doi: 10.1093/biolre/ioy248

211. Baumann CG, Morris DG, Sreenan JM, Leese HJ. The quiet embryo hypothesis: molecular characteristics favoring viability. *Mol Reprod Dev*. (2007) 74:1345–53. doi: 10.1002/mrd.20604

212. Morimoto N, Hashimoto S, Yamanaka M, Nakano T, Satoh M, Nakaoka Y, et al. Mitochondrial oxygen consumption rate of human embryos declines with maternal age. *J Assist Reprod Genet*. (2020) 37:1815–21. doi: 10.1007/s10815-020-01869-5

213. Hashimoto S, Morimoto N, Yamanaka M, Matsumoto H, Yamochi T, Goto H, et al. Quantitative and qualitative changes of mitochondria in human preimplantation embryos. *J Assist Reprod Genet*. (2017) 34:573–80. doi: 10.1007/s10815-017-0886-6

214. Li J, Zhang J, Hou W, Yang X, Liu X, Zhang Y, et al. Metabolic control of histone acetylation for precise and timely regulation of minor ZGA in early mammalian embryos. *Cell Discovery*. (2022) 8:96. doi: 10.1038/s41421-022-00440-z

215. Fragouli E, Spath K, Alfarawati S, Kaper F, Craig A, Michel CE, et al. Altered levels of mitochondrial DNA are associated with female age, aneuploidy, and provide an independent measure of embryonic implantation potential. *PloS Genet*. (2015) 11:e1005241. doi: 10.1371/journal.pgen.1005241

216. Lukaszuk K, Podolak A. Does trophectoderm mitochondrial DNA content affect embryo developmental and implantation potential? *Int J Mol Sci*. (2022) 23:5976. doi: 10.3390/ijms23115976

217. Ravichandran K, McCaffrey C, Grifo J, Morales A, Perloe M, Munne S, et al. Mitochondrial DNA quantification as a tool for embryo viability assessment: retrospective analysis of data from single euploid blastocyst transfers. *Hum Reprod*. (2017) 32:1282–92. doi: 10.1093/humrep/dex070

218. Fragouli E, McCaffrey C, Ravichandran K, Spath K, Grifo JA, Munné S, et al. Clinical implications of mitochondrial DNA quantification on pregnancy outcomes: a blinded prospective non-selection study. *Hum Reprod*. (2017) 32:2340–7. doi: 10.1093/humrep/dex292

219. Wu FS, Weng SP, Shen MS, Ma PC, Wu PK, Lee NC. Suboptimal trophectoderm mitochondrial DNA level is associated with delayed blastocyst development. *J Assist Reprod Genet*. (2021) 38:587–94. doi: 10.1007/s10815-020-02045-5

220. Ritu G, Veerasigamani G, Ashraf MC, Singh S, Laheri S, Colaco S, et al. Mitochondrial DNA levels in trophectodermal cells show no association with blastocyst development and pregnancy outcomes. *J Hum Reprod Sci*. (2022) 15:82–9. doi: 10.4103/jhrs.jhrs_103_21

221. Liu S, Li Y, Gao X, Yan JH, Chen ZJ. Changes in the distribution of mitochondria before and after in *vitro* maturation of human oocyte and the effect of in *vitro* maturation on mitochondria distribution. *Fertil Steril*. (2010) 93:1550–5. doi: 10.1016/j.fertnstert.2009.03.050

222. Bianchi S, Macchiarelli G, Micara G, Linari A, Boninsegna C, Aragona C, et al. Ultrastructural markers of quality are impaired in human metaphase II aged oocyte: a comparison between reproductive and in *vitro* aging. *J Assist Reprod Genet*. (2015) 32:1343–58. doi: 10.1007/s10815-015-0552-9

223. Motta PM, Nottola SA, Makabe S, Heyn R. Mitochondrial morphology in human fetal and adult female germ cells. *Hum Reprod*. (2000) 15 Suppl 2:129–47. doi: 10.1093/humrep/15.suppl_2.129

224. Dumollard R, Duchen M, Carroll J. The role of mitochondrial function in the oocyte and embryo. *Curr Top Dev Biol*. (2007) 77:21–49. doi: 10.1016/S0070-2153(06)77002-8

225. Nikiforaki D, Vanden Meerschaut F, Qian C, De Croo I, Lu Y, Deroo T, et al. Oocyte cryopreservation and in *vitro* culture affect calcium signalling during human fertilization. *Hum Reprod*. (2014) 29:29–40. doi: 10.1093/humrep/det404

226. Shi W, Xu B, Wu LM, Jin RT, Luan HB, Luo LH, et al. Oocyte with a dark zona pellucida demonstrate lower fertilization, implantation and clinical pregnancy rates in IVF/ICSI cycles. *PloS One*. (2014) 9:e89409. doi: 10.1371/journal.pone.0089409

227. Smeets HJ. Preventing the transmission of mitochondrial DNA disorders: selecting the good guys or kicking out the bad guys. *Reprod BioMed Online*. (2013) 27:599–610. doi: 10.1016/j.rbmo.2013.08.007

228. Tong J, Sheng S, Sun Y, Li H, Li WP, Zhang C, et al. Melatonin levels in follicular fluid as markers for IVF outcomes and predicting ovarian reserve. *Reproduction*. (2017) 153:443–51. doi: 10.1530/REP-16-0641

229. Li X, Mu Y, Elshewy N, Ding D, Zou H, Chen B, et al. Comparison of IVF and IVM outcomes in the same patient treated with a modified IVM protocol along with an oocyte-maturing system containing melatonin: A pilot study. *Life Sci*. (2021) 264:118706. doi: 10.1016/j.lfs.2020.118706

230. Bao Z, Li G, Wang R, Xue S, Zeng Y, Deng S. Melatonin improves quality of repeated-poor and frozen-thawed embryos in human, a prospective clinical trial. *Front Endocrinol (Lausanne)*. (2022) 13:853999. doi: 10.3389/fendo.2022.853999

231. Zhu Q, Wang K, Zhang C, Chen B, Zou H, Zou W, et al. Effect of melatonin on the clinical outcome of patients with repeated cycles after failed cycles of in *vitro* fertilization and intracytoplasmic sperm injection. *Zygote*. (2022) 30:471–9. doi: 10.1017/S0967199421000770

232. Morimoto N, Hashimoto S, Yamanaka M, Satoh M, Nakaoka Y, Fukui A, et al. Treatment with Laevo (L)-carnitine reverses the mitochondrial function of human embryos. *J Assist Reprod Genet*. (2021) 38:71–8. doi: 10.1007/s10815-020-01973-6

233. Xu Y, Nisenblat V, Lu C, Li R, Qiao J, Zhen X, et al. Pretreatment with coenzyme Q10 improves ovarian response and embryo quality in low-prognosis young women with decreased ovarian reserve: a randomized controlled trial. *Reprod Biol Endocrinol*. (2018) 16:29. doi: 10.1186/s12958-018-0343-0

234. Giannubilo SR, Orlando P, Silvestri S, Cirilli I, Marcheggiani F, Ciavattini A, et al. CoQ10 supplementation in patients undergoing IVF-ET: the relationship with follicular fluid content and oocyte maturity. *Antioxid (Basel)*. (2018) 7:141. doi: 10.3390/antiox7100141

235. Tamura H, Takasaki A, Miwa I, Taniguchi K, Maekawa R, Asada H, et al. Oxidative stress impairs oocyte quality and melatonin protects oocyte from free radical damage and improves fertilization rate. *J Pineal Res*. (2008) 44:280–7. doi: 10.1111/j.1600-079X.2007.00524.x

236. Hosseini FS, Shamsipour M, Yazdekhasti H, Akbari-Asbagh F, Shahraki Z, Aghaee-Bakhtiari SH. The effect of oral melatonin supplementation on MT-ATP6 gene expression and IVF outcomes in Iranian infertile couples: a nonrandomized controlled trial. *Naunyn Schmiedebergs Arch Pharmacol*. (2021) 394:1487–95. doi: 10.1007/s00210-021-02071-9

237. Kitano Y, Hashimoto S, Matsumoto H, Yamochi T, Yamanaka M, Nakaoka Y, et al. Oral administration of l-carnitine improves the clinical outcome of fertility in patients with IVF treatment. *Gynecol Endocrinol*. (2018) 34:684–8. doi: 10.1080/09513590.2018.1431769

238. Battaglia R, Caponnetto A, Caringella AM, Cortone A, Ferrara C, Smirni S, et al. Resveratrol treatment induces mito-miRNome modification in follicular fluid from aged women with a poor prognosis for *in vitro* fertilization cycles. *Antioxid (Basel)*. (2022) 11:1019. doi: 10.3390/antiox11051019

239. Ochiai A, Kuroda K, Ikemoto Y, Ozaki R, Nakagawa K, Nojiri S, et al. Influence of resveratrol supplementation on IVF-embryo transfer cycle outcomes. *Reprod BioMed Online*. (2019) 39:205–10. doi: 10.1016/j.rbmo.2019.03.205

240. Schimmel MS, Bromiker R, Hammerman C, Chertman L, Ioscovich A, Granovsky-Grisaru S, et al. The effects of maternal age and parity on maternal and neonatal outcome. *Arch Gynecol Obstet*. (2015) 291:793–8. doi: 10.1007/s00404-014-3469-0

241. Al-Shaikh GK, Ibrahim GH, Fayed AA, Al-Mandeel H. Grand multiparity and the possible risk of adverse maternal and neonatal outcomes: a dilemma to be deciphered. *BMC Pregnancy Childbirth*. (2017) 17:310. doi: 10.1186/s12884-017-1508-0

242. Islam MM, Bakheit CS. Advanced maternal age and risks for adverse pregnancy outcomes: A population-based study in Oman. *Health Care Women Int*. (2015) 36:1081–103. doi: 10.1080/07399332.2014.990560

243. Morino H, Pierce SB, Matsuda Y, Walsh T, Ohsawa R, Newby M, et al. Mutations in Twinkle primase-helicase cause Perrault syndrome with neurologic features. *Neurology*. (2014) 83:2054–61. doi: 10.1212/WNL.0000000000001036

244. Pang L, Yu W, Lv J, Dou Y, Zhao H, Li S, et al. Air pollution exposure and ovarian reserve impairment in Shandong province, China: The effects of particulate

matter size and exposure window. *Environ Res*. (2023) 218:115056. doi: 10.1016/j.envres.2022.115056

245. Levine L, Hall JE. Does the environment affect menopause? A review of the effects of endocrine disrupting chemicals on menopause. *Climacteric*. (2023) 26:206–15. doi: 10.1080/13697137.2023.2173570

246. Gaskins AJ, Hood RB, Ford JB, Hauser R, Knight AK, Smith AK, et al. Traffic-related air pollution and supplemental folic acid intake in relation to DNA methylation in granulosa cells. *Clin Epigene*. (2023) 15:84. doi: 10.1186/s13148-023-01503-y

247. Damman CJ. Perspective: nutrition's next chapter - bioactive gaps and the microbiome-mitochondria axis. *Adv Nutr*. (2023) 14:420–5. doi: 10.1016/j.advnut.2023.03.016

248. Neto IVS, Pinto AP, Muñoz VR, de Cássia Marqueti R, Pauli JR, Ropelle ER, et al. Pleiotropic and multi-systemic actions of physical exercise on PGC-1α signaling during the aging process. *Ageing Res Rev*. (2023) 87:101935. doi: 10.1016/j.arr.2023.101935

249. Okt Ma L, Cai L, Hu M, Wang J, Xie J, Xing Y, et al. Coenzyme Q10 supplementation of human oocyte in *vitro* maturation reduces postmeiotic aneuploidies. *Fertil Steril*. (2020) 114:331–7. doi: 10.1016/j.fertnstert.2020.04.002

Glossary

assisted reproductive technology	ART
in vitro fertilization	IVF
intracytoplasmic sperm injection	ICSI
preimplantation genetic testing	PGT
preimplantation genetic testing for aneuploidy	PGT-A
embryo transfer	ET
in vitro maturation	IVM
in vitro aging	IVA
diminished ovarian reserve	DOR
premature ovarian insufficiency	POI
premature ovarian failure	POF
follicle-stimulating hormone	FSH
anti-Mullerian hormone	AMH
germinal vesicle	GV
cumulus oocyte complex	COC
granulosa cells	GCs
cumulus cells	CCs
mitochondrial DNA	mtDNA
tricarboxylic acid	TCA
oxidative stress	OS
oxidative phosphorylation	OXPHOS
nicotinamide adenine dinucleotide	NADH
flavin adenine dinucleotide	FADH2
adenosine triphosphate	ATP
guanosine triphosphate	GTP
reactive oxygen species	ROS
reactive nitrogen species	RNS
electron transport chain	ETC
mitochondrial unfolded protein response	UPRmt
oogonial precursor cells	OPCs
cytoplasmic metastasis	CT
nuclear transfer	NT
spindle transfer	ST
pronuclear transfer	PNT
polar body transfer	PBT
mitochondrial membrane potential	MMP
mitochondria-vesicle	MV
mitochondria-smooth endoplasmic reticulum	M-SER

frontiers | Frontiers in Endocrinology

TYPE Systematic Review
PUBLISHED 11 July 2024
DOI 10.3389/fendo.2024.1361573

OPEN ACCESS

EDITED BY
Antonio Simone Laganà,
University of Palermo, Italy

REVIEWED BY
Michał Kunicki,
Medical University of Warsaw, Poland
Jian Liu,
Guangdong Provincial Hospital of Chinese Medicine, China

*CORRESPONDENCE
Lianwei Xu
xu_lianwei2800@shutcm.edu.cn

RECEIVED 26 December 2023
ACCEPTED 01 May 2024
PUBLISHED 11 July 2024

CITATION
Cao H, Li H, Lin G, Li X, Liu S, Li P, Cong C and Xu L (2024) The clinical value of acupuncture for women with premature ovarian insufficiency: a systematic review and meta-analysis of randomized controlled trials. *Front. Endocrinol.* 15:1361573. doi: 10.3389/fendo.2024.1361573

The clinical value of acupuncture for women with premature ovarian insufficiency: a systematic review and meta-analysis of randomized controlled trials

Hengjie Cao[1], Huize Li[2], Guangyao Lin[1], Xuanling Li[1], Shimin Liu[2], Peiqi Li[2], Chao Cong[1] and Lianwei Xu[1]*

[1]Department of Gynecology, Longhua Hospital, Shanghai University of Traditional Chinese Medicine, Shanghai, China, [2]School of Acupuncture-Moxibustion and Tuina, Shanghai University of Traditional Chinese Medicine, Shanghai, China

Objective: The aim of this study was to evaluate the therapeutic implications of acupuncture on improving ovarian function in women diagnosed with premature ovarian insufficiency (POI) through the implementation of randomized clinical trials (RCTs).

Methods: A comprehensive search of eight databases was conducted to identify RCTs up until 5 October 2023. The outcomes included the levels of sex hormones, antral follicle count (AFC), Kupperman score, and total effective rate. The risk of bias (RoB) tool was utilized to evaluate the quality of the included studies. In order to guarantee the robustness and reliability of the findings, subgroup and sensitivity analyses were performed to investigate potential sources of heterogeneity.

Results: A total of 13 RCTs comprising 775 patients were included in the study. Acupuncture demonstrated significant efficacy in reducing follicle-stimulating hormone (FSH) [SMD = 0.83, 95% CI (0.27, 1.39), I^2 = 92%, p = 0.004], enhancing estradiol levels (E_2) [SMD = 0.50, 95% CI (0.07, 0.93), p = 0.02, I^2 = 87%], and increasing anti-Müllerian hormone (AMH) [SMD = 0.24, 95% CI (0.05, 0.44), p = 0.01, I^2 = 8%], as well as improving the overall effective rate [RR = 1.22, 95% CI (1.10, 1.35), p < 0.01, I^2 = 14%]. Subgroup analysis revealed that compared with non-acupuncture therapy, the acupuncture with Chinese herbal medicine (CHM) and hormone replacement therapy (HRT) group exhibited a substantial reduction in FSH levels [SMD = 1.02, 95% CI (0.52, 1.51), I^2 = 60%, p < 0.01]. Furthermore, the acupuncture with CHM group also exhibited a substantial reduction [SMD = 4.59, 95% CI (1.53, 7.65), I^2 = 98%, p < 0.01]. However, only the acupuncture with CHM and HRT group demonstrated a significant increase in E_2 levels [SMD = 0.55, 95% CI (0.23, 0.87), I^2 = 12%, p < 0.01].

Conclusion: Acupuncture has demonstrated superiority over non-acupuncture in diminishing serum FSH levels and increasing serum E_2, AMH, and the overall efficacy rate in women diagnosed with POI. These research findings suggest the

necessity for broader-scale research with meticulous designs to fully demonstrate the efficacy and safety of acupuncture in the treatment of women with POI.

Systematic review registration: https://www.crd.york.ac.uk, identifier CRD42023467751.

KEYWORDS

premature ovarian insufficiency, acupuncture, randomized controlled trials, meta-analysis, review

1 Introduction

Premature ovarian insufficiency (POI) is a syndrome characterized by ovarian hypofunction occurring prior to the age of 40, with an approximate incidence of 1% (1). Various factors including genetic (2, 3), immunological, viral, iatrogenic (4, 5), and environmental factors are common contributors to POI, with over 50% of patients encountering an etiology that remains undetermined (6). Irregular menstruation is a common manifestation in POI patients, presenting as oligomenorrhea or amenorrhea persisting for ≥4 months. The condition is characterized by elevated levels of gonadotropins and reduced estradiol, ultimately leading to a decrease in reproductive capacity. Symptoms of POI encompass hot flashes, perspiration, reduced libido, bone rarefaction, metabolic disturbances, and other repercussions. It not only impacts fertility, mental health, and quality of life but also exerts influence on various systems, including skeletal, cardiovascular, urogenital, and nervous systems among others (6–8). The concept of POI was introduced in 2008 (9), but its diagnosis has always lacked a precise criterion. In 2016, the European Society for Human Reproduction and Embryology (ESHRE) lowered the cutoff point for follicle-stimulating hormone (FSH) in early-onset ovarian insufficiency to 25 IU/L. This adjustment has drawn attention to POI, differentiating it from premature ovarian failure (POF).

Common treatments for POI encompass hormone replacement therapy (HRT), selenium and vitamin E supplementation, exercise therapy, and more (7). HRT is sequential estrogen–progesterone therapy with progesterone supplementation for 10 to 14 days per month in addition to continuous estrogen use. HRT stands as the recommended standard protocol for individuals with POI to alleviate symptoms of low estrogen (10, 11). Additionally, HRT has the potential to prevent cardiovascular diseases and bone rarefaction. However, this therapy has limitations as it cannot enhance ovarian activity, and breast cancer is a contraindication (12). Oral hormone therapy may elevate the risk of hypertension in women (13). Furthermore, judicious assessment is imperative for the use of HRT in POI patients with conditions such as SLE, gallbladder disorders, epilepsy, or asthma (6, 14, 15). A novel therapy known as *in-vitro* activation of follicles has been introduced, with a limited number of clinical pregnancy reports; however, its efficiency falls below the optimal level (16–18). Advanced treatments, including immunotherapy, stem cells, and gene editing, are currently in the research stage (19, 20).

Acupuncture, regarded as a traditional Chinese non-pharmacological intervention, has demonstrated promising outcomes, a high degree of safety, and minimal adverse effects. It is widely utilized in the field of reproductive endocrinology (21, 22). Recently, there has been a surge in randomized controlled trials investigating the efficacy of acupuncture for POI. It is imperative to integrate and systematically evaluate these research findings. Given the revised diagnostic criteria for POI by ESHRE in 2016 and the limited attention to the impact of acupuncture on the subset of POI patients with FSH >25 IU/L, a meta-analysis and systematic evaluation of existing data were conducted to furnish a pertinent reference for clinical practice.

2 Materials and methods

The Preferred Reporting Items for Systematic Reviews and Meta-Analyses guidelines (23) were followed in the reporting of this systematic review and meta-analysis (PROSPERO registration No. CRD42023467751).

2.1 Search strategy and study selection

Eight databases were comprehensively searched, namely, the English-language databases Cochrane Library, Web of Science, EMBASE, and PubMed and the Chinese-language databases Wanfang, VIP Information, CBM, and China National Knowledge Infrastructure (CNKI) from inception up to October 2023. Our retrieval strategy comprised three main components: clinical conditions (including premature ovarian failure, primary ovarian failure, primary ovarian insufficiency, premature ovarian insufficiency, premature menopause, POI, POF), interventions (such as acupuncture, electroacupuncture, manual acupuncture,

warming needle, acupuncture therapy, needling, needles, needle therapy), and study types (RCT). No retrieval filters or limits were applied. To identify redundant papers, researchers manually examined the reference summaries of the retrieved articles. The initial screening of articles, independently conducted by the first two authors (H.J.C. and H.Z.L.), involved a thorough review of titles, abstracts, or full text to substantiate the eligibility of the studies. Any uncertainties regarding inclusion were deliberated among the other authors (L.W.X and S.M.L).

2.2 Inclusion and exclusion criteria

Studies that met the following criteria were included: 1) subjects: the standard of diagnosis was based on the clinical recommendations for the treatment of POI patients presented by ESHRE in 2016: a) women under 40 years old with amenorrhea/oligomenorrhea or symptoms of estrogen deficiency, b) oligomenorrhea or amenorrhea persisting for ≥4 months, and c) FSH level >25 IU/L on two occasions with a gap of >4 weeks; 2) intervention: acupuncture (including manual acupuncture and electroacupuncture regardless of the level of needling techniques), as well as the singular or combined use of Chinese herbal medicine or (and) HRT. Studies would be included if acupuncture was regarded as an adjuvant therapy for POI, and there were similar concomitant treatments between the experimental group and the control group; 3) controlled method: HRT, Chinese herbal medicine, or a combination of HRT and Chinese herbal medicine; 4) outcome indicators with sufficient data: effective rate, FSH, LH, E_2, AMH, etc. Blood tests were performed before and after treatment, respectively, on the second to fourth days of the menstrual cycle to evaluate the basic hormone levels during the cycle; 5) study type: RCT; and 6) availability of complete data in the literature and precise data in the experimental and control groups.

Studies that met the following criteria were excluded: 1) interventions without acupuncture treatment (e.g., massage, moxibustion, or electrostimulation without needle); 2) interventions of control groups receiving different acupuncture treatments (e.g., acupoint catgut embedding); 3) patients suffering from other endocrine diseases (e.g., polycystic ovary syndrome, thyroid dysfunction, and hyperprolactinemia); 4) lack of definite or self-made criteria for efficacy evaluation; 5) studies about animal experiments, commentaries, editorials, experience introductions, conference articles, reviews, graduation theses, and case reports; 6) duplicate publication; 7) literature with incomplete outcome index data or full texts that cannot be obtained; and 8) literature with incorrect data and unidentified authors.

2.3 Data extraction and quality evaluation

Two authors, H.J.C. and H.Z.L., independently extracted relevant data using a standardized form. Information regarding the characteristics of the study population (such as sample size, age, and disease duration), treatment specifics (including types of interventions, acupoints, and duration), and group-wise results was collected.

Meanwhile, the quality assessment of the included studies was carried out by two independent reviewers (H.J.C. and H.Z.L.) utilizing the Cochrane Collaboration's Risk of Bias tool. Any discrepancies were resolved through discussion with L.W.X.

The STRICTA (Standards for Reporting Interventions in Controlled Trials of Acupuncture: the STRICTA recommendations) (24) standard was used to evaluate acupuncture intervention measures. A response is considered "positive" by the STRICTA standard if every item is fully recorded. There were three categories for the reporting rate (N = reported RCTs/13): high ($N \geq 80\%$), moderate ($N = 50\%–80\%$), and low ($N < 50\%$).

2.4 Statistical analysis

The data management software RevMan 5.3 was employed for data organization. Each group's mean and standard deviation of the pretreatment and posttreatment results was collected. Continuous data were measured using the mean difference (MD) or standardized mean difference (SMD) with 95% confidence intervals (CIs). The following formula was used to figure out the D-value of the statistical mean and standard deviation: $S * S = S1 * S1 + S2 * S2 - 2 * R * S1 * S2$; $D = M1 - M2$ (D-value, difference before and after treatment; S, standard deviation of D-value; S1 and S2, standard deviation before and after treatment, respectively; M1 and M2, mean value before and after treatment; $R = 0.4$) (25). Statistical significance was established at $p < 0.05$ on both sides. Dichotomous variables, such as the total effective rate, were presented as the risk ratio (RR). Additionally, I^2 statistics were utilized to assess interstudy heterogeneity. In cases of non-significant heterogeneity, we adopted the fixed-effects model; otherwise, the random-effects model was employed. A subgroup analysis based on the type of intervention was conducted to explore potential sources of heterogeneity. If a meta-analysis was considered inappropriate, we would offer a qualitative description of the results. To ensure result stability, a sensitivity analysis was performed by excluding specific studies. Moreover, if at least 10 studies were included, Begg's tests and funnel plots were adopted by evaluating the p-value for publication bias.

3 Results

3.1 Included articles

Figure 1 illustrates the flowchart utilized for selecting publications. Initial database searches yielded 741 papers related to the therapeutic efficacy of acupuncture therapy in the treatment of premature ovarian insufficiency. After removing 391 duplicate publications, 350 pieces of literature remained. Upon reviewing the titles and abstracts among the remaining studies, 319 papers were excluded for failing to meet the inclusion criteria. Subsequently, 18 additional studies were excluded due to non-compliance with POI

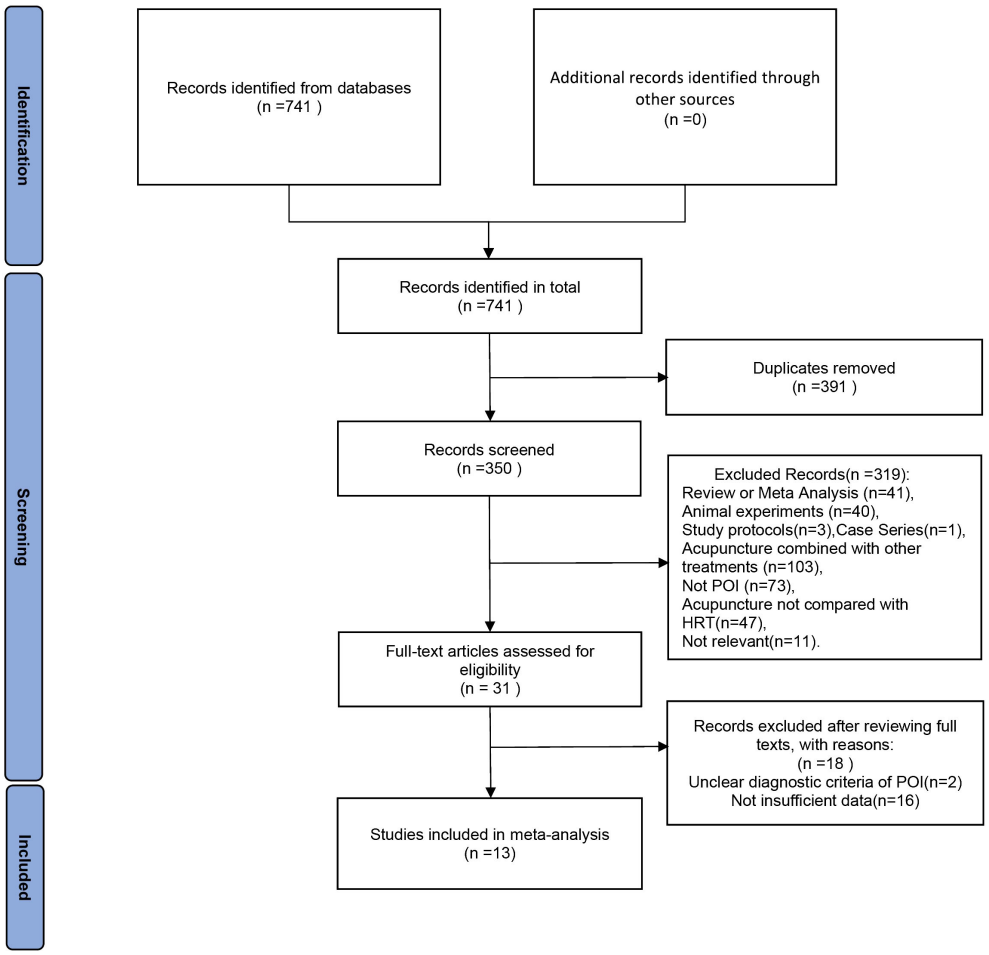

FIGURE 1
The PRISMA flowchart.

diagnostic criteria or insufficient data for evaluation. Finally, the meta-analysis included 13 RCTs published between 2019 and 2023.

3.2 Study characteristics

We incorporated 13 RCTs, all conducted in China and published in Chinese between 2019 and 2023. The studies encompassed 775 POI patients, divided into an experimental group (acupuncture group) and a control group, with 388 and 387 cases, respectively. In the studies, blood samples were collected on days 2–4 of the menstrual cycle to assess baseline sex hormone indices. Twelve of the studies collected blood samples before and after the last treatment, while the other study (26) collected blood samples before treatment and 3 months after the cessation of treatment, respectively. Among them, 13 reported FSH levels (26–38), 12 reported LH and E_2 levels (26–33, 35–38), 8 reported AMH levels (26, 27, 31–33, 35–37), 5 trials reported the total effective rate (26, 30–32, 35), and 9 presented adverse events (26, 27, 29–33, 35, 38). Baseline homogeneity was observed across all RCTs. Comprehensive details on the characteristics of the study are shown in Table 1.

3.3 Quality assessment

Except for Song (31), the methodological quality of all studies regarding selection bias was assessed as low risk due to clear procedures and concealed allocation in the patient randomization process. Given the inherent limitation that acupuncture therapy cannot be blinded, all included RCTs were categorized as “high risk” for participant and staff blinding. Incomplete outcome data and selective reporting were considered to pose a low risk of bias across all studies. Among the 13 studies, no indication of potential bias was identified (Figure 2). The quality of interventions reported was evaluated against the STRICTA list, with a mean reporting rate of 71.04% for all entries (Table 2). In summary, the quality of the included studies was considered moderate.

3.4 Outcome measurements

3.4.1 FSH levels

Thirteen studies reported FSH levels of 388 participants in the acupuncture group. Combining the results of these studies showed

10.3389/fendo.2024.1361573

TABLE 1 Study characteristics.

Study	Year	Sample size (*n*)	Age (years)		Disease duration (months)		Treatment regimen		Treatment frequency	Treatment duration (months)	Outcomes
		T/C	T	C	T	C	T	C			
Bai, (38)	2023	30/30	32.6 ± 5.8	30.8 ± 5.5	17.8 ± 7.3	16.1 ± 6.2	Acu.	HRT	5 times a week	3	①②③④⑤⑥
Liang, (37)	2022	32/30	33.56 ± 4.73	33.50 ± 4.69	NA	NA	Acu.+CHM +HRT	CHM +HRT	3 times a week	3	①②③
Zhuo, (36)	2021	40/40	34.52 ± 3.12	35.78 ± 3.27	15.6 ± 2.9	16.2 ± 3.3	Acu.+HRT	HRT	3 times a week	3	①②③④
Xu Qing, (35)	2021	30/30	33.90 ± 4.57	32.87 ± 4.86	11.07 ± 6.53	13.17 ± 6.61	Acu.+CHM	CHM	2 times a week	3	①②③④⑦
Xu Chengchao, (34)	2021	30/30	31 ± 4	29 ± 5	14.5 ± 6.0	12.2 ± 4.4	Acu.	HRT	5 times a week	3	①⑤
Liu, (33)	2021	21/22	34.36 ± 5.18	34.44 ± 5.92	20.52 ± 14.07	18.18 ± 10.37	Acu.	HRT	3 times a week	3	①②③④⑤⑥
Hui, (26)	2021	30/30	34 ± 3	34 ± 4	14.30 ± 2.36	14.25 ± 2.32	Acu.+HRT	HRT	3 times a week	3	①②③④⑥⑦
Zhang, (32)	2020	30/30	35.16 ± 3.32	36.50 ± 3.22	12.80 ± 9.03	10.86 ± 9.52	Acu.+CHM +HRT	CHM +HRT	3 times a week	3	①②③④⑦
Song, (31)	2020	30/30	34.60 ± 3.78	35.33 ± 2.99	13.00 ± 10.99	12.10 ± 10.08	Acu.+CHM +HRT	CHM +HRT	3 times a week	3	①②③④⑦
Qiu, (30)	2020	29/29	31.90 ± 4.21	32.24 ± 4.56	11.25 ± 5.56	10.89 ± 4.07	Acu.+HRT	HRT	3 times a week	3	①②③⑤⑦
Zhang, (29)	2019	25/25	31 ± 4	33 ± 4	19.2 ± 10.8	19.2 ± 9.6	Acu.	HRT	3 times a week	3	①②③
Qi, (28)	2019	30/30	31.15 ± 4.84	29.15 ± 4.86	40.56 ± 13.8	42 ± 14.52	Acu.+CHM	CHM	3 times a week	3	①②③⑥
Miao, (27)	2019	31/31	34.58 ± 0.76	34.10 ± 0.83	23.06 ± 2.18	22.39 ± 2.17	Acu.+CHM	CHM	3 times a week	3	①②③④

T, trial group; C, control group; NA, not available; Acu., acupuncture; CHM, Chinese herbal medicine; HRT, hormone replacement therapy; ① follicle-stimulating hormone (FSH); ② luteinizing hormone (LH); ③ estradiol (E_2); ④ anti-Müllerian hormone (AMH); ⑤ Kupperman score; ⑥ antral follicle count (AFC); ⑦ total effective rate.

that acupuncture dramatically reduced the levels of FSH in women with POI [SMD = 0.83, 95% CI (0.27, 1.39), I^2 = 92%, p = 0.004] (Figure 3). Sensitivity analysis was employed to confirm the robustness of the aggregated outcomes.

3.4.2 LH levels

Twelve studies involving 715 patients focused on the LH levels. Compared with the control groups, the acupuncture group had no advantage [SMD = 0.27, 95% CI (−0.02, 0.57), I^2 = 74%, p = 0.07] (Figure 4). The robustness of the combined findings was confirmed through sensitivity analysis.

3.4.3 Estradiol levels

The evaluation of the impact of acupuncture on estradiol levels yielded 12 RCTs with a total of 715 individuals. It showed a statistically significant connection between the function of acupuncture and the improvement in estradiol levels [SMD = 0.50, 95% CI (0.07, 0.93), I^2 = 87%, p = 0.02] (Figure 5). The

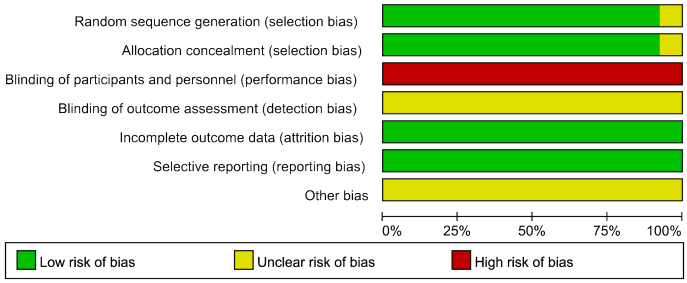

FIGURE 2
Risk of bias assessment.

TABLE 2 Quality evaluation based on the STRICTA list.

Items	Item details		Reported RCTs	%
1. Acupuncture rationale	1a	Style of acupuncture	13	100%
	1b	Reasoning for treatment provided	13	100%
	1c	Extent to which treatment was varied	0	0%
2. Details of needling	2a	Number of needle insertions per subject per session	13	100%
	2b	Names of points used	13	100%
	2c	Depth of insertion	11	85%
	2d	Response sought	8	62%
	2e	Needle stimulation	12	92%
	2f	Needle retention time	13	100%
	2g	Needle type	13	100%
3. Treatment regimen	3a	Number of treatment sessions	13	100%
	3b	Frequency and duration of treatment sessions	13	100%
4. Other components of treatment	4a	Details of other interventions administered to the acupuncture group	5	38%
	4b	Setting and context of treatment	3	23%
5. Practitioner background	5	Description of participating acupuncturists	0	0%
6. Control or comparator interventions	6a	Rationale for the control or comparator in the context of the research question,	13	100%
		with sources that justify this choice		
	6b	Precise description of the control or comparator	13	100%

(Continued)

pooled estimates remained unaffected by any individual study, as confirmed through the sensitivity analysis.

3.4.4 AMH levels

Among all studies, only eight studies reported the AMH levels. The heterogeneity dropped from 81% to 8% after the exclusion of one study (26) in the sensitivity analysis. The combined findings of seven trials with 212 individuals showed a significant increase in the AMH levels [SMD = 0.24, 95% CI (0.05, 0.44), I^2 = 8%, p = 0.01] (Figure 6).

3.4.5 KI score

Four studies reported the modified KI score (39). The results of the fixed-effects model analysis indicated that there was no statistically significant difference between the control group and the acupuncture therapy group [MD = 0.04, 95% CI (−1.71, 1.80), I^2 = 26%, p = 0.96] (Figure 7).

3.4.6 Antral follicle count

This meta-analysis of the antral follicle count (AFC) result contained 111 participants from a total of four studies. The pooled result revealed that the effects of acupuncture did not exhibit a significant difference from others [MD = 0.38, 95% CI (−0.73, 1.49), I^2 = 89, p = 0.50] (Figure 8). Furthermore, following the sensitivity analysis, the outcomes remained unchanged.

3.4.7 Total effective rate

Five studies assessed the overall effective rate (26, 30–32, 35), sticking to the same score scale including the menstrual cycle, menstrual blood volume, and general symptoms, such as palpitation and sleeplessness. Pretreatment and posttreatment evaluations were conducted, revealing a notable increase of 30% or more in symptom

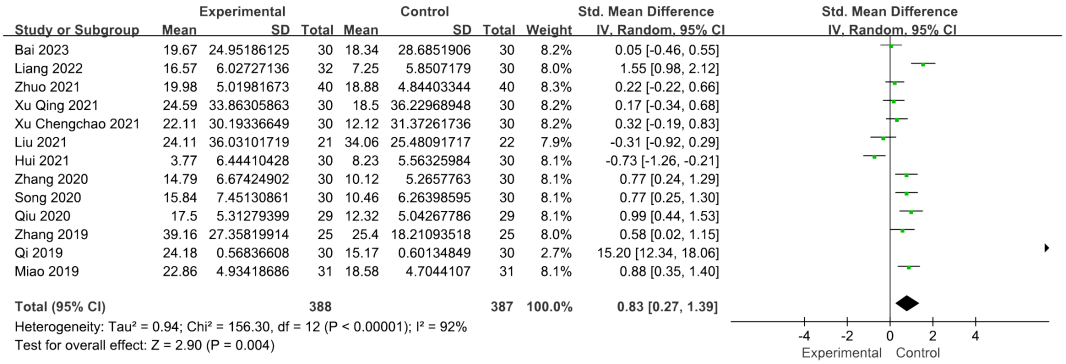

FIGURE 3
Forest plot illustrating the relationship between FSH levels and acupuncture therapy.

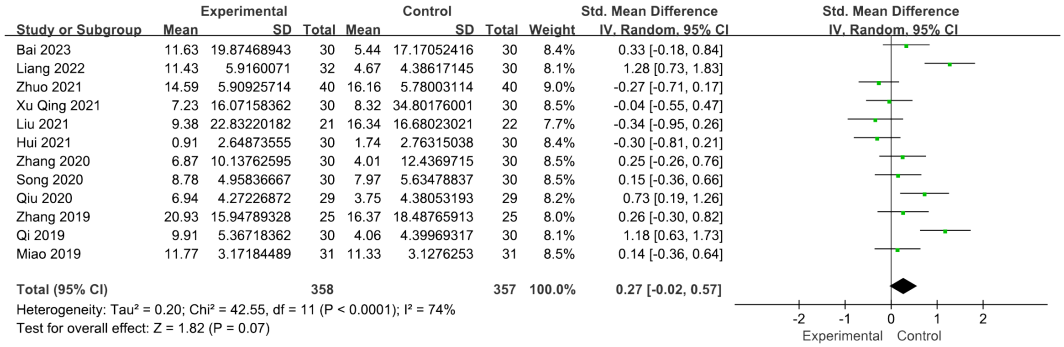

FIGURE 4
Forest plot illustrating the relationship between LH levels and acupuncture therapy.

amelioration, thereby indicating effectiveness. The study results indicated that patients who received acupuncture treatment had a higher overall effective rate compared with those who did not receive acupuncture treatment [RR = 1.22, 95% CI (1.10, 1.35), $I^2 = 14\%$, $p < 0.01$] (Figure 9). The figure revealed low heterogeneity.

3.4.8 Adverse effect

Nine of the thirteen studies reported the situation of adverse effects: five of them reported adverse effects (29, 31, 33, 35, 38), while the remaining four documented no adverse effects (26, 27, 30, 32). One study reporting abdominal distension was excluded due to insufficient detailed description (31), while the following statistics included eight studies (26, 27, 29, 30, 32, 33, 35, 38). Among 226 patients in the trial groups, 11 cases of adverse events were reported, consisting of nine cases of subcutaneous hemorrhage (33, 35, 38), one case of breast distending pain (29), and one case of needle sticking (35). In the control groups, 12 adverse events were reported in 227 patients, consisting of five cases of stomach discomfort (29, 33),

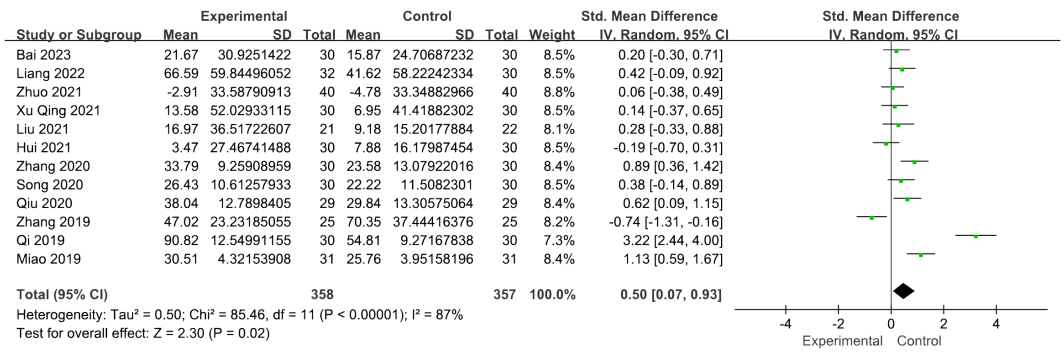

FIGURE 5
Forest plot illustrating the relationship between E_2 levels and acupuncture therapy.

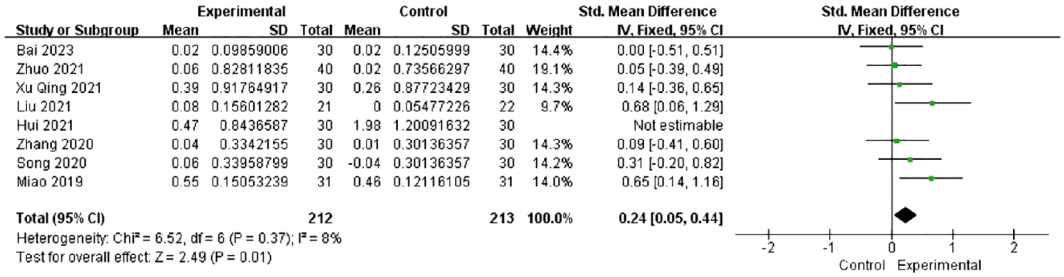

FIGURE 6
Forest plot illustrating the relationship between AMH levels and acupuncture therapy.

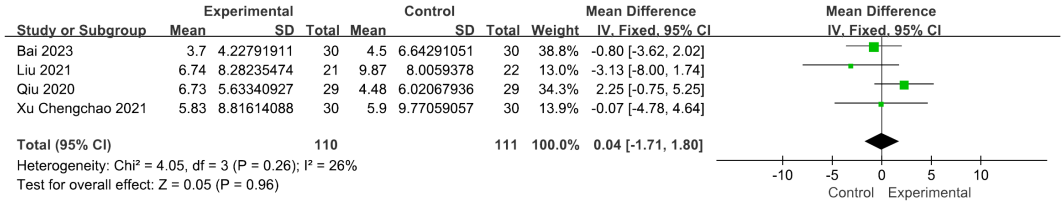

FIGURE 7
Forest plot illustrating the relationship between KI score and acupuncture therapy.

five cases of breast distending pain (29), and two episodes of menostaxis (38). Meta-analysis showed that the difference between the two groups lacks statistical significance ($p = 0.86 > 0.05$) (Figure 10).

3.5 Subgroup analysis

Due to three pooled results indicating significant heterogeneity ($I^2 > 60\%$) in the levels of FSH, LH, and estradiol, subgroup analysis was conducted based on various types of interventions.

3.5.1 FSH and LH levels

In the subgroup analysis for FSH levels, the pooled result revealed that both the acupuncture combined with CHM and HRT group [SMD = 1.02, 95% CI (0.52, 1.51), $I^2 = 60\%$, $p < 0.0001$] and the acupuncture with CHM group [SMD = 4.59, 95% CI (1.53, 7.65), $I^2 = 98\%$, $p = 0.003$] exhibited greater efficacy in lowering FSH levels compared with the non-acupuncture group (Figure 11). However, for the LH levels, no decrease in heterogeneity was observed during the subgroup analysis (Figure 12).

3.5.2 Estradiol levels

The meta-analysis indicated that the acupuncture with CHM and HRT group outperformed the control groups [SMD = 0.55, 95% CI (0.23, 0.87), $I^2 = 12\%$, $p = 0.0007$] (Figure 13). High-level heterogeneity was seen in the remaining three subcategories, including nine journals. Rather than using a meta-analysis, a qualitative description was employed. Out of the nine investigations, three (28–30) demonstrated an increase in estradiol levels of the trial groups following treatment, surpassing those of the control groups ($p < 0.05$). The remaining six (26, 27, 35–38) investigations revealed no difference between the two groups ($p > 0.05$).

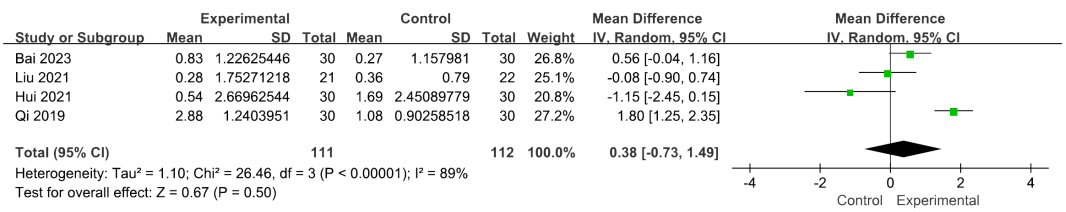

FIGURE 8
Forest plot illustrating the relationship between AFC and acupuncture therapy.

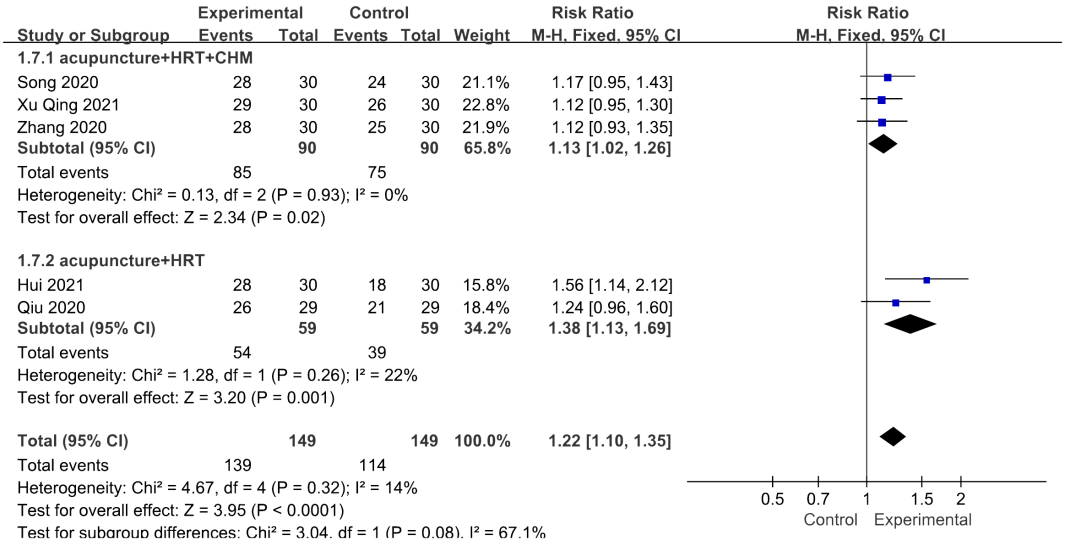

FIGURE 9
Forest plot illustrating the relationship between total effective rate and acupuncture therapy.

3.6 Publication bias

The presence of publication bias was assessed using Begg's tests, with a minimum of 10 studies being included in the analysis. There was no apparent asymmetry in the funnel plots, as shown in Figure 14. Begg's test for FSH (p = 0.06), LH (p = 0.06), and E_2 (p = 0.09) was not significant for publication bias in this meta-analysis due to p >0.05.

4 Discussion

This study represents the inaugural meta-analysis evaluating the clinical efficacy of acupuncture for POI, employing FSH >25 IU/L as the diagnostic criterion. In this investigation, we incorporated a total of 13 RCTs, involving 775 patients, to scrutinize the efficacy of acupuncture for POI. The findings are succinctly presented as follows: 1) sex hormones—acupuncture demonstrated a significant reduction in FSH levels and an increase in AMH and E_2 levels in POI patients, with negligible impact on LH levels. 2) Follicular development status—following the reduction of heterogeneity, acupuncture yielded a significant improvement in AMH levels, while no discernible difference was observed in AFC. 3) Climacteric symptoms—patients subjected to acupuncture exhibited a higher overall effective rate compared with their counterparts without acupuncture. However, the acupuncture group manifested no improvement in the Kupperman index, and the difference in adverse effects between the two groups lacked statistical significance.

FSH possesses the capability to enhance follicular development and stimulate estrogen secretion. Elevated FSH levels are associated with excessive follicular depletion, culminating in diminished follicular reserve. Lower FSH levels can enhance fertility probabilities. Serving as a biomarker of follicular development, estrogen not only protects the cardiovascular system and nerves but also prevents the risk of bone rarefaction. Addressing estrogen

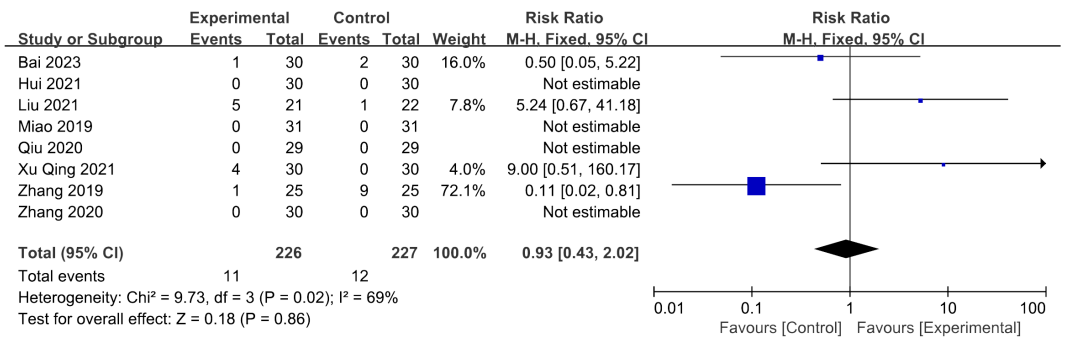

FIGURE 10
Forest plot illustrating the relationship between adverse effect and acupuncture therapy.

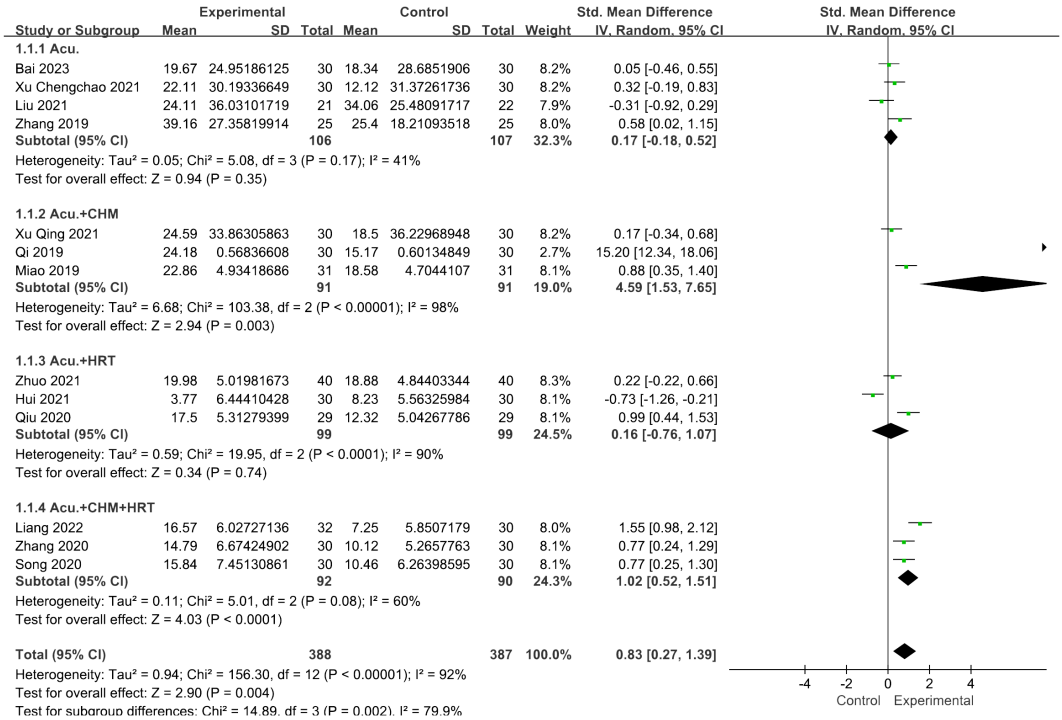

FIGURE 11
Forest plot illustrating the relationship between FSH levels and acupuncture therapy with subgroup analysis.

deficiency effectively markedly improves the quality of life for POI patients. AMH can prevent premature follicular depletion by inhibiting the recruitment of primordial follicles. According to our findings, acupuncture demonstrated the potential to lower FSH levels, elevate E_2 and AMH levels, and alleviate associated symptoms. Preantral follicle development took 85 days to mature, during which time the follicles underwent continuous growth (grades 1 to 4) and exponential growth (grades 5 to 8). The findings of the study

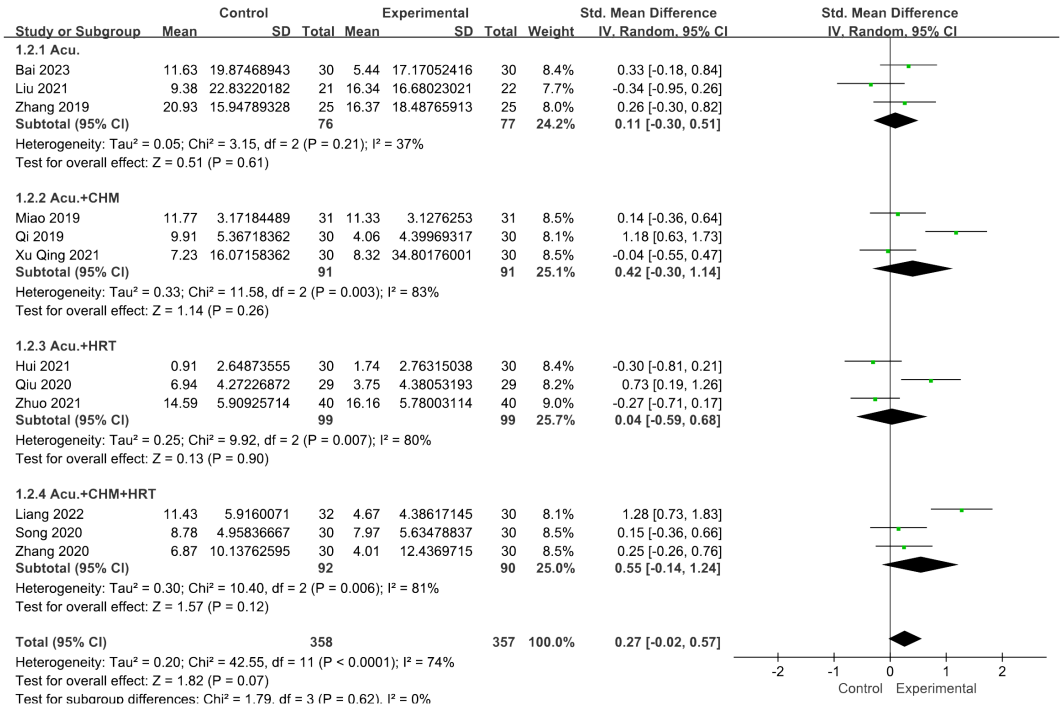

FIGURE 12
Forest plot illustrating the relationship between LH levels and acupuncture therapy with subgroup analysis.

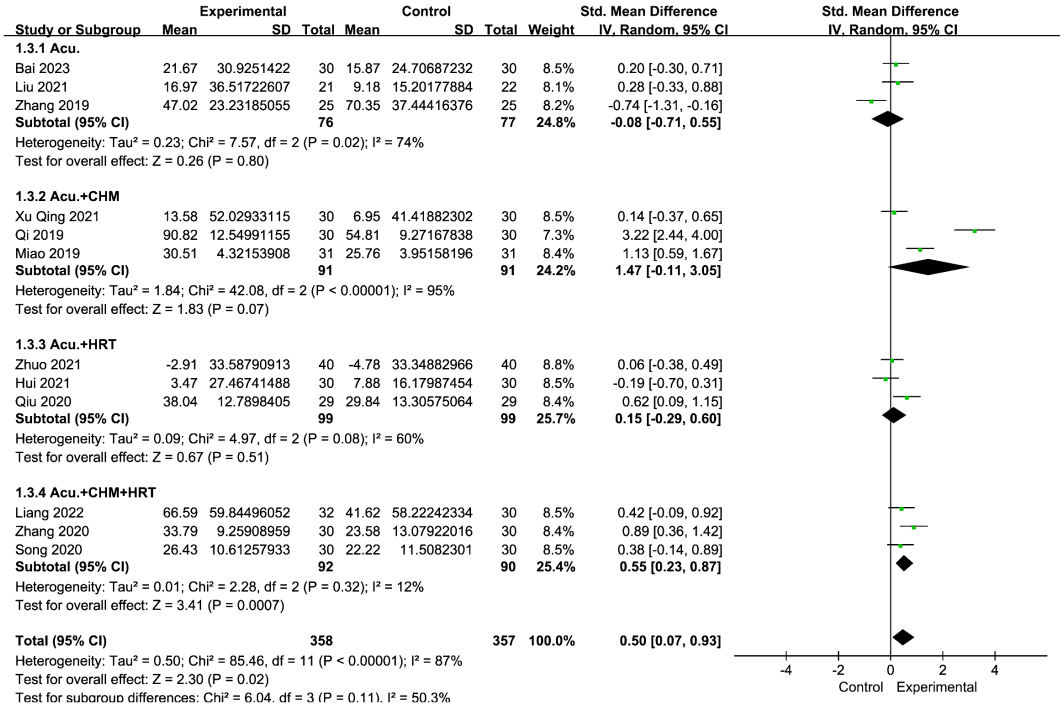

FIGURE 13
Forest plot illustrating the relationship between E_2 levels and acupuncture therapy with subgroup analysis.

suggest that acupuncture has the potential to decrease FSH levels, increase E_2 and AMH levels, and alleviate associated symptoms. However, due to the long time required for follicle development from the preantral follicle to the antral follicle, which can be observed by B-ultrasound, this study did not find any benefit of acupuncture treatment on antral follicle-related outcomes.

In contrast to previous systematic reviews, we adhered to the latest diagnostic criteria for POI as outlined by the ESHRE. Additionally, the intervention window was advanced. The literature incorporated into this study was not considered in prior relevant articles. Consistent with earlier discoveries (40, 41), our findings demonstrate the efficacy of acupuncture in lowering serum FSH levels and increasing E_2 levels. Limited research has focused on the isolated effects of acupuncture. Our study revealed that acupuncture has the potential to elevate AMH levels and the overall effective rate, exerting positive effects on menstrual disorders and perimenopausal symptoms.

Acupuncture, emerging as a novel therapy for POI, has been demonstrated to modulate a diverse array of cellular processes and pathways. In another investigation, acupuncture exhibited the capacity to stimulate Bcl-2 and diminish Bax expression in ovarian tissues, thereby mitigating granulosa cell apoptosis and impeding primordial follicle loss through the induction of antioxidant and anti-apoptotic systems (42). Additionally, Zhang et al. (43) unveiled that electroacupuncture could potentially inhibit the phosphorylation of proteins in the PI3K/AKT/mTOR pathway, leading to the restoration of serum levels of AMH, E_2, FSH, and LH, along with the proliferation of small follicles. Remarkably, electroacupuncture exhibited the potential to regulate characteristic metabolites linked to energy and neurotransmitter metabolism in the liver and kidney, thereby enhancing the menstrual cycle in the participants (44). Moreover, a recent experiment revealed that electroacupuncture could potentially stabilize hormone levels and mitigate follicular atresia by upregulating the expression of CDK6/CCND1 in murine ovarian granulosa cells (OGCs) (45).

The limitations of this systematic study are as follows: firstly, the clinical effect is susceptible to various factors such as acupoint selection, stimulation intensity, qi generation, and acupuncture techniques, lacking uniformity and objectivity at present. It may contribute to the observed heterogeneity, and no significant improvement was achieved in the subgroup analysis. Furthermore, due to limitations in the source studies, pregnancy outcomes cannot be assessed though serving as a crucial concern for reproductive-aged women with POI. Individuals with POI may experience anxiety, depression, and dyssomnia (46). Although acupuncture has demonstrated benefits for ovarian function, its impact on physical and psychological health or quality of life remains unexplored. Additionally, the thickness of the endometrium should be monitored in time after the rise of estrogen, and if necessary, progesterone should be used to transform the endometrium. Moreover, a majority of the included studies lacked explicit descriptions of double-blind procedures, resulting in methodological shortcomings. Nevertheless, the nature of acupuncture involves mutual interaction between the physician and the patient, making the application of a blinding

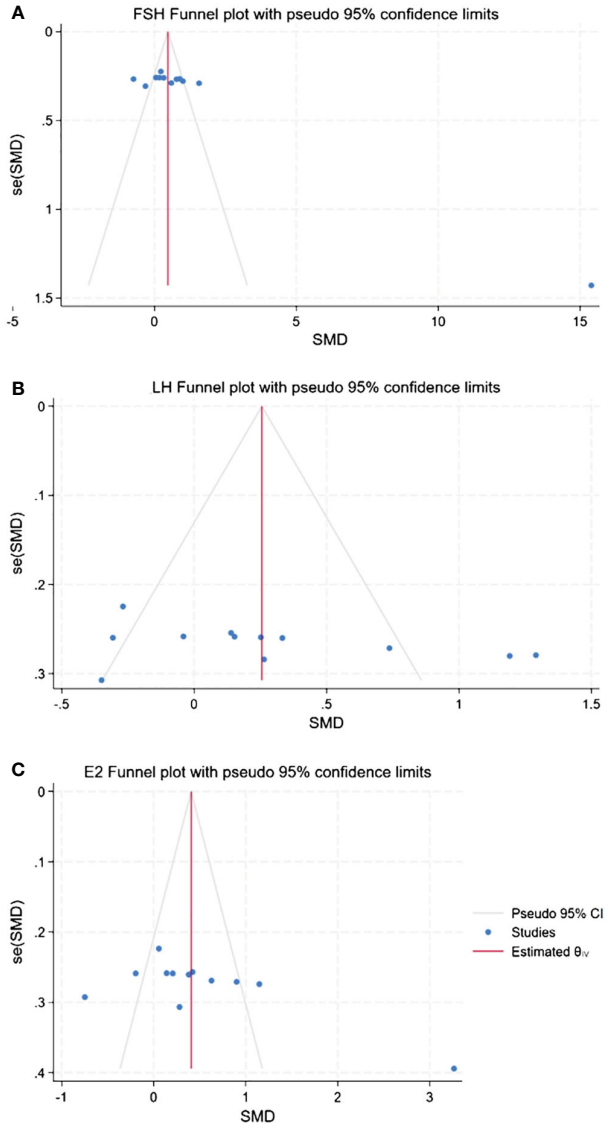

FIGURE 14
Funnel plots of publication bias. **(A)** Publication bias of FSH. **(B)** Publication bias of LH. **(C)** Publication bias of E_2.

approach challenging. Therefore, our study represents the inaugural meta-analysis and systematic review of RCTs adhering to the 2016 ESHRE criteria, with a specific focus on acupuncture for POI patients. Despite these limitations, future efforts should involve larger and higher-quality RCTs incorporating essential acupuncture outcomes to comprehensively assess its current clinical efficacy.

5 Conclusion

Considering the research findings, acupuncture emerges as a potentially efficacious alternative therapy for the treatment of POI, particularly in light of the existing deficiencies in HRT. However, the quality of evidence remains constrained due to the significant heterogeneity and the small sample effect. Future research is imperative to substantiate the efficacy of acupuncture in the treatment of POI, necessitating meticulously designed, large-scale and multicenter RCTs.

Data availability statement

The original contributions presented in the study are included in the article/Supplementary Material. Further inquiries can be directed to the corresponding author.

Author contributions

HC: Conceptualization, Data curation, Formal analysis, Investigation, Methodology, Software, Writing – original draft, Writing – review & editing. HL: Conceptualization, Data curation, Formal analysis, Investigation, Methodology, Software, Writing – original draft, Writing – review & editing. GL: Conceptualization, Data curation, Formal analysis, Investigation, Methodology, Software, Writing – review & editing. XL: Conceptualization, Data curation, Formal analysis, Investigation, Methodology, Software, Writing – review & editing. SL: Project administration, Supervision, Validation, Writing – review & editing. PL: Conceptualization, Methodology, Validation, Writing – review & editing. CC: Project administration, Supervision, Validation, Writing – review & editing. LX: Project administration, Resources, Supervision, Validation, Writing – review & editing.

Funding

The author(s) declare financial support was received for the research, authorship, and/or publication of this article. This study received funding from the Three-Year Action Plan for Further Accelerating the Development of Traditional Chinese Medicine Inheritance and Innovation in Shanghai (2021–2023) [grant number ZY(2021–2023)-0209–01] and the Shanghai Science and Technology Commission under Grant 23Y21920300. Clinical study of internal adjustment and external treatment combined with prevention and treatment of mild and medium positive Omicron infection during rehabilitation (2022-KY-ZYY-07).

Acknowledgments

We extend our gratitude to Mengxin Ye and Huirong Gao for their assistance in language editing.

Conflict of interest

The authors declare the research was conducted in the absence of any commercial or financial relationships that could be construed as a potential conflict of interest.

Publisher's note

All claims expressed in this article are solely those of the authors and do not necessarily represent those of their affiliated organizations, or those of the publisher, the editors and the reviewers. Any product that may be evaluated in this article, or claim that may be made by its manufacturer, is not guaranteed or endorsed by the publisher.

Supplementary material

The Supplementary Material for this article can be found online at: https://www.frontiersin.org/articles/10.3389/fendo.2024.1361573/full#supplementary-material

References

1. European Society for Human R, Embryology Guideline Group on POI, Webber L, Davies M, Anderson R, Bartlett J, et al. ESHRE Guideline: management of women with premature ovarian insufficiency. *Hum Reprod*. (2016) 31:926–37. doi: 10.1093/humrep/dew027

2. Zhou Y, Jin Y, Wu T, Wang Y, Dong Y, Chen P, et al. New insights on mitochondrial heteroplasmy observed in ovarian diseases. *J Adv Res*. (2023). doi: 10.1016/j.jare.2023.11.033

3. Zhang Q, Zhang W, Wu X, Ke H, Qin Y, Zhao S, et al. Homozygous missense variant in MEIOSIN causes premature ovarian insufficiency. *Hum Reprod*. (2023) 38:ii47–56. doi: 10.1093/humrep/dead084

4. Cattoni A, Parissone F, Porcari I, Molinari S, Masera N, Franchi M, et al. Hormonal replacement therapy in adolescents and young women with chemo- or radio-induced premature ovarian insufficiency: Practical recommendations. *Blood Rev*. (2021) 45:100730. doi: 10.1016/j.blre.2020.100730

5. Chemaitilly W, Li Z, Krasin MJ, Brooke RJ, Wilson CL, Green DM, et al. Premature ovarian insufficiency in childhood cancer survivors: A report from the st. Jude lifetime cohort. *J Clin Endocrinol Metab*. (2017) 102:2242–50. doi: 10.1210/jc.2016–3723

6. Hamoda H, Sharma A. Premature ovarian insufficiency, early menopause, and induced menopause. *Best Pract Res Clin Endocrinol Metab*. (2024) 38(1):101823. doi: 10.1016/j.beem.2023.101823

7. Menopause Subgroup CSoO and Gynecology CMA. [Consensus of clinical diagnosis and treatment of premature ovarian insufficiency (2023)]. *Zhonghua Fu Chan Ke Za Zhi*. (2023) 58:721–8. doi: 10.3760/cma.j.cn112141–20230316–00122

8. Gunning M, Meun C, van Rijn B, Daan N, Roeters van Lennep J, Appelman Y, et al. The cardiovascular risk profile of middle age women previously diagnosed with premature ovarian insufficiency: A case-control study. *PLoS One*. (2020) 15:e0229576. doi: 10.1371/journal.pone.0229576

9. Welt CK. Primary ovarian insufficiency: a more accurate term for premature ovarian failure. *Clin Endocrinol (Oxf)*. (2008) 68:499–509. doi: 10.1111/j.1365-2265.2007.03073.x

10. Ishizuka B. Current understanding of the etiology, symptomatology, and treatment options in premature ovarian insufficiency (POI). *Front Endocrinol (Lausanne)*. (2021) 12:626924. doi: 10.3389/fendo.2021.626924

11. Armeni E, Paschou SA, Goulis DG, Lambrinoudaki I. Hormone therapy regimens for managing the menopause and premature ovarian insufficiency. *Best Pract Res Clin Endocrinol Metab*. (2021) 35:101561. doi: 10.1016/j.beem.2021.101561

12. Cuzick J, Chu K, Keevil B, Brentnall AR, Howell A, Zdenkowski N, et al. Effect of baseline oestradiol serum concentration on the efficacy of anastrozole for preventing breast cancer in postmenopausal women at high risk: a case-control study of the IBIS-II prevention trial. *Lancet Oncol*. (2024) 25:108–16. doi: 10.1016/S1470–2045(23)00578–8

13. Kalenga CZ, Metcalfe A, Robert M, Nerenberg KA, MacRae JM, Ahmed SB. Association between the route of administration and formulation of estrogen therapy and hypertension risk in postmenopausal women: A prospective population-based study. *Hypertension*. (2023) 80:1463–73. doi: 10.1161/HYPERTENSIONAHA.122.19938

14. Mohammed K, Abu Dabrh AM, Benkhadra K, Al Nofal A, Carranza Leon BG, Prokop LJ, et al. Oral vs transdermal estrogen therapy and vascular events: A systematic review and meta-analysis. *J Clin Endocrinol Metab*. (2015) 100:4012–20. doi: 10.1210/jc.2015–2237

15. Booyens RM, Engelbrecht AM, Strauss L, Pretorius E. To clot, or not to clot: The dilemma of hormone treatment options for menopause. *Thromb Res*. (2022) 218:99–111. doi: 10.1016/j.thromres.2022.08.016

16. Yang Q, Zhu L, Jin L. Human follicle *in vitro* culture including activation, growth, and maturation: A review of research progress. *Front Endocrinol (Lausanne)*. (2020) 11:548. doi: 10.3389/fendo.2020.00548

17. Kawamura K, Cheng Y, Suzuki N, Deguchi M, Sato Y, Takae S, et al. Hippo signaling disruption and Akt stimulation of ovarian follicles for infertility treatment. *Proc Natl Acad Sci U S A*. (2013) 110:17474–9. doi: 10.1073/pnas.1312830110

18. Zhai J, Yao G, Dong F, Bu Z, Cheng Y, Sato Y, et al. *In vitro* activation of follicles and fresh tissue auto-transplantation in primary ovarian insufficiency patients. *J Clin Endocrinol Metab*. (2016) 101:4405–12. doi: 10.1210/jc.2016–1589

19. Chen ZJ, Tian Q, Qiao J. [Chinese expert consensus on premature ovarian insufficiency]. *Zhonghua Fu Chan Ke Za Zhi*. (2017) 52:577–81. doi: 10.3760/cma.j.issn.0529–567X.2017.09.001

20. Zhang S, Yahaya BH, Pan Y, Liu Y, Lin J. Menstrual blood-derived endometrial stem cell, a unique and promising alternative in the stem cell-based therapy for chemotherapy-induced premature ovarian insufficiency. *Stem Cell Res Ther*. (2023) 14:327. doi: 10.1186/s13287-023-03551-w

21. Yang L, Yang W, Sun M, Luo L, Li HR, Miao R, et al. Meta analysis of ovulation induction effect and pregnancy outcome of acupuncture & moxibustion combined with clomiphene in patients with polycystic ovary syndrome. *Front Endocrinol (Lausanne)*. (2023) 14:1261016. doi: 10.3389/fendo.2023.1261016

22. Lin G, Liu X, Cong C, Chen S, Xu L. Clinical efficacy of acupuncture for diminished ovarian reserve: a systematic review and meta-analysis of randomized controlled trials. *Front Endocrinol (Lausanne)*. (2023) 14:1136121. doi: 10.3389/fendo.2023.1136121

23. Page M, McKenzie J, Bossuyt P, Boutron I, Hoffmann T, Mulrow C, et al. The PRISMA 2020 statement: an updated guideline for reporting systematic reviews. *BMJ (Clinical Res ed.)*. (2021) 372:n71. doi: 10.1136/bmj.n71

24. Hugh M, Altman D, Hammerschlag R, Hammerschlag R, Li Y, Wu T, et al. STRICTA Revision Group. [Revised Standards for Reporting Interventions in Clinical Trials of Acupuncture (STRICTA): extending the CONSORT statement (Chinese version)]. *Zhong Xi Yi Jie He Xue Bao*. (2010) 8:804–18. doi: 10.3736/jcim20100902

25. Li P, Zhang Y, Li F, Cai F, Xiao B, Yang H. The efficacy of electroacupuncture in the treatment of knee osteoarthritis: A systematic review and meta-analysis. *Adv Biol (Weinh)*. (2023) 7:e2200304. doi: 10.1002/adbi.20220030

26. Hui J, Yang P, Wang Y, Zhao X, Li B, Xiao Y, et al. Efficacy observation of tiao ren bu shen needling method plus western medication for premature ovarian. *Shanghai J Acu-mox*. (2021) 40:551–4. doi: 10.13460/j.issn.1005–0957.2021.05.0551

27. Miao Y. *Clinical study on the treatment of premature ovarian insufficiency of kidney-deficiency and liver stagnation type by combination of acupuncture and medicine*. Hubei,China: Hubei University of Traditional Chinese Medicine (2019) 4:128–9.

28. Qi L, Su T, Yang Y, Jiang X. Clinical effect of acupuncture in the treatment of 30 patients with premature ovarian insufficiency. *Clin Res Practice*. (2019) 4:128–9. doi: 10.19347/j.cnki.2096–1413.201929055

29. Zhang J, Liu Y, Deng R, Guo Y, Yan B, Chen P, et al. Observation on therapeutic effect of "Tiaoren Tongdu acupuncture" on premature ovarian insufficiency of kidney deficiency. *Chin acupuncture moxibustion*. (2019) 39:579–82. doi: 10.13703/j.0255–2930.2019.06.003

30. Qiu J. *Clinical observation on abdominal acupuncture combined with femoston in the treatment of premature ovarian insufficiency of kidney deficiency type*. Fujian,China: Fujian University of Traditional Chinese Medicine (2020).

31. Song J. *Clinical study on the treatmet of premature ovarian insufficiency in the kidney deficiency and blood stasis type by combining acupuncture with traditional Chinese medicine*. Liaoning,China: Liaoning University of Traditional Chinese Medicine (2020).

32. Zhang S. *Clinical observation on the combination of Chinese and Western medicine and acupuncture in treating patients with premature ovarian insufficiency of kidney deficiency and liver depression syndrome*. Liaoning,China: Liaoning University of Traditional Chinese Medicine (2020).

33. Liu X. *Metabolomics of Serum Studies on the impact of acupuncture combined with hormone replacement therapy on sex hormone-related metabolites and metabolic pathways in individuals with premature ovarian insufficiency*. Hunan,China: Hunan University of Chinese Medicine (2021).

34. Xu C, Li H, Fang Y, Bai T, Yu X. Effect of regulating menstruation and promoting pregnancy acupuncture therapy on negative emotion in patients with premature ovarian insufficiency. *Chin Acupuncture Moxibustion*. (2021) 41:279–82. doi: 10.13703/j.0255–2930.20200307–0004

35. Xu Q. *Clinical study on acupuncture combined with traditional Chinese medicine in the treatment of premature ovarian insufficiency due to liver and kidney Yin deficiency*. Liaoning,China: Liaoning University of Traditional Chinese Medicine (2021).

36. Zhuo Y, Huang X, Huang Y, Wu J. Effect of regulating menstruation and promoting pregnancy acupuncture in the treatment of patients with premature ovarian insufficiency undergoing *in vitro* fertilization and embryo transfer. *China Med Herald*. (2021) 18:125-8,132.

37. Liang S, Huang X, He D. Clinical observation of combined acupuncture and medicine in the treatment of premature ovarian insufficiency with kidney deficiency and liver stagnation syndrome. *Lishizhen Med Materia Med Res*. (2022) 33:2682–4. doi: 10.3969/j.issn.1008–0805.2022.11.31

38. Bai T, Li H. Efficacy of medical moxibustion at baliao points combined with regulating menstruation to promote pregnancy acupuncture on premature ovarian insufficiency of spleen and kidney yang deficiency. *Shangdong J Traditional Chin Med*. (2023) 42:1074–9. doi: 10.16295/j.cnki.0257–358x.2023.10.010

39. Tao M, Shao H, Li C, Teng Y. Correlation between the modified Kupperman Index and the Menopause Rating Scale in Chinese women. *Patient Prefer Adherence*. (2013) 7:223–9. doi: 10.2147/PPA.S42852

40. Li Y, Xia G, Tan Y, Shuai J. Acupoint stimulation and Chinese herbal medicines for the treatment of premature ovarian insufficiency: A systematic review and meta-analysis. *Complement Ther Clin Pract*. (2020) 41:101244. doi: 10.1016/j.ctcp.2020.101244

41. Li H, Zhang J, Chen W. Dissecting the efficacy of the use of acupuncture and Chinese herbal medicine for the treatment of premature ovarian insufficiency (POI): A systematic review and metaanalysis. *Heliyon*. (2023) 9:e20498. doi: 10.1016/j.heliyon.2023.e20498

42. Tan R, He Y, Zhang S, Pu D, Wu J. Effect of transcutaneous electrical acupoint stimulation on protecting against radiotherapy- induced ovarian damage in mice. *J Ovarian Res*. (2019) 12:65. doi: 10.1186/s13048–019-0541–1

43. Zhang H, Qin F, Liu A, Sun Q, Wang Q, Xie S, et al. Electro-acupuncture attenuates the mice premature ovarian failure via mediating PI3K/AKT/mTOR pathway. *Life Sci*. (2019) 217:169–75. doi: 10.1016/j.lfs.2018.11.059

44. Chen M, He Q, Guo J, Wu Q, Zhang Q, Yau Y, et al. Electro-acupuncture regulates metabolic disorders of the liver and kidney in premature ovarian failure mice. *Front Endocrinol (Lausanne)*. (2022) 13:882214. doi: 10.3389/fendo.2022.882214

45. Geng Z, Liu P, Yuan L, Zhang K, Lin J, Nie X, et al. Electroacupuncture attenuates ac4C modification of P16 mRNA in the ovarian granulosa cells of a mouse model premature ovarian failure. *Acupunct Med*. (2023) 41:27–37. doi: 10.1177/09645284221085284

46. Xi D, Chen B, Tao H, Xu Y, Chen G. The risk of depressive and anxiety symptoms in women with premature ovarian insufficiency: a systematic review and meta-analysis. *Arch Womens Ment Health*. (2023) 26:1–10. doi: 10.1007/s00737–022-01289–7

Frontiers in Endocrinology

Explores the endocrine system to find new therapies for key health issues

The second most-cited endocrinology and metabolism journal, which advances our understanding of the endocrine system. It uncovers new therapies for prevalent health issues such as obesity, diabetes, reproduction, and aging.

Discover the latest Research Topics

See more →

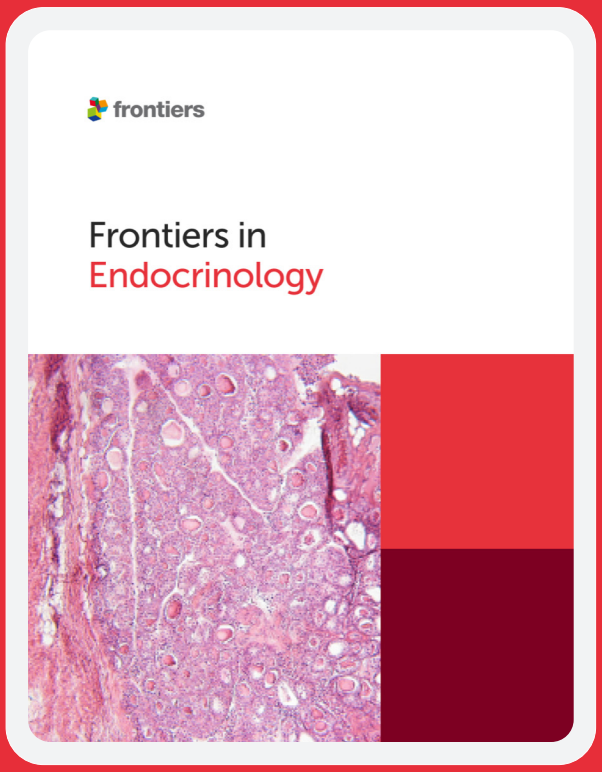

Frontiers

Avenue du Tribunal-Fédéral 34
1005 Lausanne, Switzerland
frontiersin.org

Contact us

+41 (0)21 510 17 00
frontiersin.org/about/contact